SPATIAL INEQUALITY OF INFRASTRUCTURE DEVELOPMENT IN MIZORAM

A THESIS SUBMITTED IN PARTIAL FULFILLMENT OF THE REQUIREMENTS FOR THE DEGREE OF DOCTOR OF PHILOSOPHY

VANLALROLUAHPUIA

MZU Regn. No. 4782 of 2011

Ph.D Regn. No. MZU/Ph.D./1152 of 26.10.2018

DEPARTMENT OF ECONOMICS

SCHOOL OF ECONOMICS, MANAGEMENT & INFORMATION SCIENCE

JANUARY 2026

SPATIAL INEQUALITY OF INFRASTRUCTURE DEVELOPMENT IN MIZORAM

BY

Vanlalroluahpuia

Department of Economics

Prof. Lalhriatpuii

Supervisor

Submitted

In partial fulfillment of the requirement of the Degree of Doctor of Philosophy in Economics of Mizoram University, Aizawl.

MIZORAM UNIVERSITY

DEPARTMENT OF ECONOMICS

Prof. Lalhriatpuii ***09436152046***

MZU, Tanhril-796009 ***0389-2330709***

CERTIFICATE

This is to certify that the thesis entitled **"Spatial Inequality of Infrastructure Development in Mizoram"** by Shri. Vanlalroluahpuia has been written under my guidance. This thesis is the result of his investigation into the subject and was never submitted to any other University for any research degree.

(PROF. LALHRIATPUII)

II

DECLARATION

MIZORAM UNIVERSITY

January 2026

I, Vanlalroluahpuia, hereby declare that the subject matter of this thesis is the record of work done by me, that the contents of this thesis did not form basis of the award of any previous degree to me or to do the best of my knowledge to anybody else, and that the thesis has not been submitted by me for any research degree in any other University/Institute.

This is being submitted to the Mizoram University for the degree of Doctor of Philosophy in Economics.

(VANLALROLUAHPUIA)

(Dr. K. ANGELA LALHMINGSANGI)
HoD i/c

(PROF. LALHRIATPUII)
Supervisor

ACKNOWLEDGEMENT

First and foremost, I express my deepest gratitude to the Almighty God for His grace and mercy, without which the completion of this dissertation would not have been possible.

I am profoundly grateful to my supervisor, Prof. Lalhriatpuii, whose academic expertise and professional guidance have been invaluable throughout this study. Her patience, discernment, and consistent encouragement have provided both intellectual direction and personal support. This work stands completed largely through her steadfast mentorship.

My heartfelt thanks are due to my family. To my wife and kids, for their constant encouragement, understanding, and quiet strength during the course of this endeavour. To my father and sister, whose moral support and confidence in me have been a source of motivation.

To all who have, in various ways, contributed to the fulfilment of this work, I remain deeply obliged.

(VANLALROLUAHPUIA)

TABLE OF CONTENTS

LIST OF TABLES

LIST OF MAPS

LIST OF GRAPHS

LIST OF ABBREVIATIONS

2SFCA	Two-step Floating Catchment Area
ABC	Aerial Bundled Cables
ADB	Asian Development Bank
ALR	Agricultural Link Road
API	Annual Parasite Incidence
BPL	Below Poverty Line
CAGR	Compound Annual Growth Rate
CEA	Central Electricity Authority
CHC	Community Health Centre
COVID-19	Coronavirus Disease of 2019
CV	Coefficient of Variation
DEM	Digital Elevation Model
DH	District Hospital
DMSP-OLS	Defense Meteorological Satellite Program Operational Line-Scan System
DPI	Dots Per Inch
ECG	Electrocardiogram
ECHO	Echocardiogram
EEG	Electroencephalogram
EOG	Earth Observations Group
EPSG	European Petroleum Survey Group
FRU	First Referral Unit
GDP	Gross Domestic Product
GIS	Geographic Information Systems
GSDP	Gross State Domestic Product
HH	High High (in LISA)
HL	High Low (in LISA)
HMIS	Health Management Information System
HPSA	Health Professional Shortage Area
IBEF	India Brand Equity Foundation
IMR	Infant Mortality Rate
IPD	In-Patient Department
IPHS	Indian Public Health Standards
ISRO	Indian Space Research Organisation
JASP	Jeffreys’s Amazing Statistics Program

JPL	Jet Propulsion Laboratory
KMMTTP	Kaladan Multimodal Transit Transport Project
KMO	Kaiser-Meyer-Olkin
LH	Low High (in LISA)
LHV	Lady Health Visitor
LISA	Local Indicators of Spatial Association
LL	Low Low (in LISA)
LLR	Log-Likelihood Ratio
LM	Lagrange Multiplier
MHW	Male Health Worker
MK Test	Mann-Kendall Test
MMR	Maternal Mortality Ratio
MoHFW	Ministry of Health and Family Welfare
MSHC	Mizoram State Healthcare Scheme
NCD	Non-Communicable Diseases
NDVI	Normalized Difference Vegetation Index
NH	National Highway
NHM	National Health Mission
NITI Aayog	National Institution for Transforming India
NOAA	National Oceanic and Atmospheric Administration (USA)
NTL	Night Time Lights
NVBDC	National Centre for Vector Borne Diseases Control
OECD	Organisation for Economic Co-operation and Development
OLS	Ordinary Least Square
OPD	Out-Patient Department
OSM	Open Street Map
PCA	Principal Component Analysis
PHC	Primary Health Centre
PM-JAY	Pradhan Mantri Jan Arogya Yojana
PNG	Portable Network Graphics
QGIS	Quantum Geographic Information System
Res.R	Residential Road
RM	Registered Midwives
RN	Registered Nurse
RR	Relative Risk (in SaTScan)
RR	Rural Roads
RSBY	Rashtriya Swasthya Bima Yojana
SaTScan	Spatial and Space Time Scan Statistics

SDH	Sub-District Hospital
SEM	Spatial Error Model
SH	State Highway
SLM	Spatial Lag Model
SRTM	Shuttle Radar Topography Mission
T&D	Transmission and Distribution
UHC	Universal Health Coverage
UPHC	Urban Primary Health Centre
UTM	Universal Traverse Mercator
VIF	Variance Inflation Factor
VIIRS-DNB	Visible Infrared Imaging Radiometer Suite - Day/Night Band
VNL V2	VIIRS Night-time Lights Version 2
WHO	Word Health Organization

CHAPTER-I

INTRODUCTION

1.1 INTRODUCTION

Infrastructure plays a vital role in economic development by enabling efficient resource allocation, market integration, and productivity growth. It lowers transaction costs, expands access to services, and creates positive externalities across sectors. At the same time, the distribution of infrastructure across space is not always uniform, often resulting in concentration that limits growth and welfare gains.

Historical experience reinforces this connection. Europe's railway networks integrated fragmented markets during the Industrial Revolution. The United States' interstate highways linked distant regions and supported domestic commerce. Japan's high-speed rail, introduced during its post-war recovery, became both a symbol and a driver of modernisation. In each case, infrastructure was not only a response to geographic constraints but also an instrument for advancing national goals. Where investments were distributed more evenly, economic growth tended to spread more widely, creating development that was not only faster but also more inclusive. On the other hand, in many developing countries, infrastructure investment is limited and unevenly distributed. Resources are frequently concentrated in larger urban centres, while peripheral regions receive less attention. This pattern creates inefficiencies in the use of resources and slows regional convergence.

India reflects both these successes and shortcomings. Infrastructure has expanded considerably since the 1990s, with new highways, rural electrification schemes, and the growth of health facilities. Yet provision remains uneven. Investment continues to favour urban centres and states with stronger capacity, while peripheral regions are still lagging behind. The North-Eastern region of India is one among the peripheral regions of India where the deficit in infrastructure is most pronounced. Although the region possesses abundant natural resources and a location that places it as the gateway to South-East Asian markets, its difficult terrain and inadequate infrastructure continue to limit economic progress. These gaps matter not only for the region itself but also for India's broader development, since they restrict integration into national markets and undercut the economic potential of an area strategically located at the frontier with South-East Asia.

Mizoram exemplifies this paradox. It is among the most literate states in India and enjoys a location of strategic importance, bordering both Myanmar and Bangladesh. Yet its economy remains small, dependent on public spending, and limited in industrial growth. The state's advantages have not translated into broad-based economic outcomes. This gap points directly to question of how infrastructure development has penetrated the state and whether its distribution allows its population to make full use of their human capital.

Studying the spatial distribution of infrastructure in such a context is essential. Disparities in provision affect not only welfare but also the efficiency of public investment and the prospects for sustained growth. Although traditional statistics capture broad counts of facilities or outputs, they often provide limited insight into how resources are distributed across space, especially in remote region such as Mizoram. Recent advances in spatial analysis, including geographic information systems and satellite-based measures, allow more precise examination of these questions. Night-time light radiance, in particular, has emerged as a useful proxy for economic activity as it offers granular data in settings where conventional data are sparse.

In settings such as Mizoram, where geographic constraints are severe and conventional statistics are often limited, the use of geospatial techniques alongside administrative data opens new possibilities in spatial analysis. These methods make it possible to move beyond the fixed boundaries of administrative units and to observe disparities at much finer levels of resolution. By capturing variation across space in consistent and comparable ways, they allow spatial inequality to be assessed not only between regions but also within them, across multiple dimensions of development. Such perspectives bring into view patterns that remain hidden in aggregate statistics, offering insights into processes and disparities that have rarely been documented.

1.2 SPATIAL INEQUALITY: A THEORETICAL FRAMEWORK

This section discusses the definition, approaches and theoretical background of Spatial Inequality studies.

1.2.1 Definition of Spatial Inequality

According to Krugman, “Spatial inequality refers to the concentration of economic activity and resources in specific geographic areas, leading to disparities in income, opportunities, and development between regions, such as urban versus rural areas or core versus peripheral regions.” The term *spatial inequality* combines two concepts: “spatial,” referring to geographical space, and “inequality,” denoting differences in distribution. In economics, spatial inequality signifies systematic disparities in economic and social outcomes across regions, districts, or localities. Unlike interpersonal inequality, which focuses on differences between individuals or households, spatial inequality emphasizes the territorial dimension of development, the extent to which access to resources, services, and opportunities are unevenly distributed across physical space. This locational emphasis reflects the idea that where individuals live is a fundamental determinant of their capacity to participate and benefit from the processes of growth and welfare.

1.2.2 Approaches to Spatial Inequality Studies

Spatial inequality may be analysed through three principal approaches that guide its examination in research and policy contexts.

(i) Spatial Scale Approach

The spatial scale approach focuses on the geographical level at which disparities are assessed. At the intra-urban scale, inequalities manifest within cities, as neighbourhoods vary in access to housing, healthcare, education, and public services, or in exposure to environmental hazards such as traffic congestion and air pollution. At the regional scale, differences arise across districts or provinces within a country, typically driven by variations in infrastructure, economic output, or administrative effectiveness (Kanbur & Venables, 2005). At the national and international scales, spatial inequality encompasses enduring developmental gaps between countries or world regions, influenced by trade structures, resource distributions, and historical factors (Shorrocks & Wan, 2005). Beyond these administrative divisions, research frequently employs grid-based units, especially in work with geospatial or satellite data, to enable uniform comparisons of indicators across space and time (Henderson, 2012). In many cases, a temporal dimension is incorporated at each scale, allowing analysis of how spatial disparities evolve alongside processes of growth and structural change.

(ii) Comparative Measurement Approach

This approach addresses the methods used to evaluate spatial differences. Under absolute measurement, inequality appears as direct contrasts, such as the total number of schools, hospitals, or kilometres of paved roads between one area and another. Relative measurement adjusts these figures by relevant denominators, including population size, land area, or total income, to produce per capita or proportional indicators that account for differing unit sizes. Relational measurement extends this by situating outcomes within broader spatial systems, whether through adjacency effects, commuting zones, trade linkages, or spatial econometric dependencies (Anselin, 1988). This approach underscores that the assessment of spatial inequality depends not only on the indicators selected but also on the comparative frame and statistical methods employed.

(iii) Normative Approach

The normative approach places spatial inequality within evaluations of welfare and economic progress. From the perspective of equity, disparities in access to infrastructure and services are problematic, as they limit opportunities according to place of residence rather than personal attributes. From the perspective of efficiency, such unevenness may be tolerated when it supports productivity gains from the clustering of activities, which reduce costs and promote innovation despite persistent gaps (Krugman, 1991). More recent contributions extend this debate to justice, sustainability, and social cohesion, viewing entrenched spatial divides as risks to long-term prosperity and inclusive development (Israel & Frenkel, 2018). The normative approach thus treats spatial inequality as both an empirical condition and an object of ethical appraisal, with policy interventions operating at the intersection of competing or converging goals.

1.2.3 Theoretical Background of Spatial Inequality

The study of space is as old as the economics discipline itself. Adam Smith acknowledged that the division of labour was "limited by the extent of the market," which implicitly recognized that spatial reach and connectivity condition productivity and specialization (Smith, 1776). David Ricardo's theory of comparative advantage underscored how regions differ in production potential based on endowments and trade costs, giving early shape to the idea that location produces systematic disparities (Ricardo, 1817). The early location theorists further elaborated these insights. Von Thünen (1826) modelled how transport costs and distance from markets determined land use and rents, while Weber (1929) emphasized the cost-minimization logic of industrial location, where firms balance transport expenses, labour costs, and agglomeration benefits. Lösch (1954) extended these arguments by theorizing the optimal spatial distribution of cities and regions. These early contributions established that economic outcomes are not evenly distributed but follow structured spatial patterns driven by distance, costs, and agglomeration forces.

In welfare economics, the question of spatial inequality appears through the lens of public goods and state intervention. Pigou (1920) argued that markets alone may not deliver optimal allocation when externalities or indivisibilities exist, which is often the case for infrastructure and essential services. Musgrave (1969) later framed the role of government in correcting such inefficiencies, highlighting infrastructure and health services as quasi-public goods whose distribution has profound welfare implications. Within this tradition, spatial inequality arises not merely from market forces but also from the uneven allocation of public expenditure. Unequal provision of welfare-enhancing goods such as healthcare, education, and basic infrastructure leads to disparities in individual well-being and regional productivity, justifying redistributive policy intervention.

In the mid-twentieth century, development economics deepened the understanding of spatial inequality through the lens of growth dynamics. Rosenstein-Rodan (1943) and Nurkse (1953) stressed the importance of "social overhead capital" in balanced growth, arguing that without widespread provision of infrastructure, regions may become trapped in low-level equilibria. Myrdal (1957) introduced the theory of cumulative causation, highlighting that regional disparities are self-reinforcing: advantages in one area attract further investment and talent, while disadvantaged regions fall further behind. Hirschman (1958) similarly emphasized unbalanced growth, arguing that investment often produces forward and backward linkages that concentrate activity in growth poles rather than diffusing it evenly. Williamson (1965) hypothesized that inequality tends to rise during the early stages of development as resources concentrate in leading regions before converging in later stages, although empirical findings suggest that such convergence is far from automatic. Together, these contributions highlighted that spatial inequality is not transitory but often systemic, reflecting both structural and policy-related dynamics.

Modern theories have further formalized the mechanisms of spatial concentration and divergence. The Alonso-Muth-Mills framework (Alonso, 1964; Mills, 1967; Muth, 1969) analysed the structure of urban space, showing how commuting costs, land rents, and access to public goods shape the spatial allocation of households and firms within cities and surrounding regions. Krugman (1991) introduced the "new economic geography," demonstrating how economies of scale, labour pooling, and knowledge spillovers produce centripetal forces that drive agglomeration, while congestion and land scarcity provide centrifugal counterforces. Venables (2005) extended these arguments to global and national development patterns, emphasizing that the benefits of agglomeration often accrue disproportionately to a few regions. These modern perspectives enrich the discussion as to why economic activity, infrastructure, and welfare outcomes remain concentrated even in contexts where factor endowments appear broadly similar.

While multiple traditions address spatial inequality, three theoretical strands offer particularly strong anchors for analysing disparities in contemporary development contexts. First, welfare economics emphasizes that the distribution of welfare-enhancing goods such as healthcare has both equity and efficiency implications, as uneven provision generates productivity losses alongside social inequities. Second, infrastructure economics and urban models highlight the role of roads, buildings, and other physical assets as determinants of spatial concentration, showing how unequal infrastructure provision entrenches regional imbalances. Third, theories of uneven growth and divergence demonstrate that initial disparities can persist or even widen over time through cumulative causation and agglomeration forces, challenging the neoclassical presumption of automatic convergence. Together, these theoretical traditions offer the study a distinct leg to stand on in assessing the nature of spatial inequality in Infrastructure.

1.3 MEANING AND SCOPE OF SOFT INFRASTRUCTURE

Soft infrastructure denotes the institutional and organisational arrangements that sustain the functioning of an economy and society through the provision of services, regulation, and human capital formation. It differs from hard infrastructure in that it is not primarily physical in nature but instead relates to systems and capacities that ensure effective delivery of welfare and economic activity. Principal domains of soft infrastructure include education, healthcare, public administration, legal and financial systems, and social protection mechanisms.

1.3.1 Health Infrastructure

Health infrastructure is particularly critical for balanced development. Beyond its intrinsic value as a determinant of welfare, access to quality healthcare ensures the maintenance of a productive workforce, reduces morbidity-related income losses, and enhances labour mobility. Unequal distribution of health facilities, by contrast, traps peripheral regions in cycles of deprivation: high travel costs to access urban hospitals discourage timely care, leading to both welfare losses and diminished productivity. For the purpose of this study, health infrastructure is selected as a key representative of soft infrastructure in Mizoram.

Health infrastructure comprises the facilities, personnel, equipment, and institutional arrangements that provide preventive, promotive, curative, and rehabilitative health services. The key components are:

(i) **Facilities**: Health buildings such as Sub-centres, Primary Health Centres, Community Health Centres, Sub-district Hospitals, District hospitals, and specialised facilities.

(ii) **Beds**: Inpatient care capacity, expressed as the number of available hospital beds.

(iii) **Medical equipment**: Diagnostic, surgical, and support technologies required for the functioning of facilities.

(iv) **Personnel**: Human resources including doctors, nurses, paramedical staff, and community health workers.

(v) **Health financing:** Financial mechanism such as health insurance which determine financial access and risk protection.

1.3.2 Indian Public Health Standards (IPHS 2022)

The Ministry of Health and Family Welfare (MoHFW) regulates the organisation of India's health facilities through the Indian Public Health Standards (IPHS), last comprehensively updated in 2022. The standards establish benchmarks for population coverage, bed capacity, personnel, equipment, and service responsibilities into a three-tier health system, primary, secondary, and tertiary.

At the primary level, the Primary Health Centre (PHC) is the first point of institutional care beyond the sub-centre. Each PHC is designed to serve a population of 30,000 in plain areas and 20,000 in tribal or hilly areas. According to IPHS norms, it should provide at least six beds, be staffed by a medical officer supported by nurses, a pharmacist, and multipurpose health workers, and be equipped with a basic laboratory, essential drugs, and facilities for maternal and child health services. The PHC functions as a referral unit for sub-centres while delivering preventive, promotive, and curative services.

At the secondary level, two categories of facilities are recognised. The Community Health Centre (CHC) is intended to cover a population of 80,000 to 120,000, with a minimum of 30 beds. It should be staffed by at least four medical specialists, typically a physician, surgeon, obstetrician-gynaecologist, and paediatrician, supported by nursing and technical personnel. Equipment provision includes diagnostic laboratories, x-ray machines, and a labour room, enabling the CHC to act as a first-level referral for PHCs. Above the CHC, the Sub-District Hospital (SDH) provides a larger secondary referral service, meant to serve a population of around 500,000, with 50 to 100 beds. The SDH employs an expanded cadre of specialists and support staff and is expected to provide broader diagnostic and surgical capacity, including blood storage and comprehensive emergency obstetric care.

The District Hospital (DH) represents the highest institutional form at the secondary level in the IPHS framework. It is designed to cover populations of 1.5 to 2 million, with a bed strength of 200 to 300 per one million population, adjusted for district size. Staffing includes the full complement of specialist doctors, nurses, and technical personnel, while facilities include operating theatres, intensive care units, specialty clinics, and advanced diagnostic equipment. Although officially defined as a secondary-level referral hospital, district hospitals in many states also undertake tertiary-level functions, particularly in the absence of medical colleges or regional specialty centres.

At the tertiary level, India's health system is organised around regional and specialist facilities, including medical colleges and apex hospitals. These institutions provide advanced and super-specialty care, in addition to teaching and research functions. Examples include regional cancer centres, cardiology institutes, and the network of All India Institutes of Medical Sciences (AIIMS).

1.3.3 Overview of Healthcare in India

India's healthcare system in 2020–21 comprised a tiered public infrastructure designed to deliver primary, secondary, and tertiary care, as outlined in the Indian Public Health Standards (IPHS). According to the Ministry of Health and Family Welfare (MoHFW, 2021), the public sector operated 25,778 Primary Health Centres (PHCs), 5,624 Community Health Centres (CHCs), 1,224 Sub-District Hospitals (SDHs), and 764 District Hospitals (DHs).

The overall bed density stood at approximately 5.3 per 10,000 population, far below the World Health Organization (WHO) recommendation of 30 per 10,000 (World Health Organization, 2019). Doctor density was 1 per 1,404 persons, short of the WHO norm of 1 per 1,000 (National Health Profile, 2020). Shortages extended to paramedical staff, with 1.7 nurses and midwives per 1,000 population against a global average of 3.5 (WHO, 2020). Equipment availability, particularly for advanced diagnostics such as CT scanners and ventilators, was unevenly distributed across states, contributing to urban–rural and interstate disparities.

The infant mortality rate (IMR) declined to 28 per 1,000 live births in 2020, down from 57 in 2005, while the maternal mortality ratio (MMR) was 103 per 100,000 live births (Sample Registration System, 2020; MoHFW, 2020). In Mizoram, MMR was higher at 130 per 100,000 live births due to limited emergency obstetric care (MoHFW, 2020). Non-communicable diseases (NCDs) accounted for an estimated 63% of total deaths in 2019, with cardiovascular diseases and diabetes increasing in prevalence, while communicable diseases such as tuberculosis persisted, with an incidence rate of 193 per 100,000 (World Health Organization, 2020).

Several national programmes sought to address these challenges. The National Health Mission (NHM), launched in 2005, strengthened rural and urban health systems by upgrading PHCs and CHCs and introducing mobile medical units. The Ayushman Bharat programme (2018) established Health and Wellness Centres for primary care and launched the Pradhan Mantri Jan Arogya Yojana (PM-JAY), providing insurance coverage of up to ₹5 lakh per family annually for secondary and tertiary hospitalisation (MoHFW, 2021). By 2021, immunisation coverage under the Universal Immunisation Programme reached 85% for children under five (MoHFW, 2021). However, total public health expenditure remained at 1.8% of GDP, below the global average of 6% (Government of India, 2021).

The private sector accounted for nearly 60% of hospital beds and 70% of outpatient consultations in India by 2019 (National Health Accounts, 2019). This concentration of private facilities in urban centres reinforced spatial inequalities, as rural regions, including Mizoram, relied predominantly on the public sector. Despite reforms, spatial disparities in healthcare access persisted. Only 30% of PHCs met IPHS norms for essential diagnostics, and just 15% of CHCs had the mandated complement of specialists (MoHFW, 2021).

1.4 MEANING AND SCOPE OF HARD INFRASTRUCTURE

Hard infrastructure refers to the stock of long-lived physical assets that support economic production and the delivery of basic services. It is defined as immobile, tangible capital that reduces transaction costs and enables market activity (Aschauer, 1989). Standard definitions distinguish economic infrastructure, such as transport, energy, and communications, from social infrastructure, such as health and education facilities (World Bank, 1994). These assets are immobile, capital-intensive, and long-lived, making their spatial distribution central to regional development outcomes (Gramlich, 1994).

1.4.1 Types of Hard Infrastructure

Hard infrastructure is conventionally classified into four groups:

(i) **Transport**: Roads, railways, ports, and airports that facilitate mobility of goods and people.
(ii) **Energy**: Systems of electricity generation, transmission, and distribution that sustain households and industries.
(iii) **Communications**: Telecommunication and digital networks that enable the flow of information.
(iv) **Physical structures**: Buildings and constructed facilities that accommodate residential, commercial, and institutional functions.

1.4.2 Building Infrastructure

In India, the Census defines a building as a permanent structure with a roof and walls, intended for human habitation or other use (Office of the Registrar General & Census Commissioner, 2011). Buildings are classified into residential, commercial, industrial, institutional, and mixed-use categories. Residential buildings include houses, apartments, and hostels; commercial buildings include shops, offices, and hotels; industrial buildings comprise factories and workshops; institutional buildings cover schools, hospitals, and government offices; and mixed-use structures combine residential with business or institutional activity. In spatial studies, the overall distribution of buildings, regardless of function, provides a proxy for the built environment, reflecting both settlement patterns and economic activity. In this study, building stock is assessed in terms of density per unit area and density per capita.

1.4.3 Road Infrastructure

Roads are linear corridors built for the transport of goods and people. Their classification in India follows administrative responsibility and functional role. The different types of roads used for this study are defined as follows:

(i) **National Highway (NH):** They are the arterial roads or inter-state roads connecting state capitals, ports, major industrial centres, and border regions. They are financed by the central government and maintained by the National Highways Authority of India (NHAI) or state Public Works Departments (PWDs). NHs are constructed to high technical standards, generally with paved bituminous or concrete surfaces, wider carriageways of two to four lanes, and all-weather durability. In hilly terrain, width and alignment are smaller, with increased maintenance requirements.

(ii) **State Highway (SH):** Roads that connect district headquarters and important towns within a state, and provide links to the National Highway network. They are financed and maintained by state governments. SHs are typically two-lane paved roads, but standards vary; in difficult terrain, sections may remain single-lane. They are intended for all-weather use but with lower capacity than NHs

(iii) **Rural Road (RR):** Also called village roads, these provide connectivity between villages and service centres. They are largely constructed under centrally sponsored programmes such as the Pradhan Mantri Gram Sadak Yojana (PMGSY). Design standards prescribe paved, all-weather surfaces, but in hilly regions many stretches remain gravel or semi-paved and are subject to weather-related disruptions.

(iv) **Residential Road (Res.R):** Also known as Town Roads, these are intra-urban and peri-urban roads, maintained by municipal authorities. They provide direct access to residences, businesses, and public facilities. Their quality ranges from paved surfaces in central areas to gravel or semi-paved roads in peripheral settlements.

(v) **Agricultural Link Road (ALR):** Feeder roads connecting farms and cultivation areas to the wider road network, villages or urban settlements. They are often built under state or local rural development programmes. The surfaces are commonly gravel or earthen, and their condition is strongly affected by rainfall and seasonal usage.

1.4.4 Electricity Infrastructure

Electricity infrastructure in India comprises the generation, transmission, and distribution of power. Electricity Generation is based on multiple sources, such as coal, hydroelectric, natural gas, nuclear, and renewable energy such as solar and wind. Power generated is fed into the national grid, operated under the Ministry of Power and coordinated by the Power Grid Corporation of India. The grid is divided into five regional zones, Northern, Western, Southern, Eastern, and North-Eastern, linked into a unified national network.

Electricity is transmitted from generating plants through high-voltage transmission lines to substations, where voltage is stepped down for distribution. In India, 220 kV and 132 kV lines form the main transmission backbone, while 66 kV and 33 kV lines supply power to regional and district-level load centres. Distribution is carried out through 11 kV feeders delivering power to towns and groups of villages, and low-tension 0.415 kV lines supplying individual households and small enterprises (CEA, 2018). Aerial Bundled Cables (ABC) at both 11 kV and 0.415 kV levels are increasingly used to reduce theft and technical losses. Substations are organised by voltage class, extra high voltage, high voltage, and medium voltage, each playing a role in stepping power down for eventual household and industrial consumption.

System performance is measured through installed capacity, consumption, and efficiency indicators. Installed capacity, expressed in megawatts (MW), indicates the maximum generation capability under specified conditions. Electricity consumption is measured in kilowatt-hours (kWh), where one kWh represents the use of 1,000 watts of power for one hour. Per capita consumption is the average kWh used per person per year and serves as a benchmark for access and living standards (CEA, 2020b). Voltage, expressed in kilovolts (kV), denotes the level of electrical potential applied in transmission and distribution, with higher kV suited for long-distance transmission and lower kV used for final distribution. Transmission and Distribution (T&D) losses represent the proportion of electricity lost in transit before reaching consumers. These losses remain a persistent challenge in India's power sector, averaging above 20 percent nationally in recent years (CEA, 2021).

1.5 MEANING AND SCOPE OF GEOGRAPHIC INFORMATION SYSTEMS (GIS)

A Geographic Information System (GIS) is a computer-based framework for the capture, storage, analysis, and visualization of spatially referenced data. The term derives from "geo," meaning earth, and "information system," denoting an organized structure for managing and processing data. In its modern use, GIS integrates cartography, statistical analysis, and database technology to enable the representation of spatial features and their attributes (Longley et al., 2015). By linking location with descriptive information, GIS provides a means to study spatial relationships, patterns, and processes in both natural and human systems.

1.5.1 Data Models and Analytical Tools

GIS data are represented in two primary forms: vector data and raster data, each suited to different types of spatial analysis.

(i) **Vector Data**: Vector data represent geographic features as discrete geometric shapes. Points denote specific locations, such as wells, hospitals, or individual buildings. Lines depict linear features, including roads, rivers, or power lines. Polygons define enclosed areas, such as administrative boundaries, land parcels, or lakes. These shapes provide precise locations and are ideal for mapping infrastructure or administrative units, enabling accurate analysis of spatial distributions, such as healthcare facilities across districts.

(ii) **Raster Data**: Raster data represent continuous phenomena through a grid of cells, where each cell contains a numerical value. Examples include elevation, temperature, rainfall, or satellite imagery, such as night-time lights. The cell size determines the resolution, with smaller cells offering finer detail but requiring more processing power. Raster data are well-suited for analysing spatially continuous variables, such as economic activity or environmental conditions, across regions.

Analytical work in GIS relies on specialised software platforms. Proprietary systems like ArcGIS excel in map production and spatial visualisation, while open-source options such as QGIS, and GeoDa offer flexible tools for spatial analysis, including overlay operations, network analysis, and terrain modelling. Cloud-based platforms, such as Google Earth Engine, facilitate the processing of large-scale satellite datasets, enabling rapid analysis of regional disparities. Statistical software, including Stata, SPSS, R, and Python, supports quantitative analysis of spatial data, such as regression models to assess inequalities in infrastructure access or economic output.

1.5.2 Digital Elevation Models (DEM)

A Digital Elevation Model (DEM) is a raster dataset in which each cell records the elevation of the earth's surface at that location. DEMs provide the foundation for analysing slope, aspect, watershed boundaries, and terrain effects on settlement and infrastructure distribution.

One of the most widely used global datasets is provided by NASA's Shuttle Radar Topography Mission (SRTM), which mapped most of the earth's land surface using radar interferometry. The SRTM DEM provides near-global coverage at a spatial resolution of 30 metres, with elevation values referenced to mean sea level (Farr et al., 2007). DEMs are a core input in spatial studies, particularly in regions with rugged terrain, as they allow systematic analysis of accessibility and the physical constraints of geography.

1.5.3 Night Time Lights (NTL)

Night Time Lights (NTL) data measure the visible and near-infrared light emitted from the Earth's surface at night, as detected by satellite sensors. The physical quantity recorded is radiance, which expresses the amount of light energy emitted from the ground per unit area and per unit solid angle. The standard unit used is nanowatts per square centimetre per steradian ($nW/cm^2/sr$). Here, per square centimetre refers to the area on the ground, and per steradian refers to the angular spread of light detected by the sensor, as in the portion of the sky or hemisphere from which emissions are observed.

Radiance values are not direct counts of individual light sources, such as lamps or buildings. Instead, each value represents the total radiance averaged across the spatial footprint of a satellite pixel. For example, if the resolution of the sensor is 500 metres, the radiance assigned to that pixel corresponds to the average light emission across an area of 500 m × 500 m. This means that the brightness of a single lamp is indistinguishable on its own; rather, the data reflect the combined effect of all lights within the pixel area, averaged into one radiance value.

From these radiance values, different indicators can be derived. Mean radiance is the average brightness within a chosen geographic unit, such as a district or region. Total radiance (or sum of lights) is the aggregate of radiance values across all pixels within a given area. These measures allow comparisons across space and time, showing relative intensity of human activity, infrastructure use, or economic concentration.

The NTL data most widely used in research are produced from the Visible Infrared Imaging Radiometer Suite (VIIRS), mounted on the Suomi National Polar-orbiting Partnership (NPP) and NOAA-20 satellites. VIIRS captures light emissions at a native spatial resolution of approximately 500 metres at the equator. Data are collected as the satellite passes overhead, with the central view termed nadir (directly beneath the satellite, offering the clearest observations) and peripheral views termed off-nadir (at angles from the satellite's path, which may introduce minor distortions). Annual composites are produced by aggregating daily observations into monthly averages and then yearly summaries, while filtering out transient light sources such as wildfires, auroras, or temporary flares, to produce a stable representation of persistent night-time lights (Elvidge et al., 2021).

1.6 AREA OF THE STUDY

Mizoram is one of the eight states of north-eastern India. It shares an international boundary with Myanmar to the east and south, and with Bangladesh to the west. Domestically, it is bordered by Assam to the north, Manipur to the north-east, and Tripura to the west. The state covers an area of 21,081 square kilometres. Its terrain is mountainous, with steep hills and narrow valleys, and elevations ranging from 17 metres to 2,149 metres above sea level. The state falls within seismic zone V and is therefore highly prone to earthquakes and landslides. These natural hazards frequently disrupt connectivity between the central and peripheral regions.

According to the 2011 Census of India, Mizoram’s population was 1,097,206, giving a population density of 52 persons per square kilometre. By 2023, the population is estimated to have risen to around 1.25 million. The state is one of the most urbanised in India. In 2011, 52.1 per cent of the population lived in urban areas, compared with a national average of 31.2 per cent. Aizawl district alone accounted for more than one-quarter of the state’s population, and most of this was concentrated in Aizawl city.

The economy of Mizoram remains dominated by agriculture, which employs more than half of the working population. However, the contribution of agriculture to Gross State Domestic Product (GSDP) is less than one-fifth, reflecting low productivity and structural imbalance. Services account for over 60 per cent of value added, with public administration forming a large share. Industry contributes less than 20 per cent, indicating the absence of a strong manufacturing base (Economic Survey Mizoram, 2021–22). In 2022–23, per capita GSDP was estimated at ₹308,571, while the overall GSDP was projected at ₹35,904 crore in 2023–24.

Map 1.1 Map of Mizoram

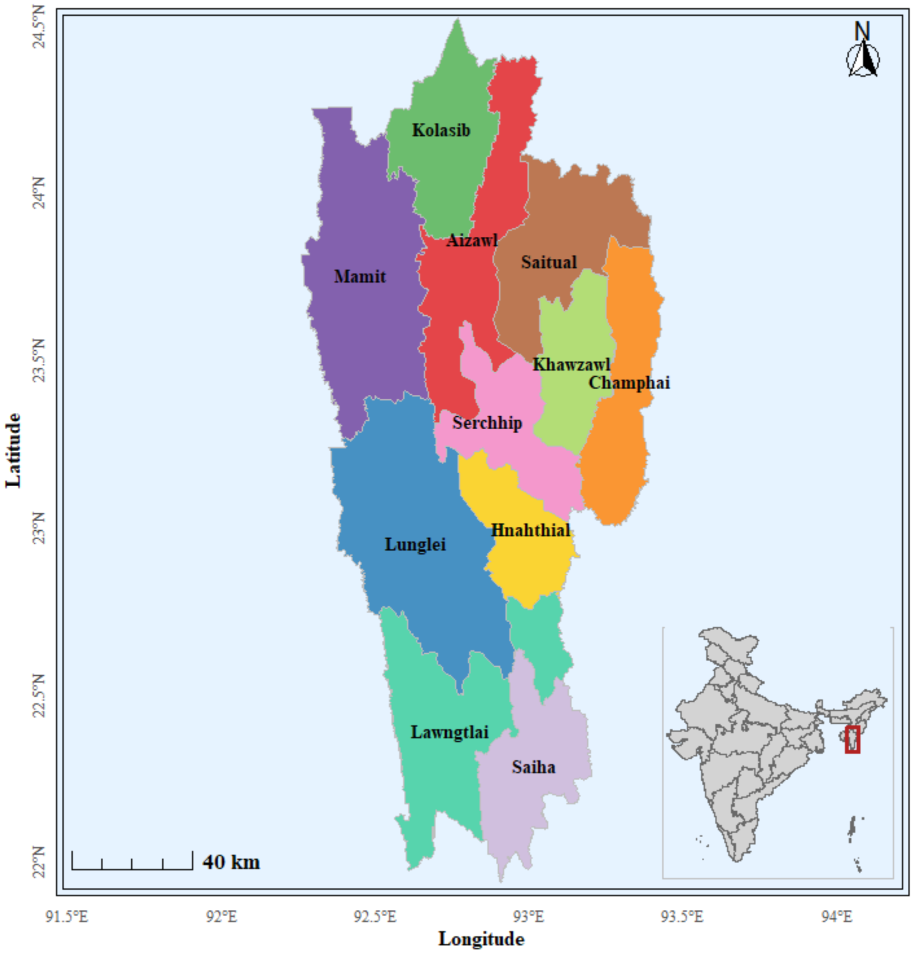

Source: Own visualisation

1.7 RESEARCH GAP

Mizoram presents a developmental paradox. Despite high literacy (92 per cent, Census 2011), economic activity remains small in scale, heavily reliant on public expenditure, and weakly industrialised. The distribution of population and enterprises is markedly uneven. Aizawl alone houses over one-quarter of the state's people, 43 per cent of registered small-scale industries, and 42 per cent of business enterprises (Statistical Handbook of Mizoram, 2022). Around 45 per cent of the state's total workers are concentrated there. The rest of the districts, except some urban centres, remain predominantly neglected, suggesting that both population and productive activity are clustered around the capital.

Mizoram's pattern of development reveals both rapid urbanisation and persistent structural imbalance. Census records show that the share of the population living in urban areas increased from 19.9 per cent in 1971 to 52.1 per cent in 2011, a pace of change well above the national average (Census of India, 1971–2011). Much of this growth has centred on Aizawl, which houses over one-quarter of the state's population and has become the administrative, commercial, and service hub. This concentration has produced signs of congestion, including rising rents and commuting costs, while peripheral districts remain comparatively less developed. Economic data reinforce these disparities. The Economic Survey Mizoram (2021–22) reports that services account for over 60 per cent of GSDP, while industry contributes less than 20 per cent, reflecting the absence of a strong manufacturing base. Agriculture continues to employ a large share of the workforce but adds less than one-fifth of total output, indicating low productivity. Poverty assessments also highlight uneven outcomes: NITI Aayog's National Multidimensional Poverty Index (2021) placed Mizoram's overall poverty rate at 11.9 per cent, but district-level figures showed higher deprivation in Lawngtlai and Mamit compared with Aizawl. Taken together, these trends suggest that while the state has urbanised rapidly, growth and welfare gains have been unevenly distributed across space, leaving peripheral areas at risk of long-term stagnation.

Mizoram's geography compounds these disparities. The state's mountainous terrain, scattered settlements, and vulnerability to landslides make the provision of infrastructure both costly and uneven. These constraints are reflected across sectors. Electrification has reached nearly all villages, yet transmission and distribution losses remain high, averaging 24 per cent (P&E Department, 2019–20). Road networks are better developed in national and state highways that converge on Aizawl, but rural and agricultural link roads remain limited in quality, reducing accessibility in peripheral areas. Health facilities also show a similar pattern: while primary and secondary centres are present in most districts, tertiary services are concentrated in Aizawl, leaving large parts of the state dependent on referral or long-distance travel.

Despite the availability of district-level statistics on facilities, road length, and electrification, economic indicators such as GSDP or Monthly Per Capita Expenditure are reported only at the state level. This prevents assessment of development below the state scale. Moreover, infrastructure data are tabular and descriptive, not spatially analysed. Without GIS-backed approaches, questions of intra-district variation in accessibility, density, and balance between core and periphery remain unresolved.

This absence of spatially informed evidence creates a gap for both scholarship and policy. Given the fact that the state's location is central to India's Act East strategy, the participation of the local population is necessary to make the trade and diplomatic relations a success, therefore a systematic spatial analysis of infrastructure in Mizoram is not only a state interest but also of national interest. More importantly, regional disparities may prevent the peripheral districts from convergence and may locked them into cycles of low infrastructure investment and weak economic performance, while over-reliance on Aizawl as the dominant hub exposes the state to congestion and diminishing returns. Addressing this gap requires a framework that can identify not only the quantity of infrastructure but also its distribution across space and its relationship to economic activity.

1.8 SIGNIFICANCE OF THE STUDY

Spatial inequality in infrastructure has a profound effect on regional development in developing economies such as India. While questions of inequality have been widely studied at both national and state levels, very little work has employed GIS-based methods in regions where data limitations and difficult terrain constrain conventional analyses. Areas with well-developed mapping and robust economic datasets are frequently prioritised in spatial research, whereas peripheral, hilly states such as Mizoram remain underexplored. This study addresses that gap by analysing the spatial distribution of infrastructure, such as health facilities, buildings, and roads, while contextualising their contribution to regional economic progress through the use of night-time Light radiance, thereby demonstrating the utility of spatial methods in data-constrained environments.

By examining disparities in health, building, and road infrastructure, the research highlights how resources are distributed, where imbalances emerge across the state, its economic implication, and explores how public finance can better allocate scarce resources to achieve optimal growth trajectory. The use of remote-sensing data, triangulated with ground data, provides a unique empirical basis in a context where policy decisions have often been shaped more by administrative convenience and political considerations than by systematic spatial analysis. The study's contribution can be considered twofold. First, it situates Mizoram within the national and regional discourse on spatial inequality and regional economic development in India. Second, it offers a methodological template to examine the distribution of infrastructure and their contribution to the wider discourse on economic development in data-scarce regions. In doing so, it opens avenues for further research and more informed policy debate, with the potential to support robust and equitable development strategies in Mizoram and beyond.

1.9 OBJECTIVES OF THE STUDY

1. To identify factors influencing access constraints and spatial disparities in health infrastructure and services across Mizoram.
2. To assess spatial disparities in density and per capita distribution of building infrastructure across Mizoram
3. To evaluate spatial patterns and inequalities in road infrastructure in Mizoram.
4. To analyse the spatial and temporal dynamics of economic activity in Mizoram.

5. To investigate the relationships and factors influencing spatial disparities in infrastructure and economic activity in Mizoram.

1.10 HYPOTHESES

1. Health facilities are spatially clustered in Mizoram.
2. The distribution of medical equipment usage is spatially clustered in Mizoram.
3. The distribution of buildings per capita in Mizoram is significantly unequal.
4. There is significant spatial autocorrelation in the distribution of road infrastructure in Mizoram.
5. Growth in economic activity exhibits significant spatial clustering in Mizoram between 2014 and 2023.
6. Spatial disparities in road and health facility infrastructures are significantly associated with spatial disparities in economic activity in Mizoram.

1.11 METHODOLOGY OF THE STUDY

The study examines the spatial distribution of infrastructure in Mizoram and the role played by disparities in infrastructure on the level economic activity in the state. Using secondary data and GIS mapping tools, the study integrates official statistics with geospatial indicators to assess disparities in health, building, and road infrastructure, and their association with patterns of economic activity in Mizoram.

1.11.1 Research Design

The study is organised into four main areas of quantitative analysis. First, it evaluates the distribution of health infrastructure in Mizoram, assessing whether facilities and services align with demographic need and whether imbalances generate welfare losses through inefficient allocation of public expenditure. Second, it examines physical infrastructure, particularly buildings and road networks, analysing their distribution and density across spatial scales and addressing questions of allocative efficiency in public investment. Third, it considers economic activity, proxied by Night Time Light (NTL) radiance, situating Mizoram within the national context and tracing changes in economic activity over a ten-year period. By examining growth trajectories at district and grid levels, the analysis assesses whether activity is converging or displaying patterns of agglomeration.

Finally, the study integrates these strands of infrastructure to test whether disparities in infrastructure reinforce or attenuate inequalities in economic activity, while also identifying the relative contribution of different infrastructure variables to economic development in the state.

Where appropriate, the research adapts its parameters to the characteristics of the data and the spatial scale under analysis, between intra- and inter-district comparisons, employing grid-based techniques, and refining indicators to capture context-specific variation. This multi-dimensional approach to infrastructure measurement enhances understanding of spatial variation and its relation to economic inequality in Mizoram.

1.11.2 Sources of Data

The study relies on secondary data drawn from authoritative statistical and administrative sources, while also using multiple sources to validate and cross check when discrepancies arise. Demographic estimates are obtained from the Census of India (2011), while health infrastructure and services are compiled from the Mizoram Hospital Statistics Report (2020–2021), Health and Family Welfare Department Annual Report (2019–2020), Mizoram State Healthcare Scheme Annual Report (2021), and National Health Mission reports (2021–2023).

Broader state-wide metrics are taken from the Mizoram Statistical Abstract (2021) and Statistical Handbook (2021–2023). The Public Works Department Report (2023) provides detailed road network data, complemented by Below

Poverty Line (BPL) records from the Directorate of Economics and Statistics, Mizoram, and malaria incidence data from the National Vector Borne Disease Control Programme (2017–2021).

Geospatial datasets include NASADEM (2021) for elevation, Earth Observations Group's VIIRS composites (2014–2023) for night-time light (NTL) radiance, Survey of India (2011) administrative boundaries, Bhuvan land-use/land-cover maps, Microsoft building footprints, and road shapefiles from OpenStreetMap and the Ministry of Rural Development. Building and road datasets are cross-validated against ISRO Bhuvan satellite imagery and other open-access sources, with corrections applied where extraneous or misclassified features (e.g., temporary shelters) are identified.

All spatial data are standardised by georeferencing to the Mizoram administrative boundary shapefile and reprojected to the Universal Traverse Mercator (UTM) Zone 46 North (EPSG:32646) coordinate reference system, ensuring consistency across layers. This preparation enabled subsequent statistical and spatial analysis to meet the research's objectives.

1.11.3 Statistical Analyses

The study employs numerous statistical tools to analyzed the different sets of data and to draw meaningful inferences, which can help in reaching the stated research objectives and hypotheses posed. The statistical tools are discussed as follows.

The Gini coefficient was computed using the **trapezoidal approximation** method, as described by Cowell (2011), which estimates the area between the Lorenz curve and the line of perfect equality. The formula used is:

$$G = 1 - \sum_{i=1}^{n-1} (X_{i+1} - X_i)(Y_{i+1} + Y_i)$$

Where:

G: Gini coefficient

X_i: Cumulative proportion of the population up to district i,

Y_i: Cumulative proportion of variables to district i

n: Number of districts (11 in this study)

The population weights (P_i) were incorporated to account for the varying population sizes across districts, ensuring that the Gini Index reflects the demographic context of Mizoram.

District level cross-sectional data of bed density (3744 beds) is analysed using the Theil T index, decomposing inequality into within-group (urban-rural) and between-group (district-level) components (Theil, 1967). The Theil T Index measures the divergence between the distribution of hospital beds and the population across Mizoram's districts, with urban and rural subgroups. It is defined as:

$$T = \sum_{i=1}^{n} \sum_{j=1}^{m} \left(\frac{b_{i,j}}{B}\right) \ln \left(\frac{b_{i,j}/B}{P_{i.j}/P}\right)$$

Where:

T: Theil T Index, representing total inequality

$b_{i,j}$:Number of health facility beds in subgroup j (urban or rural) of district i

B: Total number of health facility beds across Mizoram

$P_{i.j}$: Population of subgroup j in district i

P: Total population of Mizoram

n: Number of districts (11 in this study)

m: Number of subgroups per district (2 i.e urban and rural)

The index's decomposability allows total inequality to be expressed as:

$$T = T_W + T_B$$

Where the within-district component, capturing urban-rural disparities within each district, is:

$$T_W = \sum_{i=1}^{n} \left(\frac{b_i}{B}\right) \sum_{j=1}^{m} \left(\frac{b_{i,j}}{b_i}\right) \ln\left(\frac{b_{i,j}/b_i}{p_{i.j}/p_i}\right)$$

And the between-district component, reflecting disparities across districts, is:

$$T_B = \sum_{i=1}^{n} \left(\frac{b_i}{B}\right) \ln\left(\frac{b_{i,j}/B}{p_{i.}/P}\right)$$

Where:

b_i: Total number of beds in district *i*

$P_{i.j}$Total population of district *i*

A Theil T Index of 0 (zero) indicates perfect equality, where resources are allocated proportionally to population, while higher values signal greater inequality. The decomposition into T_W and T_B provides an in-depth understanding of the sources of in equality, whether driven by intra district (within group), i.e.

urban-rural, or inter-district variations. The decomposition into sub groups allows targeted policy recommendations (Conceicao & Galbraith, 2000).

Medical equipment usage (196,385 cases across 10 clinically relevant devices) is assessed via a bootstrapped Atkinson index at inequality aversion levels (ε = 0.5, 1, 1.5, 2), using the usage ratio (actual/expected usage) to evaluate deprivation sensitivity. Building density and per capita disparities are also examined using a bootstrapped Atkinson index (1000 permutations, ε = 0.5, 1, 1.5, 2) to estimate mean, standard deviation, and 95% confidence interval (Atkinson, 1970).

The Atkinson Index is calculated as follows:

$$\boldsymbol{A_{\varepsilon} = 1 - \left[\sum_{i=1}^{n}\left(\frac{y_i}{\mu}\right)^{1-\varepsilon}\frac{p_i}{P}\right]^{\frac{1}{1-\varepsilon}}\ ,\ \varepsilon \neq 1}$$

For ε = 1:

$$\boldsymbol{A_1 = 1 - exp\left[\sum_{i=1}^{n}\frac{p_i}{P}\ \mathrm{ln}\left(\frac{y_i}{\mu}\right)\right]}$$

Where:

$\boldsymbol{A_{\varepsilon}}$: Atkinson Index for inequality aversion parameter ε

$\boldsymbol{y_i}$**:** Medical equipment usage in district *i*

μ: Mean equipment usage across all districts

$\boldsymbol{p_i}$**:** Population of district *i*

P: Total population of Mizoram

n: Number of districts

ε = Inequality aversion parameter (tested at 0.5, 1, 1.5, and 2)

Where:

$\boldsymbol{A_{\varepsilon}}$: Atkinson Index for inequality aversion parameter ε

$\boldsymbol{y_i}$**:** Value of the resource or density metric for unit *i*.

μ: Mean value of the resource or density metric across all units.

$\boldsymbol{p_i}$**:** Weight or size of the unit *i*.

P: Total weight across all units.

n: Number of units.

ε = Inequality aversion parameter (tested at 0.5, 1, 1.5, and 2)

The parameter εgoverns the sensitivity of the index to disparities at different points in the distribution. Lower values of ε(e.g., 0.5) place more weight on moderate inequalities, while higher values (e.g., 2) emphasise extreme disparities, particularly at the lower end of the distribution. To ensure the statistical reliability of the Atkinson Index estimates, a bootstrapping procedure was implemented, a nonparametric method that provides robust standard errors and confidence intervals (Efron, B., & Tibshirani, R. J., 1993). For each εvalue, 1,000 bootstrap samples were generated by resampling with replacement from the vector of unit-level ratios. The Atkinson Index was computed for each bootstrap sample, yielding a distribution of index values. From this distribution, the mean, standard error, and 95% confidence intervals were calculated using the 2.5th and 97.5th percentiles. Additionally, the quantiles (2.5%, 25%, 50%, 75%, 97.5%) were provided to offer a comprehensive summary of the index's variability.

To construct the Health Infrastructure Index for Mizoram, a composite index using health facility, beds and medical equipment density was combined using the Principal Component Analysis (PCA). To ensure equal contribution of variables to the Principal Component Analysis (PCA), z-score standardisation is applied to transform variables to a common scale with a mean of 0 and a standard deviation of 1. The z-score for an observation x_{ij} representing the value of variable *j* (e.g., Weighted Bed per 1000) for district *i* is calculated as follows:

$$Z_{xi} = \frac{x_{ij} - \mu_j}{\sigma_j}$$

Where:

x_{ij}: Weighted value of variable *j* for district *i*

μ_j: Mean of variable *j* across all 11 districts

σ_j: Standard deviation of variable *j*

The mean μ_j is computed as:

$$\frac{1}{n}\sum_{i=1}^{n} x_{ij}$$

The standard deviation σ_j using the sample standard deviation for n = 11 districts is:

$$\sqrt{\frac{1}{n-1}\sum_{i=1}^{n}\left(x_{ij} - \mu_j\right)^2}$$

The PCA is conducted on the standardised data matrix Z, with n units and p variables, using the following steps:

- Standardized Data Matrix: The z-scores form an $n \times p$ matrix *Z*, where $n = 11$ (districts) and $p = 3$ (variables: Health Building per 1000, Weighted Bed per 1000, Weighted Equipment per 1000).

- Correlation Matrix: Since the variables are standardized (*mean = 0*, *standard deviation = 1*), the covariance matrix is equivalent to the correlation matrix *S*.

$$= \frac{1}{n - 1} Z^{\mathrm{T}} Z$$

- Eigenvalue Decomposition: The correlation matrix (*S*) is decomposed to obtain eigenvalues λ_k and eigenvectors v_k

where:

λ_k is the variance explained by the K^{th} principal component.

v_k is the loadings (weights) for each variable on PC *K*.

- Principal Component Scores: The score for district (*i*) on PC *K* is calculated as:

$$K = Z_{\mathrm{i}} v_k$$

Where:

Z_{i} is the row vector of z-scores for district *i* and

v_k is the eigenvector for PC *K*

- Proportion of Variance Explained: The proportion of total variance explained by PC (*k*) is:

$$\frac{\lambda_k}{\sum_{j=1}^{p} \lambda_j}$$

Fit test using Correlations matrix, Bartlett's Test of Sphericity and Kaiser-Meyer-Olkin (KMO) were also used (Jolliffe, 2002).

To evaluate whether health personnel per 1000 exhibits non-random spatial patterns across Mizoram, the Global Moran's I and LISA analysis is applied at district level. To tests whether road infrastructure, comprising National Highways, State Highways, Rural Roads, Residential Roads, and Agricultural Link Roads, show patterns of spatial clustering, the same set of tests are applied on a 10x10 km grid, with sensitivity tests at 5x5 km and 20x20 km grids to ensure robustness across spatial scales. Global Moran's I is expressed as:

$$I = \frac{n}{\sum_i \sum_j w_{ij}} \cdot \frac{\sum_i \sum_j w_{ij}\,(x_i - \bar{x})(x_j - \bar{x})}{\sum_i (x_i - \bar{x})^2}$$

where n is the number of samples, w_{ij} is the Queen contiguity weight, x_i is the density at location i, and $\bar{x}$ is the mean density. Local Indicators of Spatial Association (LISA) is calculated as:

$$I_i = \frac{(x_i - \bar{x}) \sum_j w_{ij}\,(x_j - \bar{x})}{\frac{1}{n} \sum_i (x_i - \bar{x})^2}$$

where local clusters (High-High, Low-Low, etc.) are identified at significance levels $p \leq 0.05, 0.01, 0.001$, highlighting areas of concentrated or sparse density (Anselin 1988).

To assess health facility accessibility, the Euclidean distance from each settlement to the nearest health facility was calculated (Noel & Guertin 2018). For a settlement at coordinates (x_s, y_s) and a health facility at (x_h, y_h), the Euclidean distance d is computed as:

$$\boldsymbol{d} = \sqrt{(\boldsymbol{x_h} - \boldsymbol{x_s})^2 + (\boldsymbol{y_h} - \boldsymbol{y_s})^2}$$

Owing to the winding nature of roads in Mizoram, an average motor vehicle is estimated to cover an aerial distance of 7 km in 1 hour, distances are converted to travel times and categorised into near (<30 minutes), moderate (< 1 hour) and far (> 1 hour) bins, reflecting economic access constraints.

Spatial clustering of health facilities (119 locations) is tested using SaTScan's Bernoulli model, with likelihood:

$$\boldsymbol{L(z)} = \left(\frac{\boldsymbol{n_z}}{\boldsymbol{n_z + m_z}}\right)^{n_z} \left(\frac{\boldsymbol{n_z}}{\boldsymbol{n_z + m_z}}\right)^{m_z} \cdot \left(\frac{\boldsymbol{N - n_z}}{\boldsymbol{N + M - n_z - m_z}}\right)^{N-n_z} \left(\frac{\boldsymbol{M - m_z}}{\boldsymbol{N + M - n_z - m_z}}\right)^{m-m_z}$$

Where $\boldsymbol{n_z}$ is the number of cases (facilities) in cluster z**,** m_z is the number of controls in cluster z**,** N is the total number of cases (119 facilities), M is the total number of controls (1000), with log-likelihood ratio (LLR = log(L(z)/L0)) and relative risk assessed via 999 Monte Carlo replications (Kulldorff, 1997).

To analyse equipment usage data the Discrete Poisson model was selected, assuming usage follows a Poisson distribution proportional to district populations. For a circular spatial window z, the likelihood function is defined as:

$$L(z) = \frac{e^{-\mu}\mu_Z^{c_z}}{C_z!} \cdot \frac{e^{-(\mu-\mu_z)}(\mu - \mu_z)^{C-c_z}}{(C - c_z!)}$$

Where c_z is the number of usage cases in cluster z, μ_z is the expected cases in cluster z, calculated as $\mu_z = P_z \cdot (C/P)$, P_z is the population in cluster in z, C is the total number of case (196,385), and P is the total population (1,354,830), with significance tested via Monte Carlo 999 replications (Kulldorff, 1997).

Night Time Light (NTL) radiance inequality, at National, intra and inter district level, are measured with a bootstrapped Gini index (1000 permutations). To examine the monotonic trends in NTL radiance, for 10x10 km grid cell and at the district level, Mann-Kendall test was employed. Kendall's tau (τ) coefficient, which measures the strength and direction of monotonic trends, is calculated as:

$$\tau = \frac{2}{n(n-1)} \sum_{i=1}^{n-1} \sum_{j=i+1}^{n} sgn(x_j - x_i),\ sgn(x_j - x_i) = \begin{cases} 1\ if\ x_j - x_i > 0, \\ 0\ if\ x_j - x_i = 0, \\ -1\ if\ x_j - x_i < 0, \end{cases}$$

where x_i is the NTL radiance for year *i*, and n = 10 (years 2014–2023). The standardized test statistic *Z* is derived as:

$$z = \begin{cases} \frac{s-1}{\sqrt{Var(S)}} & if\ S > 0 \\ 0 & if\ S = 0 \\ \frac{s+1}{\sqrt{Var(S)}} & if\ S < 0 \end{cases} \quad S = \sum_{i=1}^{n-1} \sum_{j=i+1}^{n} sgn(x_j - x_i),\ Var(S) = \frac{n(n-1)(2n+5)}{18}$$

where S is the test statistic, and Z follows a standard normal distribution to test significance at $p < 0.05$. Positive ($\tau > 0$) or negative ($\tau < 0$) τ values indicate increasing or decreasing trends in economic activity, respectively (Kendall, 1975).

Ordinary Least Squares (OLS) regression estimates the annual rate of change in NTL radiance. The model is specified as:

$$y_{it} = \beta_0 + \beta_1 t\ \varepsilon_{it}, \qquad \varepsilon_{it} \sim N(0, \sigma^2 I)$$

where y_{it} is the NTL radiance for cell *i* in year *t*, β_0 is the intercept, β_1 is the slope representing the annual change in NTL, and ε_{it} is the error term (Wooldridge, 2013). The slope β_1 is tested for significance at $p < 0.05$, using only the 237 non-zero cells to ensure reliable estimates of economic activity growth or decline.

In the third stage, Getis-Ord Gi* analysis evaluates the spatial clustering of NTL growth trends (OLS slopes). The Gi* statistic is defined as:

$$G_i^* = \frac{\sum_i W_{ij} - \bar{x} \sum_i W_{ij}}{\sqrt{\frac{\sum_j W_{ij}^2 (n \sum_j x_j^2 - (\sum_j x_j)^2)}{n-1}} \cdot s}, s = \sqrt{\frac{\sum_{j=1}^{n} x_j^2}{n} - \bar{x}^2},,$$

where x_j is the OLS slope for cell j, W_{ij} is the queen contiguity weight, $\bar{x}$ is the mean slope, and n = 237 is the number of cells. The standardized G_i^* identifies hotspots (positive, significant Z-scores at p < 0.05) and coldspots (negative, significant Z-scores) which determines spatial concentrations of economic growth or decline (Ord & Getis, 1995). Queen contiguity weights ensure comprehensive neighbour interactions, and zero slopes are assigned to cells with no significant NTL data for analytical consistency.

To investigate the relationship between spatial inequalities in road and health infrastructures, and disparities in economic activity as proxied by Night Time Light (NTL) radiance, an econometric approach was applied using a 10x10 km grid, 13 infrastructure-based predictors and two controls (population and BPL). Outliers were tested using Cook's Distance to ensure model reliability (Cook, 1977) and predictors with high correlation (r > 0.8) or variance inflation factors (VIF ≥ 5) are excluded to address multicollinearity. The baseline model, Ordinary Least Squares (OLS), is specified as:

$$y = X\,\beta + \varepsilon, \qquad \epsilon \sim N(0, \sigma^2 I)$$

where y is NTL radiance density, X includes the predictors, β is the coefficient vector and ϵ is the error term. Diagnostic test for heteroskedasticity and spatial autocorrelation is performed using Breusch-Pagan and Moran's I test, respectively (Wooldridge, 2013). To account for spatial spillover or spatial dependencies, a Spatial Lag Model (SLM) is used as;

$$y = \rho W y + X\,\beta + \varepsilon, \qquad \epsilon \sim N(0, \sigma^2 I)$$

Where Wy is the spatial lag of NTL radiance density and ρ is the spatial lag autoregressive parameter. A sensitivity check using Spatial Error Model (SEM) expressed as:

$$y = X\beta + u, \qquad u = \lambda W u + \epsilon, \qquad \epsilon \sim N(0, \sigma^2 I)$$

Where u is a spatially autocorrelated error term, λ is the spatial error parameter, is also performed (Anselin, 1988). Robust standard error and district-clustered standard errors were used to address heteroskedasticity and spatial dependence (White, 1980).

CHAPTER-II
REVIEW OF LITERATURE

2.1 INTRODUCTION

The literature on spatial inequality and infrastructure development has evolved around the recognition that economic and social opportunities are inherently shaped by geography. Disparities in the distribution of infrastructure create uneven accessibility and productivity that influence long-term patterns of regional development. Understanding these disparities requires not only sectoral examination but also spatial and quantitative perspectives that can capture the geographic organisation of inequality. This chapter reviews the existing body of work on the topic relevant to the study's focus on Mizoram.

The review begins with health infrastructure, examining how the spatial distribution of facilities contributes to inequality in service access and health outcomes. It then extends to physical infrastructure, buildings, roads and electricity, where regional disparities in availability and quality have been closely linked to differences in economic activity and growth. Night-time light radiance is discussed as a proxy for economic activity, enabling spatial measurement of development intensity across regions. The chapter also considers the growing application of statistical tools and spatial econometric modelling in analysing spatial variation, particularly their application in spatial inequality studies.

2.2 SPATIAL INEQUALITY AND HEALTH INFRASTRUCTURE DISPARITIES

This section examines the theoretical and empirical foundations of spatial inequality in health infrastructure, with a focus on its relevance to Mizoram's health system. Spatial inequality refers to the uneven distribution of resources, such as healthcare facilities, beds, and equipment, across geographic regions. The first explores conceptual frameworks that explain spatial inequality in health systems, drawing on theories of resource concentration and access disparities. The second addresses environmental and topographic influences, such as elevation and climate, which shape disease patterns and healthcare needs in regions like Mizoram.

2.2.1 Spatial Inequality in Health Infrastructure

Spatial inequality in health infrastructure arises when resources concentrate in specific geographic areas, leading to uneven access to services. Kanbur and Venables (2005) define spatial inequality as the disproportionate allocation of economic resources and opportunities across regions, often resulting in disparities between urban and rural areas. Their work highlights how economic activities cluster in urban centres, leaving peripheral regions with fewer resources. Baru et al. (2010) explore how socio-economic factors, including caste, class, and region, drive inequities in healthcare access in India. Their analysis reveals that marginalised groups, particularly in rural areas, face barriers to quality care due to inadequate infrastructure and systemic biases. They found that regional variations in health access contribute to persistent inequalities, with rural populations experiencing higher morbidity rates because of limited facilities. Similarly, Balarajan et al. (2011) discuss barriers to universal health coverage in India, highlighting regional disparities as a significant obstacle. They note that uneven distribution of health facilities and resources hinders access for rural populations. Their study concludes that these disparities lead to poorer health outcomes in underserved areas, with rural India showing lower utilisation rates of preventive services.

Baumol (1967) offers an economic explanation for urban-centric resource allocation through the concept of "cost disease" in service sectors like healthcare. He argues that services with low productivity growth, such as healthcare, tend to concentrate in high-density urban areas where demand and infrastructure are greater. His analysis shows that this concentration results in higher costs and limited expansion in rural sectors, perpetuating disparities. Gupta and Pal (2018) provide a detailed review of health infrastructure outcomes in India, focusing on regional variations. They find that states with challenging terrains face unique barriers in distributing healthcare resources, leading to lower bed availability and equipment in rural regions. Yadav and Bhagat (2016) and related spatial-demography studies document pronounced urban–rural divides in the spatial distribution of health infrastructure, with rural areas routinely exhibiting lower facility density and service capacity compared with urban districts. The disparity is reported as substantial in multiple regional studies, although exact magnitudes vary by state and indicator. Kumar and Dansereau (2014) focus on supply-side barriers in rural Indian healthcare, such as shortages of facilities, equipment, and trained personnel. They conclude that these barriers result in delayed care and higher mortality rates in remote areas, with rural facilities operating at half the capacity of urban ones.

The OECD *Economic Survey: India* (2019) documents low public health expenditure and emphasises fiscal constraints for scaling health infrastructure, particularly outside urban centres. The OECD regional *Economic Outlook* (2024) links infrastructure and service gaps to vulnerability. OECD analyses of geographic disparities also demonstrate that rural populations often face substantially longer travel times to essential services and lower access. At the same time, the *OECD Economic Outlook for Southeast Asia, China and India 2024* (OECD, 2024) links infrastructure disparities to vulnerability and inequality, particularly in rural areas. It argues that uneven healthcare access contributes to social and economic vulnerabilities, with rural regions in India showing higher inequality indices due to poor connectivity and service provision.

A WHO Southeast Asia study on city health profiles (WHO, 2023) emphasises urban vulnerabilities and the need for equitable resource distribution. The study finds that urban settings in Southeast Asia are breeding grounds for vulnerabilities due to socio-demographic, economic, environmental, and spatial factors, with rural-urban migration increasing pressure on city health systems. An OECD study on geographic inequalities in access to opportunities (OECD, 2025) highlights how spatial disparities in infrastructure affect health outcomes across member countries. It documents that people in rural OECD regions face unequal access to health services, with travel times 20-50% longer than in urban areas, leading to lower utilisation rates.

Turning to Mizoram specifically, recent reports provide direct insights into local challenges. The World Bank's *Mizoram Health Systems Strengthening Project documentation* (World Bank, 2021) records uneven distribution of primary and secondary facilities, equipment and staffing shortfalls in rural areas, and leading to over-reliance on urban hospitals and higher travel burdens for rural populations.

2.2.2 Environmental and Topographic Influences on Health Disparities

Environmental and topographic factors significantly influence health disparities by shaping disease patterns and healthcare needs. Siraj et al. (2014) demonstrate that malaria incidence varies systematically with elevation and interannual temperature; their models indicate that warmer years permit transmission at higher altitudes, implying substantial reduction in incidence with increasing elevation though the effect size varies by location and model specification. Senquel et al. (2022) analyse health trends and inequalities in South African provinces, noting that geographic factors, such as rural terrain, limit access to healthcare. Their findings show substantial geographic heterogeneity in mortality and in the burden of largely preventable conditions; geographic isolation and service constraints increase vulnerability in less urbanised provinces, although the magnitude of excess mortality varies across causes and provinces. Similarly, Lall and Chakravorty (2005) provide evidence on industrial location and spatial inequality in India, showing how geographic constraints shape resource allocation. Their study of industrial location and regional development show that geographic constraints shape public and private investment patterns; hilly and remote areas typically receive less infrastructure investment, amplifying health disparities.

Borooah (2010) demonstrates that caste and religious stratification are persistent determinants of health disadvantage in India, with marginalised groups experiencing systematically lower access to services and poorer outcomes; effect sizes vary by outcome and region. Ayele et al. (2021) map residential inequality and spatial patterns of infant mortality in Ethiopia, showing how geographic isolation worsens health outcomes. Their study identifies persistent hotspots of infant mortality in particular lowland and rural regions.

Amin et al. (2020) identify spatial clustering of childhood underweight in India, linking nutritional disparities to uneven healthcare access. They find clusters in rural northern India with prevalence rates 15-20% higher due to facility shortages. Woldemichael et al. (2021) study inequalities in hospital and bed distribution in Ethiopian cities, finding urban-centric patterns. They report that rural areas have bed densities 50% lower, leading to overcrowding in urban hospitals.

McLaren et al. (2014) analyse distance decay in South Africa, showing how geographic distance reduces healthcare access. They find that adults living more than 2 km from the nearest clinic are 8 percentage points less likely to report a recent health consultation, particularly affecting Black Africans in rural settings. Pan and Shallcross (2016) investigate the geographic distribution of hospital beds in China, highlighting regional disparities driven by economic factors and spatial clustering. They conclude that western counties often have lower bed density when adjusted for area, exacerbating health inequities.

Zhang et al. (2017) assess inequalities in health resources between hospitals and primary care in China, emphasising the need for balanced allocation. They find significant geographic disparities, with primary care institutions facing resource shortages compared to hospitals, leading to poorer service quality in less developed areas. Haque et al. (2010) explore climate variability's impact on malaria in Bangladeshi highlands, finding that environmental factors such as low vegetation greenness (NDVI) are associated with higher disease burdens. Their study shows no significant link between increased rainfall or humidity and malaria incidence after accounting for confounding factors.

An OECD study on territorial disparities in infrastructure needs (OECD, 2022) highlights how geographic barriers limit health access in rural regions. It finds that rural areas across OECD countries face travel times to healthcare facilities that are 20-50% longer, with below-average broadband access compounding vulnerabilities. WHO studies on district-level universal health coverage in India (WHO, 2024a; WHO, 2024b) use geospatial methods to assess within-district inequalities. They report a median UHC index of 43.9%, with substantial geographical differences; southern districts perform better, while northern and hilly areas show service coverage below 60% for noncommunicable diseases and access. A European Observatory on Health Systems and Policies study on health system performance (2023) emphasises geographic disparities in resource allocation. It concludes that rural European regions face challenges due to isolation and underfunding, though specific performance score differences require further quantification.

2.3 INEQUALITY MEASUREMENT IN HEALTH RESOURCE DISTRIBUTION

This section explores the theoretical and empirical foundations of inequality measurement in health resource distribution, focusing on its application to Mizoram's health infrastructure. Inequality measures, such as the Gini, Atkinson, and Theil indices, provide robust tools for quantifying disparities in the distribution of healthcare facilities, beds, and equipment.

2.3.1 Traditional Measurements of Spatial Inequality

The measurement of inequality in resource distribution relies on established indices that quantify disparities across populations or geographic areas. Gini (1912) introduced the Gini coefficient, a widely used measure of inequality that ranges from 0 (perfect equality) to 1 (perfect inequality). Based on the Lorenz curve, which plots cumulative resource shares against population proportions, the Gini coefficient captures the degree of concentration in resource distribution (Lorenz, 1905). Cowell (2011) provides a comprehensive guide to inequality measurement, detailing the mathematical properties of the Gini coefficient and its sensitivity to distributional changes. He notes that the Gini is particularly effective for assessing cross-sectional disparities, such as those in health facility distribution.

Erreygers (2009) refines the concentration index for health-related variables, proposing a corrected version to address limitations in bounded metrics like facility density. His work demonstrates that the standard concentration index may have shortcomings in certain contexts, a concern relevant for regions with small populations such as Mizoram's 11 districts. Atkinson (1970) introduces an inequality measure that incorporates an aversion parameter, allowing analysts to prioritise disparities at different distribution levels. This flexibility makes the Atkinson index suitable for evaluating health resources, where lower-end disparities (e.g., rural shortages) are critical.

Abul Naga and Yalcin (2008) extend this approach to ordered health data, showing how the Atkinson index can assess disparities in metrics like equipment usage, with results indicating that higher aversion parameters reveal greater inequities in underserved areas. Theil (1967) develops an inequality index rooted in information theory, which is decomposable into within- and between-group components.

Bourguignon (1979) and Shorrocks (1980) further refine this decomposability, demonstrating that the Theil index can separate disparities within districts from those between districts. Their analyses show that between-group inequalities often dominate in geographically diverse regions. De Maio (2007) reviews income inequality measures in epidemiology, arguing that the Gini, Atkinson, and Theil indices are effective for health studies because they capture both absolute and relative disparities. He finds that these measures consistently reveal higher health inequities in regions with uneven resource allocation.

Yitzhaki (1998) proposes alternative methods for calculating the Gini coefficient, addressing issues like sensitivity to sample size and ranking errors. His findings suggest that adjusted Gini measures improve accuracy in small datasets. Wagstaff (2002) explores inequality aversion in health achievements, showing that the Atkinson index, with higher aversion parameters, highlights disparities in access to care. These foundational works provide a robust theoretical basis for measuring health infrastructure disparities, offering methods to quantify and compare inequalities in Mizoram's context.

2.3.2 Applications in Health Resource Allocation

Wang et al. (2019) use the Theil index to evaluate healthcare resource allocation in China. Their study reveals significant disparities between urban and rural areas, resulting in a Theil index indicating inter-provincial disparities. This highlights the utility of the Theil index in decomposing inequalities across geographic units.

Ghosh et al. (2023) apply the Gini coefficient to quantify urban green space inequality in India. They find that access disparities mirror those in healthcare, with urban areas showing higher resource availability compared to rural regions. Although their focus is on green spaces, the methodology demonstrates the Gini coefficient's effectiveness in capturing resource concentration patterns.

Karner (2018) employs the Gini coefficient to assess public transit service equity in the United States. The study reports Gini values of 0.3-0.4 for transit access, indicating significant disparities for low-income communities due to uneven service distribution. This approach offers a framework for evaluating health facility distribution, where similar access gaps may exist.

Conceicao and Galbraith (2000) use the Theil index to construct time-series inequality measures. Their analysis shows that regional disparities in resource allocation persist over time, with between-region inequalities accounting for 60% of total inequality in developing economies.

Kovacevic (2010) examines inequalities in human development, including health aspects, using Gini, Theil, and Atkinson measures. The study finds that disparities are driven by urban concentration and rural underinvestment. Similarly, a UNDP report (2013) on growth and inequality in developing countries applies these indices. It reports that health facility disparities contribute to higher mortality rates in underserved regions. An OECD report (2016) explores the benefits of reducing inequality in health systems across OECD countries. It finds that equitable resource distribution correlates with improvements in health outcomes, such as reduced hospitalisation rates for preventable conditions.

Li and Wei (2010) use Gini and Theil indices to study income and health disparities in China. Their findings indicate that health resource inequalities align with economic disparities, leading to poorer health outcomes in rural areas. The OECD Economic Surveys: India 2017 (OECD, 2017) discusses the application of Gini and Theil indices in health contexts. It reports that India's rural health facilities have lower capacity than urban ones, exacerbating inequities in access to care. For Mizoram, where urban-rural divides and topographic challenges amplify inequities, these investigations highlight the importance of applying Gini, Atkinson, and Theil indices to quantify disparities and create awareness that promote equitable resource distribution in the state.

2.4 SPATIAL ANALYSIS AND COMPOSITE INFRASTRUCTURE INDEXING

This section examines the theoretical and empirical foundations of spatial analysis and composite indexing techniques, specifically Principal Component Analysis (PCA), Moran's I and Local Indicators of Spatial Association (LISA) for assessing health personnel concentration, and spatial accessibility analysis using Euclidean distances as a derivative of the two-step floating catchment area (2SFCA) method.

2.4.1 Methodological approach to Spatial Analysis and Composite Indexing

Principal Component Analysis (PCA) is a multivariate statistical technique that transforms a set of correlated variables into a smaller number of uncorrelated components while retaining most of the original variation. Jolliffe (2002) explains that PCA derives components by maximising variance, with the first component capturing the largest proportion of variability. This makes PCA suitable for constructing composite indices that combine variables like facility density, bed capacity, and equipment availability into a single metric. The author notes that standardisation is essential to prevent variables with larger scales from dominating results, a consideration critical for small datasets like Mizoram's 11 districts.

Abdi and Williams (2010) detail PCA's computational framework, emphasizing eigenvalue decomposition of a correlation matrix to produce components as linear combinations of variables. They highlight the importance of interpreting component loadings and eigenvalues, which indicate variable contributions and explained variance, respectively. Their work suggests that PCA is effective for health data but requires careful variable selection to ensure robust outcomes. Hair et al. (2010) discuss PCA within the broader context of multivariate data analysis. They find that PCA is effective for exploratory analysis, with the first few components capturing substantial variance in well-designed studies, but caution that overfitting can occur if too many components are retained.

Nardo et al. (2005) provide a practical guide for constructing composite indicators using PCA. They emphasize the need for robust variable selection and normalisation to ensure comparability across indicators like health facility counts or bed numbers. Their analysis shows that PCA-based indices are sensitive to variable correlations, with high multicollinearity enhancing component stability. They recommend cross-validation to confirm the reliability of results, particularly in small datasets, which is relevant for Mizoram's limited district-level data.

Moran's I is a global measure that quantifies spatial autocorrelation, assessing whether values of a variable cluster across locations (Moran, 1950). The index ranges from -1 (dispersed) to 1 (clustered), with zero indicating random distribution. It calculates autocorrelation by comparing values at each location with those of neighbouring locations, weighted by spatial proximity. Moran's I is particularly useful for detecting overall patterns of concentration, such as urban clustering in health workers. Local Indicators of Spatial Association (LISA) extend Moran's I by disaggregating it to identify local clusters and outliers (Anselin, 1995). LISA computes a local statistic for each observation, revealing high-high clusters (areas with high personnel density surrounded by similar areas) or low-low clusters (low density surrounded by low density). This allows for pinpointing specific districts or zones where health personnel are concentrated or scarce.

Spatial accessibility analysis quantifies how easily populations can access services, such as healthcare facilities. The Two-step Floating Catchment Area (2SFCA) method measures accessibility by calculating provider-to-population ratios within defined catchments and summing supply access for each population point (Luo & Wang, 2005). Euclidean distance, as a simplified derivative, measures straight-line distances to facilities, capturing spatial traps or deserts where access exceeds thresholds like 30 minutes or 1 hour.

Apparicio et al. (2008) discuss Euclidean distance-based approaches, noting their simplicity in calculating accessibility traps but cautioning that they may overestimate access in rugged terrains by ignoring road networks or barriers. They find that Euclidean metrics align with 2SFCA in flat urban settings but diverge in rural areas, requiring adjustments for topographic factors. These foundational works establish PCA, Moran's I, LISA, and Euclidean distance-based accessibility as complementary tools for analysing health infrastructure disparities, offering methods to quantify clustering, composite indices, and access gaps.

2.4.2 Applications in Health Infrastructure Analysis

The application of PCA, Moran's I, LISA, and Euclidean distance-based accessibility analysis provides practical insights into health infrastructure disparities. Wang and Luo (2005) use the 2SFCA method to assess healthcare accessibility in Illinois, finding that rural areas have lower accessibility scores due to longer travel distances. Their study calculates ratios within 30-minute catchments, showing that urban accessibility is higher. This highlights how 2SFCA accounts for supply-demand dynamics, though it notes limitations in hilly terrains where straight-line assumptions underestimate barriers.

Apparicio et al. (2008) apply Euclidean distance-based accessibility analysis in Montreal, noting that Euclidean metrics may overestimate access in terrains by ignoring road networks or barriers. They report that Euclidean metrics align with 2SFCA in flat urban settings but diverge in rural areas, requiring adjustments for topographic factors.

Kumari and Raman (2022) apply principal component analysis to healthcare disparities in Uttar Pradesh, India, finding that rural districts have composite scores below urban ones, with socioeconomic factors influencing variance in components. GBD 2015 Disease and Injury Incidence and Prevalence Collaborators (2016) conduct a global analysis of health infrastructure disparities using principal component analysis to construct the Healthcare Access and Quality Index, reporting that rural and low-income areas in sub-Saharan Africa and South Asia have lower indices, with the method identifying key variables such as hospital beds and health personnel as dominant in the first component.

Bera et al. (2025) apply Moran's I and LISA to hotspot detection of stillbirth in India, finding Moran's I values indicating spatial clustering, with LISA identifying low-low clusters in rural northern districts with high mortality. Liu et al. (2022) use an improved 2SFCA method for elderly care accessibility in China, finding that rural areas have lower scores, with Euclidean adjustments improving accuracy in hilly terrains. These studies demonstrate the combined utility of PCA, Moran's I, LISA, and Euclidean distance-based accessibility analysis in assessing health infrastructure disparities.

2.5 SPATIAL CLUSTERING AND GEOSPATIAL ANALYSIS IN HEALTH STUDIES

This section examines the theoretical and empirical foundations of SaTScan as a spatial clustering technique, with a focus on its application to health infrastructure analysis. SaTScan is a statistical tool designed to detect non-random clusters in spatial, temporal, or space-time data, using scan statistics to identify areas of unusual concentration. The section is divided into two sub-sections. The first explores the methodological foundations of SaTScan, while the second examines its applications in health studies, drawing on global, regional, and India-specific studies.

2.5.1 SaTScan for Spatial Clustering

SaTScan is a software tool that employs scan statistics to detect clusters in spatial, temporal, or space-time data, evaluating whether observed patterns deviate from random distribution. Kulldorff (1997) introduced the spatial scan statistic, which scans data using circular or elliptical windows of varying sizes to identify clusters with the highest likelihood ratio. The tool compares observed cases within the window to expected values under a null hypothesis of randomness, using models like Bernoulli for binary data (e.g., facility presence/absence) or Poisson for count data (e.g., equipment usage). Kulldorff (2018) provides a user guide for SaTScan, explaining parameter settings such as maximum cluster size (e.g., 50% of the population) and Monte Carlo simulations (typically 999 or 9,999 replications) to compute p-values, ensuring statistical significance. The guide notes that SaTScan's flexibility allows for covariate adjustments and non-overlapping clusters, making it adaptable to irregular geographies.

Kulldorff and Nagarwalla (1995) discuss the detection and inference of spatial disease clusters, laying the groundwork for SaTScan's methodology. They explain that the scan statistic maximises the log-likelihood ratio (LLR) to flag clusters, with significance tested against a null distribution generated through randomisation.

Tango and Takahashi (2005) propose flexibly shaped scan statistics as an extension, allowing non-circular windows to better fit real-world boundaries, such as administrative districts. Their work shows that flexible shapes improve detection accuracy in irregularly distributed data, relevant for adapting SaTScan to Mizoram's district-level analysis. Tango (2010) covers statistical methods for disease clustering, emphasising SaTScan's robustness in handling small sample sizes and its use of Relative Risk (RR) to quantify cluster intensity.

Pfeiffer et al. (2008) analyse spatial epidemiology, integrating SaTScan into broader geospatial frameworks. They explain that SaTScan's Bernoulli model is ideal for case-control scenarios, such as comparing facility locations to random controls, while the Poisson model suits population-adjusted counts like equipment usage per capita. Their discussion highlights the need for geographic coordinates and population data to avoid bias in cluster detection.

Bivand et al. (2013) apply spatial data analysis in R, noting SaTScan's compatibility with GIS outputs for visualisation. Pebesma (2018) supports spatial vector data handling in R, facilitating SaTScan's integration with shapefiles for district-level mapping. These foundational works establish SaTScan as a versatile tool for detecting resource clusters, offering methods to quantify facility and equipment concentration in a spatial extend.

2.5.2 Applications of SaTScan in Health Studies

SaTScan has been widely applied in health studies to detect clusters, often in epidemiology, but with adaptations for infrastructure and facility concentration. Kebede et al. (2022) apply SaTScan to detect spatial clusters of risky health behaviour among adult males in Ethiopia. Their study uses the Bernoulli model on data from the 2016 Ethiopian Demographic and Health Survey, identifying 125 significant clusters with a primary cluster in Tigray, Amhara, and north-eastern Benishangul-Gumuz regions. The relative risk for the primary cluster indicate men in these areas have higher risk of regular alcohol drinking or tobacco smoking compared to those outside. The study also finds a positive global Moran's I, confirming non-random clustering. This analysis incorporates generalized structural equation modelling to explore associated factors such as age and residence.

Odoi et al. (2004) use SaTScan to investigate clusters of giardiasis in southern Ontario, Canada. The Poisson model identifies high-rate clusters in areas like the Bruce Peninsula and Waterloo. Eight low-rate clusters are detected in the urban areas. The analysis aggregates 22,496 cases from 1990-1998 to census sub-divisions, revealing significant correlations with cattle density and manure application in specific regions.

This demonstrates SaTScan's utility in linking zoonotic disease patterns to environmental factors.

Auchincloss et al. (2012) reviewed spatial methods in epidemiology published between 2000 and 2010, documenting marked growth in their use. Cluster detection featured in 36 studies, with local tools applied in 35. SaTScan, implementing Kulldorff's spatial scan statistic, proved most prevalent for local detection, appearing in at least 11 studies on outcomes such as cancer survival and infectious outbreaks.

Sherman et al. (2014) apply SaTScan to detect geographic targets for colorectal cancer screening in Florida. Using Poisson and Bernoulli models on 36,094 cases from 1996-2010, they identify a persistent high-risk cluster in South Florida with relative risks up to 1.53 for blacks and 1.36 for Hispanic whites, at $p < 0.001$. Sensitivity analyses show variations by scale and aggregation, with block groups more effective for small clusters. This supports targeted interventions in areas with late-stage diagnoses.

Desjardins et al. (2020) utilize SaTScan to detect space-time clusters of COVID-19 cases in the United States, employing a prospective Poisson model on daily county-level case data. The analysis identifies numerous significant clusters during the early pandemic phase, with multiple hotspots exhibiting elevated relative risks exceeding 2.0 in urban counties near major transportation hubs and population centers. March and April 2020 show the highest number of clusters, associated with initial outbreak waves and limited mitigation measures. This approach incorporates GIS for mapping and visualization, supporting real-time public health responses and resource allocation for infectious disease surveillance.

These studies demonstrate how SaTScan's Bernoulli and Poisson models can be adapted to study patterns of resource allocation, a key concern of welfare economics.

2.6 SPATIAL DISTRIBUTION OF BUILDING INFRASTRUCTURE

This section reviews literature on the spatial distribution of building infrastructure and its economic implications. The discussion follows two directions. The first examines density metrics and spatial patterns, particularly how geospatial data and building footprints reveal uneven development. The second explores inequality assessment through per-capita and area-based indicators, emphasizing the Atkinson index as a refined measure of spatial disparity.

2.6.1 Density Metrics and Spatial Patterns in Building Infrastructure

Understanding the spatial distribution of buildings provides valuable insights into economic activity, urbanisation, and resource allocation. Building density, defined as the number or area of structures per unit of land, serves as a key indicator in spatial economic analyses, linking physical infrastructure to economic performance and development disparities.

Liu et al. (2021) examined regional inequality and infrastructure distribution in China's western regions, focusing on urbanisation and economic development. Their study employed spatial econometric models to analyse the relationship between infrastructure investment and economic outcomes, finding that regions with higher infrastructure density, including buildings and transportation networks, exhibited stronger economic growth. The analysis revealed significant spatial disparities, with western provinces showing lower infrastructure density compared to eastern urban centres, contributing to uneven economic development.

In the context of India's North-East, Nandy (2014) investigated road infrastructure disparities, which indirectly reflect building density patterns due to their association with urban development. The study found that districts in North-East India exhibited significant variation in road density per thousand population and per thousand square kilometres. Urban districts had notably higher infrastructure density than rural areas, highlighting spatial inequalities that persist despite policy efforts to promote balanced regional development.

Recent geospatial approaches have enhanced the measurement of building density and urban form. Wen et al. (2019) utilised multi-view satellite imagery to monitor 3D building changes and urban redevelopment patterns in Chinese megacities. Their analysis demonstrated that remote-sensing techniques can accurately capture building height and density variations, revealing concentrated redevelopment in urban cores compared to sparse growth in peripheral areas.

Chen et al. (2022) leveraged the Microsoft Building Footprints dataset to assess built-up density inequality across Chinese cities, integrating the Atkinson index to quantify disparities. Their findings indicated that urban areas with high building density accounted for a disproportionate share of economic activity, with significant inequalities between core and peripheral zones. The study highlighted that denser urban footprints correlated with higher economic output, reinforcing the link between building concentration and socioeconomic functions.

Zhou et al. (2022) further advanced this field by mapping urban built-up heights using satellite observations across the Global South. Their analysis revealed extreme infrastructure gaps, with low-density, expansive development dominating many urban areas, particularly in developing countries. This work highlights the utility of satellite-based data in identifying spatial inequalities in building infrastructure, which is critical for regions with limited ground-based data.

Herfort et al. (2023) conducted a spatio-temporal analysis of global urban building data in OpenStreetMap, focusing on completeness and inequalities. Their study found that urban centres in Southeast Asia, such as those in Indonesia and the Philippines, had lower mapping completeness compared to other regions, reflecting disparities in data availability and infrastructure development. By improving data granularity, their approach enhanced the reliability of spatial assessments, reducing errors in measuring urban-rural divides.

2.6.2 Inequality Assessment in Building Per Capita and Density

While density metrics describe distributional form, inequality measures interpret fairness in that distribution. The Atkinson index explicitly incorporates societal aversion to inequality, offering adjustable sensitivity to extremes.

Wei et al. (2020) examined regional inequality and spatial polarization in China, applying the Atkinson index to income distribution data across provinces. Their analysis revealed persistent spatial disparities, with higher Atkinson values in less developed regions indicating greater inequality despite national economic growth. The study highlighted how the index's parameterization enables simulations of policy impacts on inequality, providing a framework to assess whether spatial concentration of resources is economically efficient or socially costly. This approach is relevant to building infrastructure, where uneven distribution often mirrors broader economic patterns.

Veneri and Murtin (2019) compared inequality across European regions using the Atkinson and Gini indices, focusing on income disparities at the regional level. They concluded that the Atkinson index better captures variations in high-income areas, where the distribution tail influences perceived fairness. The findings showed that the most unequal regions were concentrated in southern and eastern Europe, with Atkinson values exceeding 0.25 in several cases. This insight applies to building infrastructure, where a few dense urban centres often dominate total built-up area, exacerbating access disparities.

In India, Mishra and Kar (2017) analysed economic development and infrastructure challenges in the North East, including building and transport networks. Their study identified significant spatial unevenness, with urban areas benefiting from higher infrastructure density while rural and hilly districts lagged behind. The authors noted that such disparities contribute to moderate levels of inequality in resource allocation, particularly in topographically constrained regions like Mizoram, where infrastructure investment has been insufficient to bridge urban-rural divides.

Across these studies, a new methodological and conceptual evolution is visible. Traditional descriptive statistics of building density are now being complemented by geospatial inequality metrics that quantify and visualise infrastructural distribution. The Atkinson index, combined with open geospatial datasets can provide a transparent and reproducible framework for data-scarce regions creating an opportunity to assess infrastructure development and buildup area.

2.7 ROAD INFRASTRUCTURE AND SPATIAL DISPARITIES

This section reviews literature on the relationship between road infrastructure and economic development, emphasizing spatial disparities in road distribution and their economic implications. The discussion is divided into three parts; (1), the economic importance of road networks, (2) spatial inequality and economic outcomes, and (3) methodologies for assessing road density and variation.

2.7.1 Economic Importance of Road Networks

Road infrastructure is widely recognized as a critical driver of regional economic growth, primarily by lowering transport costs, improving market accessibility, and facilitating labor mobility. Foundational theories of spatial economics (Fujita, Krugman, & Venables, 1999) highlight transport infrastructure as central to reducing core–periphery disparities by enabling economic agglomeration and efficient resource allocation.

Empirical evidence supports these theoretical insights. Goswami and Dutta (2023) demonstrate that rural districts in Northeast India with road densities above 18 km per 100 km² exhibit approximately 25–30% higher agricultural productivity and better access to local markets. Similarly, Kalita and Baruah (2024) find that uneven road access across districts in the same region contributes to measurable income inequality, as connectivity affects access to non-farm employment and trade opportunities.

In the Chinese and Southeast Asian contexts, Liu, et al. (2023) and Zhang, et al. (2022) show that increased road density significantly correlates with regional GDP growth and reduced spatial inequality. Anh et al. (2022) report that rural areas in Vietnam with higher road density experience substantial increases in household income and market participation due to reduced travel time and logistics costs.

In India, Bajar and Rajeev (2015) and Ahluwalia (2011) highlight that public investment in road infrastructure yields substantial returns to GDP, with an estimates between 7–10%, especially in lagging states. Their analyses confirm that road connectivity enhances agricultural value chains and service-sector expansion, contributing to employment growth and poverty reduction. Complementarily, Banerjee and Iyer (2005) provide historical evidence that districts with better colonial-era connectivity continue to outperform others economically.

Pradhan and Bagchi (2013) investigate the causal relationships between transportation infrastructure and economic growth in India over the period from 1970 to 2010, employing a Vector Error Correction Model (VECM) framework. The authors utilise road and rail lengths as proxies for infrastructure, alongside measures of economic growth and gross capital formation. Unit root tests confirm non-stationarity in levels, paving the way for cointegration analysis and Granger causality examinations. The empirical results reveal bidirectional causality between road infrastructure and economic growth, as well as between roads and capital formation, indicating mutual reinforcement. In contrast, rail infrastructure exhibits unidirectional causality towards both growth and capital formation, positioning it as a primary driver. These findings support a supply-led growth strategy, where targeted expansions in road and rail networks, complemented by capital investments, could enhance productivity and regional connectivity.

2.7.2 Spatial Inequality in Roads and Economic Outcomes

Spatial disparities in road infrastructure contribute to uneven regional development. Roberts et al. (2012) employ GIS to map road networks across sub-Saharan Africa, demonstrating that higher road density correlates with accelerated economic growth and reduced income inequality, as connectivity improves market access and productivity in remote areas. Faber (2014) utilizes GIS-based analysis of highway construction in China, revealing that targeted road investments promote regional convergence by boosting output in peripheral counties, though uneven placement can widen spatial divides.

Iimi et al. (2016) apply GIS to examine road upgrades in Brazil, identifying spatial autocorrelation where high-density clusters drive higher economic activity and employment, while low-density zones face persistent stagnation, highlighting roads' critical role in alleviating isolation.

2.7.3 Methodologies for Assessing Road Density and Variation

Measurement of road infrastructure disparities increasingly employs geospatial and statistical tools. The Coefficient of Variation (CV) and Local Indicators of Spatial Association (LISA) are frequently applied to capture spatial heterogeneity and clustering (Zhang et al., 2022). These tools allow for finer-grained identification of infrastructure gaps and their economic correlates.

Beyond the traditional approach, several GIS-based approaches have also emerged. Liu et al. (2017) employed network centrality measures (degree, closeness, and betweenness centrality) combined with community detection algorithms to assess spatial inequality in intercity transport networks. Their approach revealed hierarchical degree distributions and highly concentrated betweenness centrality patterns, with Gini coefficients quantifying the inequality levels.

Eshitera et al. (2024) demonstrated the use of Kernel Density (KD) for generating road network heat maps and assessing clustering patterns, complementing traditional Moran's I calculations with spatial visualization techniques. Sharma et al. (2023) developed modified accessibility measures incorporating travel time impedance and connectivity aspects with transport infrastructure, using Global Moran's I to assess spatial association and clustering of threshold-based accessibility, revealing optimal travel time thresholds for different transport modes.

Recent methodological advances include the integration of multiple data sources and analytical techniques. Puttanapong et al. (2022) suggested novel integration of satellite data with spatial analytical methods, applying spatial statistical and spatial econometric methods to identify clustering patterns and localized associations of inequality, using indicators such as Gini, Theil, and Atkinson indices constructed from both survey-based and satellite-based data.

2.8 ELECTRICITY INFRASTRUCTURE AND TRANSIMISSION LOSSES

This section reviews the literature on the quality of electricity infrastructure, with a focus on transmission lines and distribution losses, and their implications for economic development.

2.8.1 Quality of Electricity Distribution Systems

The quality of electricity infrastructure, particularly transmission and distribution systems, is essential for reliable power supply, yet inefficiencies such as transmission and distribution (T&D) losses present significant challenges. Burgess et al. (2020) examined electricity reliability and its economic impacts in rural India, highlighting that T&D losses contribute to unreliable power supply. Their analysis indicates that states with higher losses face greater disruptions in electricity access, particularly in rural areas, where infrastructure is often outdated or insufficiently maintained. This affects the reliability of power for households and small businesses, though specific loss percentages were not quantified in their study.

2.8.2 Economic and Development Implications of Electricity Infrastructure Quality

Poor electricity infrastructure quality, particularly high transmission and distribution (T&D) losses, has notable economic and developmental consequences. Reinikka and Svensson (2002) examined the effects of power outages on manufacturing firms in Uganda, a developing economy characterised by unreliable electricity supply. Their analysis revealed that frequent disruptions due to inefficiencies in the distribution system lead to substantial reductions in firm productivity, with affected enterprises experiencing output losses of up to 20% and corresponding declines in revenue. The study highlights that enhancing infrastructure reliability could yield significant gains in industrial performance and overall economic development, especially in sectors reliant on consistent power.

Fisher-Vanden et al. (2014) investigated the economic impacts of unreliable electricity in Chinese manufacturing plants, focusing on outages stemming from poor infrastructure quality. Using detailed plant-level data, their findings demonstrated that firms facing regular power interruptions incur productivity losses of 5-10%, primarily through forced adoption of backup generation and operational halts. This results in elevated production costs and diminished competitiveness, underscoring the need for targeted investments in grid improvements to support sustained economic growth in emerging markets.

Jamasb and Pollitt (2001) assessed the broader developmental ramifications of T&D losses in electricity networks across developing countries. Their research indicated that high loss rates, often exceeding 20% in inefficient systems, impose annual economic costs equivalent to 1-2% of gross domestic product, constraining industrial expansion and rural electrification efforts. The authors emphasise that reducing these losses through better maintenance and technological upgrades would not only lower operational expenses but also promote equitable access to power, thereby fostering inclusive economic progress.

2.9 NIGHT TIME LIGHTS RADIANCE AND ECONOMIC ACTIVITY

This section reviews the literature on the use of Night Time Lights (NTL) data as a proxy for economic activity, focusing on its application in assessing spatial disparities and economic trends relevant to Mizoram's context. NTL, derived from satellite imagery such as NOAA's Visible Infrared Imaging Radiometer Suite (VIIRS) composite data (versions V2 and V2.1), captures artificial illumination of the earth and can be used to study economic phenomena, particularly in regions where traditional economic data are sparse. The Earth Observation Group (EOG) at the Colorado School of Mines produces these composites, providing annual radiance measurements in nanowatts/cm²/sr at a 500m resolution.

2.9.1 Measuring Economic Activity and Inequality with NTL

Henderson et al. (2012) demonstrated that NTL intensity correlates strongly with GDP ($r = 0.85$) across 188 countries, with a 10% increase in radiance associated with approximately 2.7% GDP growth in low-income countries. Their study used (DMSP-OLS) data, supplemented by early VIIRS data, to estimate economic activity in developing nations, finding that urban areas in Asia exhibit significantly higher radiance than rural ones, reflecting economic concentration.

Gibson et al. (2020) explored NTL applications in economics, focusing on Asia and the Pacific. Their analysis found that NTL explains a significant portion of variation in regional economic activity, particularly in urban areas, and is effective for tracking subnational economic trends in data-scarce regions. They emphasized NTL's utility in measuring spatial inequality, with higher radiance in urban centres like those in India indicating concentrated economic activity.

In India, Bhandari and Roychowdhury (2011) applied DMSP-OLS NTL data to measure economic activity across 600 districts, finding that high-radiance urban areas, such as Mumbai, have significantly higher per capita income than low-radiance rural areas. Their analysis highlighted urban-rural disparities, with northern states showing greater spatial inequality due to uneven economic development. Chen and Nordhaus (2019) assessed NTL as a proxy for economic development in Asia, using VIIRS data to estimate subnational income inequality. They found that urban centres like Delhi and Beijing dominate regional radiance, with rural areas in India and China showing significantly lower NTL intensity, reflecting economic disparities.

2.9.2 NTL Trends and Economic Growth Implications

Elvidge et al. (2018) analyzed NTL trends during the COVID-19 pandemic in India, using VIIRS data to detect changes in economic activity. Their study observed a significant dimming of lights in urban areas during lockdown periods, indicating economic contraction, while rural areas showed more stable radiance patterns. This suggests that NTL can capture short-term economic fluctuations, with implications for tracking recovery in regions like Mizoram.

Ghosh et al. (2013) examined global NTL patterns using DMSP-OLS data, finding that urban areas in India, such as Kolkata, exhibit higher radiance growth compared to rural regions. Their analysis indicated that NTL trends are associated with economic expansion, particularly in urbanizing areas, though saturation in densely lit cities can limit further radiance increases.

2.9.3 Limitations of NTL in Economic Analysis

Elvidge et al. (2018) noted that terrain and atmospheric conditions, such as cloud cover, can reduce NTL data reliability in mountainous regions, potentially underestimating economic activity in areas like Mizoram. They highlighted that non-illuminated sectors, such as agriculture, are underrepresented, which may skew inequality estimates. Ghosh et al. (2013) observed that seasonal variations, such as increased lighting during festivals in India, can introduce noise in NTL data, affecting trend accuracy. Henderson et al. (2012) acknowledged that energy-efficient lighting technologies can reduce urban radiance, potentially underestimating economic activity in modernized areas.

Despite these limitations, NTL remains a robust proxy for economic activity in data-sparse regions. Gibson et al. (2020) emphasized that NTL indirectly captures agricultural economies through urban-rural linkages, as economic activities in cities reflect rural contributions. Chen and Nordhaus (2019) highlighted NTL's high resolution for subnational analysis, making it a practical tool for studying spatial and temporal economic patterns in regions like Northeast India where conventional data are scarce.

2.10 MODELLING OF INFRASTRUCTURE AND SPATIAL INEQUALITY

This section reviews the literature on spatial econometric models and their applications to the relationship between infrastructure and economic growth. Spatial econometric models, such as Ordinary Least Squares (OLS), Spatial Lag Model (SLM), and Spatial Error Model (SEM), account for spatial dependence in data, enabling the analysis of how infrastructure disparities influence economic outcomes across regions.

2.10.1 Spatial Analysis in Econometric

Anselin (1988) provides the foundational framework for spatial econometrics, establishing that the classical OLS assumption of independence among observations is often violated in geographically referenced data such as infrastructure density. He formalizes measures like Moran's I for detecting spatial autocorrelation and develops Lagrange Multiplier (LM) diagnostics to distinguish whether spatial dependence occurs in the dependent variable (lag form) or the error term (error form).

LeSage and Pace (2009) expand on this foundation by articulating the mathematical structure of the Spatial Lag Model (SLM) and Spatial Error Model (SEM). They demonstrate how the spatial weight matrix defines neighbour interactions and how SLM estimates can be decomposed into direct and indirect (spillover) effects, offering a clearer interpretation of regional interdependence.

The Spatial Error Model (SEM), as developed in Anselin's and subsequent works, captures spatial dependence arising from omitted spatial processes, such as topography or infrastructure clustering. Wooldridge (2013) reinforces the importance of correcting for heteroskedasticity and model specification errors in regression, while White (1980) introduces heteroskedasticity-consistent covariance estimators that underpin modern robust spatial inference. Cook (1977) contributes diagnostic tools for identifying influential data points, a critical step in ensuring unbiased parameter estimates in models with spatial structure.

Finally, Arbia (2014) integrates these theoretical foundations with practical guidance for model implementation in R, showing how diagnostic tests, including LM and Moran-based statistics, inform model selection. Collectively, these works establish the methodological basis for analysing spatial dependencies in infrastructure and economic development studies, ensuring that parameter estimates account for the inherent spatial structure of regional data.

2.10.2 Applications to Infrastructure and Economic Growth

Empirical applications of spatial econometric modelling have increasingly focused on examining how infrastructural distribution, especially in transport, health, and built environments, relates to regional economic performance and spatial inequality. While earlier studies often relied on ordinary least squares (OLS) to test linear associations, more recent work applies spatial models to account for spillovers and locational dependencies inherent in infrastructure networks. Across different geographical contexts, these studies highlight that infrastructure availability does not only contribute directly to economic output but also generates spatial externalities that reinforce regional interdependence.

The integration of spatial econometric methods with regional economic analysis has advanced understanding of how infrastructure contributes to growth and inequality. Rey and Montouri (1999) pioneered the application of spatial models in examining income convergence across U.S. regions. Using both the Spatial Lag Model (SLM) and the Spatial Error Model (SEM), they found that ignoring spatial dependence leads to biased conclusions about convergence rates. Their analysis demonstrated that neighbouring regions with similar income trajectories influence each other's growth paths, highlighting the spatial interdependence inherent in regional economies.

Building on this approach, Dall'erba and Le Gallo (2008) analyzed the impact of European structural funds on regional growth using spatial econometrics. Employing both SLM and SEM, they found that EU investments in infrastructure generated significant spillover effects, particularly in less developed regions of southern Europe. The findings indicated that growth benefits were not confined to the funded regions but extended to adjacent areas, illustrating the regional diffusion of infrastructure-driven development.

Kim et al. (2021) examines how infrastructure investments contribute to economic growth both within and across national borders. The authors focus on transport (road and rail), energy, and ICT (telephone, mobile, and broadband) infrastructure across 78 countries from 1960 to 2014. Using a spatial econometric framework, particularly the Spatial Autoregressive (SAR) and Spatial Durbin Models (SDM), the study measures both direct and indirect (spillover) effects on GDP. Their study suggests that broadband infrastructure and human capital have significant positive cross-border effects. They find that the development of digital connectivity in one country enhances productivity and growth in neighbouring economies. The study emphasised that infrastructure serves not only as a driver of national productivity but also as a regional public good that promotes economic interdependence and shared growth among countries.

Ertur and Koch (2007) extends the augmented Solow model by incorporating spatial dependence to capture technological interdependence and spatial externalities among European regions. The authors argue that regional economic growth is not an isolated process but one influenced by the technological and capital accumulation of neighbouring economies. The study employs Spatial Lag Models (SLM) and Spatial Error Models (SEM) to test for the presence of spatial spillovers in cross-country growth regressions. Using data from 25 OECD countries, the authors find strong and significant spatial dependence, indicating that growth in one country tends to be positively associated with the growth of its neighbours.

In China, Zhang and Lin (2020) used a GIS-based Spatial Error Model to assess the spatial impact of infrastructure on regional economic inequality. Drawing on provincial panel data and geospatial indicators of transport and digital infrastructure, their study revealed that well-connected regions exhibit stronger growth, while peripheral areas lag behind. The results suggested that infrastructure gaps contribute directly to persistent inequality, reinforcing the need for spatially balanced policy design.

Similarly, Kumar and Rao (2019) applied GIS-based SLM and SEM approaches to district-level data in India to measure how transport infrastructure affects industrial output. Their study found that improved road density significantly boosts local productivity and has positive externalities on adjacent districts. The inclusion of spatial dependence improved model accuracy, showing that traditional OLS estimates underestimate the broader economic effects of infrastructure networks.

Zusmelia et al. (2020) employ spatial lag (SLM) and spatial error (SEM) models to investigate per capita income convergence and associated inequalities across districts in West Sumatra, Indonesia, spanning 2003 to 2019. By incorporating predictors such as gross domestic product per capita, small and medium enterprises, government investment, road infrastructure (proxied by road length relative to population and area), education levels, poverty, unemployment, and urbanisation, the study found that road-to-population ratio emerges with positive coefficient, signalling that denser networks relative to inhabitants may intensify disparities through urban-centric advantages. In opposition, the road-to-area ratio yields negative coefficients evidencing that extensive coverage facilitates inter-district interactions and agglomeration economies, thereby mitigating gaps.

Arbués et al. (2015) analysed how transportation infrastructure influences regional productivity across Spanish provinces between 1995 and 2008 using a Spatial Durbin Model (SDM). This approach allows them to distinguish between direct effects of infrastructure within a province and indirect spillover effects from neighbouring areas. Using geographically referenced data on road and rail networks, the authors find that road infrastructure exerts significant positive direct and spillover effects on productivity, while rail infrastructure shows more limited and localized impacts.

Across these studies, road and building infrastructures exhibit clear spatial spillovers, captured effectively through spatial models such as SLM, SEM and SDM.

The collective evidence thus supports the analytical rationale for employing spatial econometric approaches when testing associations between infrastructural endowments and economic activity.

2.11 CONCLUSION

The reviewed literature collectively cements that infrastructure and economic development are deeply spatial processes, often unevenly distributed, mutually reinforcing, and shaped by regional context. For Mizoram, these spatial dimensions are not peripheral but central to understanding development outcomes. Mizoram's strategic location within the emerging Kaladan Multimodal Transit Transport Project (KMMTTP) and India's Act East Policy positions it as a key node in the country's eastward integration, linking local economic transformation with transnational connectivity objectives.

The literature reviewed demonstrates that spatial patterns of infrastructure and economic activity are best understood through integrative approaches that combine geospatial data with econometric analysis. Studies across Asia and other developing regions have tested and validated these methods in examining how roads, buildings, and public facilities relate to economic performance and regional disparities. However, despite growing evidence from national and international contexts, there remains empirical gap in the application of such spatially grounded frameworks within Northeast India, particularly in Mizoram. The review therefore substantiates the research design and highlights Mizoram as an important but underexamined case in the spatial economics literature.

CHAPTER-III

DATA SOURCING AND PREPARATION

3.1 INTRODUCTION

This chapter presents an account of the data sourcing and processing procedures central to the study. It encompasses the retrieval of secondary datasets, their refinement, and the application of specialised techniques to render them suitable for hybrid quantitative and spatial analysis. The inclusion of a dedicated chapter for these operations stems from the intricate nature of the preparatory work, documentation of which can ensure transparency and supports full replicability. In a region like Mizoram, characterised by recent administrative restructuring and diverse topographic features, standard datasets often require substantial adaptation. For instance, extrapolating population figures from the 2011 census to 2021 necessitates adjustments for the 2019 district reorganisation, a process involving growth rate calculations and boundary realignments. Similarly, constructing a composite index for health infrastructure demands careful selection of variables, assignment of weights grounded in local service delivery priorities, and normalisation to enable meaningful comparisons.

The chapter proceeds sequentially through key components. It begins with the extrapolation of census data to produce 2021 population estimates, applying interpolation techniques to address decadal intervals and administrative boundary adjustments. This is followed by the sourcing and validation of health infrastructure records against official reports. The construction of a composite index incorporates variable selection and weighting based on local priorities. Geospatial data preparation integrates building footprints and road networks via multi-source compilation, manual enhancements, and alignment to state boundaries.

Raster processing for Night Time Lights (NTL) includes clipping, noise reduction through thresholding, and area normalisation to serve as proxies for economic activity. Elevation data are refined to yield district-level statistics for zonation and inclusion as explanatory variables. Standardised procedures for map creation accommodate diverse visualisation needs across choropleth, buffer, and statistical outputs. The chapter concludes with an overview of the software tools that enabled these operations. Collectively, these steps transform raw inputs into analytical-ready datasets, laying the groundwork for the empirical examinations in subsequent chapters.

3. 2 CENSUS EXTRAPOLATION FOR 2021 POPULATION ESTIMATES

The primary objective of this thesis is to analyse secondary data across Mizoram's 11 districts in 2021. However, the absence of an official 2021 census and the 2019 district reorganization, which redefined administrative boundaries, necessitated the development of population estimates for 2021 to enable accurate stratification and decomposition of the secondary data. The 2011 Census of India data, which provide village- and town-level population figures for Mizoram's eight districts at the time, cannot be directly applied to 2021 secondary data due to demographic changes and the creation of three new districts, namely Hnahthial, Khawzawl, and Saitual. This section outlines the methodology for extrapolating the 2011 census data to estimate the 2021 population at the village, town, and district levels to ensure compatibility with the reorganized district structure and to facilitate robust analysis of the secondary data.

The primary data source of the estimation is the Official Census of India 2011, which provides detailed demographic information, including total population, rural and urban proportions, and the decadal population growth rate (2001–2011) of 23.48% for Mizoram. The 2011 census reported Mizoram's population as 1,097,206, with 52.11% in urban areas and 47.89% in rural areas. Village and town-level population data were obtained from the Census 2011 for Mizoram's eight districts in 2011, Aizawl, Champhai, Kolasib, Lawngtlai, Lunglei, Mamit, Saiha, and Serchhip.

To account for the 2019 district reorganization, the study relied on the Government of Mizoram's notification dated 3 June 2019, which detailed the reallocation of villages and towns to form the new districts of Hnahthial, Khawzawl, and Saitual. This notification served as the authoritative reference for mapping 2011 census units to the 2021 district structure.

3.2.1 Population Extrapolation Method

To estimate the 2021 population, the study applied the decadal growth rate of 23.48% (2001–2011) to the 2011 population data at the village and town levels, assuming a constant growth rate over the 2011–2021 period. This approach is widely used in demographic studies when recent census data are unavailable, as noted by Vijayanunni (2018), who emphasizes the reliability of historical growth rates for short-term projections in India. The extrapolation formula is:

$$P_{2021} = P_{2011} \text{ x } (1 + r)$$

Where:

P_{2021} = Estimated population in 2021

P_{2011} = Population in 2011 (from Census 2011)

r = Decadal growth rate (23.48% or 0.2348)

For each village and town listed in the 2011 census, the 2011 population was multiplied by 1.2348 to derive the 2021 population estimate. This granular approach ensured that population estimates were accurate at the smallest administrative units, which is critical for subsequent stratification of secondary data, as recommended by the Census of India's guidelines for demographic analysis (Census of India, 2011)

3.2.2 District Reorganization and Population Reallocation

The 2019 district reorganization created significant challenges, as the new districts were formed by reallocating villages and towns from multiple existing districts, rather than simple bifurcations. For instance, Hnahthial was carved out of Lunglei, Khawzawl from Champhai, and Saitual from portions of Aizawl and Champhai. The issue was further compounded by the fact that some peripheral villages were reassigned to the non-bifurcated districts based on local sentiments.

To address this, the study undertook the following steps:

1. **Village and Town Reassignment**: Using the Government of Mizoram's 3 June 2019 notification, each village and town from the 2011 census was reassigned to its corresponding 2021 district. This process involved cross-referencing the Census 2011 village and town directories with the new district boundaries to ensure accurate mapping.
2. **Population Aggregation**: The extrapolated 2021 population estimates for each village and town were aggregated to compute the total population for each of the 11 districts. This resulted in a total estimated population of 1,354,830 for Mizoram in 2021, consistent with external projections.

3.2.3 Rural and Urban Population Estimates

To facilitate stratification of secondary data by rural and urban areas, the study applied the 2011 census rural (47.89%) and urban (52.11%) proportions to the 2021 population estimates. However, district-specific variations were considered, reflecting Mizoram's uneven urbanization patterns. For example, Aizawl has a significantly higher urban proportion (77.3%) due to its role as the state capital, while districts like Lawngtlai are predominantly rural (17.7% urban). These proportions were applied to the extrapolated 2021 district populations to estimate rural and urban populations, as shown in Table 1. This approach aligns with studies on urbanization in Northeast India, which highlights the importance of maintaining historical rural-urban distributions for demographic analysis (Singh, 2017).

The estimated 2021 population served as the foundation for stratifying secondary data, such as medical equipment usage, by district and rural-urban classification. This stratification was essential to account for inter district and intra district disparities in healthcare resource utilization. The population estimates enabled the decomposition of secondary data into meaningful subgroups, following standard statistical techniques for stratified sampling (Cochran, 1977). This ensured that the analysis of 2021 observation data was aligned with the updated district structure and demographic context.

The resulting district-level population estimates are presented in Table 3.1.

Table 3.1 **Mizoram Population Projection 2021**

SN	Districts	Census 2011	Population 2021		
			Urban	Rural	Total
1	**Aizawl**	364,791	347963	83889	450444
2	**Champhai**	71,209	23728	87174	87929
3	**Hnahthial**	28,468	8875	26278	35152
4	**Khawzawl**	35,931	16692	27676	44368
5	**Kolasib**	83955	57885	45783	103668
6	**Lawngtlai**	117894	25721	119855	145575
7	**Lunglei**	132,960	61523	102656	164179
8	**Mamit**	86364	18397	88245	106642
9	**Saiha**	56574	31006	38852	69858
10	**Saitual**	54,123	14347	48103	66831
11	**Serchhip**	64,937	39537	40647	80184
*	**Mizoram**	1,097,206	645673	709157	1354830

Note: Own calculation based on Census 2011 data

3.2.4 Limitations

The use of the 2001–2011 decadal growth rate assumes that population growth trends remained stable over the 2011–2021 period. While this is a standard approach in demographic projections, it may not fully capture changes in fertility, mortality, or migration, as evidenced by the National Family Health Survey (NFHS-5, 2019–2021), which reported a decline in Mizoram's total fertility rate to 1.9 children per woman.

The reliance on 2011 rural-urban proportions also assumes stable urbanization patterns, which may be affected by recent urban growth in Aizawl and other district headquarters. Moreover, the 2019 district reorganization introduced complexities, as villages and towns were reassigned across multiple districts. The use of the 3 June 2019 notification ensured accurate mapping, at the same time the absence of an official 2021 village-level population estimates necessitated this extrapolation approach.

Estimating Mizoram's 2021 population at the village, town, and district levels, addresses the challenges posed by the absence of 2021 census data and the 2019 district reorganization. By extrapolating Census 2011 data using the 2001–2011 decadal growth rate and reassigning villages and towns to the updated district structure, the method provides a robust framework for stratifying secondary data. Hence forth, for the sake of analysis in this thesis, the estimated 2021 population in Table 3.1, will be referred to as *Population Projection (2021)* whenever necessary.

3.3 SECONDARY DATA SOURCING FOR HEALTH INFRASTRUCTURE

Secondary data were primarily sourced from government publications, selected for their reliability and alignment with the study's spatial scope. The Mizoram Statistical Abstract (2021) served as the primary reference, providing comprehensive district-level data on population, healthcare facilities, and auxiliary variables such as road networks and area (Directorate of Economics and Statistics, 2021). The Mizoram Hospital Statistics Report (2020–2021) was extensively used for detailed information on unit level beds, outpatient department (OPD) visits, inpatient department (IPD) admissions, and medical equipment usage across facility types, including District Hospitals (DHs), private hospitals, Sub-District Hospitals (SDH) (Department of Health and Family Welfare, 2021). The Health Institutions Report from the National Health Mission (NHM) Mizoram (2022) provided supplementary data on the number and location of health facilities, addressing gaps in the primary sources (NHM Mizoram, 2021).

The National Health profile (2020, 2021& 2022), National Rural Health Statistics (2020-21, 2021-22) NHM Annual Health Report (2020-21) were extensively used whenever state level data were missing, for instance rural health facility staffing (National Heath Mission, 2022). However, national level reports have limitations as they do not capture district level data, except in the case of national Health Management and Information System (HMIS) which offers granular data. Additional data on insurance schemes, such as the Rashtriya Swasthya Bima Yojana (RSBY) and Mizoram State Healthcare Scheme (MSHCS), were sourced from publicly available reports to contextualize health service access (mizoramdata.mizoram.gov.in).

The choice of 2021 as the reference year aligns with the Population Projection (2021), derived by extrapolating Census 2011 data using decadal growth rates, as detailed in Section 2.1. This year was selected due to its comprehensive and granular data availability, enabling cross-verification across multiple sources. The 2021 data from the Mizoram Health Department also align with the Ministry of Health and Family Welfare's Management Information System (MIS) reports, which are the most recent publicly available datasets due to delays in central reporting (HMIS.mohfw.gov.in).

3.3.1 Data Validation and Triangulation

The secondary data exhibited inconsistencies, such as missing entries, non-standardized reporting, and incomplete facility details, necessitating a systematic validation process. The following steps were employed to ensure data quality:

1. **Cross-Verification**: Data from the Mizoram Statistical Abstract (2021) were cross-checked with the Mizoram Hospital Statistics Report (2020–2021) National Rural Statistic Report (2021-22), and NHM Mizoram (2022) to verify the number, type, and location of healthcare facilities. For instance, discrepancies in PHC counts were resolved by prioritizing NHM Mizoram (2022) data, which provided detailed facility lists. Similarly, bed allocations (totalling 3,744 beds: 918 rural, 2,826 urban) were validated by comparing hospital-level records from the Mizoram Hospital Statistics Report (2020–2021) with district-level aggregates in the Mizoram Statistical Abstract (2021).

2. **Field Observations**: Where secondary data were unclear or ambiguous field observations prior and interview with locals were used to fill gaps. This approach ensured accuracy in facility geolocation and operational status, particularly for rural PHCs and CHCs.

3. **Handling Missing Data**: Missing or NA entries, such as incomplete equipment usage records, were addressed by triangulating with MIS reports submitted to the central government (MoHFW, 2021). Where data for the study period (2020–2021) were unavailable, data from the preceding or subsequent year, whichever was available, were used.

4. **Urban-Rural Disaggregation**: Heath Data were disaggregated into urban and rural categories based on Census 2011's notified urban and rural segregation (Office of the Registrar General & Census Commissioner, 2011). This classification was cross-verified with District Commissioner's website to ensure alignment with Mizoram's 2019 district reorganization.

3.3.2 Other Data Sourcing

Data were aggregated at the district level for consistency with the study's spatial framework, reflecting Mizoram's 11 districts post-2019 reorganization. Staffing data, unavailable at the institutional level, were sourced from district-level aggregates in the Mizoram Statistical Abstract (2021), supplemented by NHM Mizoram (2022) where possible.

3.4 PREPARATION OF COMPOSITE HEALTH INFRASTRUCTURE INDEX

Principal Component Analysis (PCA) was employed to construct a composite Health Infrastructure Index by reducing the three standardized weighted variables, Health Building per 1000, Weighted Bed per 1000, and Weighted Equipment per 1000 into a single dimension.

3.4.1 Theoretical and Empirical Basis for Variable Selection

The selection of variables for the Health Infrastructure Index is grounded in a confluence of theoretical imperatives and empirical realities pertinent to Mizoram's health landscape. Mizoram, like much of India's North East, exhibits pronounced spatial disparities, with urban centres such as Aizawl endowed with advanced health facilities, whilst remote districts like Lawngtlai and Mamit grapple with resource paucity. These disparities, reflective of broader regional inequalities in India (Bhagat, 2010), necessitate variables that can quantify variations in health infrastructure to inform equitable policy interventions. The chosen variables are justified by the following considerations:

1. **Alignment with Health Systems Frameworks**: The variables correspond to the World Health Organization's (WHO, 2010) framework for health

systems, which identifies infrastructure encompassing facilities, beds, and equipment as pivotal for service delivery. Health Building per 1000 reflects physical access to care, Weighted Bed per 1000 measures the capacity for inpatient treatment, and Weighted Equipment per 1000 gauges technological sophistication. These dimensions are critical in Mizoram, where geographical barriers exacerbate access disparities, particularly in rural areas (Anand & Bärnighausen, 2004).

2. **Data Availability and Reliability**: In developing economies like India, data constraints at the district level are a significant challenge, particularly in peripheral regions like North East India. Variables which are widely used in the literature such as Infant mortality rates (IMR), Maternal Mortality Rate (MMR), Crude Birth Rate (CDR), Crude Death Rate (CBR), etc. are often either incomplete or inconsistent across Mizoram's districts. The selected variables were therefore derived from reliable sources such as Mizoram Health Statistics Report (2020–2021), Statistical Abstract of Mizoram (2020-2021), Gazette Notified List from NHMMizoram.org and validated through field visits.

3. **Suitability for Composite Index Construction**: PCA requires variables that are correlated yet distinct to yield a meaningful composite index (Jolliffe, 2002). The selected variables are interrelated—larger facilities often have more beds and equipment—but measure unique aspects (access, capacity, technology), ensuring the index provides a holistic yet non-redundant representation of health infrastructure.

3.4.6 Health Building per 1000 Population

This variable quantifies the number of health facilities per 1,000 population, encompassing a range of establishments from tertiary Hospitals to Sub-Centres, reflecting the physical accessibility of healthcare services. The following variables are the sub-components of Health Buildings per 1000 Population with the weightage given to each sub component.

- **Hospitals**: Tertiary and district hospitals, weighted higher (weight = 0.35) for their comprehensive services, including surgical, ICU beds, diagnostic services and specialist care. Hospitals included both Government and private Hospitals. No distinction is made in the context of preparing this infrastructure index because the Government of Mizoram is the licensing authority for private hospitals and all private hospitals operate under the monitoring and authority of the Directorate of Health and Family Welfare Department, Mizoram. Apart from following the rules and regulations set by the Government, the Mizoram Government also extents facilities such as medical reimbursement and health care coverage for patients treated in private hospitals. Therefore, they are included in the infrastructure index as Hospitals along with Government Hospitals.

- **Sub-District Hospitals:** They are mid-tier tertiary facilities (weighted moderately (Weight= 0.25) that bridge the gap between district Hospitals and Rural hospitals like CHCs and PHCs. They are generally located in smaller urban towns which are remotely located from the district capitals.

- **Community Health Centres (CHCs)**: They are mid-tier facilities, weighted moderately (weight = 0.2) for basic inpatient and outpatient services. Often equipped with 20-30 beds, basic diagnostic laboratory, general physician, nurses, and support staffs.

- **Urban Primary Health Centres (UPHCs)**: They are small facilities like PHCs designed under the National Urban Health Mission (NUHM), with 20-30 beds and basic services like outpatient care, non-communicable disease (NCD) screening, they are weighted the lowest (weight = 0.1) due to limited nature and their focus on primary health care.

- **Primary Health Centres (PHCs)**: Rural centres focusing on outpatient care, maternal health, and preventive services, weighted the lowest along with UPHCs (weight= 0.1). They act as the first point of contact between the villagers and a qualified doctor. They provide services such as Outpatent treatment, maternal and child health services, immunization, Disease surveillance and control for TB, malaria etc. They provide basic laboratory service. There are some cases of PHCs being located in the District Hospitals itself for instance in Khawzawl Districts. However given the geographical constraints and economic state of Mizoram, these are practical cost saving polices therefore we count them as a separate unit wherever they may exist together.

Although they are part of the healthcare system in Mizoram, some facilities were excluded in the creation of the index for health Buildings. They are;

- **Sub-Centres**: Smallest units, often single-room facilities in remote villages, delivering basic services such as immunisation and antenatal care. However, we have excluded sub-centres in this analysis because they do not have any broad comparable facilities such as beds, health equipment with the rest of the above variables. Moreover, some health Sub-centres do not independently operate in certain towns and villages, often the PHCs houses the subcentres and its impractical to map them because they're of dissimilarities in set. However, given the fact that all sub-centres work under the guidance of the PHCs, the practical threshold is kept at PHC level.

- **Private Clinics and Laboratories**: Private clinics are located mainly in urban areas where there is an abundant supply of specialists. They include specialized consultation clinics, dental clinics, skin clinics, eye clinic, Diagnostic test clinics, etc. whose functions are largely independent of the government health initiatives. Given the fact that they serve a wide array of services and also the nature of their impermanence which is dependent on the availability of doctors or specialists, makes them less relevant in mapping an index.

3.4.7 Weighted Health Facility Bed per 1000 Population

This component measures beds from the selected health facilities, decomposed per 1,000 population. It is further weighted by facility type to capture qualitative differences of the health infrastructure considered, reflecting each district's ability to address serious health conditions requiring hospitalization.

- **District Hospital Beds**: Beds in referral or district hospitals and private hospitals, weighted highest (weight = 0.35) for their role in advanced care, such as ergonomic beds, 24/7 monitoring equipment, oxygen lines, extra bedding area for attendants in private hospitals, private non-ICU rooms, etc.

- **Sub-District Hospital beds:** They are typically general warded beds with basic bedside lockers, privacy screens and shared toilets. Although District Hospitals have general wards Sub Districts hospitals do not have specialized monitoring equipment or the luxury to upgrade patients into ICUs. Moreover, they are mainly equipped to treat acute common illnesses or general ward conditions. Therefore, they are weighted lower than district level Hospital beds at 0.25. Some Sub-District Hospitals have facility to treat Leprosy and Ayush section but they are mainly concentrated on non-specialized inpatient conditions

- **CHC Beds**: Beds in community health centres, like sub-district hospitals are also weighted moderately at 0.20 because they provide basic general ward bed services without any specialized care. They are for general purpose acute common illnesses for the rural areas.

- **PHC and UPHC Beds**: Limited beds in primary health centres, weighted lowest (weight = 0.1) due to rudimentary infrastructure. Their services are more into preventive care and emergency casualty ward before serious patients are transferred to CHCs, or District Hospitals.

Bed counts were sourced from Mizoram Hospital Statistics Report (2020–2021) and partially verified during field visits, as it was practically impossible to visit all of them especially the rural PHCs. For all the district hospitals, sub-district hospital, CHCs and UPHC/PHCs Weights were assigned at a value of 0.35, 0.25, 0.2 and 0.1 respectively, based on their utility and functionality. The weighted sum is further divided by the district's Population Projection (2021) calculated from Census 2011 data.

3.4.8 Weighted Equipment per 1000 Population

To select the vast array of health equipment used across various health services in Mizoram two approaches were employed. Firstly, the report on Medically Certified Deaths by leading causes as per International Classification of Disease (ICD 10) was extracted from the Mizoram Statistical Abstract of Mizoram (2021). Major causes of death in Mizoram such as Diseases of the circulatory system, respiratory system, digestive system, endocrine, nutritional, metabolic diseases, etc. were identified, with a total count of 3,318 deaths.

The causes of death were reordered by the number of deaths for clarity. Then detection and treatment services are then aligned based on clinical relevance (e.g., ECG and Echo for circulatory diseases, Chemotherapy for neoplasms). Some disease groups (e.g., Diseases of the Eye) have no relevant services from the list, as they provided services focus on systemic conditions. As a result, 10 health services and equipment were selected, namely Bronchoscopy, Chemotherapy, Dialysis, CT-Scan, Electrocardiogram (ECG), Echocardiography (Echo), Endoscopy, Ultrasound, Radiotherapy and X-ray.

Secondly, the usage of these health services and equipment was extracted from Mizoram Hospital Statistics Report (2021). Usage of these services and equipment was given primary factor in creating the weightage. Higher usage indicates greater demand and importance in the healthcare system. For example, X-Ray (76,766 uses) and Ultrasound (44,965 uses) are the most used services, reflecting their broad applicability. At the same time utility in preventing deaths was also given secondary factor. Services that detect or treat diseases with the highest mortality rates, for instance ECG and Echo, which have the highest death toll (e.g., circulatory diseases: 579 deaths, digestive diseases: 555 deaths) were prioritized. Therefore, they were divided into three tier groups:

- **Top-Tier** (Broad Impact, High Usage): X-Ray, Ultrasound, ECG & CT-Scan
- **Mid-Tier** (Targeted impact & Moderate Usage**)**: Echo, Chemotherapy, Radiotherapy, and Dialysis
- **Low-Tier** (Specific Usage): Bronchoscopy and Endoscopy

The length and breadth of application for these services and equipment with respect to their relevance in Mizoram was considered. Thus, services and equipment that apply to multiple high-mortality diseases are ranked higher. Consequently, a weightage was prepared as the following:

- **X-Ray** (Weight = 0.18): Recoded 76,766 uses**,** detects infectious diseases (494 deaths), respiratory diseases (456 deaths), neoplasms (424 deaths), injuries (107 deaths), and COVID-19 (8 deaths). It has the highest usage, availability across all districts and broad applicability across multiple leading causes of death.

- **Ultrasound** (Weight = 0.14): Recoded 44,965 uses, detects digestive diseases (555 deaths), infectious diseases (494 deaths), neoplasms (424 deaths), perinatal conditions (139 deaths), pregnancy-related issues (146 deaths), and circulatory diseases (579 deaths).

- **ECG** (Weight = 0.12): It has 24,348 recoded usage, primary detection tool for circulatory diseases (579 deaths), the leading cause of death. High usage and directly addresses the top cause of death, though less versatile than X-Ray or Ultrasound.

- **CT-Scan** (Weight= 0.11): It was used 12,566 times as per record Detects circulatory diseases (579 deaths), digestive diseases (555 deaths), infectious diseases (494 deaths), neoplasms (424 deaths), respiratory diseases (456 deaths), injuries (107 deaths), and neurological disorders (56 deaths). Moderate usage but applicable to nearly all high-mortality diseases, enhancing diagnostic accuracy.

- **Echo (Weight = 0.10):** It has 1,066 recorded uses**,** detects circulatory diseases (579 deaths), complementing ECG for heart condition diagnosis. It has Lower usage but highly specific for the top cause of death, making it critical for targeted prevention.

- **Chemotherapy** (Weight = 0.09): With a record usage of 7,447**,** used mainly for treatment of neoplasms (424 deaths) which is one of the top causes of death in Mizoram. However, it ranks lower than the other because of its moderate usage and limited utility to one disease group.

- **Radiotherapy** (Weight = 0.8)**:** With a recorded usage of 8,486, it treats neoplasms like chemotherapy. Although it has a higher usage than chemotherapy it complements Chemotherapy therefore rank lower.

- **Dialysis** (Weight = 0.07): There was a recorded 11,839 usage. It treats kidney complications linked to digestive diseases (555 deaths), endocrine diseases (76 deaths), and genitourinary diseases (8 deaths). Although it records moderate usage its usage is limited to specific conditions, often as a last resort rather than a preventive measure.

- **Endoscopy** (Weight = 0.06): It has a moderate usage of 10425 in 2021. It is given lower weight in the ranking as its diagnostic role in gastrointestinal issues (including stomach cancer) is important but less immediate than chemotherapy or dialysis. Its impact depends on follow-up treatments.

- **Bronchoscopy** (weight = 0.5): It has low usage of 258 in 2021. However, it is highly efficient in detecting respiratory diseases (456 deaths) and neoplasms (424 deaths) which earns itself a spot in the ranking.

- **Excluded Equipment:** Other equipment such as Magnetic resonance imaging (MRI), was excluded because they was no data specific to MRI usage at the time of data collection, and the overall usage data on Perfusable Tissue Fraction (PTF), which MRI is part of was only 46 usages, thus appropriately excluded from the ranking.

Weights were assigned based on equipment classifications as mentioned above, with the weighted sum divided by the district's Population Projection (2021). Technological capability is paramount in rural settings like Mizoram, where diagnostic and treatment shortages hinder health outcomes. Field observation confirmed the quality and scale of diagnostic capacity, thus validating the weightage.

Despite the efforts, there are certain limitations and concerns that needs to be addressed in assigning the weights. Health Facility weights were applied based on standardized assumptions of care levels, with DHs weighted at 0.35 while PHCs/UPHCs at 0.1. Field observation finds that the same type of unit differs widely across space in capacity and scale. However, these weights were deliberately kept conservative, since available secondary data does not consistently reflect the actual service capacities of similarly labelled facilities across districts

In the context of Mizoram, where urban centres like Aizawl boast advanced facilities and rural districts like Mamit face resource scarcity, PCA ensures that the index reflects the combined influence of access (buildings), capacity (beds), and technology (equipment), as weighted sub components and further standardized. The methodology is particularly apt for small datasets, such as the 11 districts here, and is widely used in spatial inequality studies to create composite indices (Abdi & Williams, 2010).

3.5 PREPARATION OF DATA FOR SPATIAL ANALYSIS

To analyse spatial disparities in health infrastructure across Mizoram, Geographic Information Systems (GIS) were employed to create choropleth maps visualizing the distribution of health facilities and population characteristics. This methodology outlines the preparation of spatial data using Quantum Geographic Information System (QGIS) and the rendering of maps through R software.

3.5.1 Shapefile Preparation for Health Infrastructure Analysis.

A shapefile reflecting Mizoram's 2019 district reorganization were created using QGIS. The process ensured accurate spatial representation of administrative boundaries and health infrastructure, following these steps:

1. **Mizoram Boundary Shapefile**: A shapefile for Mizoram's state boundary with district demarcation was constructed based on the 2019 district reorganization notification (Government of Mizoram, 2019). It was prepared in three coordinate reference systems: Universal Traverse Mercator (UTM) Zone 46 North (EPSG:32646) for the main analyses, while EPSG 4326 (WGS84) and EPSG 3857 (Pseudo-Mercator) were also created for projected mapping, facilitating compatibility with visualization tools.

2. **Urban and Rural Settlement Shapefile**: A shapefile delineating urban and rural settlements was adapted from the Survey of India's 2011 Census shapefile for India (Survey of India, 2011). The shapefile was cropped to Mizoram's boundaries and realigned to reflect the 2019 district structure, ensuring consistency with current administrative divisions.

3. **Health Facility Shapefile**: A shapefile was developed to map health facilities, including District Hospitals (DHs), private hospitals, Sub-District Hospitals (SDHs), Community Health Centres (CHCs), and Primary Health Centres (PHCs). Coordinates for each facility were assigned at building centroids using EPSG 3857 projected maps.

3.5.2 Buildings Shapefile Sourcing and Preparation

The analysis of buildings in Mizoram, represented as vector polygons, forms a critical component of the infrastructure assessment for Mizoram. This dataset facilitates the evaluation of building density across the state and supports a descriptive analysis in conjunction with the Atkinson Index to measure inequality in spatial distribution. To ensure comprehensive coverage, building data were sourced from two distinct datasets, as no single source provided complete information for all districts. The subsequent processing steps aimed to integrate these sources, refine the data for relevance, and align them with Mizoram's administrative boundaries. These procedures were conducted using Quantum Geographic Information System (QGIS) software, promoting replicability through standardised geospatial tools and methods.

Data sourcing began with the Microsoft Global Buildings Footprint (MDF) dataset for the districts of Mamit and Kolasib, where alternative sources exhibited gaps in coverage (Microsoft, 2024). The MDF dataset comprises of building footprints derived from high-resolution satellite imagery. To obtain the relevant data, quad keys were generated for the entire state of Mizoram at a zoom level of 10, which corresponds to a spatial resolution suitable for district-level analysis. This zoom level balances detail with computational efficiency, capturing building outlines without excessive granularity that might introduce noise from minor structures. The resulting footprints were exported as a shapefile and clipped to the two district, Mamit and Kolasib District boundary in QGIS.

For the remaining nine districts (Aizawl, Champhai, Hnahthial, Khawzawl, Lawngtlai, Lunglei, Saiha, Saitual, and Serchhip) building data were extracted from OpenStreetMap (OSM) (OpenStreetMap Contributors, 2023). OSM provides crowdsourced geospatial data, including building polygons contributed by volunteers and validated through community processes. Extraction involved querying the OSM database directly within QGIS using the built-in OSM query tool. The query targeted all features tagged as buildings within the bounding box encompassing the 9 districts of Mizoram, ensuring that only relevant polygons were retrieved. This approach yielded a shapefile compatible with the MDF data of the previous two districts.

Following data acquisition, the two shapefiles underwent preprocessing to create a unified dataset. First, the coordinate reference system (CRS) of each shapefile was verified and standardised to EPSG:4326 (WGS 84). This step prevented spatial distortions during subsequent operations. The shapefiles were then sub-set to Mizoram's administrative boundaries by clipping them against a reference boundary shapefile for the state, the preparation of which is mention in section 3.5.1 of this chapter. Clipping removed any extraneous features extending beyond the state's borders, focusing the dataset exclusively on Mizoram. Finally, the two clipped shapefiles were merged into a single layer using QGIS's merge vector layers tool, which combines geometries and attributes while resolving any overlapping polygons through union operations.

To enhance the dataset's applicability for the intended analysis, an area-based threshold was applied to exclude small structures. Polygons with an area smaller than 13.94 m^2, equivalent to dimensions of approximately 10 feet by 15 feet, were filtered out. This threshold was selected based on local contextual knowledge of Mizoram's built environment, where structures below this size often represent animal shelters, jhum (shifting cultivation) huts, or temporary working sheds rather than permanent human dwellings or industrial facilities. The exclusion was implemented in QGIS by calculating the area attribute for each polygon using the field calculator and then selecting and deleting features that fell below the threshold. This refinement ensured that the final dataset prioritised buildings indicative of population density and economic activity, thereby improving the accuracy of density comparisons.

The processed dataset, now a cohesive shapefile of building polygons aligned to Mizoram's boundaries, enables robust comparisons of building density at the district level. It also supports the application of the Atkinson Index for assessing inequality in the distribution of infrastructure, providing insights into spatial disparities that inform policy recommendations. All steps described here utilise open-source tools and publicly available datasets, allowing for replication by researchers with access to similar software and data sources.

3.5.3 Road Infrastructure Shapefile Preparation

The preparation of shapefiles for road infrastructure involved the compilation and refinement of data to represent Mizoram's network accurately. This process resulted in the classification of roads into five categories: National Highways (NH), State Highways (SH), Rural Roads (RR), Agricultural Link Roads (ALR), and Residential Roads (Res.R). These categories capture the diversity of road types in the state, from major arterial routes to local access paths. Road lengths were computed in the Universal Transverse Mercator projection (UTM Zone 46N, EPSG:32646) to maintain precision in measurements, given the state's hilly topography. The final dataset was validated through comparison with multiple authoritative sources, yielding a total mapped length of 14,377.37 kilometres and an average density of 68.2 kilometres per 100 square kilometres across Mizoram's area of 21,081 square kilometres.

Data acquisition commenced with the extraction of road features from OpenStreetMap (OSM) using QGIS. A targeted query retrieved line geometries for highways, Grand Trunk roads, primary and secondary state highways, residential or town roads, and tracks within Mizoram's extent (OpenStreetMap Contributors, 2023). This source provided a broad baseline, but discrepancies arose in classification when compared to official government records, particularly in distinguishing between road hierarchies and functional roles.

To address these inconsistencies, additional data were obtained from the Ministry of Rural Development's GeoSadak portal under the Pradhan Mantri Gram Sadak Yojana (PMGSY) programme (Ministry of Rural Development, 2022). This dataset classified roads in Mizoram into categories such as National Highways (NH), Major District Roads (MDR), Other Tracks (OT), Rural Roads (RR), Other District Roads (ODR), Rural Road Tracks (RR Tracks), Rural Road Village Roads (RR VR), and State Highways (SH). The PMGSY data focused on rural connectivity, offering detailed shapefiles that complemented the OSM coverage.

The two datasets were then cross-referenced in QGIS to reconcile differences and derive the five standardised categories for analysis. National Highways encompassed major inter-state routes managed by the National Highways Authority of India. State Highways included primary intra-state links under the Mizoram Public Works Department (PWD). Rural Roads aggregated village and district-level paths, including those from PMGSY initiatives. Agricultural Link Roads were identified as specialised connectors to farming areas, often funded by departments like Agriculture or Horticulture. Residential Roads covered local streets and tracks inside buildup area, incorporating community-maintained or private paths. This reclassification ensured alignment with local usage patterns while resolving overlaps, such as merging MDR and ODR into broader groups where appropriate.

However, the combined data remained incomplete, spanning records from 2014 to 2023 and omitting contributions from various agencies. These included the State PWD for highways, the Border Roads Organisation (BRO) for strategic frontier routes, and other entities such as the Agriculture and Horticulture Departments, the Mahatma Gandhi National Rural Employment Guarantee Act (MGNREGA) schemes, Member of Legislative Assembly (MLA)-funded projects, as well as community-initiated or privately built roads.

To complete the network, supplementary mapping drew from high-resolution satellite imagery with a cutoff year of 2023. Sources comprised the Indian Space Research Organisation's (ISRO) Bhuvan portal for national geospatial data, Google Earth for detailed visual overlays, Esri's World Imagery basemap for global coverage, and the European Union's Copernicus programme, specifically Sentinel-2 optical imagery from the Copernicus Open Access Hub (European Space Agency, 2023). Missing or incomplete segments were manually digitised in QGIS by tracing visible road alignments on these layers. This step proved labour-intensive, requiring iterative verification across multiple views to account for terrain variations.

Coordinate reference systems played a key role in this process. Digitisation alternated between EPSG:3857 (Web Mercator) for web-based imagery compatibility, EPSG:4326 (WGS 84) for geographic alignment, and EPSG:32646 (UTM Zone 46N) for metric accuracy in length calculations. Layers were projected, merged, and harmonised in QGIS to eliminate distortions. Once compiled, each of the five road category shapefiles was clipped to the Mizoram boundary shapefile established in Section 3.5.1, removing any extraneous segments. For visualisation, colour coding was applied: yellow for NH, orange for SH, blue for RR, red for ALR, and purple for Res.R. These individual layers were then unified into a single comprehensive road network shapefile via QGIS's merge tool.

For subsequent analytical purposes, the road shapefiles were further subsetted to a gridded framework derived from the state boundary. Grids of 5x5 km, 10x10 km,, and 20x20 km were generated in QGIS, allowing segmentation of road data for density and distribution assessments at varying scales.

Certain limitations persist in the dataset. The total mapped length of 14,377.37 kilometres surpasses the Mizoram PWD's reported figure of 6,554.63 kilometres for 2023, as it incorporates additional elements like agricultural links, residential paths, informal tracks, jeep roads, community-maintained segments, and border routes not always documented in official PWD inventories. Satellite imagery sources may overlook some roads, especially older or disused ones, owing to dense forest canopy, steep hill slopes, shadowing effects, and oblique imaging angles prevalent in Mizoram's rugged landscape. These factors could lead to minor underrepresentation in remote areas, though the multi-source approach mitigated such gaps to the extent possible.

3.6 PREPARATION OF NIGHT TIME LIGHT RASTER FILE

Night Time Light (NTL) data offer a proxy for economic activity and urban development. Preparation of these raster files involved acquiring global composites, cropping them to relevant boundaries, applying filters to reduce noise, normalising values for comparison, and generating visual outputs. The process covered the years 2014 to 2023 to capture temporal trends. All operations prioritised accuracy in radiance measurements and spatial alignment.

3.6.1 Data Acquisition and Clipping

Annual composite raster files from the Visible Infrared Imaging Radiometer Suite (VIIRS) Nighttime Lights (VNL) Version 2 dataset were downloaded from the Earth Observation Group (EOG) at the Colorado School of Mines. This dataset provides cloud-free average radiance values in nanowatts per square centimetre per steradian ($nW/cm^2/sr$), derived from the Day/Night Band (DNB) sensor. The selection of yearly composites ensured consistency for long-term analysis across the ten-year period.

For each year, the global raster was first clipped to India's national boundaries using the official shapefile from the Survey of India. A second clipping operation then subset the data to Mizoram's state boundary, as prepared in Section 3.5.1. These steps generated twenty raster files in total: ten for India and ten for Mizoram. Clipping was performed in R with the 'terra' package, which handles vector and raster operations efficiently.

The raster files were cropped to the shapefile's extent, and masked to retain only pixels within the specified boundary in R. The output was saved as a new TIFF file for each year and region. Aggregate statistics such as total radiance, mean radiance, and median radiance, were extracted from these clipped raster files. Extractions used zonal statistics functions in 'terra', applied to the state boundary for Mizoram-level summaries and to district boundaries for finer-scale insights.

3.6.2 Threshold Application, Normalisation, and Visualisation

To filter out residual background noise, stray light, and sensor artifacts, radiance values below 0.5 nW/cm²/sr were set to zero in all processed rasters. This threshold aligns with established practices in VIIRS NTL analysis. NASA's Black Marble nighttime lights product suite: Algorithm theoretical basis document (ATBD) Version 1.0 specifies that NTL composite values less than 0.5 nW/cm²/sr are set to zero to remove residual noise, particularly in land applications. Research by Román et al. (2018) in the NASA Black Marble suite Empirical studies, such as those by Tan (2023) in urban illumination contexts, discard values below 0.5 nW/cm²/sr, noting that over 80% of such pixels represent noise in rural areas. Zhang et al. (2025) apply the same threshold in cross-sensor validations to correct for temporal noise. This approach ensures the dataset focuses on persistent anthropogenic light sources while excluding ephemeral or false signals.

3.6.3 Measurement and Visualisation

Area measurements for normalisation drew from the UTM Zone 43N projection (EPSG:32643), selected for its metric properties that preserve distances in Mizoram's latitude range. Total radiance was divided by administrative area to yield radiance per square kilometre (nW/cm²/sr/km²). This metric facilitates comparisons of light intensity across regions of varying sizes.

Visual representations of the NTL data were created in R for both national and state scales. The process involved loading the raster with 'terra', applying bilinear interpolation to smooth at a resolution factor of two. Outliers were clamped at the 99th percentile to manage extreme values. Plots employed a NASA-inspired colour ramp, progressing from black through reds and oranges to white, to depict radiance gradients realistically. This visualisation method highlighted spatial patterns in artificial illumination for India (extent: 68°E to 97°E, 8°N to 37°N) and Mizoram.

3.7 PREPARATION OF ELEVATION RASTER FILE

A high-resolution digital elevation model (DEM) was prepared for Mizoram using NASA's Jet Propulsion Laboratory (JPL) NASADEM dataset (NASA JPL, 2021). The global raster was downloaded from OpenTopography (OpenTopography, 2023), processed, and clipped to the Mizoram boundary shapefile in QGIS to focus on the state extent.

Zonal statistics were computed in R for each district, extracting the highest elevation, lowest elevation, median elevation, and mean elevation using the 'terra' package functions. These metrics supported analyses of malaria incidence patterns, including the division of Mizoram into three elevation zones, and served as one of the independent variables in spatial modelling of economic activity in Mizoram.

3.8 GENERAL PROCEDURE FOR MAP GENERATION

Maps served to illustrate spatial patterns across various infrastructure elements in Mizoram. These included choropleth representations of health facilities and population distribution, as well as depictions of building densities, road networks, and advanced spatial analyses such as Local Indicators of Spatial Association (LISA), Getis-Ord Gi* hotspot detection, Mann-Kendall trend tests, and regression models including Ordinary Least Squares (OLS), Spatial Lag Model (SLM). RStudio and QGIS facilitated data integration and rendering for all maps. The process began with importing shapefiles via the sf package to handle spatial vector data. Relevant attribute data, such as population figures from official abstracts or infrastructure metrics derived from earlier sections, were joined to these geometries. For health-related maps, urban and rural population data were categorised into quantiles per 1,000 residents to support colour gradations. Health facility locations, including their centroid coordinates, were transformed into spatial objects and projected to EPSG:3857 for compatibility with base maps.

Data validation followed to maintain integrity. This step converted values to numeric formats where necessary and replaced missing entries with zeros to avoid errors in computations. For maps beyond health infrastructure, such as those for buildings and roads, the procedure adapted to incorporate grid-based frameworks. Grids of 5x5 km, 10x10 km, and 20x20 km were created from the Mizoram boundary shapefile and used to clip and aggregate data layers. This enabled localised density calculations and supported the application of spatial statistics like Moran's I, LISA and Getis-Ord Gi* for identifying clusters, and Mann-Kendall for temporal trends.

Visualisation relied on the ggplot2 package. The shapefile polygons were shaded according to metrics like population density or infrastructure concentration, with colour palettes drawn from the RColorBrewer package and also custom designs. In health maps, facility points appeared at centroids, accompanied by 7 km buffer zones as semi-transparent red circles, generated via the st_buffer function in sf to denote service catchments. Each map featured a legend detailing categories and types, a descriptive title, and annotations citing sources. Exports occurred as high-resolution PNG files at 600 DPI through the ggsave function, promoting clarity for replication.

3.9 SOFTWARE AND TOOLS EMPLOYED

The analyses relied on a suite of specialised software and tools to handle data processing, spatial computations, and visualisation. SaTScan version 10.3.2 facilitated spatial cluster detection through scan statistics (Kulldorff, 2018). QGIS version 3.34.0

(Prizren) served as the primary platform for geospatial editing, layer integration, and output visualisation (QGIS Development Team, 2023). RStudio supported data preparation, statistical modelling, and raster operations, leveraging packages such as sf for vector handling (Pebesma, 2018) and dplyr for data manipulation (Wickham et al., 2023). GeoDa enabled calculations of global and local Moran's I indices as well as LISA statistics for autocorrelation assessments. JASP version 0.18.3 performed descriptive statistics and hypothesis testing. Microsoft Excel managed table formatting and basic chart generation. This combination ensured efficient workflows across quantitative and spatial tasks.

3.10 CONCLUSION

This chapter has detailed the systematic sourcing, processing, and integration of diverse datasets essential to the complete the study. The resulting outputs such as population estimates, comprehensive road and building shapefiles, Night Time light rasters, and elevation statistics, equip the study with reliable inputs for spatial inequality assessments and economic modelling. This documentation is also done with the hope that it serves the broader purpose of aiding future researchers in Mizoram, offering accessible processes and datasets that can be adapted or extended for regional studies at different spatial scale.

CHAPTER-IV

SPATIAL INEQUALITY IN HEALTH INFRASTRUCTURE IN MIZORAM

4.1 INTRODUCTION

This chapter contains an analysis of the health infrastructure and health services distribution of Mizoram at a granular level, from primary healthcare, secondary healthcare and tertiary level health care. It presents both the descriptive and inferential statistics concerning health infrastructure distribution and service utilisation across the length and breadth of Mizoram. Data from Secondary sources such as those from Mizoram Statistical Abstract (2021), Mizoram Hospital Statistics Report (2021), Census of India (2011), and other various digital publications from the state and national (NHM Mizoram, 2022; NHM MOHFW 2020-2022), will be analysed using statistical tools and geospatial tools. Observations from field visits, conversations with health officials and interaction with the locals will also be employed to triangulate the statistics and will be exhaustively applied to bridge the gap in secondary data. For the sake of uniformity across multiple secondary data points, especially with respect to analytical tools such as Quantum Geographic Information System (QGIS) that uses shapefiles in the official names, official designated names of district and towns from Census 2011 is adopted in the analysis. For instance, Saiha, also known locally as Siaha, will be called by its official Census 2011 name, Saiha.

Essentially this chapter can be divided into three main parts, part 1 deals with raw data with descriptive statistics, part two deals with economic externalities and inferential statistics, and part three deals with hypothesis testing. GIS based studies will be employed in each section to validate the findings.

Part one for the most part will deal with the topographic nature of Mizoram and its decease burdens, setting the stage for the rest of chapter. The sections will further deal with key variables such as medical buildings, medical beds, medical equipment, health personnel, utilisation of health facilities, and other key variables for a comprehensive dive into the healthcare system of Mizoram and understand their spatial distribution across the state. Tables, choropleth maps with geo references, and some descriptive statistics will be employed.

Part two delivers descriptive and inferential statistics on health infrastructure in Mizoram by triangulating the descriptive statistics and GIS finding to analysed key economic externalities. The aggregated raw data will be further analysed by employing the Principal Component Analysis (PCA) to construct a composite health infrastructure index of Mizoram capturing the underlying variance structure of the data. Findings from the prior sections are utilised to corroborate and reinforce the PCA results.

Part three primarily focuses on hypothesis testing through spatial clustering analysis using Spatial and Space-Time Scan Statistics (SaTScan) Bernoulli model and Discrete Poisson Model. These spatial analyses will test spatial concentration and clustering of healthcare in Mizoram, identifying patterns of urban-centric resource concentration. The SaTScan statistics, including relative risk, log likelihood ratio, and p-values, along with findings from other spatial tools, will be used to triangulate the presence of concentration and clustering in the healthcare system of Mizoram.

4.2 CLIMATIC DISEASE RISK ZONATION OF MIZORAM

Elevation governs temperature and humidity, key factors in the transmission of tropical diseases. Mizoram's topography, ranging from 28 to 2147 metres, shapes its environmental conditions and influences the concentration of tropical diseases in some regions. By looking at the elevation of the state, this analysis attempts to situate each district by their median elevation, categorizing them into 3 distinct groups, lowlands, midlands and highlands, enabling further analysis whether health resources are optimally allocated in the state.

A high-resolution elevation map, using NASA's Jet Propulsion Laboratory (JPL 2021) digital elevation map (DEM)) for the state of Mizoram was prepared, the elevation data was calculated using R and the output is further visualized using a hypsometric system. The blue hues mark low elevations while the red hues indicate higher altitudes. The findings are presented in Map 4.1.

Map 4.1

Mizoram Elevation Map

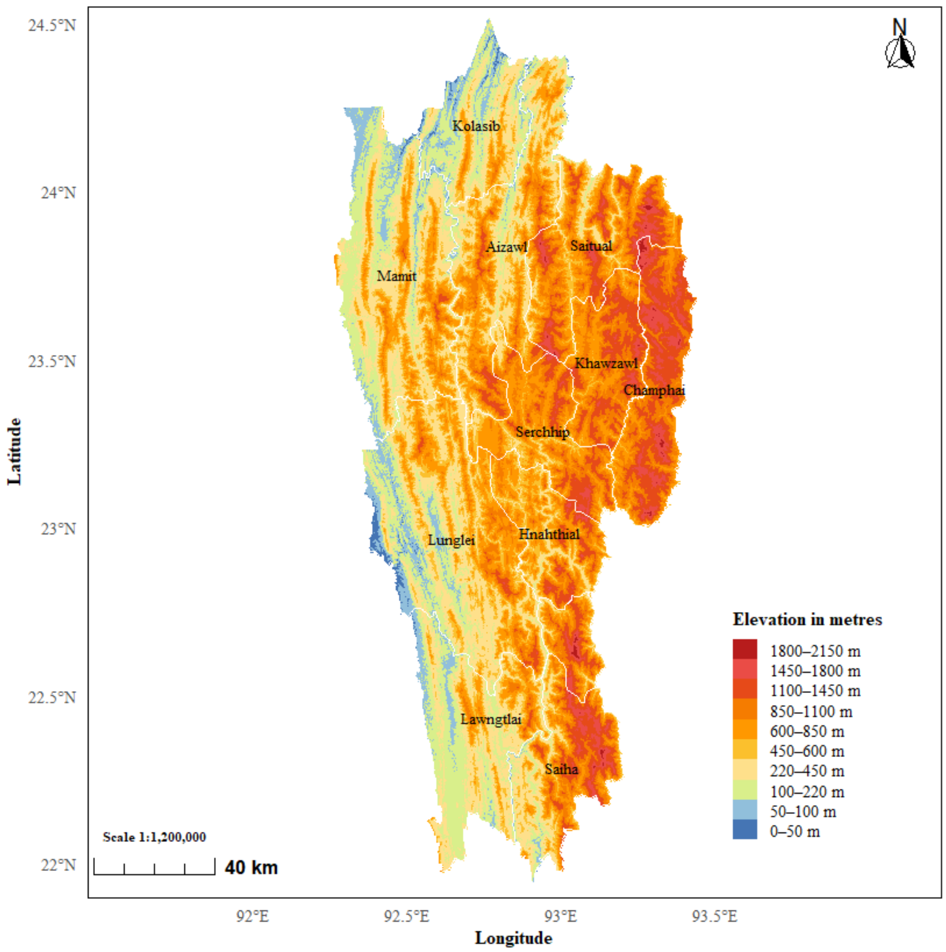

Note: Elevation data from NASA JPL (2021) NASADEM via OpenTopography

4.2.1 Insights from Elevation Mapping

The analysis found that Mizoram primarily lies between 17 m to 2149 m above sea level, a mean elevation of 610.2 m and a median elevation of 565 m. At a resolution of 30 m, the JPL data showed that 25% (1st quintile) of the data points are below an elevation of 284 metres, 75% (3rd quintile) are below 869 metres above the sea level. In other words, the mean elevation (610.5 m) exceeds the median (562 m), indicating a right-skewed distribution driven by high peaks like Phawngpui Tlang, while most of the terrain consists of moderately elevated but steep hills and valleys. The lower elevations (0–450 m) have warmer temperatures and higher rainfall while Mid-to-high elevations (450–2,149 m) are cooler throughout the year (FSI, 2021). The state being located northeast of the Bay of Bengal, the elevation gradient causes higher rainfall in the western lowlands compared to the eastern highlands, peaking during the month of June-September (Meteorological Data of Mizoram, 2021).

4.2.2 Zonal Statistics Analysis

A zonal statistics analysis was conducted with the JPL (2021) data, aligning with Mizoram's post-2019 district bifurcation. The analysis calculated highest, lowest, mean, and median elevations for each district, results are presented in the table below.

Table 4.1 Mizoram District Elevation Statistics

SN	District	Highest point	Lowest point	Mean Elevation	Median Elevation
1	Aizawl	1685	18	565	535
2	Champhai	2132	407	1150.1	1139
3	Hnahthial	1738	176	735.1	693
4	Khawzawl	1860	453	985.2	973
5	Kolasib	1150	25	263	193
6	Lawngtlai	2149	32	432	315
7	Lunglei	1546	17	423.4	396
8	Mamit	1460	25	366.5	311
9	Saiha	2014	35	769.9	737
10	Saitual	2003	53	869.5	835
11	Serchhip	1863	188	844	815
*	Mizoram	2149	17	610.5	562

Source: Own Calculations

The analysis reveals significant topographical variation across the 11 districts of Mizoram. Champhai District records the highest mean (1,150.1 m) and median (1,139 m) elevations, reflecting its highland terrain, while Kolasib has the lowest mean (263 m) and median (193 m), indicative of its low-lying areas. The highest point in Mizoram (2,149 m) is in Lawngtlai, whereas the lowest points (17

m) occur in Lunglei district corresponding to its river valleys near the Indo-Bangladesh border. Districts such as Aizawl, Hnahthial, Saiha and Serchhip show moderate mean elevations (565–844 m), while outliers like Champhai and Khawzawl exceed 985 m, contributing to the state's right-skewed elevation distribution.

4.2.3 Elevation Based Tropical Disease Burden in Mizoram

Low-elevation areas with high rainfall are particularly susceptible to tropical diseases due to environmental conditions that support vector survival. Malaria, in particular, thrives in low-lying regions where warm temperatures and abundant water bodies create ideal mosquito breeding habitats. To test the relationship between elevation and malaria incidence in Mizoram, the median elevations for 639 settlement points, each with a 3 km buffer was plotted using the Mizoram Boundary shapefile. These elevations were correlated with malaria Annual Parasite Incidence (API, cases per 1,000 population) data from the National Centre for Vector Borne Diseases Control (NVBDC, 2017–2021) across Mizoram's Health districts.

Table 4.2 Malaria Annual Parasite Incidence (API) Mizoram

SN	Health District	2017	2018	2019	2020	2021
1	Aizawl East	0.29	0.04	0.13	0.06	0.1
2	Aizawl West	0.41	0.25	0.29	0.15	0.22
3	Lunglei	9.19	6.83	15	19.83	0.2
4	Saiha	3.1	1.66	4.23	6.16	0.71
5	Kolasib	1.35	0.4	0.26	0.38	0.38
6	Mamit	9.24	8.67	21.14	7.57	14.76
7	Champhai	0.04	0.04	0.13	0.14	26.22
8	Lawngtlai	20.37	16.22	25.89	24.33	6.66
9	Serchhip	0.14	0.12	0.26	0.26	12.84

Source: Malaria data from NVBDC (2017-2021) & Own calculation

The Spearman correlation analysis (Table 4.3) reveals a strong negative relationship between settlement elevation and malaria API for 2017–2020.

Specifically, API_2017 and API_2018 show highly significant correlations (r = -0.857, p = 0.011), followed by API_2020 (r = -0.810, p = 0.022) and API_2019 (r = -0.707, p = 0.050). These results indicate that higher elevations are associated with lower malaria incidence. In contrast, API_2021 shows a weak positive correlation (r = 0.286, p = 0.501), likely due to reduced outdoor activity during COVID restrictions, limiting exposure to mosquito-prone areas.

Table 4.3 Elevation and Malaria API Correlation

Variable	Spearman Correlation	p_Value
API_2017	-0.857	0.011 **
API_2018	-0.857	0.011**
API_2019	-0.707	0.05*
API_2020	-0.81	0.022*
API_2021	0.286	0.501

Source: Own calculation

Note: *** p < .001, ** p < .01, * p < .05

These findings suggest that low-elevation regions, particularly in Mizoram's western belt, have slower water drainage from eastern highlands, leading to abundant water bodies and higher humidity. These conditions foster mosquito breeding, increasing malaria transmission. When planning for health interventions, it is imperative to account for these inherent natural advantages and disadvantages of regional topography, not just on population-based decomposition.

Based on the median elevation of each district, and their apparent tropical disease risks, such as Malaria, an elevation based tropical disease risk zones for Mizoram is deemed necessary to understand the spatial differences and unique needs of each region. Consequently, the 11 districts are divided into 3 elevated zones, namely, lowlands, midlands and highlands. Four districts, Kolasib, Lawngtlai, Lunglei and Mamit, were classified as Lowland district base on their median elevation and their higher risk to tropical maladies. Five districts, Aizawl, Hnahthial, Saiha, Saitual and Serchhip, having had a moderate risk and an overall higher elevated land, were designated as Midland districts, and two districts, Champhai and Khawzawl with low risks as Highlands. Map 4.2 illustrates the median elevation and zoning of the 11 districts into 3 categories, the western districts being shown in a reddish hue, midland districts in yellow and highland districts in green hue. The colouring, a reversal of the hypsometric elevation, is intended to highlight the tropical disease risk faced by each district.

Map 4.2

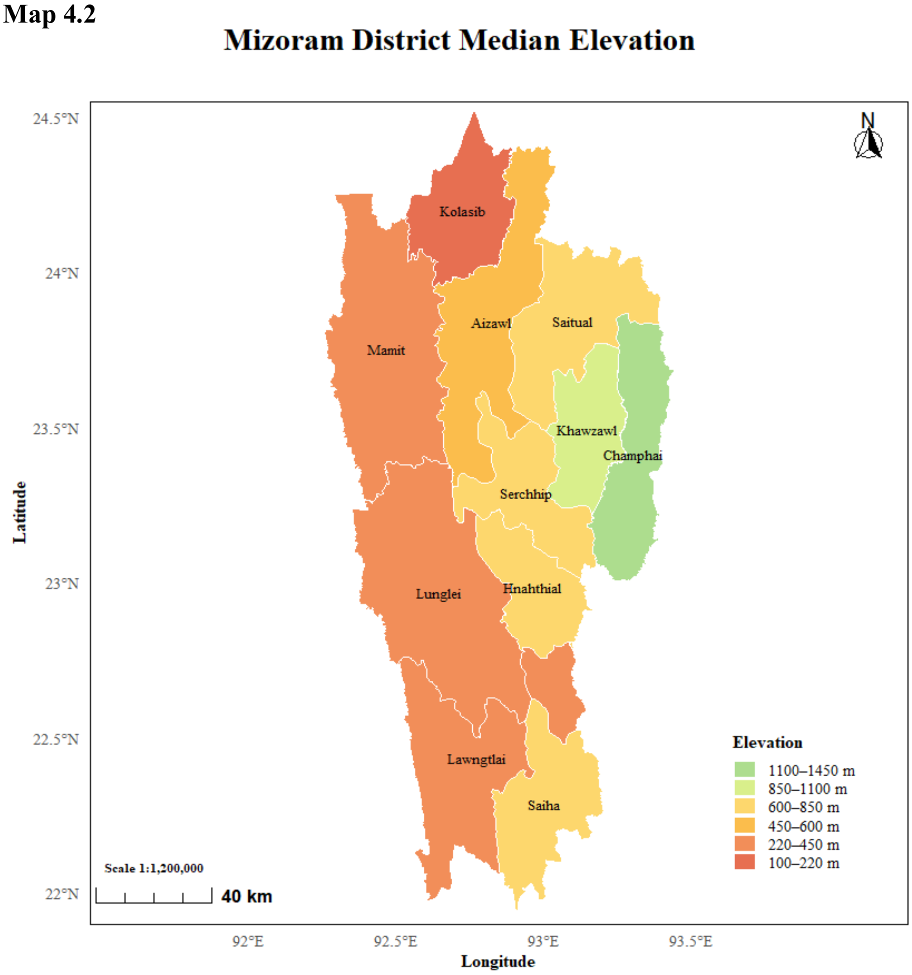

Note: Elevation data from NASA JPL (2021) NASADEM via OpenTopography

By considering these factors, the zoning provides a multidimensional approach, apart from population decomposition, to understand the spatial dimension of public health and its preventive measures. It bears mention that the Elevation-Based Disease Risk Zones is not meant to capture the broad spectrum of health issues in Mizoram but rather to show a naturally inherent variation and disadvantages among the regions of Mizoram based on elevation and the proliferation of tropical disease in these areas. It does not take into consider lifestyle induced diseases, respiratory diseases and other health hazard endemic in some regions.

4.2.4 Implications for Public Health Analysis

Zoning each district by elevation enables more precise public health interventions. For example, vector control measures, such as insecticide-treated nets for malaria and dengue or improved sanitation to reduce typhoid and leptospirosis can be tailored to zone-specific risks. Vaccination campaigns for Japanese encephalitis may prioritize lowland areas with rice cultivation. This elevation-based framework also supports spatial epidemiological research by linking topography with disease patterns, particularly relevant in tropical regions like Mizoram where elevation significantly shapes health risks. By aligning with global approaches to environmental health mapping, the zoning system offers a transferable model for geographies having the same similar context as Mizoram.

4.3 DISTRIBUTION OF HEALTH INFRASTRUCTURE IN MIZORAM

This section presents a detailed overview of the spatial distribution of health infrastructure across Mizoram, encompassing Primary Health Centres (PHCs), Community Health Centres (CHCs), Sub-District Hospitals (SDHs), and District Hospitals (DHs). The analysis includes both absolute facility counts and population-adjusted metrics to assess infrastructure adequacy relative to demographic demand. By examining disparities across districts, this descriptive assessment aims to highlight patterns of healthcare availability, identify underserved regions, and provide a baseline for evaluating spatial inequality in the state.

4.3.1 Absolute Distribution of Health Infrastructure in Mizoram

The following table (Table 4.3) captures the district wise distribution of Primary Healthcare Centres such as Primary Healthcare Centre (PHC), Secondary Healthcare centres such Community Healthcare Centres (CHC), Sub-District Hospitals (SDH), and District Hospitals. Tertiary Healthcare Centres such Government Hospitals and of Private Hospitals, spread across Mizoram's 11 districts in the year 2021.

Table 4.4 **District wise Distribution of Health Facility in Mizoram 2021**

SN	Districts	PHC	CHC	SDH	Govt Hospitals	Private Hospitals	Total
1	Aizawl	12	3	1	3	16	35
2	Champhai	6	0	0	1	2	9
3	Hnahthial	4	0	0	1	0	5
4	Khawzawl	4	1	0	1	0	6
5	Kolasib	5	1	0	1	1	8
6	Lawngtlai	6	1	0	1	2	10
7	Lunglei	8	0	1	1	4	14
8	Mamit	8	1	0	1	0	10
9	Saiha	4	0	0	1	1	6
10	Saitual	5	1	0	1	0	7
11	Serchhip	5	1	0	2	1	9
*	Mizoram	67	9	1	14	27	119

Source: Mizoram Statistical Abstract (2021), Mizoram Hospital Statistics Report (2021)

The table 4.4 reveals that Mizoram has a total of 119 health facilities, comprising 67 Primary Health Centres (PHCs), 9 Community Health Centres (CHCs), 2 Sub-District Hospital (SDH), 15 Government Hospitals, and 26 Private Hospitals. Aizawl district has the highest number of health facilities (35), including 12 PHCs, 3 CHCs, 3 Government Hospitals, and 16 Private Hospitals, suggesting it is the hub for healthcare in Mizoram. Primary Health Centres (PHCs) are the most widespread facility type, with 67 units distributed across the rural and urban areas of the state. Aizawl has the highest number of primary health centres (6 PHCs and 6 UPHCs), followed by Lunglei (6 PHCs and 2 UPHC) and Mamit (8 PHCs) while

Hnahthial, Khawzawl and Saiha receive the lowest (4) number of PHC. UPHC in Aizawl (6), Lunglei (2) and Champhai (1) are included in their PHC counts.

Mizoram has limited Community Health Centres (CHCs). Only 9 CHCs exist in the state, concentrated in Aizawl district (3), Khawzawl (1), Kolasib (1), Lawngtlai (1), Mamit (1), Saitual (1), and Serchhip (1). Five districts namely, Champhai, Hnahthial, Lunglei, Saiha, and Saitual have no CHCs. Only two Sub-District Hospital (SDHs) exists in Aizawl and Lunglei district, indicating that there is a gap in the link between the primary and secondary-level of healthcare infrastructure in some districts. At the District level there are 14 Government Hospitals and 26 Private Hospitals statewide. Aizawl has the highest number of both Government hospitals (3) and Private Hospitals (16), Lunglei district second the list with one government hospital and four private hospitals. Serchhip district owns two government hospitals (2) and the rest of the districts have one government Hospital each. Private hospitals are also located in Lawngtlai (2), Champhai (2), Kolasib (1) and Saiha (1). Hnahthial, Khawzawl, Mamit, and Saitual have no private hospitals.

Mizoram's health infrastructure distribution aligns closely with its urbanization rate of 51%, but this has resulted in a centralization of services. Aizawl dominates the state's healthcare landscape, hosting 16 private hospitals, 3 District Hospitals (DHs), 1 SDH, and 12 PHCs/UPHCs. In contrast, districts like Hnahthial, contributing just 4.2% to the state's total infrastructure, relying solely on Primary Health Centres and a single government District Hospital. Similarly, marginalization is observed in Khawzawl and Saiha, each accounting for less than 8% of total facilities and exhibiting limited access to comprehensive care.

4.3.2 Population based Decomposition of Health Facility in Mizoram.

To further illuminate the distribution of health facility in the state, population dynamics is applied to secondary data to arrive at district-wise distribution of health facilities per 1,000 population through Population Projected (2021), with estimated population of all districts including the three new districts.

Table 4.5 **District-Wise Health Facility per 1000 Population (2021)**

SN	District	PHC per 1000	CHC per 1000	SDH per 1000	Hospital per 1000
1	**Aizawl**	0.078	0.007	0.002	0.042
2	**Champhai**	0.102	0.000	0.000	0.034
3	**Hnahthial**	0.142	0.000	0.000	0.028
4	**Khawzawl**	0.135	0.023	0.000	0.023
5	**Kolasib**	0.077	0.010	0.000	0.019
6	**Lawngtlai**	0.069	0.007	0.000	0.021
7	**Lunglei**	0.085	0.000	0.006	0.030
8	**Mamit**	0.094	0.009	0.000	0.009
9	**Saiha**	0.086	0.000	0.000	0.029
10	**Saitual**	0.105	0.015	0.000	0.015
11	**Serchhip**	0.112	0.012	0.000	0.037
*	**Mizoram**	0.050	0.007	0.001	0.030

Source: Own calculation from Mizoram Statistical Abstract (2021), Mizoram Hospital Statistics Report (2021) & Population Projection (2021)

Table 4.5 highlights the resultant Primary Health Centre per 1000 population, Community Health Centre per 1000 population, Sub District Hospitals per 1000 population, and Hospitals per 1000 population. At the bottom of the table, in the unnumbered row (*), the state's total count is also included to serve as an average of the state. Mention must be made that apart from combining the PHC and UPHC data earlier, the government hospitals and private hospitals are now integrated under one column. This is done so to avoid over-granulation of the data and to further enhance the interpretability of inferential statistics.

When measured per 1,000 population, districts like Hnahthial (0.142), Khawzawl (0.135), and Saitual (0.105) appear to have the highest facility densities. Aizawl, despite its dominance in absolute facility counts, records a lower overall facility density (0.078) lower than the state average (0.088). Its hospital density remains high (0.044), reflecting the concentration of tertiary care services. On the other hand, districts such as Lawngtlai (0.062) and Kolasib (0.077) fall below average across most metrics, which may indicate limited care relative to their populations.

Graph 4.1

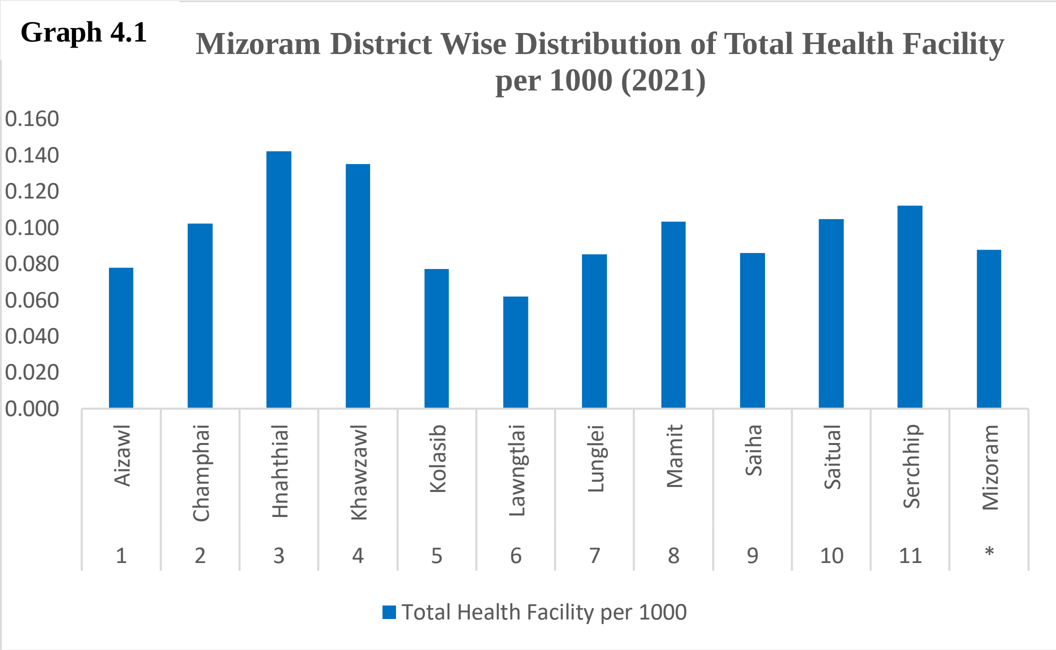

Some peripheral districts like Champhai and Saiha perform better than expected in per capita terms, even though previous indices such as the Mizoram Human Development Index (2013) ranked them lower in broader development outcomes, indicating an improved facility density since. Lunglei, Mizoram's largest district by area, presents a mixed case: despite hosting several primary, secondary and tertiary hospitals, its overall facility density (0.085) remains modest, suggesting challenges related to both space and distribution. In comparison with national averages (PHC: 0.023, CHC: 0.004, Hospital: 0.003 per 1,000), Mizoram performs well across all categories, which is commendable given the state being one of the most disadvantaged in terms of economic resources. The picture, though, is not entirely the whole story. While facility-per-population ratios are relatively high, low score in secondary and tertiary infrastructure remains a concern for many districts, and the concentration of secondary and tertiary units in urban areas is concerning. Overall, the per capita distribution complicates the earlier picture drawn from absolute figures. Rural districts may seem better served in numerical terms, but this often reflects smaller populations rather than better infrastructure.

4.4 GINI INDEX ON HEALTH FACILITY DENSITY

To further investigate the cross-sectional distribution of healthcare facilities across Mizoram's districts the Gini Coefficient was employed. Districts were ranked by population density while equal weight method was applied using the trapezoidal rule. Bootstrapping was also added to enhance the robustness and interpretability of the result.

4.4.1 Gini Index Result on Facility Density among Districts

The bootstrapping performed at 1000 iterations give a Gini value of 0.302, a mean of 0.29, the lower bound at 0.242 and upper bound being 0.334, with 95% Confidence level. Table 4.6 presents the Gini result and Graph 4.2 illustrate the Lorenz curve.

Table 4.6 **Bootstrap Gini Result on District Facility Density**

Gini_Coefficient	Mean	Std_Error	CI_Lower_95	CI_Upper_95
0.302	0.29	0.001	0.242	0.334

Note: Own calculation

Although the result suggests a moderate level of inequality, it requires caution in interpretation. Hnahthial, a fairly new rural district created in 2019, drives the inequality (0.142 health facility per 1,000, population 35,152) ranking the highest, followed closely by another new district Khawzawl (0.135, population 44,368) and another sparely populated Serchhip district (0.112) with a population 80,184. Aizawl came at third from the bottom quintile (0.078, population 450,444, 35 facilities) and Kolasib (0.077, population 103,668) rank the lowest (Table 4.7).

Graph 4.2

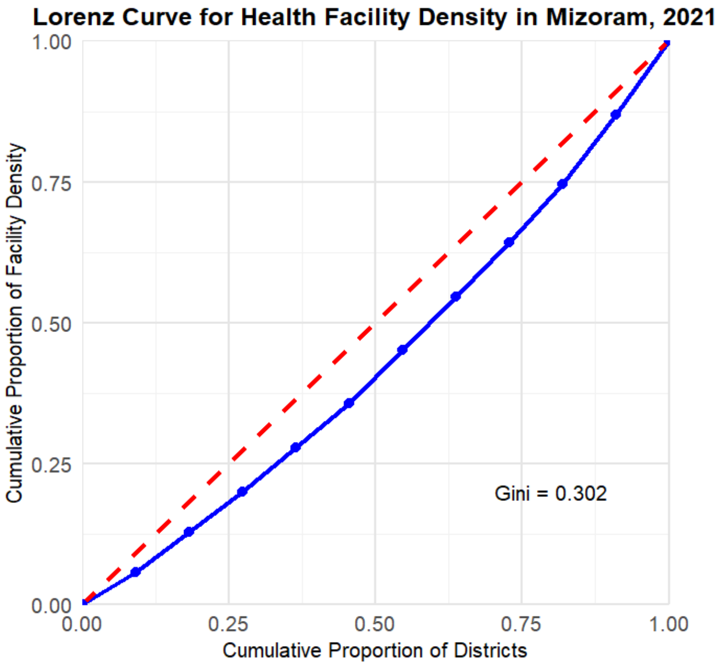

Table 4.7 Gini Bootstrapping Quintile Distribution

Quintile	District	Facility_ Density	Mean_ Density	SD_ Density
1	Kolasib	0.077	0.074	0.007
2	Lunglei	0.085	0.082	0.008
3	Champhai	0.102	0.094	0.009
4	Saitual	0.105	0.104	0.01
5	Hnahthial	0.142	0.129	0.011

Note: Own calculation

The result isn't completely unexpected as we have seen from the population-based decomposition table earlier. The quintile ranking shows a counterintuitive pattern: districts like Hnahthial and Saitual appear in the top quintiles despite limited infrastructure beyond primary care mainly due to spare population. For instance, Hnahthial's high facility density is driven by five PHCs, yet it lacks secondary services. This inflates its rank, giving a misleading impression of high health access. Conversely, Aizawl, which holds 35 facilities including 20 tertiary-level units, is ranked lower due to its large population base. This suggests that population-based density metrics can understate facility concentrations in urban centres while overstating coverage in smaller districts.

These results highlight a key methodological limitation: the current metrics do not account for facility type, service level, or functional accessibility. As a result, districts with many low-tier facilities and small populations dominate the upper quintiles, while urban areas with broader service provision appear under-resourced.

Moreover, the use of district-level aggregation conceals significant intra-district variation. Preliminary evidence suggests that residents in higher-ranked districts frequently travel to Aizawl for care, indicating a centralization of actual service delivery that the Gini index fails to capture. These findings point to the need for a more refined, multidimensional measures that reflect not just quantity, but also quality and accessibility of healthcare infrastructure.

4.5 GIS MAPPING OF HEALTH INFRASTRUCTURE IN MIZORAM

To further our inquiry into the distribution of health facilities in Mizoram, we will employ geographical Information System (GIS) analyses to examine the spatial distribution of health facilities across Mizoram, addressing the Gini coefficient’s limitations in capturing facility proximity, and concentration of resources. By mapping facility locations against topographic and demographic data, these methods will reveal disparities obscured by population-weighted metrics. Geospatial approaches, including choropleth visualizations and accessibility metrics, will contextualize the distribution.

4.5.1 GIS Mapping of Primary Health Centres

A choropleth map of PHC locations and district PHC density, using secondary data, is prepared below. The PHC Coordinates were plotted using QGIS based on CRS ESPG 3857, with Population Projection (2021) data enabling PHC density evaluation with 3-kilometre catchment radii. This analysis presents findings on PHC allocations, allowing assessment of spatial allocation beyond population-normalised metrics.

Districts such as Hnahthial and Khawzawl exhibit relatively high PHC density, followed by Serchhip and Saitual, in terms of calculated ratios and point distribution. Their spatial coverage appears consistent with their population dispersal, suggesting closer alignment between service location and settlement geography. These areas, recently carved from larger districts, retained redistributed infrastructure following administrative restructuring. With a lower population base their facility density went up. The choropleth map (Map 4.3) and the findings of the exercise are present as follow.

Map 4.3 Distribution of Primary Health Centres in Mizoram

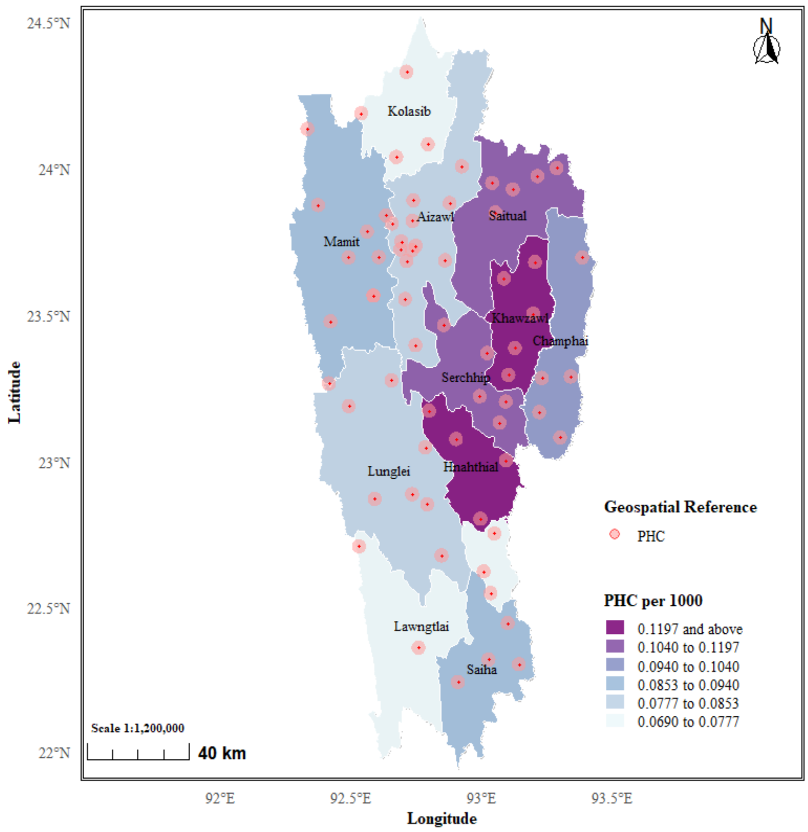

Source: Own visualisation based on Mizoram Health Institutions (2018), Mizoram Statistical Abstract (2021)

By contrast, districts, such as Kolasib and Lawngtlai presents sparser PHC placements followed closely by Lunglei. These districts show extensive areas without any proximate facility, raising concerns about geographic accessibility. Given the region's challenging topography and poor transport connectivity, the absence of facilities in these zones indicates potential service exclusion that may not be fully captured by per capita ratios.

Mamit, Saiha and Champhai seems occupy the mid-tier in terms of facility density. While they seem to be doing much better than the bottom districts, we can see visible intra-district variations in each of them, potentially resulting in some areas being marginalised.

Aizawl district presents a divergent case. Although it records low PHC density overall, the spatial clustering of facilities near the urban core suggests that rural segments within the district, particularly its far northern areas, are under-served. This uneven internal distribution raises concerns about intra-district disparities in access to primary care, even where overall service levels appear sufficient at the district scale.

A broader spatial pattern emerges clearly from the map: there is a visible North–South divide in PHC distribution, with northern regions exhibiting denser and more evenly placed facilities compared to the sparse coverage in the south. An East–West gradient is also noticeable, with eastern zones generally showing stronger spatial reach than their western counterparts. The spatial distribution of primary care is concerning given the visible fact that the western tropical disease high risk zones, mapped earlier, are poorly served whereas the moderate and low risk zones are thoroughly served. This observed pattern is rather counterintuitive to any general understanding of spatial epidemiology and may in fact result in the marginalisation of areas where primary care demand is relatively high. The mapping of the facility locations, highlights these spatial contrasts, which population-based metric alone cannot reveal.

4.5.2 GIS Mapping of Secondary Healthcare Centres

The following choropleth map shows two geo location of secondary healthcare facilities, Community health Centres and Sub-District Hospital in Mizoram in 2021. Both layers highlight the critical role secondary healthcare infrastructure plays in bridging the gap between rural populations and tertiary services, especially in a state defined by difficult terrain, scattered settlements, and recurrent monsoon-related disruptions.

Map 4.4 Distribution of CHC and SDH in Mizoram

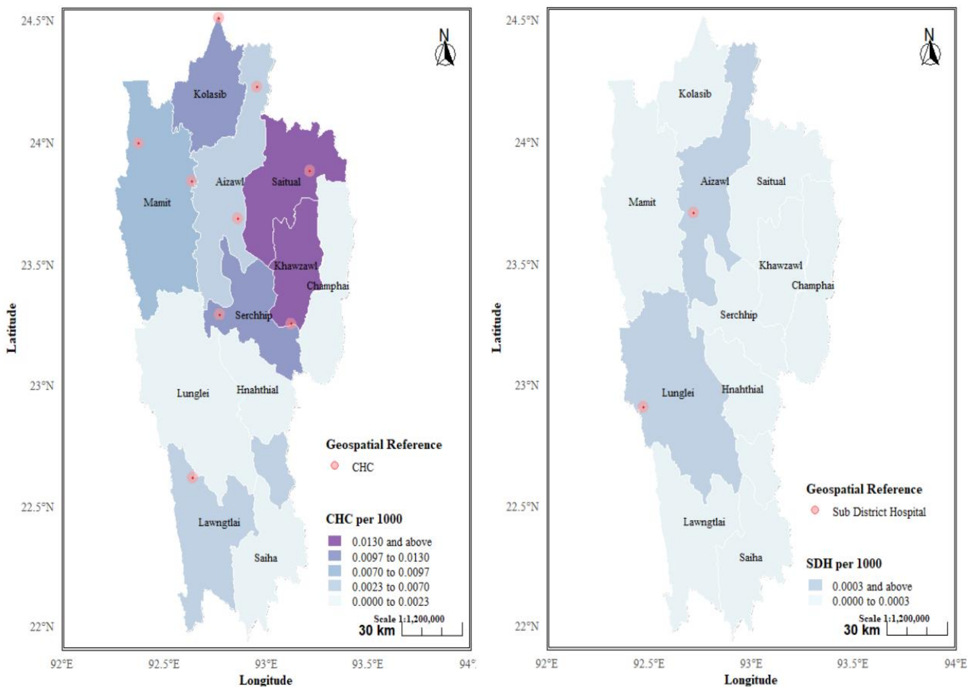

Note: Own visualization based on Mizoram Health Institutions (2018), Mizoram Statistical Abstract (2021)

The left panel, illustrating CHC density per 1,000 population, reveals a distinct spatial divide. CHCs are more densely clustered in the central-northeastern districts, particularly Khawzawl, Saitual, and Serchhip. A general north-central concentration is visible, with CHCs fairly dispersed in the upper half of the state, aligned in a northwest-southeast axis. In contrast, southern and southwestern districts, including Lawngtlai, Saiha, and parts of Lunglei, exhibit either minimal or complete absence of CHCs. Geospatial markers in the map confirm that CHCs are not uniformly spread but are concentrated in more elevated or centrally accessible regions. The spatial logic appears partially consistent in the north, but becomes more fragmented and sparser in the south.The right panel illustrate the distribution of Sub-District Hospital (SDH) in the state. Only two districts host an SDH, Lunglei and Aizawl. The SDH in Lunglei sits on the Indo-Bangladesh border catering to the secondary health needs of the rural residents whereas the other SDH sits in the Aizawl city municipal area. The rest of the districts remain entirely devoid of an SDH infrastructure.

Both maps collectively highlight the dire nature of secondary care in the state, with 4 districts without a CHC and 9 district without any SDH. On top of this paucity in secondary facilities, we can see a subtle yet pronounced regional disparity in the distribution, with a marked deficit in the southern districts. While some clustering is evident around regional nodes, large spatial voids persist, particularly in the western lowland high-risk zones.

4.5.3 Discussion on Secondary Healthcare Gaps

The spatial mismatch revealed by the choropleth highlights systemic gaps in Mizoram's secondary healthcare infrastructure. The Indian Public Health Standards (IPHS 2012) prescribe one CHC per 80,000 population, to be strategically positioned to bridge accessibility gaps between PHCs and tertiary facilities. CHCs are designed to serve as First Referral Units (FRUs)—handling maternal health, minor surgeries, basic diagnostics, and emergencies. However, the maps suggest that Mizoram's CHC allocation deviates from this mandate. Several districts, particularly in the south, fall short of the recommended coverage, undermining referral efficiency.

The geographical clustering of CHCs in the north-central districts appears to favour population cores or administrative hubs, rather than spatial equity. In terrain-challenged regions like Mizoram, such placement decisions amplify regional health disparities, especially where monsoon disruptions, road failures, or long travel times are frequent. SDHs, intended to offer more advanced services than CHCs including specialist consultation and diagnostic support, are almost entirely absent. The lone functional peripheral SDH in Tlabung (Lunglei district) is well-situated in a vulnerable lowland region but, as field observation indicates, suffers from severe under-resourcing. Lacking adequate staffing, equipment, or supporting PHC networks, its real-world function barely surpasses that of a large PHC, thus failing its IPHS role as a secondary referral hub.

Further compounding the issue is the nominal upgrade of former SDHs in districts like Khawzawl, Saitual, and Hnahthial. While these were reclassified as District Hospitals following administrative bifurcation in 2019, their operational capacities remain stagnant, rendering them ineffective in absorbing rural patient loads or offering higher-order services.

The consequence is twofold: (1) tertiary hospitals in Aizawl and Lunglei become overburdened, and (2) rural patients are forced to bypass intermediate care, bearing the full brunt of financial, temporal, and physical access costs. This creates a cascading effect of inequality, wherein location determines the quality and level of care accessible, despite official parity in service designation.

Addressing this issue demands urgent spatial reallocation and infrastructure upgrading. CHCs must be extended to underserved southern districts, with placement based on terrain, settlement isolation, and climate vulnerability rather than population density alone. Simultaneously, existing SDHs must be functionally upgraded to meet secondary care standards, including staffing norms, diagnostic infrastructure, and linkages with PHCs. Without such targeted intervention, Mizoram's healthcare pyramid remains top-heavy, with rural peripheries structurally excluded from equitable access.

4.5.4 GIS Mapping of Hospitals in Mizoram 2021

Map 4.5 illustrates the distribution of hospitals across Mizoram's 11 districts, measured in terms of hospital density per 1,000 population. The dataset, sourced from the Mizoram Hospital Statistics Report (2021) shows hospitals with red circles denoting 3 km catchment area and the blue-to-purple gradient scale reflecting district-wise hospital density.

Map 4.5 Distribution of Hospitals in Mizoram

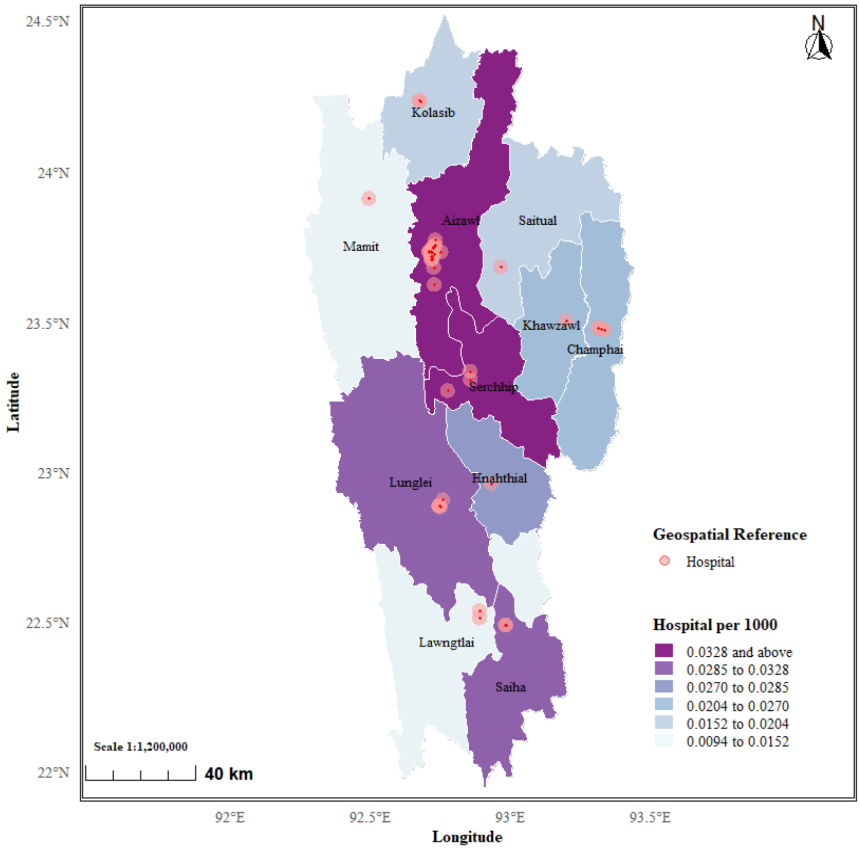

Source: Own visualisation based on Mizoram Hospital Statistics Report (2021)

Aizawl district emerges as the state hotspot in tertiary care, displaying the highest hospital density (0.044). Its urban core shows high spatial agglomeration, with hospitals concentrated within a small area, signifying superior access for urban residents. In stark contrast, southern districts like Lawngtlai, Saiha, and parts of Lunglei are more thinly populated with hospitals, despite their expansive land coverage and ecological vulnerability. Peripheral western regions especially parts of Mamit and Lawngtlai, are noticeably underserved. Aizawl's central clustering creates a visible centripetal pattern, where hospitals are pulled toward the state's administrative and economic core, while remote, western lowland, and high-risk zones remain without adequate tertiary support.

Mid-tier hospital densities are seen in Serchhip (0.037) and Champhai (0.034), where facilities are more dispersed but still accessible owing to their smaller geographic bounds. On the lower end of the spectrum, Mamit (0.009), Saitual (0.015), and Khawzawl (0.023) exhibit sparse tertiary infrastructure, often represented by just one or two hospitals for the entire district.

An observable spatial trajectory also follows the alignment of National Highway 2 (NH-2), the main arterial route bisecting the central highland spine of Mizoram. This concentration along the north-south highway corridor reflects transport-oriented facility placement. However, it leaves the western belt and deep southern fringes with limited coverage, reinforcing spatial isolation and access delays for rural populations

4.5.5 Discussion on the distribution Hospitals in Mizoram

The choropleth reveals dense clustering and overlapping in the state's capital, and also in urban regions of Lawngtlai, Lunglei and Serchhip, indicating concentrated tertiary infrastructure. At the same time, visible intra-district disparities, particularly across the western and southern fringes, highlight uneven access within districts themselves. The current population-based allocation has left large peripheral and rural regions relatively underserved. While these institutional placements are largely fixed, improving physical connectivity, especially rural road links to tertiary hubs is evidently essential for ensuring timely access for remote residents.

4.5.6 GIS Mapping of Result of Overall Healthcare Facilities in Mizoram

Map 4.6 presents the full spatial layout of Mizoram's public health infrastructure, overlaying the locations of all Primary Health Centres (PHCs), Community Health Centres (CHCs), Sub-District Hospitals (SDHs), and Hospitals on a district-wise density gradient. This composite view illustrates the broader structure of the healthcare network across the state and intra-district asymmetry.

Map 4.6 Distribution of Health Facilities in Mizoram

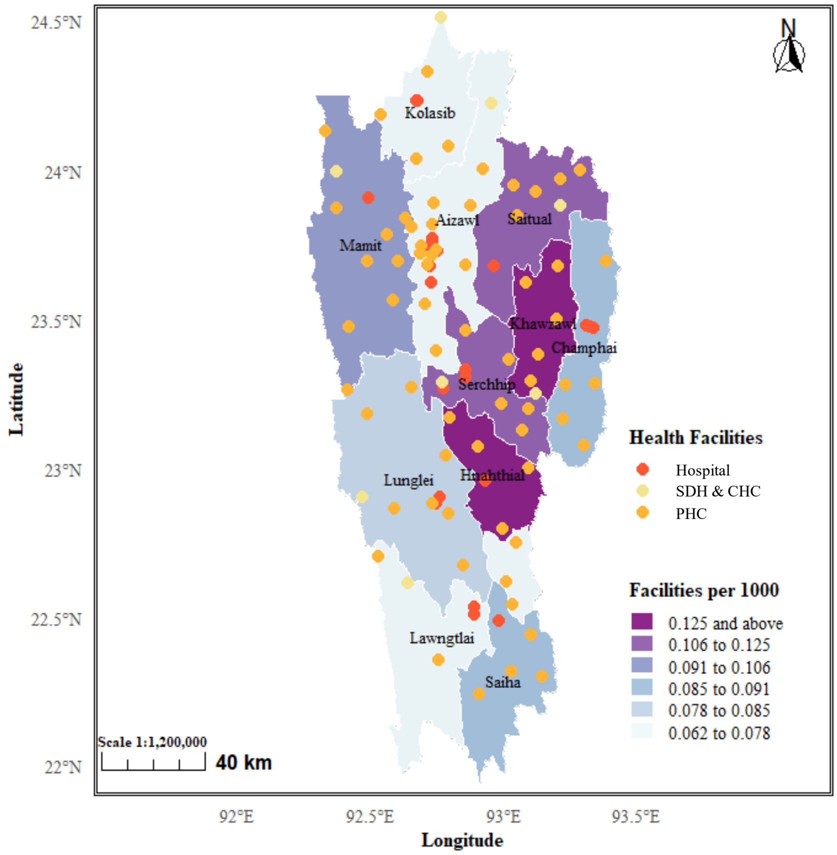

Source: Own visualisation based on Mizoram Health Institutions (2018), Mizoram Statistical Abstract (2021)

Clusters of health facilities are most visibly concentrated in the central and eastern districts, with dense overlaps in urban and peri-urban areas such as Aizawl, Lunglei, and Serchhip. In contrast, the western and southern districts, particularly Mamit, Lawngtlai, and parts of Lunglei exhibit an apparent spatial paucity. Several segments along the western and southwestern frontiers remain sparsely dotted, if at all, suggesting limited physical presence of formal health infrastructure.

The spatial alignment of facilities largely follows the NH-2 corridor, forming a linear pattern from the northern to the southern spine of the state. Facilities are positioned along this transport axis, leaving settlements further from this corridor at a relative disadvantage. This is especially evident in the west-facing slopes and interior forested regions of the southern districts. A degree of intra-district disparity is also visible. For instance, while some district headquarters show considerable facility agglomeration, surrounding rural blocks have minimal coverage. Some CHCs and SDHs appear strategically placed at a moderate remove from the urban hubs, yet in other areas, these facilities are clustered within existing tertiary-rich zones, limiting their intended function as intermediate access points.

The eastern belt, though less populated, is better served than the west in terms of spatial distribution, indicating a tilted allocation pattern favouring population density over geographic spread. These imbalances reveal that although overall facility counts may seem adequate, spatial reach remains uneven.

4.5.7 Discussion on Health Infrastructure Mapping

The spatial layout in Choropleth 4.6 reflects a cumulative pattern observed across the previous facility-specific maps: the system is anchored around a few high-density cores while substantial gaps persist in the outer peripheries. The agglomeration of PHCs, CHCs, and hospitals in and around Aizawl, Lunglei, and Serchhip suggests a layering effect, where new facilities are often established near pre-existing ones. This clustering may benefit from resource sharing and administrative convenience but does little to improve service for isolated or vulnerable regions.

The lack of spatial balance is especially pronounced in the western and southern stretches, where limited facility presence correlates with difficult terrain and sparser road infrastructure. While facility placement decisions may have been influenced by administrative accessibility and demand load, the consequence is a geographically uneven healthcare environment. These are not new allocations, and many have been in place for over a decade. As such, spatial redistribution is unlikely in the near future. However, gaps in geographic accessibility, particularly for rural populations, can still be addressed through improved referral linkages, mobile services, or investments in transport and telemedicine systems.

The composite georeferencing of health facilities reveals an uneven distribution across healthcare tiers, with some regions exhibiting a higher concentration of facilities than others. A distinct spatial pattern in facility placement indicates inconsistent allocation across the state. Furthermore, the distribution, primarily based on population, largely overlooks regions with higher disease loads and risks. To address these disparities, future planning must prioritize detailed analysis of distribution patterns and disease burden to ensure equitable facility placement across all tiers.

4.5.8 Boundary Classification and Reporting Issues

Some facilities appear spatially located in one district but are reported under another in official records. Lengpui PHC, for instance, is located within the geographical boundary of Mamit but is attributed to Aizawl district in HMIS. This results from a misalignment between administrative and health reporting boundaries.

4.6 DISTRIBUTION OF BEDS IN MIZORAM

This section aggregates the raw count of health facility beds across Mizoram’s districts in 2021, highlighting variations in healthcare infrastructure allocation among the districts. The term “health facility beds” used here refers to beds in Primary Health Centres (PHCs), Community Health Centres (CHCs), Sub-District Hospitals (SDHs), and District Hospitals, encompassing all levels of care without distinguishing bed types example, ICU or maternity. Data are compiled from the Mizoram Statistical Abstract (2021) and the Mizoram Hospital Statistics Report (2021). Subsequent sections will employ graphs and choropleth maps to further explore these distributions and their implications for healthcare access.

4.6.1 Absolute Health Facility Beds in Mizoram

Table 4.8 summarizes the distribution of 3,744 health facility beds across 11 districts, segmented by PHCs (648 beds), CHCs (270 beds), SDHs (80 beds), and District Hospitals (2,746 beds) at an average of roughly 340 beds per district.

Table 4.8 Distribution of Health Facility Beds in Mizoram 2021

SN	Districts	PHC	CHC	SDH	Hospitals	Total Beds
1	**Aizawl**	98	90	50	1841	2079
2	**Champhai**	50	0	0	142	192
3	**Hnahthial**	40	0	0	30	70
4	**Khawzawl**	40	30	0	21	91
5	**Kolasib**	50	30	0	80	160
6	**Lawngtlai**	60	30	0	105	195
7	**Lunglei**	90	0	30	220	340
8	**Mamit**	80	30	0	30	140
9	**Saiha**	40	0	0	160	200
10	**Saitual**	50	30	0	30	110
11	**Serchhip**	50	30	0	87	167
*****	**Mizoram**	648	270	80	2746	3744

Source: Mizoram Statistical Abstract (2021), Mizoram Hospital Statistics report (2021)

In absolute numbers, Aizawl district has the most beds, 2,079 (55.5% of the total), with 1,841 in District Hospitals (88.6% of its total), indicating a strong concentration of bed facilities. Hnahthial has the fewest beds, 70 (1.9%), primarily in PHCs (40 beds). All districts lag significantly behind Aizawl's scale of concentration. The limited number of mid tier care beds, 270 CHC beds and 90 SDH beds, across the state suggests constrained intermediate care capacity, potentially straining the linkage between the primary and secondary system.

Lawngtlai (195), Lunglei (340), Saiha (200 beds) and Champhai (192 beds) have moderate bed counts but remain far below Aizawl's level. These findings suggest that, beyond the uneven distribution of health facility buildings, bed capacity is also unevenly allocated across Mizoram's civil hospitals, potentially exacerbating spatial inequality.

4.6.2 Health Facility Beds per 1000 in Mizoram in 2021

The equitable distribution of health care facilities is critical for ensuring access to quality care, particularly in a geographically challenging state like Mizoram. Table 4.8 presents the distribution of health facility beds per 1,000 population across Mizoram's districts in 2021, disaggregated by primary, secondary and tertiary levels, calculated based on the Mizoram Statistical Abstract (2021) and Population projection (2021).

The state average of 2.76 beds per 1,000 population is below the World Health Organization's recommended 3.5 beds per 1,000 (WHO, 2010), reflecting a general scarcity of healthcare infrastructure. Aizawl district stands out with the highest bed density at 4.62 per 1,000, driven by a substantial concentration of private hospital beds (0.284 per 1,000), which account for 61.5% of its total capacity.

Table 4.9 Health Facility Beds Per 1000 in Mizoram 2021

SN	Districts	PHC	CHC	SDH	District Hospitals	Total Beds
1	Aizawl	0.22	0.20	0.11	4.09	4.62
2	Champhai	0.57	0.00	0.00	1.61	2.18
3	Hnahthial	1.14	0.00	0.00	0.85	1.99
4	Khawzawl	0.90	0.68	0.00	0.47	2.05
5	Kolasib	0.48	0.29	0.00	0.77	1.54
6	Lawngtlai	0.41	0.21	0.00	0.72	1.34
7	Lunglei	0.55	0.00	0.18	1.34	2.07
8	Mamit	0.75	0.28	0.00	0.28	1.31
9	Saiha	0.57	0.00	0.00	2.29	2.86
10	Saitual	0.75	0.45	0.00	0.45	1.65
11	Serchhip	0.62	0.37	0.00	1.09	2.08
*	Mizoram	0.48	0.20	0.06	2.03	2.76

Source: Own calculation based on data from Mizoram Statistical Abstract (2021), Mizoram Hospital Statistics (2021)

Southern districts lag in primary care bed availability, with similar deficiencies in secondary care (CHC and SDH), alongside Champhai in the east.

Tertiary care shows Aizawl with the highest bed concentration, followed by Saiha, while Lunglei, Serchhip, and Champhai form a middle tier. Lawngtlai, Hnahthial, Khawzawl, Saitual, Kolasib, and Mamit exhibit lower tertiary bed density, with Mamit the least served. The uneven distribution can increase healthcare access barriers, higher out-of-pocket costs, and overburdened urban facilities, particularly for rural populations deepening inequality in the state.

Map 4.7 visualizes the spatial distribution of health facility beds per 1,000 population from Table 4.9, showing four panels for PHC, CHC, SDH, and District Hospitals beds distribution.

Map 4.7 Health Facility Beds Per 1000 in Mizoram (2021)

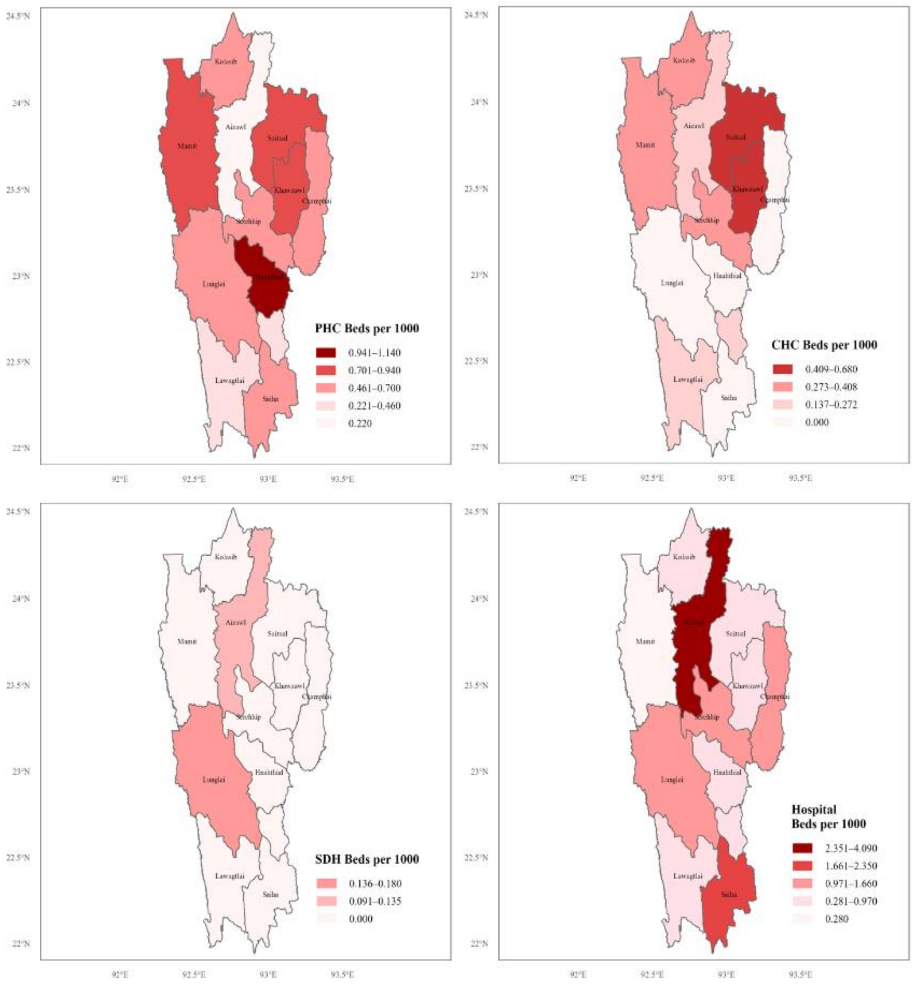

Note: Own visualisation based on data from Mizoram Statistical Abstract (2021) & Mizoram Hospital Statistics Report (2021)

4.6.3 Discussion on Urban centric Concentration of Beds

The concentration of beds in Aizawl, driven by a high concentration of tertiary care, reflects both policy bias and private sector dynamics in resource allocation. The substantial presence of private hospital beds in Aizawl, facilitated by past government's policies, exacerbates this urban-centric model, as private providers typically favour economically vibrant areas.

Map 4.8 Total Health Facility Beds Per 1000 in Mizoram ((2021)

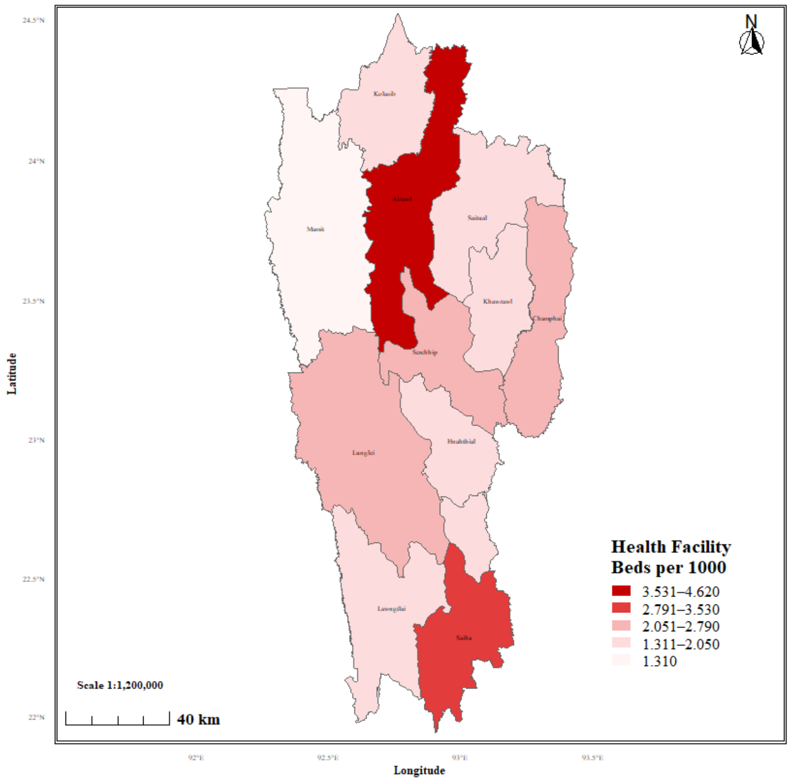

Source: Own visualisation based on Mizoram Statistical Abstract (2021), Mizoram Hospital Report (2021)

Aizawl's concentration of health facility beds results in a density of 4.62 per 1,000 population, exceeding the OECD average of 4.4 per 1,000 and surpassing high GDP per capita countries like Switzerland (4.48 per 1,000) and Iceland (2.84 per 1,000), is a remarkable anomaly. Aizawl's bed density is comparable to mountainous OECD urban regions, such as Oslo, Norway, with a bed density of approximately 4.5 per 1,000 in 2021 (Health at a glance, 2021). Compared to the Indian Public Health Standards (IPHS) 2012 benchmark of 1 to 2 beds per 1000, the concentration in Mizoram is absurdly disproportionate (IPHS, 2012). While urban concentration of tertiary care is common in developing countries, the scale in which Aizawl is agglomerated is unreasonable, far exceeding typical urban concentrations in developing countries around the world. For instance, developing nations like South Africa, with approximately 2.8 hospital beds per 1,000 people nationally, has a concentration of 2.7 beds per 1,000 in Johannesburg (Gauteng Department of Health, 2018). Ethiopia, with 0.3 beds per 1,000 nationally, has its capital Addis Ababa at 1.8 beds per 1,000 (Woldemichael et al., 2021). The Philippines, with 1.0 bed per 1,000 nationally, has 1.35 beds per 1,000 in the Metro Manila region (Statista, 2021).

Concentration imposes high out-of-pocket costs for travel and treatment, especially for those who poor but not destitute poor to qualify for free healthcare but must bear these expenses. The consequences of this skewed distribution could profoundly impact Mizoram's overall well-being, particularly in rural and peripheral hinterlands. Aizawl's small area (0.33% of the State), is inadequate to serve the entire state, especially for southern districts facing long travel times and geographic isolation.

The low bed density in high-risk tropical zones like Mamit, Kolasib, Lawngtlai, and Lunglei may also increase case fatality rates for endemic diseases like malaria. Chronic conditions requiring ongoing medical attention, such as diabetes or cardiovascular diseases, may also be underserved in rural areas, potentially worsening health outcomes and increasing long-term morbidity. These issues and concerns perpetuate spatial inequality, undermining equitable healthcare access and highlighting the need for policy interventions to rebalance resources and enhance rural healthcare infrastructure.

4.7 ANALYSIS OF BED ALLOCATION USING THIEL-T INDEX

To assess disparities in healthcare resources across Mizoram, data from Population projection (2021), and bed allocations for rural and urban areas of Mizoram was sorted from Mizoram Statistical Abstract (2021) and Mizoram Hospital Statistics Report (2021). The data cover 1,354,830 people, 709,157 rural and 645,673 urban, spanning 3,744 beds, 918 rural and 2,826 urban, sorted into urban and rural subgroups per district for within-group analysis and into district totals for between-group comparisons. This approach enabled accurate estimation of inequality contributions made within districts and between the 11 districts of Mizoram. Consequently, a Theil-T index analysis was performed. Key results are discussed below while other details of the analysis, such as tables are provided in the Appendix I & II.

4.7.1 Result of Theil T Index

The analysis yields a Theil-T index of 0.2532, derived from the sum of within-group and between-group components, indicating a moderate level of inequality in health facility bed allocation in Mizoram. The within-group inequality contributes 0.1324 or 52.3% and the between-group inequality contributes 0.1209 or 47.7% of the total Theil-T Index.

Table 4.10 **Theil-T Index Decomposition of Health Facility Bed Inequality in Mizoram, 2021**

Metric	Value
Total Theil-T Index	0.2532
Within-Group Theil-T	0.1324
Between-Group Theil-T	0.1209
Percentage Within-Group	52.3
Percentage Between-Group	47.7

Note: Own calculation

The near-equal contribution of these components, within-group and between group, indicates that both urban-rural disparities within districts and variations across districts are significant drivers of overall inequality. The index value suggests that while geographic disparities may exist, the state overall does not exhibit severe inequality as population density is an equalizing factor, consistent with earlier analyses.

4.7.2 Theil-T Within Group Result

The within-group inequality, Table 4.10, quantifies disparities between urban and rural areas within each district, weighted by district population shares. Lawngtlai (0.0358) and Lunglei (0.0325) are the largest contributors of inequality, accounting for approximately 27% and 25% of the total within-group component, respectively. These districts exhibit pronounced urban-rural gaps, with Lawngtlai's urban areas having 4.082 beds per 1,000 persons compared to 0.751 in rural areas, and Lunglei's urban areas at 4.064 versus 0.877 in rural areas. A finding consistent with earlier GIS studies.

Table 4.11 Thiel-T Within Group Contribution

District	District Pop Share	Within Theil
Aizawl	0.3324	0.0276
Champhai	0.0649	0.0121
Hnahthial	0.0259	0.0019
Khawzawl	0.0327	0.0016
Kolasib	0.0765	0.0005
Lawngtlai	0.1075	0.0358
Lunglei	0.1212	0.0325
Mamit	0.0787	0.0004
Saiha	0.0516	0.0138
Saitual	0.0493	0.006
Serchhip	0.0592	0.0001

Note: Own calculation

Aizawl also contributes significantly (0.0276), driven by its urban hospital bed allocation of 5.434 per 1000 persons compared to 2.241 in rural areas. Champhai's within-group contribution (0.0121), although small, reflects a gap between urban (5.985 beds per 1,000 persons) and rural (0.918) allocations, while Saiha's (0.0138) arises from a similar urban-rural divide, 5.161 vs. 1.029 beds per 1000. In contrast, Kolasib, Mamit, and Serchhip show near-negligible within-group inequality (0.0005, 0.0004, 0.0001), as urban and rural allocations are closely aligned reflecting their balanced urban-rural bed distributions. The dominance of within-group inequality at 52.3% highlights that addressing urban-rural disparities within some districts is necessary in Mizoram.

4.7.3 Theil-T Between Group Result

The between-group inequality, Table 4.11, examines variations in average bed allocation across districts. Aizawl, with an average of 4.615 beds per 1,000 persons and a population share of 33.24%, contributes substantially to between-group inequality (0.2848), reflecting its high bed availability relative to the state mean of 2.764 beds per 1,000 persons. Districts with below average bed allocations, such as Lawngtlai (1.340, -0.0377), Mamit (1.313, -0.0278), and Saitual (1.197, -0.0179), contribute negatively, indicating their relative resource scarcity. The between-group contribution, 47.7% of inequality, highlights regional disparities, reflecting a consistent North-South disparity we have seen from earlier analyses, here shown by disproportionate share of health facility beds among the districts.

The Theil-T results complement earlier analyses of healthcare disparities in Mizoram. GIS mapping identified a North-South disparity, with Lawngtlai and Lunglei hosting 18 spatial deserts within 7 km facility buffers, aligning with their high within-group Theil-T contributions (0.0358, 0.0325) due to rural bed shortages (0.751 and 0.877 beds per 1,000 persons).

Table 4.12 Thiel-T Between Group Result

District	District Pop Share	District Beds per Capita	X_k / μ	$ln(X_k / \mu)$	Between Contribution
Aizawl	0.3324	0.004615	1.67	0.5129	0.2848
Champhai	0.0649	0.002525	0.9138	-0.0901	-0.0053
Hnahthial	0.0259	0.001991	0.7206	-0.3276	-0.0061
Khawzawl	0.0327	0.002051	0.7424	-0.298	-0.0072
Kolasib	0.0765	0.001543	0.5584	-0.5829	-0.0249
Lawngtlai	0.1075	0.00134	0.4849	-0.7243	-0.0377
Lunglei	0.1212	0.002071	0.7495	-0.2884	-0.0262
Mamit	0.0787	0.001313	0.4752	-0.7445	-0.0278
Saiha	0.0516	0.002863	1.036	0.0354	0.0019
Saitual	0.0493	0.001197	0.4333	-0.8367	-0.0179
Serchhip	0.0592	0.002083	0.7538	-0.2825	-0.0126

Source: Own calculation

Mamit and Kolasib, flagged for tropical disease risk, show low within-group inequality (0.0004, 0.0005) but negative between-group contributions (-0.0278, -0.0249), indicating overall bed scarcity that may heighten health vulnerabilities. These findings suggest that policy interventions should prioritise increasing bed availability in rural areas of districts like Lawngtlai and Lunglei, where urban-rural disparities are most pronounced, and redistributing resources to districts with low allocations, such as Mamit and Saitual, to address regional inequalities.

4.7.4 Limitations

It bears noting that, although the Thiel-T Index is a robust and reliable measure of spatial inequality, it is not without limitations. It assumes all beds offer comparable healthcare, which may oversimplify difference in quality of care. The GIS-based study prior showed that some districts rely on lower-quality primary health centre beds while others offer unprecedented OCED level hospital bed density. The Thiel-T also fails to capture the role distances play in equitable healthcare access. In other words, the Theil-T index captures bed quantity disparities but not quality or accessibility. Nevertheless, the decomposition of within districts and between districts provides a clear basis to identify where spatial inequality exist and can help redirect targeted spatial interventions to enhance equitable healthcare access in Mizoram (Theil, 1967).

4.8. DISTRIBUTION OF MEDICAL EQUIPMENT IN MIZORAM

To analyse the nature of medical equipment distribution in Mizoram, 10 types of units, out of 16, were selected, based on clinical relevance from the Mizoram Hospital Statistics Report (2021). The types of diagnostic unit selected are Ultrasound, ECG, CT-Scan, ECHO, Chemotherapy, Radiotherapy, Dialysis, Bronchoscopy, and Endoscopy.

4.8.1 Absolute distribution on Medical Equipment in Mizoram

Graph 5.6 represents the total number of medical equipment hold by each district in 2021.

Graph 4.3 **Absolute Share of Medical Equipment by District (2021)**

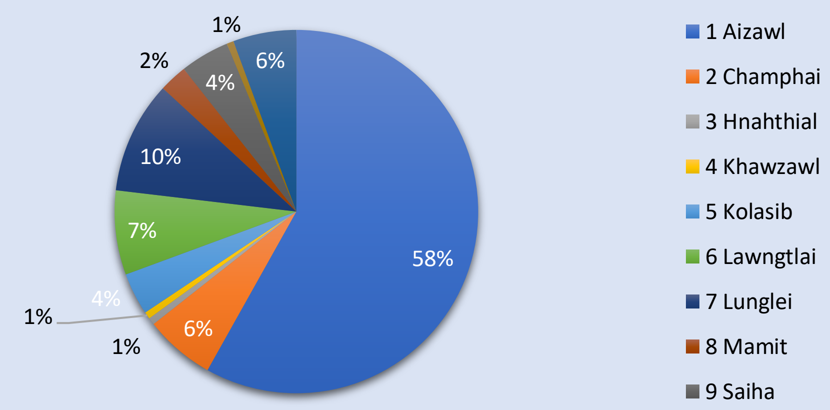

Aizawl, the state's main healthcare centre, holds 93 units (58.1%), including 18 X-ray machines, 16 Ultrasounds, 17 ECGs, 9 CT-Scans, 7 ECHO machines, 4 Chemotherapy units, 1 Radiotherapy unit, 7 Dialysis units, 3 Bronchoscopy units, and 11 Endoscopy units, reflecting its concentration of health facilities. In contrast, districts like Hnahthial, Khawzawl, and Saitual each have only one X-ray machine, indicating limited diagnostic capacity. Lunglei (16 units) and Lawngtlai (12 units) have moderate resources but lack advanced equipment like CT-Scans or ECHO. Other districts, Champhai, Kolasib, Mamit, Saiha, and Serchhip range from 4 to 10 units, mostly low-end technology like X-ray, Ultrasound, and ECG.

Across Mizoram, X-ray (37 units), ECG (34 units), and Ultrasound (29 units) are most common, while Chemotherapy (6 units) and Radiotherapy (1 unit) are scarce, suggesting limited cancer care. Endoscopy (21 units) and Dialysis (12 units) are somewhat better distributed but still concentrated in Aizawl. This distribution as illustrated by chart 5.1 suggests an overall low technological reach, highly concentrated, common with developing countries around the world.

4.8.2 Medical Equipment per 1000 in Mizoram

In this section the per capita distribution of medical equipment, measured by medical equipment per 1,000 population, across Mizoram's 11 districts is analysed. Statewide, Mizoram averages 0.118 equipment units per 1,000 people, with X-rays (0.027) being the most widely distributed while Radiotherapy (0.001) being the least distributed.

At the district level, Aizawl exhibits the highest per capita availability at 0.206 units, with notable densities in X-ray (0.040), Ultrasound (0.036), ECG (0.038), and CT-Scan (0.020). Champhai (0.114) and Serchhip (0.112) form the mid-tier, with access primarily to basic diagnostics (X-ray, Ultrasound, ECG). Lunglei (0.097), Saiha (0.100), and Lawngtlai (0.082) followed with moderate access but limited advanced equipment, such as Lunglei's CT-Scan (0.006) and Chemotherapy (0.006). The least equipped districts—Saitual (0.015), Khawzawl (0.023), Hnahthial (0.028), Kolasib (0.058), and Mamit (0.038)—rely almost solely on X-ray units.

Map 4.9 Medical Equipment Per 1000 in Mizoram (2021)

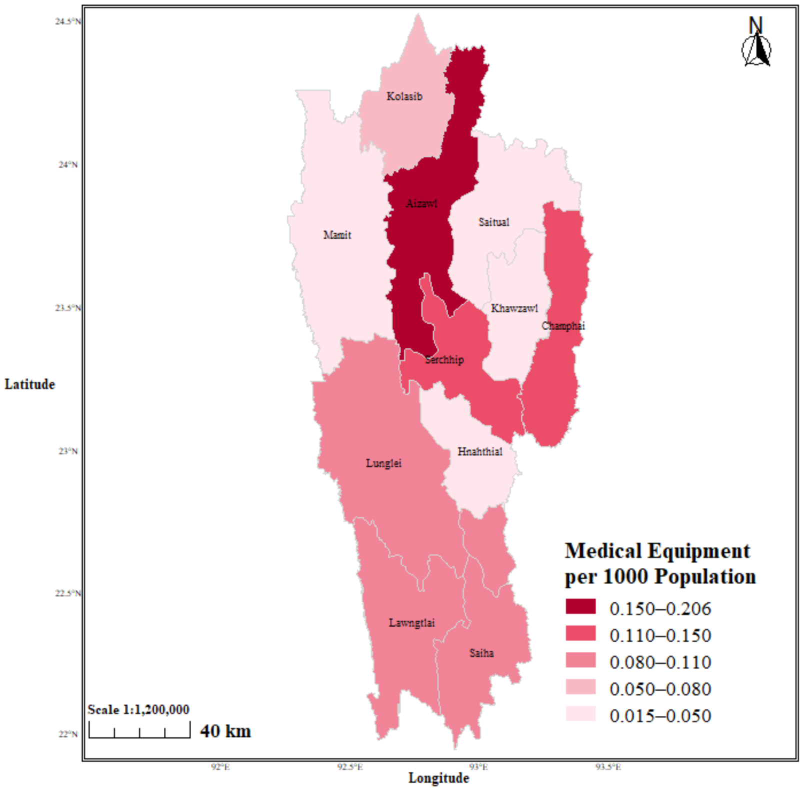

Note: Own Visualisation based on data from Mizoram Hospital Statistics (2021)

Map 4.9 illustrates the medical equipment per 1000 population in Mizoram, showing that medical technology is concentrated in Aizawl District. Districts such as Hnahthial, Mamit, Saitual, and Khawzawl have scare medical equipment resource relative to their population. The other districts such as Serchhip and Champhai occupy the second tier while Kolasib, Lunglei, Lawngtlai and Saiha are barely better off than the bottom districts. This analysis shows that most of Mizoram's advanced medical equipment is concentrated in Aizawl district, while other districts have very limited access. The analysis also reveals that Mizoram is lagging behind in the Medtech space compared to the rest of India, many districts rely on basic medical equipment and there is little specialization except in the case of Aizawl.

4.9 MEDICAL EQUIPMENT USAGE INEQUALITY

This analysis examines whether the usage of the 10 medical equipment types, namely X-ray, Ultra sound, ECG, CT-Scan, ECHO, Chemotherapy, Radiotherapy, Dialysis, Bronchoscopy, and Endoscopy, reflects population-based expectations. From the previous sections, we have established that Aizawl is a healthcare hub, meaning patients flow to the city. At the same time the lack of patient migration data makes it impossible to fairly quantify actual disparities as the actual usage data may be skewed.

To measure equity, the study compares actual usage of medical equipment to an expected benchmark derived from each district's population share (table 5.10). This approach assumes that, in an ideal scenario, usage should align proportionally with population, reflecting uniform healthcare needs across districts. By calculating expected usage as the product of a district's population share and total usage, the approach highlights disparity which otherwise was not captured by the actual usage data. Deviations from this expected benchmark, captured as usage ratios, may point to underlying issues in access or resource distribution.

Table 4.13 Medical equipment Expected Usage in Mizoram 2021

District	Population	Actual Usage	Expected Usage	Migration Proxy	Usage / Expected
Aizawl	450,444	140,888	65,293	**75,595**	2.158
Champhai	87,929	8,761	12,746	−3,985	0.687
Hnahthial	35,152	488	5,095	−4,607	0.096
Saiha	69,858	5,326	10,126	−4,800	0.526
Kolasib	103,668	8,956	15,027	−6,071	0.596
Khawzawl	44,368	146	6,431	−6,285	0.023
Serchhip	80,184	4,689	11,623	−6,934	0.403
Lunglei	164,179	16,298	23,798	−7,500	0.685
Saitual	66,831	566	9,687	−9,121	0.058
Mamit	106,642	2,882	15,458	−12,576	0.186
Lawngtlai	145,575	7,385	21,101	**−13,716**	0.350

Source: Own calculation base on Mizoram Hospital Statistics Report (2021)

Evidently, Aizawl receives all the migrating diagnostic users, 75,595 in total, whereas all other districts witnessed patients departing from their healthcare system. Lawngtlai and Mamit district sees the highest number of patients migrating, hinting a severe lack of health facility in their respective districts.

Aizawl dominates with 140,888 usage record against an expected 65,293, yielding a usage ratio of 2.158. In contrast, Khawzawl (146 actual usage, ratio 0.023) and Hnahthial (488 usage, ratio 0.096) show minimal activity, while Lunglei's 16,298 instances (ratio 0.685) indicate moderate usage, showing its potential as a secondary health hub. These ratios highlight a skewed distribution, with most districts falling far below their expected share, losing patients to Aizawl. This finding corroborates the earlier findings on spatial concentration of health facility, suggesting that concentration of medical equipment mirrors concentration of health facilities causing widespread economic cost for peripheral districts in accessing healthcare.

Graph 4.5 illustrates the expected disparity from Table 4.13 against the equality line (ratio=1).

Graph 4.4 Service Utilization Disparity by District

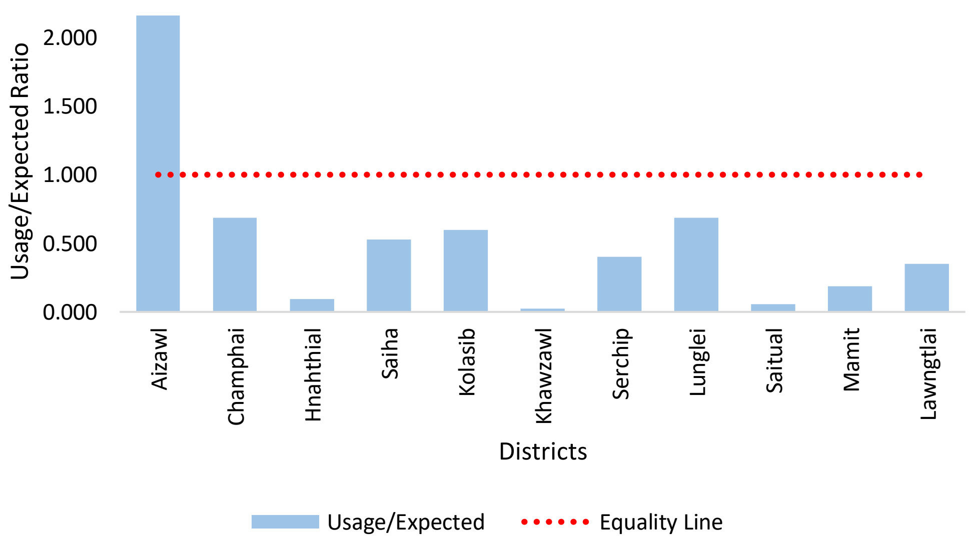

The graph visually highlights the imbalance in service utilization across districts, with Aizawl far exceeding the expected ratio while all other districts fall below the equality line. This indicates that diagnostic equipment utilization is heavily concentrated in Aizawl, with significant underutilization in the rest of the state. The difference is especially concerning for some districts, as seen by their near-zero ratios.

4.9.1 Atkinson Index on Medical Equipment Utilization

To test the statistical significance of disparities in service usage, the Atkinson Index was calculated at inequality aversion levels (ε) of 0.5, 1, 1.5, and 2, allowing for a graduated assessment of inequality under increasing sensitivity to deprivation. Bootstrapping was applied to ensure the robustness of these estimates, minimizing the influence of sample variability. As the level of aversion to inequality increases, the index places greater weight on under-served districts, helping to reveal how deep the disparities become when more emphasis is placed on those with the least access. The resulting values are summarized below.

Table 4.14 **Atkinson Index Summary**

ε	Atkinson_Index	Mean	Std_Error	CI_Lower_95%	CI_Upper_95%
0.5	0.597	0.578	0.137	0.251	0.789
1	0.714	0.690	0.116	0.413	0.867
1.5	0.812	0.787	0.096	0.532	0.911
2	0.877	0.842	0.092	0.581	0.937

Source: Own calculation

The Atkinson Index results reveal pronounced disparities in equipment usage. At $\varepsilon = 0.5$, the index is 0.597, with a bootstrap mean of 0.578, a standard error of 0.137, and a 95% confidence interval (CI) from 0.251 to 0.789. As ε increases (at $\varepsilon = 1$), the index rises to 0.714, with a mean of 0.690, CI 0.413 to 0.867. The inequality becomes even more severe at higher levels of ε, with the Atkinson index rising to 0.812 at $\varepsilon = 1.5$ and 0.877 at $\varepsilon = 2$. This progressive steepening of inequality with higher ε values highlights the extent to which aggregate figures can obscure deep structural imbalances. While moderate inequality is evident even at low aversion levels, the sharply rising Atkinson scores at ε = 1.5 and 2 suggests that a small number of districts are absorbing most of the shortfall in access. This not only validates the spatial concentration of health infrastructure but also reveals that marginal improvements would yield the greatest equity gains if targeted toward these severely underserved areas.

Graph 4.5 **Atkinson Index of Access to Health Equipment**

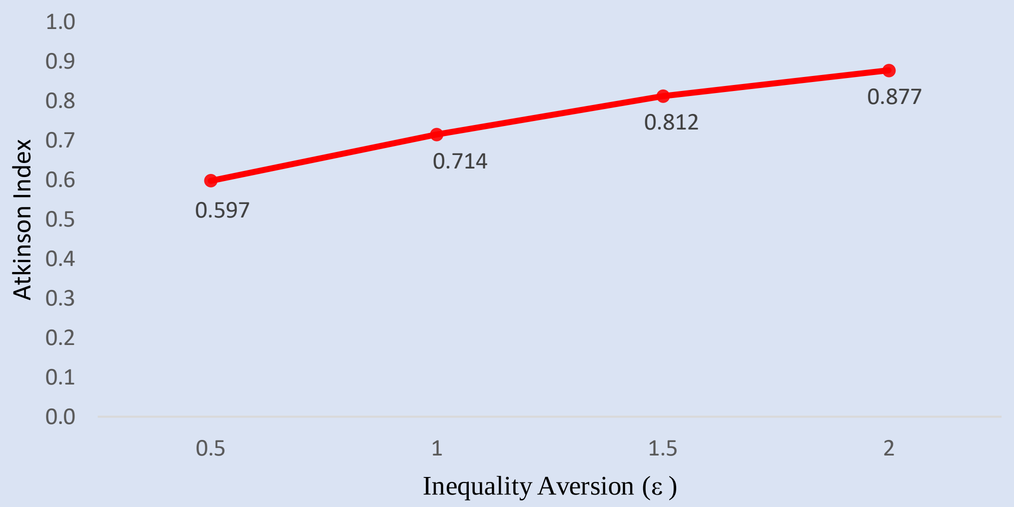

Graph 4.6 illustrates the Atkinson Index values, at ε = 0.5, 1, 1.5 and 2, against the expected usage ratio to show how inequality intensifies with greater aversion to low ratios. These values also suggest that the burden of unequal access is concentrated at the bottom end of the distribution. In other words, districts already lacking in medical equipment are disproportionately worse off, and the inequality deepens the further down the distribution one looks. This reflects not just a numerical trend, but also the ground reality, the most underserved districts have minimal access to essential health technologies. The Atkinson index here does more than capture variation, it confirms that the lower end of the healthcare system in Mizoram is under significant strain.

4.9.2 Discussion on Atkinson Index Results

The disparities shown by the Atkinson Index aligns with patterns of healthcare centralisation observed in other developing regions of the world (O'Donnell et al. 2008). The Atkinson Index values, particularly $\varepsilon = 0.5$, suggests severe inequality in access. In other words, the inequality of healthcare access in Mizoram is concerning even from a low inequality aversion threshold. This implies that redistributing medical equipment to align with population shares could enhance equity without reducing total services (Atkinson 1970).

Beyond this apparent disparity, the bigger issue is that Mizoram as a whole is lagging behind much of India in medical technology. This feat contradicts the fact that India is one of the largest markets in the Medtech space, both in Asia and the world (IBEF 2023). The result suggests a culmination of decades of neglect in the health sector in Mizoram. Public investment must not only correct the uneven geographic distribution of medical technology but also close the broader technological gap. What's needed is a targeted, outcome-oriented policy, grounded in budgetary commitments, not merely symbolic measures driven by political optics.

It bears noting that addressing the imbalance is not just about moving equipment from one place to another. Certain technologies especially those used in cancer care like radiotherapy (including linear accelerators, cobalt machines etc.) requires special infrastructure, trained personnel, and strict safety protocols. It is not practical or medically advisable to place them in every district. A more realistic solution would be to improve regional spatial access without trying to redistribute everything equally, using clinical relevance and disease burden of each district as a guide.

Ultimately, fixing this kind of spatial gap means more than just redistribution. It requires investment in infrastructure and support systems so that specialized services can be safely and effectively delivered outside the capital. Without that, redistribution alone will not solve the problem, in fact it could even create new ones.

4.10 SPATIAL AUTOCORRELATION ANALYSIS OF MEDICAL PERSONNEL

This section analysis the distribution of health personnel, specifically doctors and nurses, across Mizoram at the absolute and per 1000 metrics. Doctors include General practitioners, Dentists and Ayush Doctors, whereas Nurses and Health workers include, Registered Nurse (RN), Registered Midwives (RM), Lady Health Visitor (LHV), Male Health Worker (MHW) and Auxiliary Nurse Midwife (ANM) spread across govt and private health institutions across the state of Mizoram. Table 4.15 presents the district-wise distribution.

Table 4.15 District wise Distribution of Health Personnel in Mizoram 2021

SN	Districts	Doctors	Doctors per 1000	Nurse & HW	Nurse & HW per 1000
1	Aizawl	395	0.877	811	1.800
2	Champhai	34	0.387	127	1.444
3	Hnahthial	12	0.341	72	2.048
4	Khawzawl	11	0.248	66	1.488
5	Kolasib	35	0.338	119	1.148
6	Lawngtlai	36	0.247	106	0.728
7	Lunglei	55	0.335	176	1.072
8	Mamit	28	0.263	136	1.275
9	Siaha	20	0.286	71	1.016
10	Saitual	15	0.224	85	1.272
11	Serchhip	44	0.549	133	1.659
*	Mizoram	685	0.506	1902	1.671

Source: Mizoram Statistical Abstract (2022)

Aizawl, the urban and administrative hub, exhibits the highest physician density at 0.877 doctors per 1,000 population, far exceeding the state average of 0.506, while peripheral districts such as Saitual and Khawzawl lag significantly below the threshold. Nurse and health worker (HW) density similarly varies, with Hnahthial leading at 2.05 per 1,000, contrasted by critical shortages in Lawngtlai (0.73) and Saiha (1.02). These variations point to a maldistribution of clinical workforce, undermining horizontal equity and highlighting systemic inefficiencies in aligning health workforce deployment with population health needs across regions.

4.10.1 Global Moran's I and LISA Analysis of Health Personnel in Mizoram

To analyse the spatial distribution of health personnel in Mizoram Global Moran's I was employed using the Queens contiguity method in GeoDa. To further understand the localised nature of the distribution the Local Moran's I or LISA was also employed in QGIS. Due to the skewness of the raw data, particularly the high score of Aizawl, log transformation on the total health personnel was done to normalized the per 1000 distribution.

4.10.2 Result of Global Moran's I analysis on Health Personnel per 1000

The Global Moran's I statistic indicates a positive but weak spatial autocorrelation in the distribution of health personnel across Mizoram's districts (I = 0.071). However, with a Z-value of 0.9707 and a pseudo p-value of 0.1720 based on 999 permutations, the result does not attain statistical significance at conventional confidence thresholds. This suggests that the observed spatial clustering may be due to random chance rather than an underlying spatial process.

The absence of statistically significant global spatial autocorrelation can be interpreted as a reflection of the unique centrality and primacy of Aizawl in the state's health system architecture. Aizawl hosts a disproportionately high concentration of medical personnel relative to other districts, functioning as the administrative and tertiary care nucleus of Mizoram. However, this concentration is spatially isolated, as adjacent districts do not exhibit similarly elevated health workforce densities. This spatial heterogeneity, characterized by a high-value outlier surrounded by low-value neighbours, dilutes global spatial association measures.

Graph 4.6 Moran's I Statistics on Health Personnel per 1000 in Mizoram

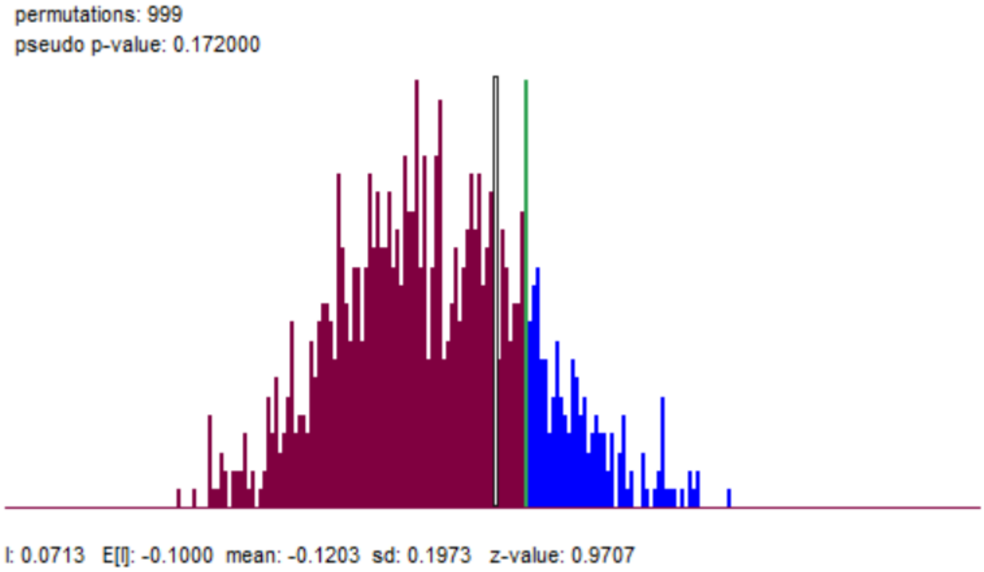

Note: Own calculation and visualization from GeoDa

It is important to note that the insignificant P value doesn't suggest that there is no concentration in health services, rather that there is no significant clustering of similar districts, meaning there is no district that is well served as Aizawl in its vicinity. This is one of the biggest limitations in spatial autocorrelation techniques such as Moran' I when applying to inequality studies with low observation points. The result highlights that the distribution of health personnel is shaped more by administrative decisions and the centralization of infrastructure in urban areas like Aizawl, rather than by the actual healthcare needs of the population or goals of equitable regional access.

4.10.3 Result Local Moran's I (LISA) on Health Personnel per 1000

The Local Moran's I analysis provides a more granular view of spatial clustering in the distribution of health personnel across Mizoram. Unlike the global test, local indicators of spatial association (LISA) revealed statistically significant spatial clusters and outliers in several districts. The results are presented below.

Table 4.16 Health Personnel Local Moran's I Summary Table

District	Local Moran's I	*Z*-score	P Value	Cluster_Type
Lawngtlai	0.209	0.6681	0.2637	High-Low (HL)
Saiha	1.3391	1.7289	0.0411*	High-Low (HL)
Saitual	-0.4228	-1.791	0.0394*	Low-Low (LL)
Aizawl	-0.2629	0.205	0.4214	Low-High (LH)
Champhai	0.0148	0.3834	0.3234	High-High (HH)
Kolasib	-0.5497	-1.8872	0.0267*	Low-Low (LL)
Mamit	-0.1844	-0.9207	0.1575	Low-Low (LL)
Serchhip	0.3431	1.6856	0.0485*	High-High (HH)
Khawzawl	0.0092	0.3983	0.3203	High-High (HH)
Hnahthial	-0.4105	-0.5719	0.2973	Low-High (LH)
Lunglei	-0.2747	-1.1495	0.1278	Low-Low (LL)

Source: Own Calculation

Saiha emerges as a statistically significant high-low outlier ($Z = 1.73$, $P = 0.0411$), indicating a district with a relatively high number of health personnel surrounded by districts with comparatively low values, suggesting a form of positive spatial outlier. Conversely, Saitual and Kolasib are identified as low-low clusters ($P < 0.05$), where both the district and its neighbours exhibit low health personnel density, signalling pockets of structural deprivation.

Additionally, Serchhip and Khawzawl register as high-high clusters, denoting localized concentrations of relatively better health staffing in contiguous regions. In contrast, Aizawl, despite being the district with the highest overall workforce density, does not form a significant cluster, and is instead categorized as low-high, further reinforcing the spatial isolation of its resource concentration, result consistent with the Global Moran's I analysis.

The LISA results, when mapped, reveal that the distribution of health personnel in Mizoram is marked by localized spatial clustering rather than uniform regional patterns. While the Global Moran’s I indicated no significant overall spatial autocorrelation, the local statistics identify specific districts exhibiting significant clustering or spatial outlier behaviour.

Map 4.10 Health Personnel Local Moran's I Clusters

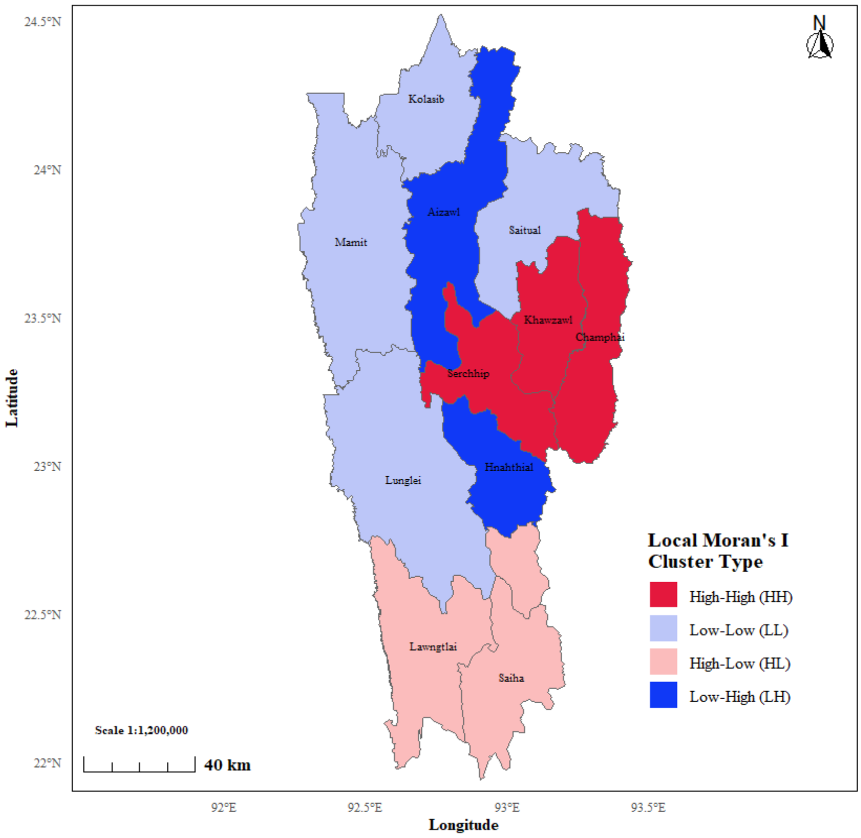

Source: Own visualisation based on data from Mizoram Statistical Abstract (2022)

These results point to spatial heterogeneity in workforce distribution, with certain districts showing relatively high or low staffing levels in contrast to their neighbours. This suggests that while some areas benefit from local concentrations of health personnel, others remain comparatively underserved. Interestingly, the LISA revealed that there is no high-high or high low clusters among the districts which were earlier identified as lowland high disease risk zones on the western belt of Mizoram. The LISA also flagged Saiha (HL) as a higher concentration of health personnel than Lawngtlai (LH). The result suggests that non only the western belts are poorly severed in infrastructure, they are also relatively poorly served in health personnel.

4.11 HEALTHCARE CATCHMENT AREA AND SPATIAL DESERTS

To map the healthcare catchment area of all health facilities and to identify possible areas of spatial deserts in Mizoram, the geo-locations of the total health facilities, Hospitals, SDHs, CHCs, and PHCs, are superimposed upon the settlement areas of Mizoram to show the accessibility gradient in healthcare. The population projection (2021) is used as the base map, and settlements are geo-located as per Survey of India (2011) data.

4.11.1 Healthcare Catchment Area in Mizoram

From each of health facility centroid mapped earlier, a 7 km buffer is drawn with lower opacity to denote their catchment areas. A map denoting all the settlement points (759), colour gradient (purple) using low intensity for densely populated areas and high intensity for the sparsely populated areas, is also laid underneath to show effective coverage. The catchment is drawn at a cutoff of 7km to denote an approximated effective travel distance of 1 hour.

The mapping (Map 4.11) reveals that the state capital region, Aizawl is the core healthcare hub of state, both its interior and peripheral areas being well covered by the myriads of buffers blooming out of it, enlarging its catchment area. Being the state's capital, it is an economic high access zone, medically a hotspot in healthcare facilities. Its rural areas are also relatively well covered by PHCs and CHCs. Some possibly underserved areas can be seen up in its northern borders, but generally it can be seen as the ideal compared to the rest of the districts.

In the north and eastern region of the state, pockets of underserviced regions appear in Kolasib and Champhai region, and also in some areas of the upper western region in Mamit district. The biggest lagging regions are the three southern districts, mainly Lawngtlai, Lunglei and Saiha. Several pockets appear more in these regions than the northern regions. The south western districts can be called lagging regions, healthcare wise, and also in a larger sense of economic development. The western belt of the state sees consistent paucity in facility location and service accessibility.

The accessibility gradient reiterates the same pattern from the earlier mapping findings, a North-South disparity and a rather pronounced East-West spatial disparity pattern.

Map 4.11 Health Facility Catchment Area in Mizoram 2021

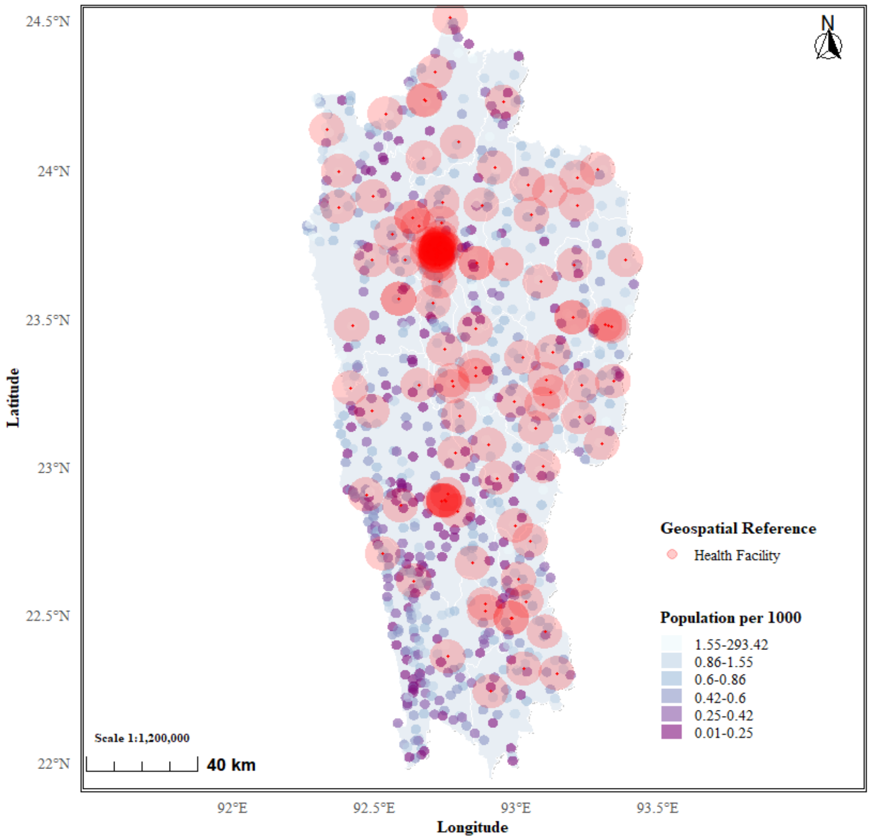

Note: Own visualisation based on Mizoram Statistical Abstract (2021). Survery of India (2014) & Mizoram Hospital Statistics Report (2021)

In the north and eastern region of the state, pockets of underserviced regions appear in Kolasib and Champhai region, and also in some areas of the upper western region in Mamit district. The biggest lagging regions are the three southern districts, mainly Lawngtlai, Lunglei and Saiha. Several pockets appear more in these regions than the northern regions. The south western districts can be called lagging regions, healthcare wise, and also in a larger sense of economic development. The western belt of the state sees consistent paucity in facility location and service accessibility.

The accessibility gradient reiterates the same pattern from the earlier mapping findings, a North-South disparity and a rather pronounced East-West spatial disparity pattern.

The catchment mapping reveals several clustering and overlapping of catchment areas, particularly in the central and eastern regions of the state, revealing uneven allocation pattern. It is evident that spatial equity, in terms of catchment or coverage, was not a prime factor when health facilities were initially allocated in the state. As population grows, this resulted in overlapping allocations, costly and sub-optimal, at the same time prone to economic externalities. Given that what has been allocated cannot be uprooted, with careful planning, these externalities can be reduced in the future.

4.11.2 Spatial Health Inequality Traps in Mizoram

To identify healthcare access spots or spatial paucity pockets, in Mizoram, Euclidean distances from 752 settlements to the nearest health facilities were considered, assuming a constant speed of 7km/hr, also keeping in mind the topography of Mizoram. This mapping allows the estimation of travel time to the nearest facility, PHC, CHC, SDH, or hospitals

4.11.3 Results and Findings

Table 4.17 reveals that that nearly 33% of 752 settlements in Mizoram, 248 in total, fall into the category of poor spatial access, requiring more than one hour of travel to reach an institutional doctor. Another 250 settlements are within a one-hour travel window, while 254 are well within thirty minutes of care. This distribution reflects a significant gradient in access to institutional healthcare across the state.

The most deprived settlements are heavily concentrated in the western and southern districts. Lawngtlai accounts for 89 of the "Far" settlements, followed by Lunglei with 51 and Mamit with 31. Together, these districts host over two-thirds of the most underserved areas. In contrast, districts located in the northern and northeastern parts of Mizoram, including Serchhip, Khawzawl, and Kolasib, report fewer such settlements, reflecting a recurring north-south and east-west spatial divide.

Table 4.17 **Nearness of Settlements to Health Facility by Districts (2021)**

SN	District	Near (<30 min)	Moderate (< 1hr)	Far (> 1 hr)
1	Aizawl	49	28	14
2	Champhai	18	14	13
3	Hnahthial	13	9	8
4	Khawzawl	19	11	3
5	Kolasib	15	19	7
6	Lawngtlai	27	30	89
7	Lunglei	30	57	51
8	Mamit	30	36	31
9	Saiha	19	22	13
10	Saitual	13	8	16
11	Serchhip	21	16	3
*	Mizoram	254	250	248

Source: Own Calculation

These pockets of inaccessibility correspond to what experts identified as spatial health traps, zones where terrain, remoteness, and weak service presence interact to produce chronic access deficits. Notably, these clusters are located in low-lying, high-disease-burden zones, where seasonal flooding and recurrent landslides frequently sever road connectivity. These environmental and infrastructural constraints compound the challenge of timely access to care.

Map 4.12 Presents the health deprivation zones where the red dot depict far, orange depicts moderate and yellow depicts settlements that with their nearest health facility. The light green circles represent the catchment area of 7 km buffer.

Map 4.12 Health Facility Access Deprivation Zones in Mizoram (2021)

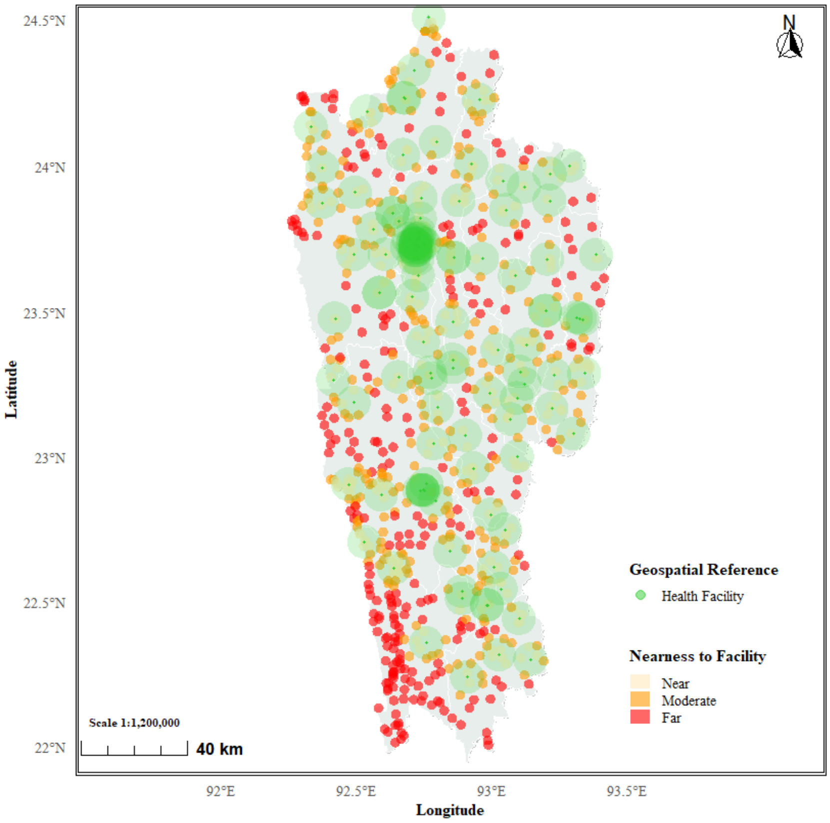

Note: Own visualisation based on Mizoram Statistical Abstract (2021), Survey of India (2014) & Mizoram Hospital Statistics Report (2021)

4.11.4 Discussion

In global comparative terms, these areas resemble Health Professional Shortage Areas (HPSAs), where the demand for medical care far outpaces the availability of medical personnel. Many of these regions would fall below the minimum threshold of 1 doctor per 3,500 population, often exacerbated by logistical and supply chain constraints in facility provisioning. The southwestern clusters of Mizoram are emblematic of these conditions and thus merit spatially targeted intervention.

What distinguishes these spatial pockets from other underserved areas in the state is their epidemiological and demographic profile. Despite relatively higher population densities and documented disease loads, particularly in tropical diseases, these regions lack appropriately equipped First Referral Units (FRUs) and intermediate healthcare infrastructure. As a result, patients are often forced to migrate to urban centres, including Aizawl and Lunglei town, to access basic or emergency care. This pattern not only imposes high opportunity costs on patients but also contributes to the systemic overcrowding of tertiary facilities. Field observations reinforce this assessment. In many rural settlements, the challenge is not only the absence of a facility, the poor quality of services at existing PHCs compound the issue. Understaffing, lack of diagnostic tools, and poor medicine availability erode trust in local centres, compelling patients to bypass them altogether in favour of distant secondary or tertiary units. This drives up travel and treatment costs while adding pressure to urban health infrastructure.

Improving conditions in these primary care facilities, staffing, equipment, and drug availability, could restore confidence and re-anchor care-seeking behaviours within rural areas. In parallel, enhancing rural road connectivity, especially routes that connect isolated valleys to ridge-top settlements, could reduce effective travel times and increase resilience during seasonal disruptions. These interventions, while modest in cost compared to new construction, offer potentially transformative effects. They can reduce tertiary hospital overcrowding, improve healthcare equity, and generate broader welfare gains across the state. Addressing Mizoram's spatial health traps, therefore, is not only a matter of infrastructure, but of realigning services to match the state's geographic and demographic realities.

4.11.5 Limitations of the Study

Methods like the Two-Step Floating Catchment Area (2SFCA) uses 5 to 20 km aerial distance as a health catchment area. This may be applicable for flat plain areas, but for Mizoram, especially in the rural hinterlands, a 7 km buffer can result in a 1-hour travel time due to the difficult terrain. For example, the village Saibawh lies right on the edge of the 7 km buffer drawn from Bungtlang South PHC. However, by road, it takes over 1 hour and 40 minutes from Saibawh to reach

Bungtlang South PHC. That said, this is not the norm in every part of the state. Generally, settlements lying on the same mountain ridge have shorter travel time compared to settlements separated by deep river valleys. Therefore, the 7 km buffer serve as a good proxy for Mizoram.

The 7 km at hour may seem like a snail's pace for some regions of the world, but Mizoram's meandering rural roads, it is quite fast. This method to translate the Euclidian straight line into time may not be replicable for other parts of the world, in fact may be redundant especially in places where road networks are thoroughly mapped. Nevertheless, these measures serve as a good starting point to understand the nature of spatial access in regions with difficult terrain like Mizoram.

4.12 HEALTH INSURANCE AND HEALTHCARE CONCENTRATION IN MIZORAM

The agglomeration of private health care facilities in Aizawl can be seen as a positive, especially in light of the covid 19 pandemic. However, it is also a double edged-sword. The concentration of healthcare facilities in the state's capital, particularly private hospitals, suggests a cascading result of misaligned allocation and misaligned incentives, perpetuating inequities in access to health care in Mizoram.

The absence of adequate secondary care infrastructure, such as CHCs and SDHs, compels rural populations to seek treatment in urban centres, often at significant personal cost. While primary care through PHCs is accessible throughout the state, save some underserved regions, the deficiency in secondary care throughout the state undermines the health system's ability to provide timely, cost-effective interventions for conditions requiring intermediate expertise. This gap requires deeper examination as private hospital concentration in Aizawl (59% of the total) warrants scrutiny as it suggests market failure and externalities in Mizoram healthcare market.

The following graph illustrates the growth of insurance claims (red and blue lines) and claims rates (dotted lines) for the Rashtriya Swasthya Bima Yojana (RSBY) and Mizoram State Health Care Scheme (MSHCS) from 2011 to 2021, sourced from mizoramdata.mizoram.gov.in (data is appended in Appendix III).

Graph 4.7

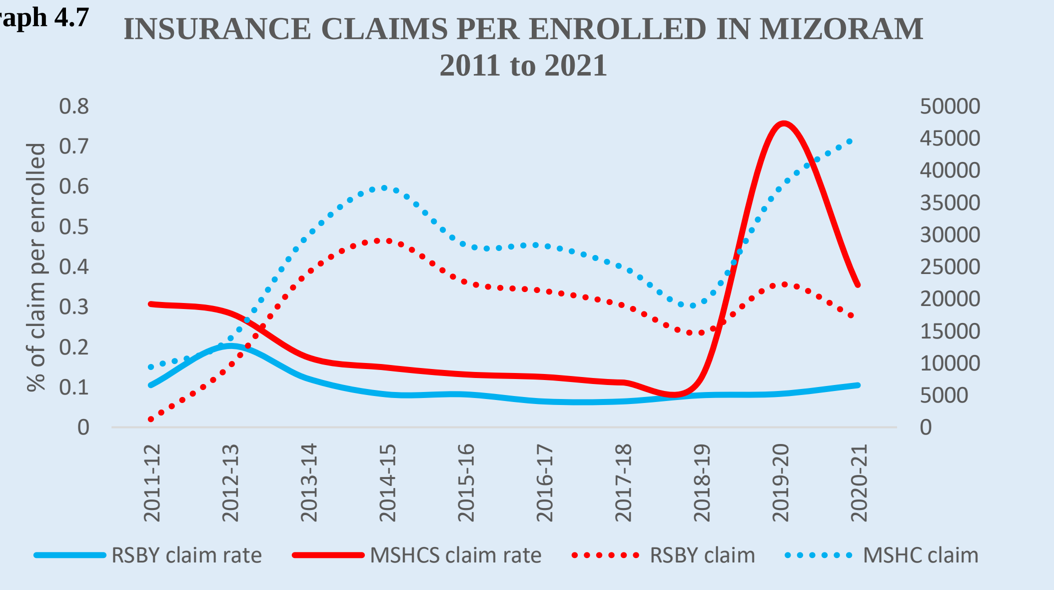

Analysis of RSBY and MSHCS over this decade reveals that insurance claims outpaced enrolment, suggesting systemic overuse. RSBY's claims grew at a compound annual growth rate (CAGR) of 33.22% compared to a 29.32% enrolment CAGR, with a high payout ratio of 97.5% in 2020–21. This rapid growth in claims, facilitated by a 90:10 Central and state funding split, indicates lax oversight, potentially encouraging provider overbilling (Dror et al., 2016).

4.12.1 Supply-side Moral Hazard

If we look at data on ten of the largest private hospitals in Aizawl, Table 4.18, the high OPD to IPD conversion rate and the high rate of non-surgical non-delivery IPDs, suggests some of the private hospital in Aizawl may be involved in moral hazard.

Table 4.18 Mizoram Private Hospitals Key Indicators 2021

SN	Name of Hospital	OPD to IPD Conversion rate (%)	Hospital Mortality Rate (%)	Non-surgery & Non-Delivery IPD (%)	IPD Insured in PMJAY & MSHCS (%)
	Private Hospitals				
1	Synod Hospital, Durtlang	26.24	2.63	35.94	7.89
2	Aizawl Adventist Hospital	24.66	1.74	83.25	44.93
3	Aizawl Hospital	33.2	3.82	23.59	0
4	Ebenezer Medical Centre	15.1	7.12	21.88	0
5	LRM Ramhlun	12.68	4.69	77.67	0
6	Greenwood Hospital	48.02	3.68	67.96	2.76
7	Redeem Hospital, College Veng	7.37	4.87	100	38.34
8	Trinity Hospital, Melthum	16.07	4.63	61.79	85.67
9	BN Hospital	9.43	3.43	62.6	13.48
10	City Hospital	13.48	5.46	73.37	22.64
	Govt Hospitals				
1	Civil Hospital, Aizawl	4.08	4.85	-34.42	59.8
2	Civil Hospital, Lunglei	4.66	3.64	0.61	30.62

Source: Own calculation based on data from Mizoram Hospital Statistics Report (2021)

Table 4.18 shows ten largest private hospitals in Mizoram on their OPD to IDP conversion rate, Hospital Mortality rate, percent of non-surgical and non-delivery IPDs from total IPDs that includes low acuity conditions, and the percent of IPDs insured in the studied insurance schemes. Two of the largest government hospitals in Mizoram are also included at the bottom as reference.

The proportion of non-surgical and non-delivery IPD cases is notably higher in private hospitals, ranging from 21.88% (Ebenezer Medical Centre) to 100% (Redeem Hospital, College Veng), with most exceeding 60%. In contrast, Civil Hospital, Lunglei reports a near-zero value (0.61%), while Civil Hospital, Aizawl shows an anomalous negative percentage (-34.42%), due to surgical and delivery cases (16,007) exceeding total IPD cases (11,908). This suggests that Civil Hospital, Aizawl, does not admit all of its patients who receive surgeries due to limited vacancy of beds.

Insurance coverage under PM-JAY and MSHCS varies widely. Private hospitals show diverse insured IPD percentages, from 0% (Aizawl Hospital, Ebenezer Medical Centre, LRM Ramhlun) to 85.67% (Trinity Hospital), with notable coverage at Aizawl Adventist Hospital (44.93%) and Redeem Hospital (38.34%). Government hospitals report higher insured IPD shares, at 59.8% (Civil Hospital, Aizawl) and 30.62% (Civil Hospital, Lunglei), reflecting their role in serving insured populations. These patterns suggest that insurance schemes influence inpatient utilisation, particularly in certain private hospitals with high insured IPD proportions.

Interestingly, MSHCS's claims rose at a 14.69% CAGR against a 12.30% enrolment CAGR, with a notable spike in 2019–20 (0.671 claims per enrolled family) but a low payout ratio of 29.7% in 2020–21, reflecting stringent state scrutiny and rejection of excessive claims under state funding. The 25% claims rate in 2020–21 suggests high utilisation, possibly driven by beneficiaries seeking care for minor conditions treatable at Primary Health Centres (PHCs), particularly incentivised by transport allowances (₹1,000 in-state, ₹10,000 outside Mizoram). This points to demand-side moral hazard, exacerbated by low enrolment fees (₹100 for BPL, ₹1,000 for APL) and high coverage of up to ₹3 lakh per family, (Nandi et al., 2015).

In 2009, the Government of Mizoram secured a US$25 million (₹117.8 crore) loan from the Asian Development Bank (ADB) to establish a corpus fund for the Mizoram State Health Care Scheme (MSHCS). The corpus, placed in fixed deposits, generates ₹11–12 crore annually in interest, which is used to cover claim reimbursements and administrative expenses, ostensibly without placing direct pressure on the state budget. However, this financing model carries overlooked risks. The loan is denominated in U.S. dollars, while returns are in Indian rupees, exposing the corpus to exchange rate volatility. Based on an assumed interest rate of 3–4%, annual repayments amount to approximately ₹3.53 crore during the grace period (2009–2014) and rise to ₹12.27 crore from 2014 to 2029. Over this 15-year period, total repayments could exceed ₹184 crore, an amount that could have funded substantial health infrastructure investments, such as the upgradation of all PHC or the construction of 9–18 CHCs.

The allocation of funds to loan repayments, rather than rural health care infrastructure, reflects misaligned priorities and incentives. High claims rates and increasing outside-Mizoram treatments (24% of claims in 2013–14) reflects supply-side moral hazard, for example, overbilling and a demand-side driven moral hazard, referrals driven by transport allowances. These perpetuate health care agglomeration, at the expense of equitable access and further exacerbating disparities. The fact that the burden of financing healthcare is increasingly becoming mandatory rather than voluntary speaks volume about its unintended externalities.

4.12.2 Rural Healthcare Avoidance Paradox

The habit of the rural-dweller in avoiding their nearest primary healthcare centre mainly driven by real or perceived gaps in staffing, equipment, and expertise, is an issue documented by (Hurtado-de-Mendoza & Song, 2023). Rural residents often make the arduous journey to urban health centres, secondary or tertiary, whichever is the nearest, despite their ailments being treatable at their nearest primary health centres. This is costly if we consider the time and economic losses incurred by the rural patients as well as the accompanying care giver, a problem well documented by Yadav et al., (2022)

The problem does not end there, it overloads the secondary and tertiary healthcare systems with conditions that can be sometimes considered medically trivial, like uncomplicated deliveries, diagnosis and treatment of urinary tract infections (UTIs) or acute respiratory infections (ARIs) etc. which a well-equipped PHC is supposed to handle. Furthermore, the overcrowded hospitals in the urban regions demand more investments thinning out the funds that is supposed to improve rural facilities. This condition is also documented by Jain & Nandraj (2023) in Rajasthan and it seems to be self-perpetuating in Mizoram leading to an agglomeration of health facilities in the urban region, specifically Aizawl.

4.12.3 Rural Patient Migration Estimates

The Rural Healthcare Avoidance Paradox hypothesizes that rural Mizoram residents bypass understaffed and under-resourced Primary Health Centres (PHCs), seeking care at urban hospitals like Aizawl's, overloading them and prompting urban-focused investments that perpetuate the cycle. Table 4.19 highlight the hypothesized migration pattern based on Inpatient Department admission during the year 2020-21 in Mizoram.

Aizawl, with 33.25% of Mizoram's population, accounts for 57.51% of inpatient admissions (175,173 vs. expected 101,241.22; +73.02% migration proxy), while rural districts like Khawzawl (-87.88% IPD proxy), Saitual (-80.10%), and Hnahthial (-62.74%) show significant underutilization of local facilities.

Table 4.19 IPD Migration Proxy in Mizoram 2021

SN	District	Actual IPD	Expected IPD	Migration Proxy IPD %
1	Aizawl	175173	101241.22	73.02
2	Champhai	12222	19762.8	-38.15
3	Hnahthial	2943	7899.39	-62.74
4	Khawzawl	1208	9967.98	-87.88
5	Kolasib	14936	23301.78	-35.89
6	Lawngtlai	10755	32706.87	-67.11
7	Lunglei	45397	36893.27	23.06
8	Mamit	5357	23975.17	-77.66
9	Saiha	22126	15701.02	40.92
10	Saitual	2990	15024.12	-80.1
11	Serchhip	11408	18003.29	-36.63

Source: Own calculation bases on data from Mizoram Hospital Statistics Report (2021)

Despite sustained efforts under the National Rural Health Mission since 2005 to improve last-mile delivery, a persistent distrust in rural public health systems continues to drive patient migration toward urban centres. As shown in Table 4.16, Aizawl Civil Hospital operates under severe strain, with negative admission capacity for surgical cases (-34.42% among non-low-acuity patients).

Simultaneously, 83% of the state's private hospitals are concentrated in Aizawl, indicating that they absorb much of the overflow from the overburdened public sector. Government responses have largely focused on expanding services to meet this growing urban demand, creating an ecosystem that sustains itself through inward patient flows.

This phenomenon may be described as the rural healthcare avoidance paradox. The intuitive solution seems straightforward, improve services in the source regions, build trust, and reduce aversion. Yet in practice, the paradox persists. Interventions often target symptoms rather than the root causes, and continued neglect in rural healthcare systems reinforces the pattern of avoidance. As a result, the system reproduces itself. Further study on patient migration in Mizoram could unravel the drivers of rural healthcare avoidance and disproportionate urban healthcare utilization.

4.12.4 Diseconomies of Scale in Concentration

While urban concentration may initially yield efficiency gains through specialization, shared infrastructure, and economies of scale, healthcare systems often face diminishing returns beyond a certain threshold. Diseconomies of scale emerge when rising demand begins to overwhelm capacity, driving up costs and eroding service quality. In Aizawl, the continued absorption of patients from underserved districts has pushed the system toward this tipping point. What began as a practical response to uneven regional access has gradually become a structural bottleneck, one where neither city residents nor referred patients can reliably access timely adequate care.

This pattern of private hospital agglomeration is not accidental; it reflects a natural response to sustained patient inflows from underserved districts. As public capacity in rural and peripheral regions remains limited, Aizawl absorbs both the unmet demand and the economic signals it generates. Private enterprises, recognizing this concentrated demand, establish themselves within proximity of existing health network, particularly around the District Civil Hospital. In effect, the city has become a healthcare catchment for the entire state, a role that both reflects systemic gaps and reinforces them. Unless infrastructure in other districts is expanded and adequately equipped, this pattern of medical centralization will persist, intensifying congestion, distorting service quality, and exacerbating access asymmetries.

Map 4.13 shows a two-panel map of urban Aizawl buildup area, highlighting public health facilities (10) and a nearby catchment of Sairang and Lengpui at the top right, with their 7 km catchment area (green). The right panel shows the concentrated private hospitals (16 in total), with a 7 km buffer (pale red) depicting their catchment area.

Map 4.13 Public and Private Health Facility Overlapping in Aizawl

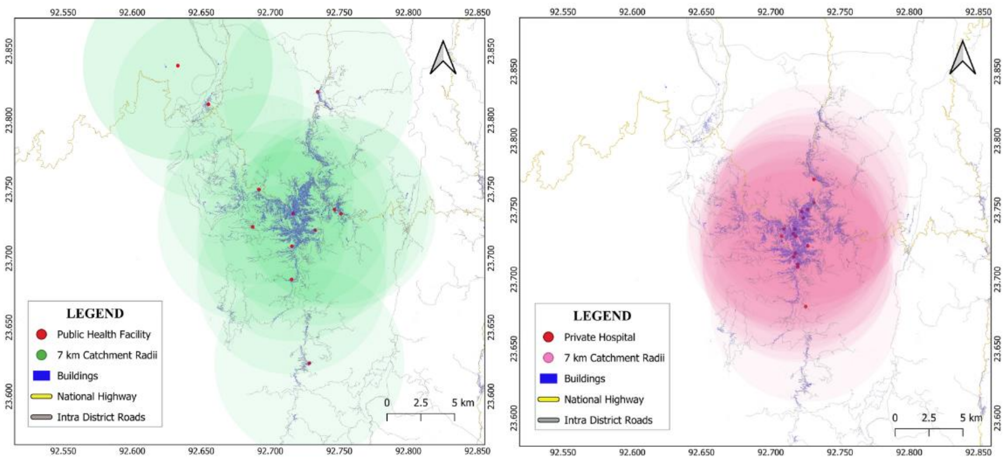

Note: Own visualisation in QGIS based on data from Mizoram Hospital Statistics Report (2021)

The level of overlapping catchment area is huge especially given that Mizoram is among one of the most sparsely populated states in India. The high overlapping of service area suggests an unnatural pattern of agglomeration fuelled by economic externalities. It must also be noted that in Aizawl, the externalities have contributed to a dense clustering of not just private hospitals but pharmacies, clinics and other specialized care effectively turning medical demand into a driver of intra-city congestion. The result is a spatial paradox: the very heart of care delivery becoming part of the most congested zones, far from ideal for patients.

Another lesser-discussed consequence of insurance backed centralization is the reduced accessibility of public health services for the real residents. As the DH absorbs increasing patient loads from across the state, urban population face longer wait-times, appointment backlogs, and reduced service availability. While referral patients from other districts are often covered under public health schemes, many urban residents, particularly those in the lower-middle income bracket, fall outside these entitlements. As a result, they are more likely to rely on private providers, often at a higher personal cost. This creates an implicit cross-subsidy, where the city's health infrastructure caters to external demand, while local users absorb higher out-of-pocket expenses. Such misalignment not only undermines equity but also weakens the core principle of universal, tiered access within the public system.

Thus, it can be argued that the current health financing arrangement in Mizoram presents a structural paradox. The state government, already the principal provider of advanced healthcare, including tertiary services through the District Civil Hospitals, the Mizoram State Cancer Institute, and the Referral Hospital with its attached medical college, has also assumed the role of health insurer. This dual position produces redundancy and injects avoidable externalities in the healthcare market. In other words, the government is paying patients to bypass its own facilities, reimbursing costs incurred in private hospitals both within and outside the state. The outcome is a perverse incentive structure: while public hospitals remain the default provider for the poor, wealthier beneficiaries capture disproportionate advantage by leveraging state-subsidised insurance for treatment in private institutions inside Mizoram and beyond.

This redundancy is not only inefficient but also fiscally regressive. Public funds that could be reinvested to strengthen the existing government health facilities are instead diverted to private providers. What makes the current arrangement seem unnecessarily extraneous is also the fact that the government hospitals, at the tertiary level, are the most superior in scope and capacity compared to any private hospital in the state. Furthermore, the outflow of reimbursements for care outside the state channels state resources into strengthening health infrastructure elsewhere, while simultaneously depriving the local system of the funds necessary for expansion. In this way, the current insurance mechanism has become less a safety net for the citizens than a mechanism of disinvestment, hollowing out investment in public institutions that the majority of people depend on.

In the long run, today’s insurance-driven healthcare market may well be remembered as a catastrophic policy detour. A model that sounds western, feels benevolent, and sold as fiscally responsible, but in practice, has produced an ecosystem where supply and demand do not align anymore, price signals have collapsed while access remains inequitable. In other words, it is an experiment in market distortion, ignoring the inherent asymmetry and public-good characteristics of healthcare (Arrow, 1963). By introducing a third player, the MSHCS, it distorts incentives by separating the buyer from the payer, and the payer from the user, contrary to what economic reasoning stands for. As individuals do not directly bear the full cost of their consumption, third party payment mechanism distorts the market (Friedman, 1980). The result is an ecosystem where everyone pays more, patients, providers, and the government, yet health outcomes remain stubbornly dismal. What is being introduced does not resemble economic efficiency, but rather a precarious financial mechanism whose sustainability relies on an intergenerational economic burden.

4.13 HEALTH INFRASTRUCTURE INDEX OF MIZORAM

This section constructs a composite Health Infrastructure Index (HII) for the 11 districts of Mizoram: Aizawl, Champhai, Hnahthial, Khawzawl, Kolasib, Lawngtlai, Lunglei, Mamit, Saiha, Saitual, and Serchhip. The index employs Principal Component Analysis (PCA) to synthesize three standardized input variables: health buildings per 1,000 population, weighted hospital beds per 1,000 population, and weighted medical equipment units per 1,000 population. These variables are computed from disaggregated secondary data with detailed derivation procedures outlined in the theoretical framework chapter. The Composite index through PCA is an attempt to provide a unified metric of health infrastructure capacity across districts and is intended to complement the GIS based studies.

4.13.1 Weighted Variables

The weighted variables for the health infrastructure index are presented below in Table 4.20. Aizawl registers the highest bed availability at 1.52 beds per 1,000 population, alongside the highest density of health equipment (0.024 units per 1,000) which validate its position as the state's primary healthcare hub. On the other end, districts like Mamit, Saitual, and Khawzawl show persistently low values across all three components. Saitual has the lowest recorded equipment availability at just 0.0027 per 1,000, while Mamit reports the lowest bed density (0.23 per 1,000).

Table 4. 20 Weighted Variables of Health Infrastructure Index

SN	District	Health Building per 1000	Health Facility Beds per 1000	Health Equipment per 1000
1	Aizawl	0.019536	1.519945	0.024132
2	Champhai	0.018765	0.622093	0.013306
3	Hnahthial	0.021336	0.412494	0.005121
4	Khawzawl	0.021412	0.391048	0.004057
5	Kolasib	0.013505	0.376201	0.008489
6	Lawngtlai	0.012708	0.334879	0.009892
7	Lunglei	0.017055	0.569500	0.011695
8	Mamit	0.013597	0.229741	0.004595
9	Saiha	0.015746	0.858885	0.013313
10	Saitual	0.015711	0.321707	0.002693
11	Serchhip	0.021825	0.516936	0.013095

Source: Own calculation based on data from Mizoram Statistical Abstract (2021), Mizoram Hospital Statistics Report (2021)

Interestingly, smaller districts such as Hnahthial, Khawzawl, and Serchhip show higher relative values for health buildings per capita, suggesting more favourable facility-to-population ratios even if those facilities are limited in capacity or equipment. These patterns point to a geographically uneven distribution of healthcare infrastructure, differing capacity and technology which was highlighted in prior sections of this analysis chapter.

4.13.2 Fit Test for Principal Component Analysis

To confirm the suitability of Principal Component Analysis (PCA) for the Mizoram Health Infrastructure Index (HII), the correlations among health buildings, beds, and medical equipment per 1,000 population were assessed. Bartlett's Test of Sphericity, which evaluates whether variables are sufficiently correlated for PCA, yielded a chi-square value of 15.03 (df = 3, p = 0.0018), indicating adequate correlations. The Kaiser-Meyer-Olkin (KMO) measure of sampling adequacy, which assesses shared variance, was 0.50 overall (0.48 for buildings, 0.50 for beds and equipment), reflecting the small sample size of 11 districts but supporting PCA given the significant Bartlett's test. Table 4.21 presents the correlation matrix, showing a strong beds-equipment correlation (r = 0.905) and weaker correlations with buildings (r = 0.294 and 0.185), alongside fit test results. These findings validate PCA for the Health Infrastructure Index for Mizoram.

Table 4.21 Fit Tests for Principal Component Analysis

Metric	Buildings_per_1000	Beds_per_1000	Equipment_per_1000
Correlation Matrix			
Buildings_per_1000	1	0.294	0.185
Beds_per_1000	0.294	1	0.905
Equipment_per_1000	0.185	0.905	1
KMO Measure of Sampling Adequacy	0.48	0.5	0.5
Bartlett's Test of Sphericity	Chi-square: 15.03, df: 3, p-value: 0.0018		

Source: Own calculation

4.13.3 Z-score Standardization of the Weighted Variables

In preparing the data for Principal Component Analysis (PCA), the three weighted variables are further standardized to Z-scores. This step rescales the variables to a common mean of 0 and standard deviation of 1, ensuring equitable contribution to the analysis despite their differing ranges. This standardization, detailed in chapter 3, is essential to capture Mizoram's health infrastructure disparities accurately. By eliminating scale-driven bias, it allows the PCA to extract latent dimensions that reflect true structural variations in the data rather than numerical magnitude alone. Moreover, it enhances the interpretability of factor loadings by placing all indicators on a comparable scale. The resulting standardized values form the basis for constructing the composite Health Infrastructure Index. The Standardized *Z*-score table is presented below.

Table 4.22 Standardized Values (Z-Scores) for Health Infrastructure Variables

District	Health_Buildings_Per_1000	Beds_per_1000	Equipment_per_1000
Aizawl	0.635	2.647	2.293
Champhai	0.408	0.173	0.532
Hnahthial	1.166	-0.405	-0.799
Khawzawl	1.189	-0.464	-0.972
Kolasib	-1.143	-0.505	-0.251
Lawngtlai	-1.378	-0.619	-0.023
Lunglei	-0.096	0.028	0.27
Mamit	-1.116	-0.908	-0.885
Saiha	-0.482	0.825	0.533
Saitual	-0.493	-0.655	-1.194
Serchhip	1.311	-0.117	0.498

Source: Own calculation based on data from Mizoram Statistical Abstract (2021), Mizoram Hospital Statistics Report (2021)

The standardisation table in Table 4.22 preserves the substantive structure of the original weighted data of Table 4.20. The relative positioning of districts remains consistent as previously established. In this formulation, standardisation serves not to reinterpret the data but to refine it for further analysis, maintaining fidelity to the conceptual weighting framework. The Z-scores thus offer a scale-independent lens through which the disparities underneath the distribution can be precisely extracted for the principal component extraction.

4.13.4 Principal Component Analysis

Principal Component Analysis was employed to construct a composite Health Infrastructure Index, from table 5.12, by reducing the three standardized weighted variables, Health Building per 1000, Weighted Bed per 1000, and Weighted Equipment per 1000, into a single dimension, Principal Component 1 (PC1) that maximises the variance across the 11 districts of Mizoram. PCA transforms the Z-scores into orthogonal components, with PC1 capturing the primary pattern of health infrastructure variation, making it suitable for a composite index to quantify spatial disparities. Key output of the analysis is detailed below.

Table 4.23 Variance Explained by Principal Components

Component	Standard Deviation	Proportion of Variance	Cumulative Proportion
PC1	1.421	0.673	0.673
PC2	0.945	0.298	0.971
PC3	0.297	0.029	1

Source: Own calculations based on data from Mizoram Statistical Abstract (2021), Mizoram Hospital Statistics Report (2021),

Table 4.23 presents the proportion of variance explained by the three principal components derived from the standardized health infrastructure indicators. The first principal component (PC1) exhibits a standard deviation of 1.421 and accounts for 67.3% of the total variance, indicating that it captures the most dominant pattern of variation across districts. The substantial explanatory power of PC1 also supports its use as the primary index for ranking district-level health infrastructure, given its ability to summarize dimensions of the other variables into a single interpretable metric.

The second principal component (PC2), with a standard deviation of 0.945, contributes an additional 29.8% of the total variance, raising the cumulative variance explained to 97.1% when combined with PC1. This indicates that nearly all meaningful variability in the dataset is concentrated within the first two dimensions, while the third component (PC3) adds only marginal explanatory value (2.9%).

This distribution of explained variance reflects the internal structure of the dataset, where the input variables, though distinct, exhibit considerable overlap in what they capture. The steep decline in variance from PC2 to PC3 confirms that the third component carries minimal additional information. On this basis, the first two components are retained for interpretation, as they together account for over 97% of the total variance. PC1 alone, explaining 67.3%, forms the core of the composite index, while PC2 provides secondary dimensional insight without significantly altering the rankings.

4.13.5 PCA Loadings Result

The loadings for PC1 reveal that beds per 1,000 population, with a value of -0.680, is the strongest contributor, indicating that bed capacity primarily drives PC1. This suggests that there is ample variation in infrastructure capacity. And followed closely by per 1,000 population at -0.662, also reflects the importance of technological resources in health facilities.

Table 4.24 Loadings of Health Infrastructure Variables on PCA

Variable	PC1	PC2	PC3
Health_Buildings_Per_1000	−0.316	0.944	0.090
Beds_per_1000	-0.680	-0.159	-0.716
Equipment_per_1000	-0.662	-0.288	0.692

Source: Own calculations based on data from Mizoram Statistical Abstract (2021), Mizoram Hospital Statistics Report (2021),

Health buildings per 1,000 population, with a loading of -0.316, has the weakest influence, suggesting that facility density varies less or correlates less strongly with beds and equipment across the 11 districts. The negative loadings suggest there is an inverse relationship, where higher values in these variables correspond to lower PC1 scores, and vice versa. The PCA loadings result suggests that districts with greater infrastructure provision in beds, equipment, or buildings tend to have more negative PC1 scores, reflecting stronger health infrastructure, while those with lower provision have positive scores. The larger absolute loadings for beds and equipment demonstrate their greater contribution to PC1 compared to health buildings, indicating that PC1 is more sensitive to variability in hospital capacity and equipment availability. This finding aligns with field observations in Mizoram, where facilities with limited beds or equipment contribute less to utilization, as migration of patients remain unabated.

4.13.6 Principal Component Result

The Mizoram Composite Health Infrastructure Index is constructed using the reversed scores of the first principal component (PC1) derived from Principal Component Analysis (PCA) and presented in Table 4.25.

Table 4.25 Mizoram Composite Health Infrastructure Index 2021

SN	District	Reversed PC1
1	Aizawl	3.517
2	Saiha	0.761
3	Serchhip	0.665
4	Champhai	0.599
5	Lunglei	0.167
6	Hnahthial	-0.435
7	Khawzawl	-0.583
8	Kolasib	-0.871
9	Lawngtlai	-0.872
10	Saitual	-1.391
11	Mamit	-1.556

Source: Own calculation based on data from Mizoram Statistical Abstract (2021), Mizoram Hospital Statistics Report (2021)

This index ranks the state's 11 districts based on their relative availability of health infrastructure per 1,000 population, with higher values indicating stronger provisioning of beds and equipment. PC1, which explains 67.3% of the total variance, is predominantly shaped by variables related to bed capacity (loading: –0.680) and equipment availability (loading: –0.662), with a smaller influence from health building density (loading: –0.316). As the original PC1 scores are negatively signed due to the direction of variable loadings, they are reversed to ensure that higher index values reflect better infrastructure.

Aizawl leads the reversed PC1 index with a score of 3.517, reflecting its urban dominance in bed and equipment provision. Saiha (0.761), Serchhip (0.665), and Champhai (0.599) rank next, indicating moderate infrastructure, while Mamit (-1.556), Saitual (-1.391), and Lawngtlai (-0.872) rank lowest, highlighting rural deficits. The index further highlights the concentration of advanced health resources in urban areas, with mid-tier districts like Lunglei (0.167) and rural districts like Hnahthial (-0.435) and Khawzawl (-0.583) showing limited bed and equipment capacity.

To complement the PC1 based index, PC2 scores, which explain 29.8% of the variance and primarily capture health building density per 1,000 population (loadings of 0.944), is also presented below in Table 4.26 for reference.

Table 4.26 Principal Component Analysis PC2 Results

SN	District	Reversed PC2
1	Khawzawl	1.477
2	Hnahthial	1.396
3	Serchhip	1.113
4	Champhai	0.204
5	Saitual	-0.017
6	Lunglei	-0.173
7	Aizawl	-0.482
8	Mamit	-0.654
9	Saiha	-0.740
10	Kolasib	-0.927
11	Lawngtlai	-1.196

Source: Own calculation on R based on data from Mizoram Statistical Abstract (2021), Mizoram Hospital Statistics Report (2021)

However, caution is warranted in interpreting PC2 rankings, as Aizawl's lower position (-0.482, 7th) reflects its lower building density per population due to its large urban population, not a lack of facilities. Evidently, PC2 ranks Khawzawl (1.477), Hnahthial (1.396), and Serchhip (1.113) highest, reflecting dense facility networks, often in rural areas, while Lawngtlai (-1.196), Kolasib (-0.927), and Saiha (-0.740) rank lowest reflecting their low per capita facility. PC2's focus on buildings highlights districts with high primary health centre coverages, complementing PC1's emphasis on overall facets of health infrastructure in Mizoram.

4.13.7 Findings from the Principal Component Analysis

District rankings on PC1 show a steep gradient in the availability of core resources. While Aizawl ranks highest, as expected, what emerges more clearly is the substantial mid-tier positioning of districts like Serchhip, Champhai, and Saiha, which, despite their peripheral location, maintain modest levels of inpatient and equipment provision. In contrast, western and northern districts such as Mamit, Saitual, and Kolasib sit at the lower end, with reversed PC1 scores below –0.8 amplified by their deficits in advanced clinical capacity. The Theil-T index for beds (0.2532), with nearly half the inequality attributable to between-district variation, reinforces this uneven distribution. These patterns suggest that while vertical investment in infrastructure has occurred, it has done so unevenly, without a clear alignment to regional accessibility or population-weighted service needs.

PC2 introduces a different spatial narrative. Districts such as Khawzawl, Hnahthial, and Serchhip lead on this component, driven by a high density of health buildings relative to population. These regions, particularly in the east and central belts, show signs of institutional coverage expansion, possibly influenced by administrative reorganization and decentralization. However, a high PC2 score does not equate to higher service capability. For instance, Hnahthial, despite scoring highly on PC2 due to its numerous PHCs, ranks low on PC1, indicating that its facilities lack adequate beds and functional equipment. This mismatch illustrates a structural misalignment between infrastructure spread and infrastructure depth. This pattern, primary care lacking compliance with IPHS 2012 norms for diagnostics and referrals, is a recurring theme witnessed during field visits all throughout the state.

Spatially, southern and western districts, notably Lawngtlai, Mamit, and Lunglei, consistently underperform across both components. These regions face the dual burden of low facility density and weak capacity, a configuration that severely limits local access and increases reliance on long-distance referrals. The situation is particularly acute in southern pockets where GIS mapping has revealed travel distances exceeding 80 km to the nearest primary healthcare facility, let alone secondary care. This creates what health economists identify as spatial treatment bottlenecks, where even timely access to primary care fails to translate into effective coverage due to upstream referral limitations.

Together, PC1 and PC2 point to a layered problem: quantitative expansion in infrastructure has not been matched by functional readiness, particularly in peripheral and resource-poor regions. The clustering of PHCs without corresponding investment in personnel, beds, and equipment may offer administrative coverage but delivers limited clinical value. What emerges from actual service utilisation is that although facilities are spread across districts, actual service delivery remains functionally centralized, leaving large segments of the population with inadequate access to comprehensive services. Bridging this gap will require more than scaling up inputs, it needs structural connectivity, ensuring that each district is not only served for coverage but also equipped for continuity of care across primary and higher tiers.

4.13.8 Discussion of the PCA Results

Policy interventions should enhance PCA findings to allocate beds and med-tech infrastructures where they are most needed. Spatially optimal allocation of bridging facilities such as CHCs in poorly served areas, and upgrading DHs in newly created districts are critical to achieve equity in health access.

In Saitual, health infrastructure remains structurally weak. While the district has a network of facilities in place, their capacity is limited. Investments should prioritize expanding bed strength and upgrading equipment at its existing District Hospital (DH) and Community Health Centres (CHCs), ensuring they can manage both inpatient care and essential diagnostics.

Map 4.14 Mizoram Composite Health Infrastructure Index (2021)

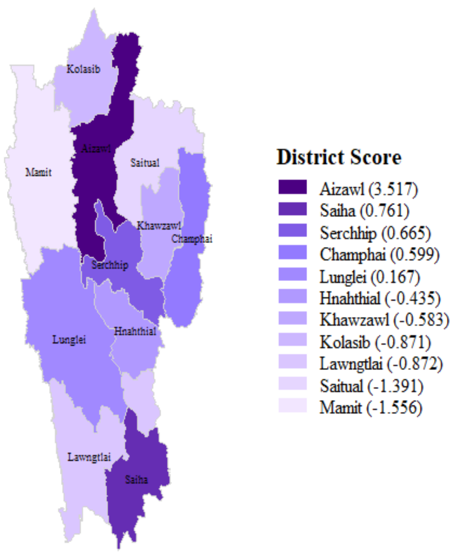

Note: Author's Visualisation based on findings from Principal Component Analysis.

Khawzawl performs well in terms of facility density but lacks the technological foundation needed to deliver quality care. Targeted investments in diagnostic equipment and digital systems would enhance the utility of its existing PHC and CHC network, closing the gap between structural availability and service readiness. In Hnahthial, access issues are both geographic and infrastructural. The eastern region lacks a functional secondary care centre, which increases the load on the DH. The DH itself requires improvements in bed capacity and equipment to function effectively as a referral point for surrounding rural areas.

Kolasib presents a case of moderate coverage but under-capacity. Additional inpatient beds and investment in core technologies, especially in maternal and diagnostic services, are necessary to support its growing population and reduce dependence on Aizawl. Mamit, particularly its southwestern region, faces severe infrastructure deficits. Here, bed capacity is low and equipment availability is limited, raising risks for delayed or incomplete treatment. Addressing these gaps requires both facility upgrades and targeted deployment of mobile or satellite diagnostic services.

Champhai, while moderately equipped, has spatial access challenges in its northern belt. One or more strategically located PHCs would enhance geographic coverage, while system-wide upgrades in bed capacity and clinical equipment would reduce avoidable referrals. Lawngtlai, one of the state's most underserved districts, requires a multi-tiered strategy. The western and southwestern regions face significant spatial isolation. New PHCs and improved secondary care capacity, particularly in bed and diagnostic provision are critical. Without addressing these gaps, even basic care will remain unreachable for large segments of the population.

Lunglei holds potential as a tertiary referral centre for southern Mizoram. However, this role is constrained by limited beds and outdated equipment in its facilities, particularly in its DH. A new CHC in the northwestern part of the district could also alleviate intra-district spatial barriers and support better triaging of cases that could alleviate its overloading. Saiha demonstrates comparatively balanced infrastructure, with a PC1 score of 0.761 and above-average bed capacity (2.86/1000). The district would benefit from better staffing and robust public-private partnerships to supplement service delivery, especially in diagnostic and specialist care. Improving road connectivity would further expand effective access.

Aizawl, given its large and rapidly growing population, faces a different set of challenges compared to the rest of the state. The sheer volume of demand necessitates intra-district and intra-urban decentralisation, particularly to prevent service overload at its District Hospital (DH). Establishing urban Community Health Centres (CHCs) with a focus on maternal and child health could offload non-tertiary cases and improve care continuity at the first point of contact. Importantly, this decentralization has broader urban implications: it can also help alleviate systemic congestion in the city, where multiple economic and administrative functions have become spatially concentrated. Reducing pressure on central health nodes is not just a medical necessity but part of a more coordinated approach to managing urban agglomeration in Aizawl.

At the same time, the growing dominance of the private health sector, concentrated in the Aizawl Municipal area, raises concerns. While it expands choice for higher-income groups, it risks exacerbating out-of-pocket burdens for those who fall outside the eligibility for free public services but cannot afford sustained private care. A regulatory and referral structure is needed to balance the public-private interface, prevent unnecessary medical expenditure, and ensure equitable access across socioeconomic groups.

PCA highlight resource specific bottlenecks for each district, suggesting that inequalities are not uniform across all healthcare inputs, some districts are low on equipment, some on beds, and some on physical buildings. The findings allow a spatially designed intervention that addresses the specific needs of each district. Pairing PCA findings with Thiel T findings and GIS studies can help where PHCs, CHCs, SDHs must be allocated, where beds should be allocated, where investment in equipment should be directed, where mobile clinics go and where telemedicine can focus. It gives policy makers a powerful scientific tool to allocate scare resources with results that can lead to efficiency and avoid economic externalities, like moral hazard, in the healthcare sector.

4.13.9 Limitations of the Principal Component Analysis

While the principal component analysis (PCA) effectively ranks Mizoram’s 11 districts by health infrastructure through the Composite Health Infrastructure Index (PC1) and facility density (PC2), several limitations inherent to the PCA approach and data constraints warrant consideration. These limitations, while not diminishing the index's utility in identifying spatial disparities, suggest areas for refinement in future analyses to enhance precision and comprehensiveness.

A key limitation of this index lies in the functional ambiguity of infrastructure categories. Although DHs are assumed to provide comprehensive services as per IPHS 12 recommendations, field observation showed disparities to a point where some DHs functioned like a primary health centre. Some districts lack basic med-tech like Ultra-sound, while urban facilities in other district offer advanced diagnostics such as MRI, which were not captured in the secondary data used. To avoid misrepresentation, the weighting scheme avoids over-amplifying DHs. However, this means the index may understate quality differences in high-capacity hospitals, particularly in urban areas like Aizawl. Future analyses would benefit from integrating service-level functionality or real-time equipment inventories.

The PCA's structure, with PC1 (67.3% variance) emphasizing beds (-0.680) and equipment (-0.662) over buildings (-0.316), splits infrastructure dimensions across components, as PC2 (29.8%) captures facility density (building loading: 0.944). While this split, noted in earlier discussions, accurately reflects the data's correlation structure, beds and equipment correlate more strongly than buildings, it requires both PC1 and PC2 to fully represent health infrastructure. For instance, Hnahthial's high PC2 (1.396, 0.142 buildings) contrasts with its low PC1 (-0.435, 0.028 equipment), indicating dense PHCs but limited advanced capacity. This mismatch in allocation of facility and accompanying infrastructure deters a definitive Composite Infrastructure. At the same time, it also highlights a rather obscure but common practice, delivery of public infrastructure with limited or no functionality, the hall mark of developing nations.

The PCA's reliance on per 1,000 population metrics for buildings, beds, and equipment limits its ability to capture absolute infrastructure scale across districts with varying population sizes. While per 1,000 metrics, aligned with inequality measures like Theil-T (0.2532 for beds) and Gini (0.40 for facilities), ensure comparability, they may underrepresent the total infrastructure in populous districts like Aizawl (431,836 population, 0.078 buildings) compared to smaller districts like Hnahthial (35,152 population, 0.142 buildings). This affects PC2's rankings, as Aizawl's mid-tier score (-0.482) reflects population-driven density rather than absolute facility count. Southern districts like Lawngtlai (PC2: -1.196) face similar issues, where low absolute infrastructure exacerbates spatial traps. Future analyses could incorporate absolute counts alongside per capita metrics to better reflect total infrastructure scale (Nardo et al., 2005).

The absence of data on building size or number of floors represents another constraint. The PCA relies on the number of health buildings per 1,000, sourced from the Mizoram Statistical Abstract (2021), but does not account for their physical scale, such as square footage or floor count, which could indicate capacity differences. For example, earlier GIS analyses noted differing spatial structures in sizes when view from satellite pictures. This limitation may undervalue the infrastructure strength of districts with larger buildings, affecting PC2's facility density rankings. Including building size metrics in future datasets would provide a more nuanced assessment of physical infrastructure distribution.

4.14 SPATIAL AND SPACE-TIME SCAN STATISTICS OF HEALTH INFRASTRUCTURE

This section tests the hypothesis that healthcare facilities in Mizoram are significantly clustered in urban district of Aizawl, contributing to urban-rural health service inequities. Using Spatial and Space-Time Scan Statistics (SaTScan) with a Bernoulli model, 119 facilities (67 PHCs, 42 hospitals, 9 CHCs, 1 SDH) and 1000 randomly generated controls across 1119 locations were analysed. Secondary and non-significant clusters are reported for transparency to provide a fair assessment of Mizoram's health resource distribution.

4.14.1 Results of SaTScan Analysis

SaTScan analysis identified a primary cluster in Aizawl district, centred at Redeem Hospital (23.724261 N, 92.726685 E), with a radius of 4.72 km and a span of 8.18 km. The cluster comprises 22 facilities (18 hospitals, 4 PHCs) and 1 control point (Control926). The facilities included in the cluster are:

1. Hospitals: Civil Hospital Aizawl, Kulikawn Hospital, Alpha Hospital, BN Hospital, Mizoram State Cancer Institute, Synod Hospital Durtlang, Adventist Hospital, Nazareth Hospital, Bethesda Hospital, Aizawl Hospital & Research Centre, Care Hospital, Grace Nursing Home, Ebenezer Medical Centre, LRM Hospital, City Hospital, Redeem Hospital, Rosewood Hospital, Trinity Hospital.
2. PHCs: Chawlhhmun UPHC, Hlimen UPHC, Lawipu UPHC, ITI 10 UPHC.

The cluster covers approximately 70 km² (~0.33% of Mizoram's 21,087 km²), containing 18 of Aizawl's 20 hospitals and 4 PHCs. The relative risk (RR) of 10.81 indicates that facilities are 10.81 times more likely to occur within this cluster than elsewhere, with a 95% confidence interval of 8.12–14.39, approximated using standard methods (Kebede et al., 2021). The SaTScan metric for Aizawl is present in Table 4.27.

Table 4.27 SaTScan Result for Aizawl Cluster

Metric	Value
Population (cases + controls)	23
Number of Cases	22 (18.5% of 119 facilities)
Expected Cases	2.45
Observed/Expected Ratio	8.99
Relative Risk (RR)	10.81 (95% CI: 8.12–14.39)
Log Likelihood Ratio (LLR)	47.236959
P-value	$< 10^{-15}$ (Monte Carlo rank 1/1000)
Gini Coefficient	0.2407 (optimal at 3%)

Source: Own calculation on SaTScan

The log likelihood ratio (LLR) of 47.236959 exceeds the critical value of 13.438945 for $p < 0.001$, and the p-value of $< 10^{-15}$ (Monte Carlo rank 1/1000) confirms high statistical significance. The Gini coefficient of 0.2407, optimal at 3%, is indicative of a highly concentrated cluster, consistent with urban-centric resource allocation.

Map 4.15 Health Infrastructure Clustering in Mizoram (2021)

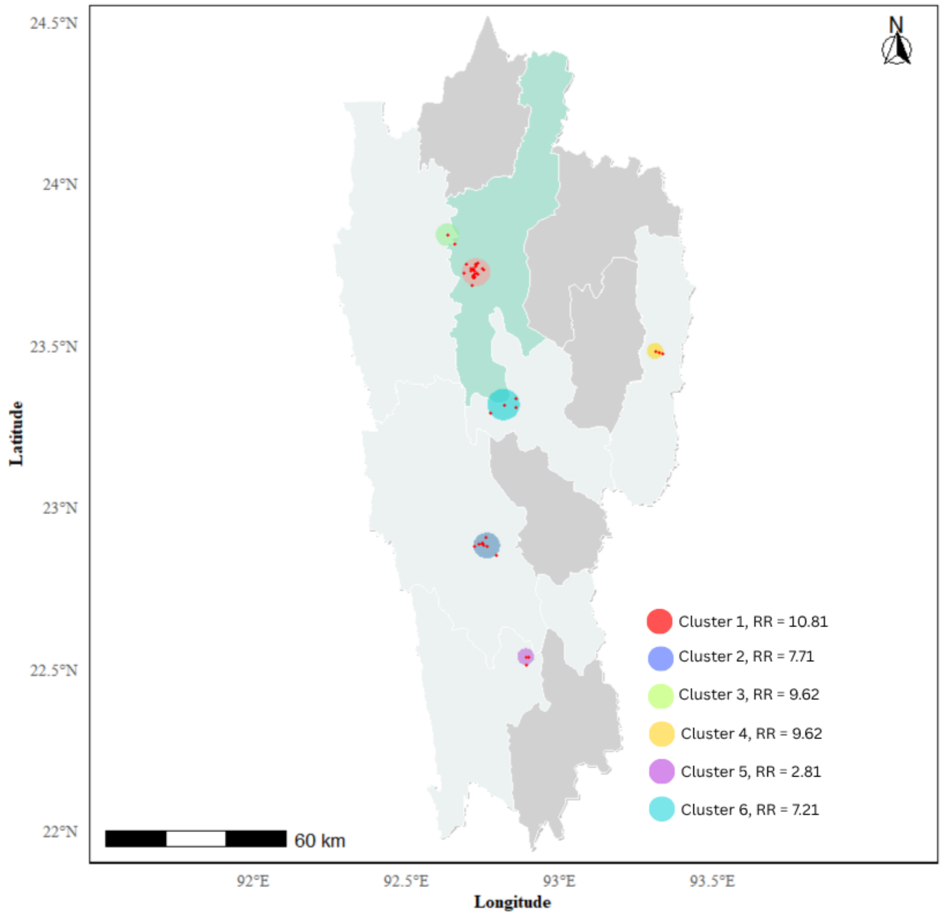

Note: Author's own visualisation based on SaTScan result

4.14.2 Hypothesis Evaluation

The SaTScan's identification of urban Aizawl, cluster 1, strongly supports the alternative hypothesis (H_1), demonstrating significant clustering of healthcare facilities. The 22 facilities, including 18 hospitals and 4 PHCs, represent 18.5% of Mizoram's 119 facilities within a 4.72 km radius, covering just 0.33% of the state's area. The RR of 10.81 and p-value $<10^{-15}$ indicates a substantial deviation from a random spatial distribution, where only 2.45 facilities would be expected. This concentration aligns with Aizawl's role as Mizoram's administrative and economic hub. The single control point (Control 926) constitutes only 4.3% of the cluster's points, reinforcing that the RR is driven by cases. As a result, the null hypothesis (H_0) of random spatial distribution was rejected.

The Gini coefficient of 0.2407 reflects the localised nature of the clustering, that 3% of the study area (or clusters) accounts for a disproportionate share of facilities (22 out of 119), confirming a highly localised cluster. This is reinforced by the cluster's small radius (4.72 km or 0.33% of Mizoram's 21,087 km²) contains 18.5% of all health facilities.

4.14.3 Secondary and Insignificant Clustering Report

Secondary and non-significant clusters identified by SaTScan, are also reported. A secondary cluster in Lunglei district (centred at 22.879495 N, 92.761851 E, 4.37 km radius) includes seven facilities: Civil Hospital Lunglei, Christian Hospital, Faith Hospital, Hope Hospital, John William Hospital, Sazaikawn PHC, and Bunghmun PHC, with two control points. This cluster has a relative risk of 7.71, an LLR of 11.320739 (exceeding the critical value of 9.704170 for $p < 0.05$), and a p-value of 0.013 (Monte Carlo rank 7/1000), indicating statistical significance but a smaller scale compared to Aizawl (7 vs. 22 facilities). This result shows that Lunglei town is a secondary health hub in the southern regions of Mizoram.

Four non-significant clusters were also detected: Cluster 3 (Lengpui - Sairang, 3.84 km, RR = 9.62, p = 0.701) includes one CHC, Sairang PHC, and Lengpui PHC. Cluster 4 (Champhai, 2.68 km, RR = 9.62, p = 0.701) includes Civil Hospital Champhai, Med-Aim Hospital, and DM Hospital. Cluster 5 (Lawngtlai, 2.81 km, RR = 9.62, p = 0.701) includes Civil Hospital Lawngtlai, Lairam Christian

Medical Centre, and Christian Hospital Lawngtlai and Cluster 6 (Serchhip, 5.33 km, RR = 7.21, p = 0.987) includes Civil Hospital Serchhip, Integrated Ayush Hospital, Mercy Hospital, and Thenzawl CHC. These clusters, with high relative risks but non-significant p-values, reflect sparse facility distribution in remote and peripheral districts. For reference, Table 4.28, summarises the metrics for all detected clusters in the study area.

Table 4.28 Health Facility Clusters in Mizoram 2021

Cluster	Location	Radius (km)	RR (95% CI)	LLR	P-value
1	Aizawl	4.72	10.81 (8.12–14.39)	47.236959	$< 10^{-15}$
2	Lunglei	4.37	7.71 (4.32–13.76)	11.320739	0.013
3	Lengpui/Sairang	3.84	9.62 (3.84–24.09)	6.757314	0.701
4	Champhai	2.68	9.62 (3.84–24.09)	6.757314	0.701
5	Lawngtlai	2.81	9.62 (3.84–24.09)	6.757314	0.701
6	Serchhip	5.33	7.21 (2.88–18.05)	4.617776	0.987

Source: Own calculation in SaTScan

4.14.4 Robustness

The findings are supported by the use of 1000 control points which ensures sufficient statistical power for Monte Carlo simulations, yielding reliable p-values, as recommended by SaTScan guidelines (Kulldorff, 2018). The 7 km maximum radius is appropriate for Mizoram's hilly terrain and facility density, approximated 1hour travel distance, and the data-driven 4.72 km radius of the Aizawl cluster minimises arbitrariness in cluster definition (Tango & Takahashi, 2005).

The 'no geographical overlap' criterion used in the analysis guarantees that the Aizawl cluster is distinct from other clusters, preventing conflation with rural patterns and enhancing the clarity of urban-centric findings (Kulldorff & Nagarwalla, 1995). The LLR of 47.236959 significantly exceeds the critical value of 13.438945, and the p-value remains robust even if simulations are increased to

9999 replications, indicating stability against random variation. The Bernoulli model's assumption of spatial randomness for controls is reasonable given the random generation of control points across Mizoram's geographical bounds, validating the cluster's significance (Kulldorff, 1997).

4.14.5 Limitations

The model has limitations that warrant consideration. The Bernoulli model assumes spatial randomness for control points, which may not fully account for Mizoram's complex topography or population density variations unintentionally oversimplifying facility distribution in the state. Incorporating population-weighted controls, such as residents under the umbrella of the buffer, in future analyses could address this. The non-significant clusters (e.g., Champhai, Lawngtlai) exhibit high relative risks (e.g., 9.62) but lack statistical power due to low case counts, limiting the detection of other clustering. This constraint reflects Mizoram's sparse health facility network.

Finally, the analysis focuses on facility locations without considering service capacity or quality, which may influence actual healthcare access (Kebede et al., 2021). Nonetheless these limitations do not undermine the study's finding that there is significant clustering of health facility in the state. The analysis provides strong evidence to reject the null hypothesis (H_0) of spatial randomness in favour of the alternative hypothesis (H_1): healthcare facilities in Mizoram are significantly clustered in Aizawl district. The primary cluster, mid-point at Redeem Hospital (23.724261 N, 92.726685 E) with a 4.72 km radius, contains 22 facilities (18.5% of the state's total) in just 0.33% of Mizoram's area, with a relative risk of 10.81 (95% CI: 8.12–14.39) and a p-value < 0.001 (Monte Carlo rank 1/1000). This confirms a marked urban-centric concentration of healthcare, aligning with Aizawl's role as the state's growth pole. The findings validate the existence of spatial inequalities in health service access, the rest of the districts in Mizoram exhibit sparse or non-significant clustering.

4.15 SPATIAL AND SPACE-TIME SCAN STATISTICS ON CONCENTRATION OF MEDICAL EQUIPMENT USAGE IN MIZORAM

This section analyses the spatial distribution of medical equipment usage across Mizoram in the year 2021, focusing on identifying areas with unusually high-concentration diagnostic usage. The study leverages on recorded usage of 10 medical equipment, such as, X-ray, Ultrasound, ECG, CT-Scan, ECHO, Chemotherapy, Radiotherapy, Dialysis, Bronchoscopy, and Endoscopy, which were selected through clinical relevance, such as data on ICD 11 leading causes of death, across Mizoram's 11 districts to detect significant clusters of medical equipment usage. Using SaTScan software, the analysis provides insights into regional disparities in healthcare resource utilization, with potential implications for policy and resource allocation.

4.15.1 Results of the SaTscan Analysis on Equipment Usage in Mizoram

The SaTScan analysis examined 196,385 medical equipment usage cases across Mizoram's 11 districts in 2021. The SaTScan considered a total population of 13,54,830, employing a Discrete Poisson model. The analysis was configured exclusively for spatial scanning, employing a circular spatial window with a maximum cluster size of 50% of the population at risk. The scan targeted areas with high rates of medical equipment usage, with no geographical overlap permitted for secondary clusters. A single significant cluster was detected in Aizawl district.

Aizawl district cluster captures 140,888 usage cases (71.7% of total cases), far exceeding the expected 65,292.65 based on its 33.3% population share. The relative risk (RR) of 5.10 indicates that usage is 5.10 times higher in Aizawl than in other districts during the study period (2020-21). The log likelihood ratio (LLR) and p-value < 0.001 (Monte Carlo rank 1/1000) confirms high significance of concentration. Furthermore, a sensitivity test with a 20% population-at-risk limit (270,966) detected no secondary clusters, indicating that the Aizawl cluster overshadows all other districts in health equipment utilisation.

Table 4.29 details the cluster's metrics and Map 4.16 depict the resultant SaTScan shapefile output.

Table 4.29 Statistical Metric for Medical Equipment Cluster 2021

Metric	Value
Location	Aizawl District
Coordinates	23.724350 N, 92.719174 E
Population	450,444 (33.3% of 1,354,830)
Number of Cases	140,888 (71.7% of 196,385)
Expected Cases	65,292.65
Observed/Expected Ratio	2.16
Relative Risk (RR)	5.1
Log Likelihood Ratio (LLR)	60,651.225016
P-value	< 0.001 (Monte Carlo rank 1/1000)

Source: Own calculation in SaTScan based on data from Mizoram Statistical Abstract (2021) & Mizoram Hospital Statistics Report (2021)

4.15.2 Hypothesis Evaluation

The results reject the null hypothesis (H_0) of uniform medical equipment usage per 1000 population across Mizoram's 11 districts in favour of the alternative hypothesis (H_1): usage is significantly concentrated in Aizawl, (RR = 5.10, $p < 0.001$). This confirms Aizawl's urban-centric dominance in diagnostic access, supporting the hypothesis of spatial inequality in functional healthcare resources.

4.15.3 Observation

Aizawl's 71.7% share of diagnostic procedures, including advanced services like Chemotherapy and Radiotherapy, highlights the concentrated nature of healthcare in Mizoram. Remote or Peripheral districts such as Hnahthial (488 uses) and Khawzawl (146 uses), are limited to basic diagnostics such as X-rays, shows they are technologically handicapped. This parallels the facility clustering analysis, where Aizawl hosts 18.5% of facilities in a 4.72 km radius (RR = 10.81, $p < 0.001$), evidencing a dual structural-functional urban bias. The high concentration of health facilities in urban region not only affects the state as whole, intra-district variation in Aizawl district from the Thiel T Index, also shows that peri-urban residents within the districts also bear the brunt of unequal access to healthcare.

The cluster is visualized in Map 4.16 using the shapefile produced by the SaTScan analysis.

Map 4.16 Diagnostic Access Concentration in Mizoram (2021)

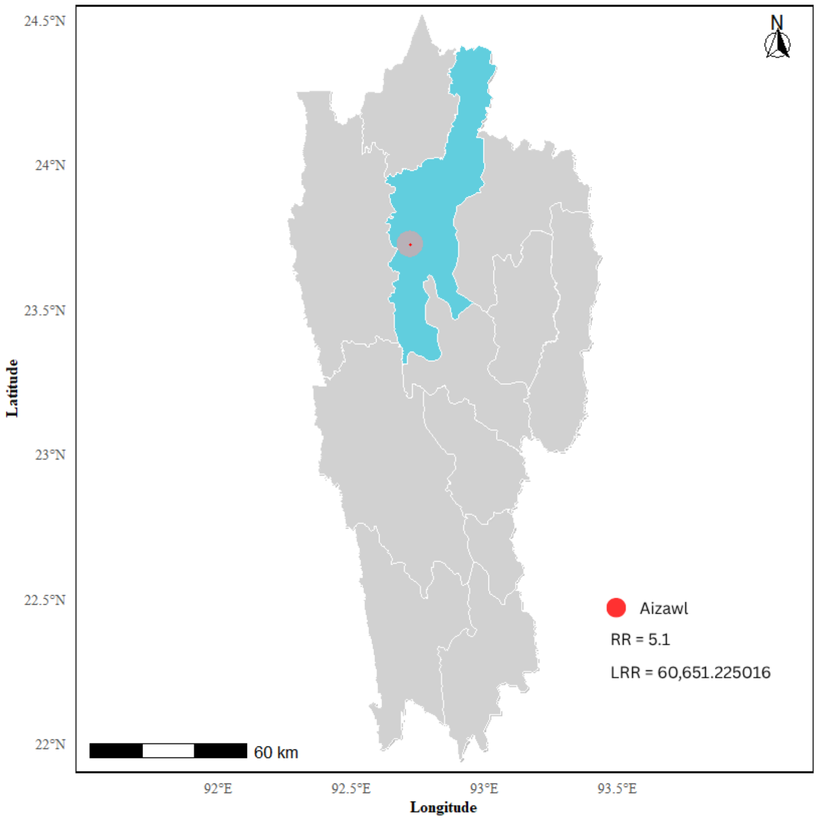

Note: Author's visualisation based on SaTScan result

4.15.4 Robustness and Sensitivity

The 999 Monte Carlo replications performed in the analysis ensures reliable p-values, minimizing Type I errors (Kulldorff, 1997). The Poisson model suits count-based, centroid-aggregated data, outperforming spatial autocorrelation tools, such as Moran's I, LISA and Getis-Ord Gi*, due to the nature of clustering and concentration bound within a 3.7 km^2 space. The absence of any contiguous neighbour district, which is also relatively abundant in observable case, leads to these tools flagging Aizawl as an outlier High-low, with no statistical significance. The Discrete Poisson model through SaTScan flags concentration without having to have this relatively rich contiguous neighbour. Furthermore, the sensitivity test at 20% population-at-risk result reinforces Aizawl's overwhelming concentration, as districts have low case counts, for instance Khawzawl's 146 uses, preclude secondary clusters.

4.15.5 Limitations

The centroid aggregation at 0 km radius stems from necessity, the uneven nature of district boundaries and the need to aggregate district-level data for fear of double counting under the catchment area in a highly concentrated cluster like Aizawl, that may potentially obscure intra-district variations in Aizawl District. This was partially mitigated by the Thiel T within group analysis in the descriptive section. Nevertheless, future studies can benefit from a demarcated municipal ward or village council level shapefile that can effectively segregate population within and beyond.

The absence of patient migration data in Mizoram is a limiting factor, especially when assessing utilisation of services at the district level. The high usage in Aizawl as against its expected usage suggests considerable patients from other districts visit the capital for diagnostic services. Future studies can benefit from patient mitigation data. This can be achieved by increasing the granularity of data collection by the government.

The absence of secondary clusters limits insights into diagnostic access in other regions of Mizoram, despite showing hopeful facility clustering in the previous SaTScan analysis. As previous analyses suggest, this is likely due to the highly concentrated nature of Medtech in Aizawl, reinforcing the prior findings that patients migrated for diagnostic services.

The lack of data at the primary level and secondary level suggests the absence of a uniform technological standard threshold within the state, as shown by the level of disparity even at the district level. Further compounded by the lack of usage data with the private clinics may, together risk underestimation of the true scale of diagnostic access throughout Mizoram. Given the population size of Mizoram, the population size of the study is robust enough for the analysis given that institutional facilities dominate Mizoram's diagnostic services. Nevertheless, these extra data points can immensely help future studies, especially those focusing on smaller spatial zones.

The SaTScan analysis rejects the H_0, confirming significant concentration of medical equipment usage in Aizawl ($RR = 5.10$, $p < 0.001$), in favour of the H_1. Aizawl's 71.7% share of diagnostics is a sobering reminder that unchecked concentration of health infrastructure in one place can result in agglomeration of interconnected services, perpetuating spatial disparities in functional healthcare access.

4.16 CONCLUSION

The findings in this chapter reveals multidimensional spatial inequality, spanning spatial locations of health infrastructure, their capacity in care, technological reach, and the nature of service delivery in the health sector of the state of Mizoram. This chapter showed that health infrastructure in Mizoram is unevenly distributed. Urban areas of Mizoram hold a disproportionate share of facilities, personnel, and equipment, while rural and high-risk areas face persistent shortages. These gaps reflect allocation patterns that emphasize population size rather than spatial coverage or disease burden. As a result, large parts of the state continue to operate with limited access to essential care.

Addressing the observed disparities requires more than increasing infrastructure or reallocating it based on population metrics. Health service delivery is conditioned not just by availability, but by functional integration across all levels of care. A system that expands primary services without ensuring linkage to higher tiers will fall short in managing complex or chronic conditions. While geographic coverage is necessary, it is not sufficient. Effective provision depends on whether referral systems are operational, whether advanced diagnostic and treatment capacity is spatially distributed, and whether institutional planning reflects actual patterns of disease burden rather than administrative convenience. Without addressing these multi-tiered constraints, ranging from care specialisation to the placement of core technologies, access gains may be shallow and uneven. A more resilient health system requires investments that prioritize structural connectivity, spatially optimised centres that puts equity over centralisation.

CHAPTER-V

SPATIAL INEQUALITY IN HARD INFRASTRUCTURE IN MIZORAM

5.1 INTRODUCTION

This chapter examines the spatial distribution and economic implications of spatial inequality in hard infrastructure in Mizoram, focusing on buildings, road and electricity infrastructure, with economic activity proxied by Night Time Lights (NTL) radiance. Building on Chapter 4's analysis of health infrastructure, it extends the study of spatial inequality by investigating how uneven access to physical infrastructure shapes patterns of economic development in the state.

The buildings infrastructure, represented as vector polygons for Mizoram's 11 districts, are sourced from Global ML Buildings Footprint (Microsoft, 2023) and OpenStreetMap (OSM) (OpenStreetMap Contributors, 2023) datasets, and processed in QGIS. District-wise summary statistics, including average buildings per square kilometres, are presented alongside choropleth maps to visualize spatial patterns. Inter-district disparities in building density and concentration of settlements are also quantified using the Atkinson index to capture inequality in the distribution.

The digitized road networks, disaggregated into National Highways, State Highways, Rural Roads, Agriculture Link Roads and Residential roads, are sourced from OSM (OpenStreetMap Contributors, 2023) and cross referenced with Ministry of Rural development (MoRD) digital road network (Digital Sadak) and published road data of Mizoram Public Work Department (MPWD) through Mizoram Statistical Abstract (2023). Disparities in road density, measured per 100 km², are assessed using coefficients of variation (CV) and tested for spatial clustering through Global Moran's I and Local Indicators of Spatial Association (LISA).

Data from Electricity Infrastructure is sourced from Report of the Mizoram Power and Electricity Department and also reports from Mizoram Statistical Abstract (2023). However, due to good spatial coverage (98% of all settlements), spatial analysis is not performed. Instead, descriptive analysis of in the quality, challenges and prospects is made.

Night Time Light (NTL) radiance data was collected through the Annual Composite (V2 and V2.2) data from Earth Observation Group (EOG), via NOAA's Visible Infrared Imaging Radiometer Suite (VIIRS) data. The data is then process and use as a proxy for economic activity, situating Mizoram within the national context. Gini coefficient is used to quantify disparities, while district-wise and grid-based temporal trends (2014–2023) are tested using the Mann-Kendall method. Hotspot analysis (Getis-Ord Gi*) is applied to the linear regression slope values of NTL, identifying spatial clustering of gains and stagnation in economic activity in the state.

To assess the relationship between infrastructure and economic outcomes, spatial econometric models (OLS, spatial lag, and spatial error) are estimated at the grid scale. Explanatory variables include road density by type, population density, poverty levels, building counts, and elevation, with NTL density as the dependent variable. Diagnostics and sensitivity tests are performed to account for spatial dependence and heterogeneity. Analyses are conducted using QGIS for spatial processing, R for statistical and spatial econometric modelling. By integrating descriptive, inequality, temporal, and regression approaches, the chapter provides a comprehensive account of spatial inequality in Mizoram's infrastructure and its implications for development.

5.2 SPATIAL INEQUALITY IN BUILDING INFRASTRUCTURE

The distribution of building infrastructure serves as a key indicator of spatial development patterns within Mizoram. This section examines the extent of such infrastructure across the state's districts to assess variations in density and their implications for regional equity. By evaluating building density, the analysis reveals disparities in the allocation of built environments, which reflect broader socio-economic trends. The application of the Atkinson Index further quantifies these inequalities, providing a measure of how unevenly resources are spread. This approach allows for an exploration of whether certain districts experience disproportionate concentrations of infrastructure relative to others. Through descriptive and quantitative methods, the following subsections present findings that highlight the spatial distribution of buildings infrastructure in Mizoram.

5.2.1 Spatial distribution of Building Infrastructure in Mizoram

Map 5.1 displays the spatial distribution of building infrastructure across Mizoram, mapped within a coordinate-referenced bounding box spanning approximately 92.2°E to 93.5°E longitude and 21.9°N to 24.5°N latitude.

Map 5.1 Buildings Infrastructure in Mizoram 2023

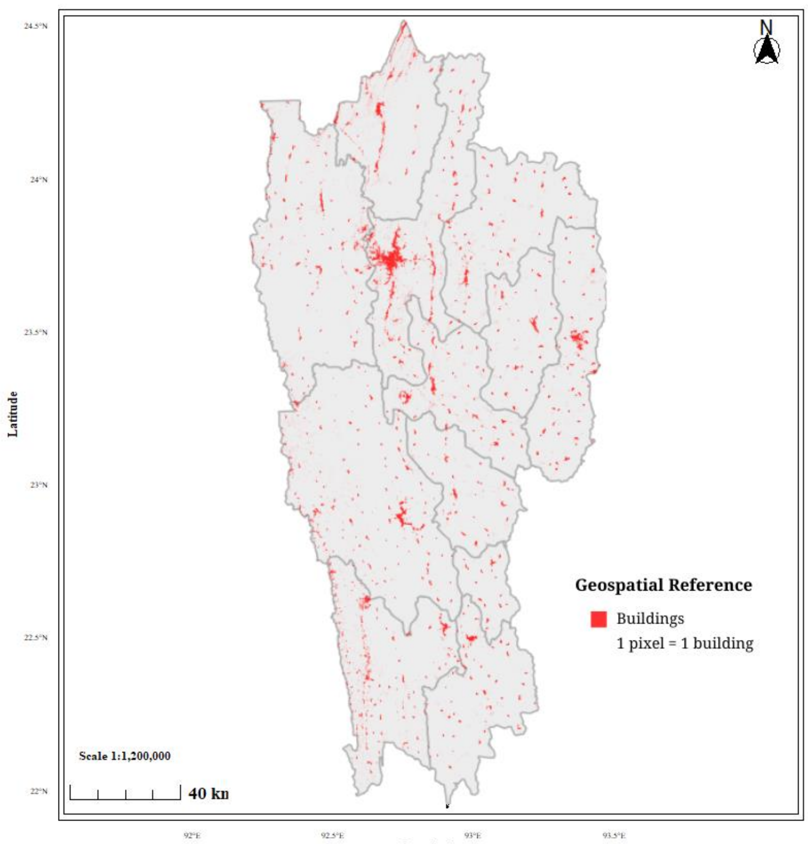

Source: Microsoft Global ML Building Footprints (2023); OpenStreetMap contributors (2023)

Individual buildings are represented as red pixel markers positioned at the centroids of valid building polygons. District boundaries are also shown and labelled for geographic orientation. The use of pixel markers allows building presence to remain visually legible at this scale without distorting the overall spatial pattern. All data have been projected in EPSG 32646, UTM Zone 46N, to maintain consistency across spatial layers. The map shows that building concentration is visually higher in the north-central part of the state, corresponding to Aizawl district, where the capital city is located.

Table 5.1 presents the number of buildings, total area (in km²), and resulting building density (buildings per km²) across the eleven districts of Mizoram

Table 5.1 Mizoram District-wise Building Density

SN	District	Buildings	Area_km2	Density
1	Aizawl	90101	2089.26	43.13
2	Champhai	27350	1530.71	17.87
3	Hnahthial	9287	1100.89	8.44
4	Khawzawl	12419	1139.79	10.9
5	Kolasib	27326	1582.13	17.27
6	Lawngtlai	34240	2473.89	13.84
7	Lunglei	33528	3415.74	9.82
8	Mamit	27284	3097.92	8.81
9	Saiha	15111	1509.47	10.01
10	Saitual	19157	1822.14	10.51
11	Serchhip	19951	1338.26	14.91

Source: Microsoft World Buildings (2023) & OpenStreetMap (2023)

The number of buildings varies considerably across Mizoram's districts, with Aizawl registering the highest count at 90,101, while Hnahthial records only 9,287. District area also shows high variation, ranging from 1,100.89 km² in Hnahthial to 3,415.74 km² in Lunglei, indicating substantial differences in the spatial extent of administrative units. Building density, expressed as buildings per square kilometre, ranges between 8.44 in Hnahthial and 43.13 in Aizawl. Among the 11 districts, three stand out with density above 15 buildings/km²: Aizawl (43.13/km²), Champhai

(17.87/km²), and Kolasib (17.27/km²). On the other hand, the lowest densities are observed in Hnahthial (8.44/km²), Mamit (8.81/km²), and Lunglei (9.82/km²), suggesting relatively sparse settlement patterns.

Aizawl's dominance is evident not only in the absolute number of buildings but also in its density, which is over twice that of Champhai, the next highest district. This suggests a concentration of settlement and infrastructure in the state's central hub. Districts such as Lunglei and Lawngtlai, despite their large land areas (3,415.74 km² and 2,473.89 km², respectively), exhibit moderate building counts (33,528 and 34,240), which translates into relatively low density, indicating dispersed settlement patterns. Mid-range values are observed in districts such as Serchhip (14.91/km²) and Khawzawl (10.90/km²), where the building distribution balances between compact and dispersed forms. The contrast between compactly settled districts such as Aizawl and Champhai, and sparsely settled ones, such as Hnahthial and Mamit, indicates a highly heterogeneous distribution of built infrastructure across Mizoram.

5.2.2 Atkinson Index on Building Density in Mizoram

The Atkinson Index is employed to quantify spatial inequality in building density across Mizoram's 11 districts, with inequality aversion parameters (ε) set at 0.5, 1, 1.5, and 2. Higher ε values emphasize disparities at the lower end of the density distribution, giving greater weight to districts with sparse infrastructure. To ensure statistical reliability, bootstrapping with 1000 replications generates 95% confidence intervals, accounting for variability in the estimates. The results of the Atkinson Index analysis are presented in Table 5.2.

Table 5.2 Atkinson Index Summary of Building Density

ε	Atkinson Index	Mean	Std. Error	CI Lower 95%	CI Upper 95%
0.5	0.066	0.055	0.032	0.01	0.108
1	0.116	0.1	0.056	0.019	0.197
1.5	0.155	0.136	0.074	0.031	0.271
2	0.185	0.16	0.085	0.034	0.324

Source: Own calculation

At ε = 0.5, the Atkinson Index is 0.066, indicating a modest level of inequality in the spatial distribution of building infrastructure across Mizoram's districts. As ε increases to 1.0, 1.5, and 2.0, the index rises to 0.116, 0.155, and 0.185, respectively, reflecting greater sensitivity to disparities in districts with lower building density, such as Hnahthial, Mamit, and Lunglei. The bootstrapped 95% confidence intervals widen with higher ε values, ranging from 0.010–0.108 at ε = 0.5 to 0.034–0.324 at ε = 2.0, due to increased sensitivity to extreme disparities in low-density districts. The central estimates remain consistent across aversion parameters, confirming the robustness of the measurement.

The results highlight that while overall building density distribution appears relatively balanced at lower ε values, inequality becomes more pronounced when prioritizing districts with sparse infrastructure. For example, Aizawl's building density (43.13 buildings/km²) is over five times higher than that of Hnahthial (8.44 buildings/km²). Such disparities are amplified at higher ε values, where the index focuses on the lower end of the distribution.

5.2.3 Atkinson Index Analysis on Buildings per Capita in Mizoram

This section tests the hypothesis that the distribution of buildings per capita across Mizoram's districts is unequal, indicating significant spatial inequality in infrastructure provision relative to population needs. The analysis employs an epsilon value of 1 to assess inequality while maintaining a balanced focus on deviations across the distribution, supplemented by sensitivity checks across epsilon values of 0.5, 1.5, and 2.0 to evaluate the robustness of findings.

Results are reported with statistical metrics to ensure transparency and robustness in evaluating spatial economic disparities. Analysis was conducted using the Atkinson index on buildings per capita, calculated as the number of buildings divided by the 2023 population for each of Mizoram's 11 districts. The data, sourced from Table 5.1 and population estimates, yield buildings per capita values ranging from 0.192 (Aizawl) to 0.373 (Hnahthial). The Atkinson index is computed with 1000 bootstrap replications to estimate the mean, standard error, and 95% confidence interval, ensuring robust statistical inference for epsilon values of 0.5, 1.0, 1.5, and 2.0.

5.2.4 Results of Atkinson Index tests on buildings per Capita

The Atkinson index for buildings per capita at $\varepsilon = 1$ is 0.009, with a bootstrap mean of 0.008 and a standard error of 0.003. The 95% confidence interval, derived from percentile bootstrap methods, ranges from 0.003 to 0.014. The result indicates that there is moderate inequality in the distribution of buildings per capita, and shows that districts with dense buildings, such as Aizawl have more buildings than their population would warrant.

Table 5.3 Statistical Metrics for Atkinson Index ($\varepsilon = 1$)

Metric	Value
Atkinson Index	0.009
Bootstrap Mean	0.008
Standard Error	0.003
95% Confidence Interval (Lower)	0.003
95% Confidence Interval (Upper)	0.014

Source: Own calculation

5.2.5 Hypothesis Evaluation

Since 95% confidence interval, Atkinson Index at **ε = 1**, does not include zero, the null hypothesis of no inequality (H_0) is rejected at the 5% significance level. The positive Atkinson index indicates a statistically significant degree of inequality in the distribution of buildings per capita across Mizoram's districts. This inequality suggests uneven infrastructure provision relative to population needs, potentially reflecting disparities in economic development or resource allocation.

The Atkinson index, though statistically significant, may underestimate the true extent of inequality due to the nature of the buildings data, spatial footprints of structures. In urban areas, the prevalence of multi-storied buildings, typically averaging three to four stories, contrasts with predominantly single-storied structures in other districts, suggesting a substantially greater inequality in infrastructure provision than the modest index values indicate.

5.2.6 Sensitivity Analysis

Across all epsilon values, the 95% confidence intervals exclude zero, consistently supporting the rejection of the null hypothesis. The Atkinson index increases with higher epsilon values, from 0.004 at epsilon = 0.5 to 0.018 at epsilon = 2.0, reflecting greater sensitivity to districts with lower buildings per capita.

Table 5.4 Atkinson Index Summary of Building per Capita

ε	Atkinson Index	Mean	Std. Error	CI Lower 95%	CI Upper 95%
0.5	0.004	0.004	0.001	0.002	0.007
1	0.009	0.008	0.003	0.003	0.014
1.5	0.014	0.012	0.004	0.005	0.021
2	0.018	0.016	0.005	0.006	0.027

Source: Own calculation

This trend indicates that inequality becomes more pronounced when prioritizing the lower tail of the distribution, yet the modest index values suggest a relatively balanced distribution overall. The consistency of statistical significance across epsilon values reinforces the robustness of the finding that spatial inequality exists in buildings per capita, aligning with economic concerns about equitable resource allocation. The absence of overlap with zero in all confidence intervals underscores the reliability of the conclusion, independent of the specific inequality aversion parameter chosen.

5.2.7 Limitation of the Analysis

The building footprint dataset, captures the spatial distribution of structures across Mizoram's districts. However, it does not account for building height, function, or quality, which is a limitation in performing a near perfect representation of density and per capita analyses. In some urban areas where buildings commonly rise to three or four stories, the dataset treats these multi-storied structures the same as single-storied ones prevalent for the rest of the state, potentially underrepresenting the extent of infrastructure disparities. This limitation is particularly relevant for the per capita analysis, as building capacity per person is not reflected in raw counts, but spatial footprint. Additionally, the dataset may not fully capture functional differences, such as residential versus commercial buildings, which could influence interpretations of infrastructure equity. With only 11 districts in Mizoram, the confidence intervals widened at higher epsilon values. Despite these constraints, the bootstrap methodology enhances the robustness of the Atkinson index estimates while the integration of OSM data and Microsoft data provides a sufficiently representative dataset for district-level comparison of settlement patterns and offers a broad picture of the spatial distribution of buildings infrastructure within the confines of the state.

Overall, the Atkinson index analyses reveal significant spatial inequalities in Mizoram's building infrastructure, both in terms of density and per capita distribution. For building density, the Atkinson index ranges from 0.066 ($\varepsilon = 0.5$) to 0.185 ($\varepsilon = 2.0$), with 95% confidence intervals consistently excluding zero, indicating statistically significant inequality.

For buildings per capita, the Atkinson index ranges from 0.004 ($\varepsilon = 0.5$) to 0.018 ($\varepsilon = 2.0$), with confidence intervals also excluding zero that suggests an unequal distribution at buildings infrastructure in Mizoram. The modest index values although may have understate inequality due to dense multi-storied buildings in districts such as Aizawl, it supports the finding by suggesting that inequality could be more severe than can be statistically tested with the available data. Nevertheless, the consistency of findings across both analyses suggests targeted investments in southern and western districts of Mizoram could address this imbalance and support equitable regional development.

5.3 SPATIAL INEQUALITY IN ROAD INFRASTRUCURE

This section analyses the spatial distribution of road infrastructure by types across Mizoram using a GIS-based approach (see Chapter 3 for road mapping process). The Coefficient of Variation (CV) is employed to examine inter-district disparities and their implications for economic development in Mizoram. Spatial autocorrelation analyses, including Moran's I and Local Indicators of Spatial Association (LISA), are conducted to assess clustering patterns.

5.3.1 Road Typology and Distribution by District

The mapped road network is segregated into five types: National Highways (NH), State Highways (SH), Rural Roads (RR), Agricultural Link Roads (ALR), and

Residential Roads (Res.R). Road lengths are calculated using the Universal Transverse Mercator projection (UTM Zone 46N, EPSG:32646) to ensure accuracy. The shapefiles are also validated against multiple road network sources.

In Map 5.2 (left panel), National Highways (NH) connect Mizoram to other states and neighbouring countries, funded by the central government and maintained by the National Highways Authority of India (NHAI) and Mizoram's Public Works Department (PWD).

Map 5.2 National Highway and State Highway in Mizoram 2023

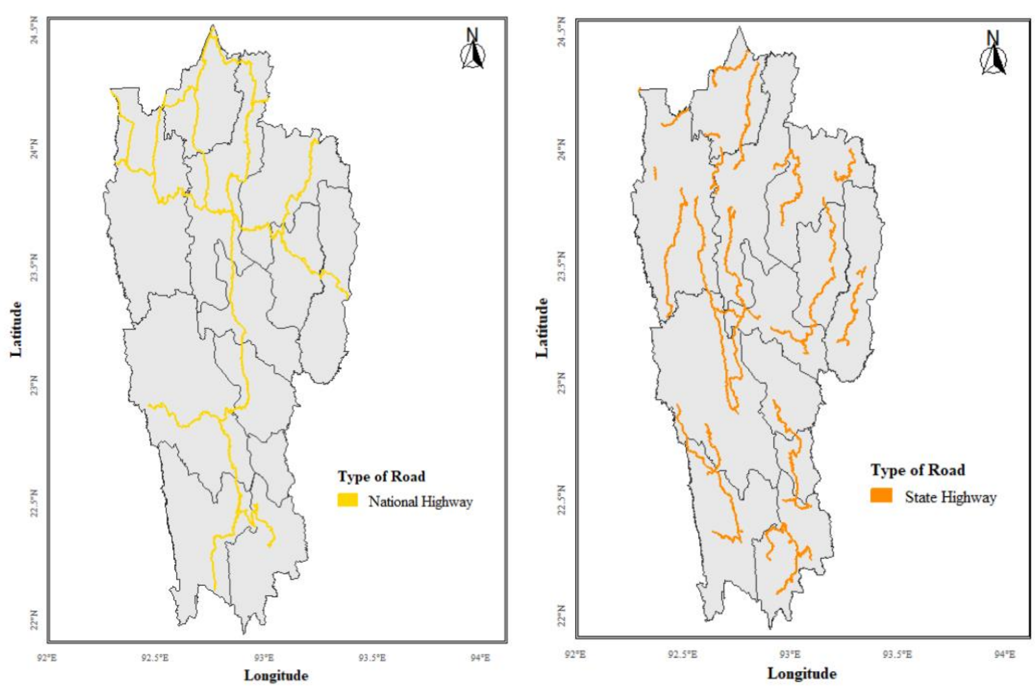

Source: OpenStreetMap Contributors (2023) & Own Mapping

Key routes include NH-2, from New Vervek to Tuipang via Aizawl, Serchhip, Lunglei, and Lawngtlai; NH-6, the Indo-Myanmar trade route from Bairabi to Zokhawthar via Kolasib, Aizawl, Saitual, Khawzawl, and Champhai, intersecting NH-

2 at Seling; NH-306A, from Saiphai to New Vervek; NH-102B, from Khawkawn to Kawlkulh in Saitual District; NH-302, from Lunglei to Tlabung for Indo-Bangladesh trade; NH-108, from Kanhmun (Mamit District) to Aizawl; NH-502A, from Zero Point to Saiha and the Kaladan Multi-Modal Transit Transport Project road from Lawngtlai to Zochawchhuah, linking to Sittwe and Paletwa ports in Myanmar. They total 1,424.882 km with an average density of 7.845 km per 100 km².

Map 5.2 (right panel) shows roads classified as State Highways (SH) in this study which links districts and key settlements, maintained by Mizoram's PWD. Key routes include the World Bank-funded road from Aizawl to Lunglei via Thenzawl, which also meets NH-2 at Serchhip via the Mat River Valley; Keitum to Khawzawl via East Lungdar, Biate, and Chawngtlai, meeting NH-102B near Pawlrang; Lawngtlai to Tlabung via Chawngte; Lunglei to Rawpuichhip via Buarpui and N. Kanghmun; Marpara to Dampui in Mamit District; Champhai to S. Khawbung via Khuangleng; and Kawlchaw East to Lope via Serkawr, Tuipang, and Zawngling in Saiha District. These routes span 1,850.158 km with an average density of 8.413 km per 100 km². This analysis includes a broader set of roads than the 170 km of officially designated as State Highways by the PWD (Statistical Handbook, 2023).

The roads classified as Rural Roads (RR) in Map 5.3 (left panel) are roads that connect villages and satellite towns to National and State Highways, maintained by Mizoram's PWD and, for some border routes, the Border Roads Organisation. They include Village Roads, Major District Roads, Other District Roads, and Border Roads, serving as vital arteries for areas unserved by major highways. These roads shorten travel distances across Mizoram's parallel mountain ridges, providing essential access to markets and services for rural communities. While most are surfaced, some tracks remain under surfacing efforts, as observed in 2023 satellite imagery. They total 3,741.340 km with an average density of 17.679 km per 100 km².

Map 5.3 Rural Roads and Agricultural Link Roads (ALR) in Mizoram

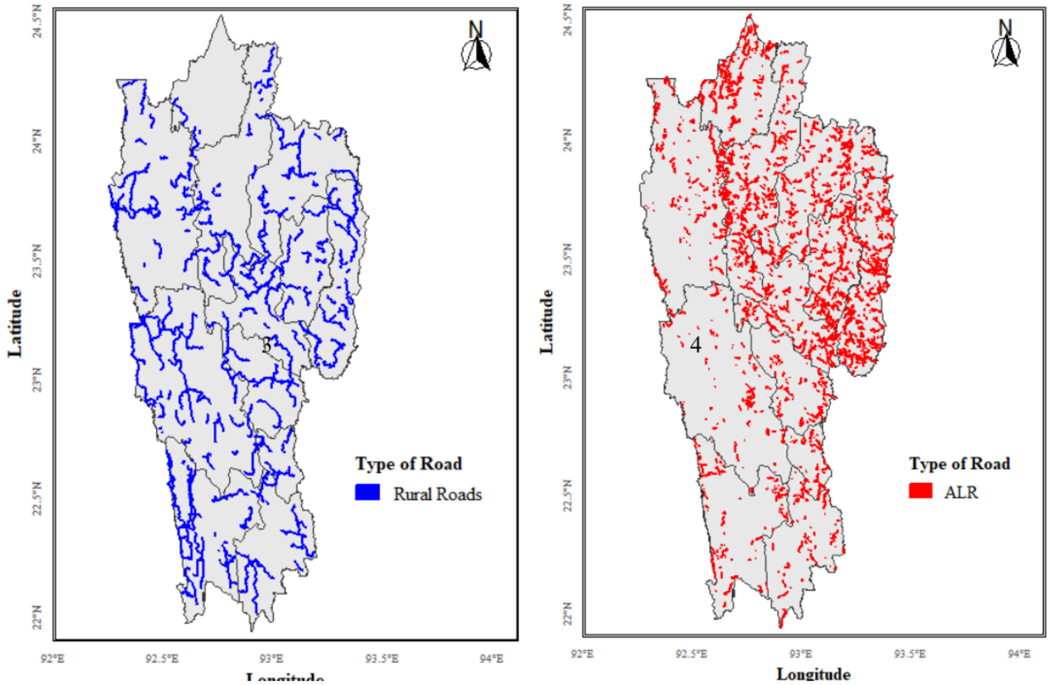

Source: OpenStreetMap Contributors (2023) & Own Mapping

Roads classified as Agricultural Link Roads (ALR) in this analysis (Map 5.3, right panel) are roads that connect rural settlements to economic sources, including farmlands, quarries, river basins, mining sites, and small or medium enterprise production centres. Funded through government schemes such as the Pradhan Mantri Gram Sadak Yojana, MGNREGA, agriculture programmes, and MLA funds, or occasionally by community and private initiatives, these dirt tracks, locally known as jeep roads, facilitate transport of agricultural and industrial goods to markets via National and State Highways. Maintenance is primarily handled by local communities, with some surfaced with gravel or bitumen and others remaining unsurfaced, as observed in 2023 satellite imagery. They total 5,197.374 km with an average density of 28.987 km per 100 km².

Map 5.4 Residential Roads and Total Roads in Mizoram 2023

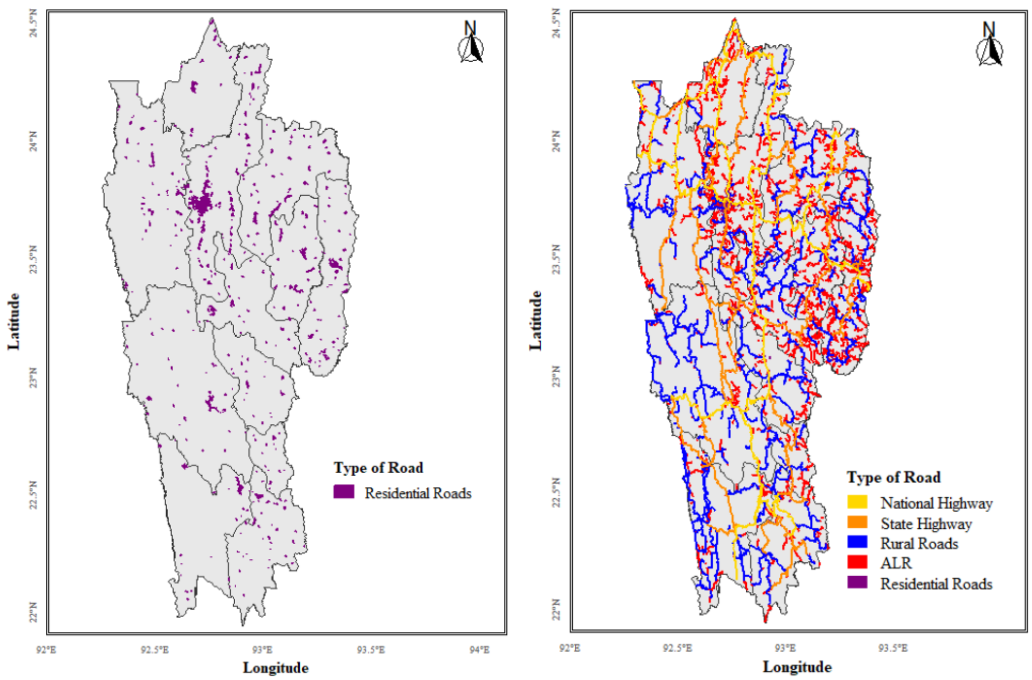

Source: OpenStreetMap Contributors (2023) & Own Mapping

The network of roads classified as Residential Roads (Res. R) provide connectivity within towns and villages, linking homes, schools, and local amenities. Maintained by Mizoram's PWD in urban areas and by village or local councils in rural settings, these roads are typically paved with bitumen or cement in towns, while rural roads may remain unpaved, consisting of dirt or gravel tracks, as observed in 2023 satellite imagery. They total 2,264.437 km with an average density of 11.058 km per 100 km².

Although not exhaustive, this GIS dataset of roads covers a wider range of roads than existing records and is expected to enhance further analysis at a granular level.

5.3.2 District wise Road length and Density

The GIS analysis reveals that National Highways (NH) with the longest extent is found in Mamit (199.32 km), followed by Lunglei (178.08 km) and Kolasib (164.30 km). Table 5.5 presents the summary of road length by type in details.

Table 5.5 Length of Roads by District in Mizoram 2023

SN	District	NH	SH	RR	ALR	Res.R	Total Roads
1	Aizawl	319.67	170.59	302.28	818.81	798.3	2409.66
2	Champhai	41.35	82.2	386.4	898.37	249.8	1658.12
3	Hnahthial	61.93	50.72	214.82	220.32	52.19	599.98
4	Khawzawl	87.51	107.68	196	525.39	175.37	1091.95
5	Kolasib	164.3	131.9	43.44	433.93	105.14	878.71
6	Lawngtlai	132.33	228.09	658.29	397.8	136.34	1552.85
7	Lunglei	178.08	243.39	643.27	232.16	146.64	1443.55
8	Mamit	199.32	234.41	405.99	406.61	143.66	1390
9	Saiha	72.52	200.26	266.84	189.91	108.66	838.19
10	Saitual	132.2	162.22	287.5	564.75	230.46	1377.13
11	Serchhip	60.82	129.93	329.34	500.57	116.58	1137.23
*	Mizoram	1450.02	1741.39	3734.18	5188.64	2263.15	14377.37

Source: OSM Contributors (2023) & Own Mapping.
Note: NH = National Highways, SH = State Highways, RR = Rural Roads, ALR = Agricultural Link Roads, Res.R = Residential Roads

State Highways (SH) are most extensive in Lunglei (243.39 km), followed by Mamit (234.41 km) and Lawngtlai (228.09 km). Rural Roads (RR) have the greatest length in Lawngtlai (658.29 km), followed by Lunglei (643.27 km) and Champhai (386.40 km). Agricultural Link Roads (ALR) are longest in Champhai (898.37 km), followed by Aizawl (818.81 km) and Saitual (564.75 km). The state's Residential Roads (Res. R) are most prominent in Aizawl (798.30 km), followed by Champhai (249.80 km) and Saitual (230.46 km).

The mapped road density by districts is presented in Table 5.6. In terms of road network density measured in km per 100 km², Aizawl has the highest density in National Highways (NH) at 13.75 km per 100 km², followed by Kolasib (12.21) and Khawzawl (7.72).

Table 5.6 Road Density by District in km per 100 km² in 2023

SN	District	NH	SH	RR	ALR	Res.R	Total Density
1	Aizawl	13.75	7.34	13.01	35.23	34.35	103.67
2	Champhai	2.7	5.37	25.23	58.66	16.31	108.26
3	Hnahthial	5.63	4.61	19.51	20.01	4.74	54.5
4	Khawzawl	7.72	9.5	17.29	46.35	15.47	96.33
5	Kolasib	12.21	9.8	3.23	32.24	7.81	65.28
6	Lawngtlai	5.33	9.18	26.5	16.01	5.49	62.51
7	Lunglei	5.21	7.12	18.82	6.79	4.29	42.24
8	Mamit	6.43	7.56	13.1	13.12	4.64	44.85
9	Saiha	4.84	13.37	17.82	12.68	7.25	55.96
10	Saitual	7.28	8.94	15.84	31.11	12.69	75.86
11	Serchhip	4.5	9.62	24.39	37.07	8.63	84.22
*	Mizoram	6.87	8.25	17.7	24.59	10.73	68.14

Source: OSM Contributors (2023 & Own Mapping.
Note: NH = National Highways, SH = State Highways, RR = Rural Roads, ALR = Agricultural Link Roads, Res.R = Residential Roads

State Highways (SH) have the greatest density in Saiha at 13.37 km per 100 km², followed by Serchhip (9.62) and Kolasib (9.80). Rural Roads (RR) are most dense in Lawngtlai district at 26.50 km per 100 km², followed by Champhai (25.23) and Serchhip (24.39). Agricultural Link Roads (ALR) sees the highest density in Champhai at 58.66 km per 100 km², followed by Khawzawl (46.35) and Serchhip (37.07). Residential Roads (Res.R) have the greatest density in Aizawl 34.35 km per 100 km², followed by Champhai (16.31) and Khawzawl (15.47). The total density of all road type is this highest in Champhai district at 108.26 km per 100 km², followed by Aizawl (103.67) and Khawzawl (96.33).

Map 5.5 highlights the density per km^2 trend in a 10x10 km grid in Mizoram, with the yellow colour showing higher road density while the blue shows lower road density.

Map 5.5 Spatial Distribution of Road Density by 100 km^2 in Mizoram

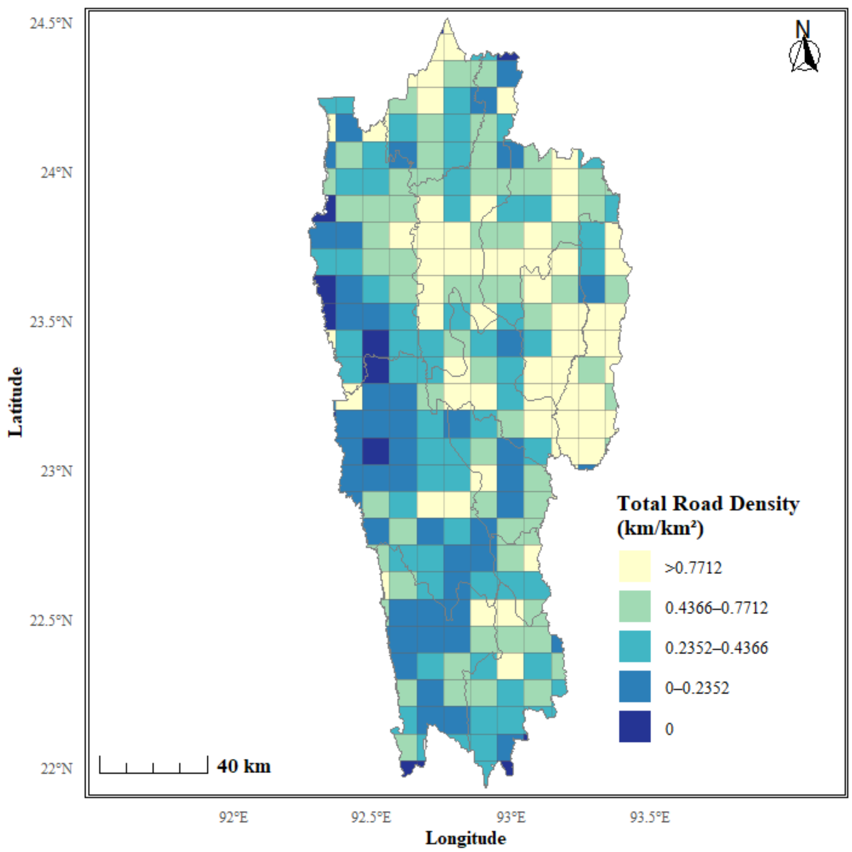

Source: OpenStreetMap Contributors (2023) & Own Mapping

5.3.3 Coefficient of Variation of Road Infrastructure Distribution

To test the variation of the density of roads by district, a coefficient of variation analysis is employed. Table 5.6 presents the Coefficient of Variation (CV) for road density across Mizoram's 11 districts, highlighting disparities in road infrastructure distribution.

The 2023 spatial distribution of road infrastructure in Mizoram exhibits unmistakable and severe inequality, particularly where roads serve economically and socially critical functions. With a coefficient of variation of 80% for Res.R and 57% for ALR, the data points to a systemic neglect of peripheral settlements and rural economic linkages. National Highways (48%) and Rural Roads (37%) further show entrenched disparities. Although the aggregate CV for total road density is at a moderately high inequality of 32%, this masks structural imbalances that skew resources toward specific regions. In an agrarian state like Mizoram, such disparities in agricultural and rural road access directly undermine economic resilience and equitable development.

Table 5.7 Coefficient of Variation (CV) of Road Density by Road Type

Road Type	CV (%)
National Highways (NH)	48%
State Highways (SH)	28%
Rural Roads (RR)	37%
Agricultural Link Roads (ALR)	57%
Residential Roads (Res.R)	80%
Total Road Density	32%

Source: Own Calculation

The observed disparities in road infrastructure, particularly in Residential Roads (CV: 80%) and Agricultural Link Roads (CV: 57%), indicate a significant imbalance in public investment across districts. In the context of an agrarian economy like Mizoram, the variation in Agriculture Link Rads suggests uneven access to essential infrastructure that supports both rural livelihoods and urban residential development.

While some level of spatial variation is expected due to topography or population density, the scale of disparity across publicly funded road categories, especially those directly tied to socio-economic mobility, raises important questions about the equity and inclusiveness of infrastructure planning in the state. The concentration of investment in certain districts points to the need for more transparent, data-driven, and regionally responsive infrastructure policies. Addressing this inequality is not merely a technical challenge but a necessary step toward ensuring that public resources serve all regions equitably, in line with developmental and constitutional commitments.

5.4 SPATIAL CLUSTERING OF ROAD INFRASTRUCTURE

This section tests the hypothesis that road infrastructure in Mizoram exhibit significant spatial autocorrelation, indicating significant spatial clustering. A 10x10 km grid was used to divide the state into 258 cells. Global Moran's I was calculated for five road types: National Highways (NH), State Highways (SH), Rural Roads (RR), Agricultural Link Roads (ALR), and Residential Roads (Res.R). Queen contiguity is employed to assess spatial autocorrelation. Sensitivity tests on 5x5 km and 20x20 km grids is also performed to access the consistency of clustering patterns across spatial scales. Results are reported with statistical metrics are present as with tables and maps to ensure transparency.

5.4.1 Global Moran's I Results on Spatial Clustering in Road Infrastructure

The Global Moran's I values for all five road types indicate statistically significant spatial clustering of all road types across the 10×10 km grid cells (Table 5.8).

Agricultural Link Roads (ALR) show the strongest clustering, with a Moran's I of 0.386, $p < 0.001$, and a z-score of 11.609. National Highways (NH) also exhibit high clustering, with a Moran's I of 0.274, $p < 0.001$, and $z = 8.215$. Residential Roads (Res.R) display a moderate degree of clustering at 0.141 ($p < 0.001$, $z = 5.837$). State Highways (SH) report a Moran's I of 0.118 ($p < 0.001$, $z = 3.582$), while Rural Roads (RR) register the lowest clustering value among the five types at 0.101 ($p < 0.001$, $z = 3.140$). Despite variation in the strength of clustering, all results are statistically significant and confirm that road infrastructure is not randomly distributed across space.

Table 5.8 Global Moran's I Statistic for Road Density in Mizoram 2023

Road Type	Moran's I	P-value	Z-value
National Highway	0.274	0.001	8.215
State Highway	0.118	0.001	3.582
Rural Roads	0.101	0.001	3.14
Agricultural Link Roads	0.386	0.001	11.609
Residential Roads	0.141	0.001	5.837

Source: Own calculation

The high clustering of Agricultural Link Roads ($I = 0.386$) suggests a tight concentration of agricultural infrastructure in select pockets, particularly in central, northern and eastern region, leaving vast parts areas of the southern and southwestern arable lands under-utilised. This supports the view that access to agricultural mobility is limited to preferred zones, which is a significant concern in an agrarian context. National Highways ($I = 0.274$) also show concentrated patterns, with major corridors appearing to be spatially limited to central-east and northeast stretches, bypassing large interior and peripheral regions. Residential Roads, despite a lower Moran's I (0.141), reveal evident urban bias, aligning with denser cells in district centres, while outer cells remain sparsely connected.

The clustering of State Highways (I = 0.118) and Rural Roads (I = 0.101) is weaker, but their statistical significance still reflects patterned infrastructural presence, largely favouring the northern belt and middle-lower spine, while border districts and southern areas show consistent gaps. Overall, the spatial clustering confirms that certain zones enjoy repeated infrastructural attention while others remain persistently excluded, which suggests that structural inequalities in regional access and development opportunity exist in the state.

5.4.2 Local Indicator of Spatial Autocorrelation (LISA) Results

The spatial clustering of road density across Mizoram's 10x10 km grid (258 cells) was further analysed using Local Indicators of Spatial Association (LISA) analysis at a significance level of $p \leq 0.05$. This analysis identifies areas of concentrated high or low road density for National Highway (NH), State Highway (SH), Rural Road (RR), Agricultural Link Road (ALR), and Residential Road (ResR). Table 5.7 presents the LISA cluster counts, highlighting significant spatial autocorrelation and areas lacking connectivity.

Table 5.9 summarizes the LISA cluster counts for road density across Mizoram's 258-cell 10x10 km grid at $p \leq 0.05$ for five road types.

Table 5.9 LISA Cluster Summary Table

Road Type	High-High	High-Low	Low-High	Low-Low	Not Significant
National Highway	19	0	11	0	228
State Highway	11	0	10	2	235
Rural Road	7	0	11	0	240
Agricultural Link Road	28	1	4	21	204
Residential Road	8	0	4	0	246

Source: Own Calculation

Agricultural Link Road (ALR) has 28 High-High cells, 1 High-Low cell, 4 Low-High cells, 21 Low-Low cells, and 204 Not Significant cells, totaling 258 cells. National Highway (NH) reports 19 High-High cells, 11 Low-High cells, and 228 Not Significant cells, summing to 258 cells. State Highway (SH) shows 11 High-High cells, 10 Low-High cells, 2 Low-Low cells, and 235 Not Significant cells, totaling 258 cells. Rural Road (RR) has 7 High-High cells, 11 Low-High cells, and 240 Not Significant cells, summing to 258 cells. Residential Road (ResR) records 8 High-High cells, 4 Low-High cells, and 246 Not Significant cells, also totaling 258 cells. Map 5.5 presents the LISA map for Agricultural Link Road density in Mizoram in 2023.

Map 5.6 LISA Cluster of Agricultural Link Road in Mizoram

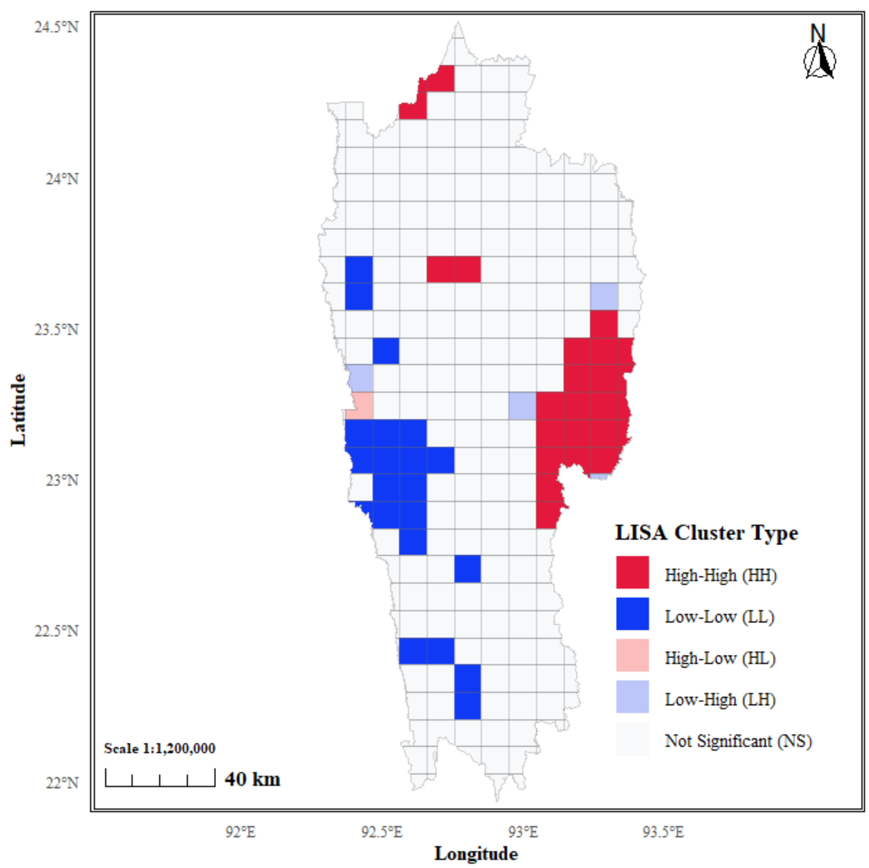

Source: Own visualisation based on GIS data from OSM Contributors (2023) & Own Mapping

The LISA analysis reveals distinct spatial clustering patterns, showing infrastructure disparities in Mizoram. Agricultural Link Roads (ALR) exhibit the strongest clustering, with 28 High-High cells indicating concentrated agricultural connectivity and 21 Low-Low cells highlighting significant gaps in rural access, potentially limiting agricultural development. National Highways (NH) and State Highways (SH) show moderate clustering, with 19 and 11 High-High cells, respectively, suggesting localized major transport routes, but minimal Low-Low clusters (0 for NH, 2 for SH) indicate few areas completely lack these roads. Rural Roads (RR) and Residential Roads (ResR) display limited clustering, with 7 and 8 High-High cells and no Low-Low clusters, reflecting their dispersed distribution. The high proportion of Not Significant cells (204 for ALR to 246 for ResR) suggests that significant clustering is confined to specific areas, emphasizing the need for targeted infrastructure investments to address connectivity gaps.

5.4.3 Sensitivity and Robustness Tests

To assess the robustness of the Global Moran's I results, sensitivity tests were conducted using alternative grid resolutions of 5×5 km and 20×20 km, alongside the primary 10×10 km grid. These tests evaluated the consistency of spatial autocorrelation patterns for all road types, National Highways (NH), State Highways (SH), Rural Roads (RR), Agricultural Link Roads (ALR), and Residential Roads (ResR), across different spatial scales.

The 5×5 km grid (1,032 cells) produced stronger Moran's I values for all road types, reflecting finer spatial resolution and enhanced statistical power. ALR maintained a high Moran's I of 0.389 ($z = 22.506$, $p < 0.001$), closely aligned with the 10×10 km result (0.386). NH (0.271), SH (0.194), RR (0.236), and ResR (0.223) also exhibited significant clustering ($p < 0.001$), with elevated z-scores due to the increased number of observations.

These results highlight the detection of more localised spatial patterns, particularly for ALR, which showed 28 High-High clusters in Table 5.7. In contrast, the 20×20 km grid (64 cells) showed broader but less sensitive patterns. ALR continued to exhibit strong clustering (Moran's I = 0.421, z = 6.541), and NH remained significant (0.307, z = 5.243). However, SH (0.009, $p = 0.364$) and RR (0.038, $p = 0.211$) showed non-significant autocorrelation, likely due to spatial smoothing at this coarser scale. ResR retained moderate clustering (0.138, $p = 0.004$), consistent with urban concentration. These findings confirm the stability of ALR and NH results across spatial scales, while SH and RR are more sensitive to resolution.

Robustness checks were also performed for the LISA analysis using stricter significance thresholds. At $p \leq 0.01$, ALR retained 20 High-High clusters, while NH had 12 at $p \leq 0.001$, these reduced to 9 and 3 respectively. Other road types show minimal significant clusters under stricter thresholds. While fewer clusters were detected, the persistence of ALR and NH under all conditions confirms the reliability of the primary 10×10 km results. Collectively, the sensitivity analyses validate the spatial clustering patterns and confirm that they are not just a construct of grid size or statistical thresholds.

5.3.4 Hypothesis Evaluation

The null hypothesis (H_0) posits that road infrastructure in Mizoram is randomly distributed across the state, with no significant spatial clustering, as indicated by a Global Moran's I of zero for all road types. The alternative hypothesis (H_1) asserts that road infrastructure exhibits significant spatial clustering, as indicated by a Global Moran's I greater than zero for all road types.

The Global Moran's I values range from 0.101 (Rural Roads) to 0.386 (Agricultural Link Roads), with z-scores from 3.140 to 11.609 and p-values < 0.001 for all road types. Since all Moran's I values are positive and statistically significant, the null hypothesis of random distribution is rejected at the 1% significance level. The results confirm significant spatial clustering of road infrastructure across Mizoram. Agricultural Link Roads show the strongest clustering ($I = 0.386$, $z = 11.609$), indicating concentrated agricultural connectivity in central, northern, and eastern regions. National Highways ($I = 0.274$, $z = 8.215$) and Residential Roads ($I = 0.141$, $z = 5.837$) also exhibit notable clustering, reflecting urban and major corridor concentration. State Highways ($I = 0.118$, $z = 3.582$) and Rural Roads ($I = 0.101$, $z = 3.140$) show weaker but significant clustering, primarily in northern and central areas. These findings suggest uneven infrastructure distribution, with southern and southwestern regions less connected.

Sensitivity tests on 5x5 km and 20x20 km grids, as detailed in Section 5.4.3, confirm the robustness of these results, particularly for ALR and NH, reinforcing the conclusion of significant spatial clustering across varying spatial scales.

5.4.5 Limitations of the Study

The spatial analysis of road density using Moran's I and LISA is subject to certain limitations. Road data derived from satellite imagery may be affected by forest canopy cover, which is extensive in Mizoram, potentially obscuring smaller or less formal roads. Furthermore, the classification of road types is complicated by the involvement of multiple agencies, beyond the Mizoram Public Works Department, including BRO, CPWD, and various state and local programmes. This introduces some uncertainty in attributing specific road segments to standardised categories. The analysis also does not distinguish between functional and under-construction roads, which may affect the accuracy of density as a proxy for accessibility.

Additionally, historical disparity in district formation and development means that road infrastructure in older districts such as Aizawl is more established, while newer districts like Hnahthial are still developing their networks. While this reflects structural realities, it may influence comparative interpretations. Finally, the study does not incorporate road quality due to limitations in detecting surface types via remote sensing. These factors do not detract from the overall findings but should be considered when interpreting the spatial patterns presented.

In conclusion, this study reveals a spatially uneven distribution of road infrastructure in Mizoram. The analysis identifies statistically significant clustering across all road types, with Agricultural Link Roads and National Highways exhibiting the most pronounced spatial concentration in central, northern, and eastern regions of the state. State Highways and Rural Roads favour northern and central redistricts while the distribution of Residential Roads aligns with urban centres. These patterns point to an uneven distribution of infrastructure, with some regions consistently more connected than others. The clustering of Agricultural Link Road agricultural connectivity is concerning as it constrains agricultural and economic opportunities, particularly for the southern and southwestern regions of the state. Targeted investments in the lagging districts could enhance connectivity and promote balanced regional development. Future research could build on this work by incorporating temporal comparisons, road quality metrics, and operational status data to deepen the understanding of infrastructure inequality in Mizoram and regions with similar geographic constraints.

5.5. A REVIEW OF ELECTRICITY INFRASTRUCTURE OF MIZORAM

Mizoram’s electricity infrastructure has improved significantly between 2016 and 2023, as reported in the Statistical Abstract of Mizoram 2023. The state’s total installed power capacity more than doubled, rising from 29.35 MW in 2016–17 to 62.70 MW in 2022–23. This growth was driven primarily by hydroelectric expansion (up to 38.35 MW) and the addition of 23.85 MW of solar capacity, most of which came online in 2022–23. Domestic electricity consumption rose from 233.90 million units (MU) to 284.69 MU, while per capita consumption increased from 322.22 kWh to 439.42 kWh, reflecting improved access and usage, especially in urban areas (Appendix IV, V & VI). By 2022–23, electricity had reached 717 of Mizoram's 725 inhabited villages, an electrification rate of almost 99 percent. Per capita consumption has also grown steadily, rising from 322 kWh in 2016–17 to 439 kWh in 2022–23. These are notable achievements given the state's difficult terrain and scattered population.

Table 5.10 Number of Electrified Villages (2022-2023)

District	No. of Electrified Villages	Percent Electrified
Mamit	91	97.85%
Kolasib	36	100.00%
Aizawl	60	100.00%
Champhai	43	100.00%
Serchhip	34	100.00%
Lunglei	131	99.24%
Lawngtlai	164	97.04%
Siaha	70	100.00%
Saitual	36	100.00%
Khawzawl	26	100.00%
Hnahthial	26	100.00%
Total	**717**	**98.90%**

Source: Statistical Handbook of Mizoram 2023

Despite these gains, the state continues to struggle with very high transmission and distribution (T&D) losses. The T&D figures have fluctuated sharply, from 15.8 percent in 2019–20 to nearly 29 percent in 2020–21, before settling at 24 percent in 2022–23. From an economic perspective, these losses are significant. They mean that nearly a quarter of electricity purchased never reaches the consumer. This strains state finances, as the government often absorb the shortfall through subsidies. Ultimately, the costs come down to the households and firms. High losses also translate into weaker service quality, more frequent outages, damaged equipment, and less reliable supply for businesses and homes.

Table 5.11 Transmission & Distribution Losses in Percentage

Year	T&D Losses (%)
2016 to 2017	25.53
2017 to 2018	21.7
2019 to 2020	15.82
2020 to 2021	29.05
2021 to 2022	28.31
2022 to 2023	24

Source: Statistical Handbook of Mizoram (2023)

From an economic perspective, these losses are significant. They mean that nearly a quarter of electricity purchased never reaches the consumer. This strains state finances, as the government often absorb the shortfall through subsidies. Ultimately, the costs come down to the households and firms. High losses also translate into weaker service quality, more frequent outages, damaged equipment, and less reliable supply for businesses and homes.

Table 5.12 Length of Power Lines in Mizoram in 2020

Power Line	Voltage Type	Length (circuit km)
132 kV	High Voltage	760.30 km
66 kV	Medium	111.42 km
33 kV	Medium	1483.42 km
11 kV	Low	5613.15 km
LT (0.415 kV)	Low	3319.07 km
11 kV ABC	Low	12.61 km
LT ABC	Low	127.97 km

Source: Statistics of Lines, Annual Report 2019-20: P&E, Dept, Mizoram

Data from the Department's 2019–20 Annual Report suggest why these inefficiencies may persist (Table 5.12). Mizoram's network is heavily tilted toward smaller lines. The state has about 2,200 km of higher-capacity lines (132 and 33 kV combined), but more than 8,900 km of smaller 11 kV and low-tension lines. Intuition suggests that electricity travels very long distances on small, weaker lines that are more vulnerable to losses and breakdowns. The number of major substations is also limited, just 11 High Voltage stations and 62 medium stations serving the entire state. This relatively sparse backbone infrastructure, combined with extensive reliance on smaller lines, suggests a structural mismatch that may explain why losses remain so high and why outages and transformer failures are common in the state.

Furthermore, household consumption forms the overwhelming share of electricity use in Mizoram, while industrial demand remains marginal. This suggests that the economic returns from the current power infrastructure are skewed, with large amounts of energy directed to sustaining households rather than fuelling productive growth. In a situation where technical losses consume nearly a quarter of total supply, the burden falls disproportionately on ordinary consumers and on state finances, while opportunities to expand industrial and commercial usage remain limited.

Reducing these losses would yield considerable benefits. Strengthening the backbone of the system, adding more medium-sized substations so that electricity does not have to travel as far on small lines. In cities, it could also be worth considering underground cabling in select corridors. Upgrading older, weaker lines in rural areas, and reconfiguring how towns and villages are connected, could also help to bring losses down. While these measures require investment, they could pay off through lower system costs, fewer outages, and better service for both households and businesses. Addressing transmission inefficiencies could therefore release capacity not only to improve reliability for households but also to enable room for expansion of more productive demand in the future.

From the data available on electrification, it is evident that Mizoram experiences a spatially equal distribution of electricity infrastructure, nearing full coverage. Due to the non-availability of district level or village level spatial data on electricity consumption, the study is limited to table summary and drawing general inferences and cannot effectively map spatial quality parametres. Nonetheless the data suggests that state has achieved a commendable electrification. Although the efficiency and reliability of its electricity system remain constrained, these structural imbalances can be addressed through investment in quality infrastructure.

5.6 SPATIAL INEQUALITY IN NIGHT TIME LIGHT RADIANCE

This section analyses Night Time Light (NTL) radiance across India for contextual understanding and focuses on Mizoram to assess patterns of economic activity. The study employs the Earth Observation Group's (EOG) Visible Infrared Imaging Radiometer Suite (VIIRS) Night Time Light (VNL) V2 and V2.2 datasets, which provide annual average radiance at a 500-meter resolution. In the absence of district-level economic indicators, NTL offers a comparable metric for economic activity in the state. The analysis presents an overview of the distribution of NTL radiance for India in 2023 to position Mizoram within the national context, analyses NTL radiance distribution in Mizoram, and presents intra and inter district study based on the Gini Coefficient.

5.6.1 All India Spatial Inequality in Night Time Light Radiance (2023)

Night Time Light radiance data for 2023 from the VIIRS Night Time Light (VNL) Version 2.2 dataset are analysed to compute total radiance for India's 36 administrative units, comprising 28 states and 8 union territories. The spatial distribution of these data is presented in Map 5.6, based on the EOG V2 Annual Composite (2023).

In 2023, India's total radiance per Area km² was 6.045 nW/cm²/sr per km², derived from a total radiance of 19,762,916.841 nW/cm²/sr across an analysed area of 3,270,051 km². This metric reflects the distribution of artificial illumination and economic activity across the country's administrative regions.

The Gini coefficient for total radiance per Area km² across the 36 states and union territories is calculated using a bootstrapping approach (1000 iterations) to assess inequality in radiance distribution. The results are presented in the table below.

Table 5.13 Bootstrap Gini Result on Total Radiance India (2023)

Gini	Mean	Std_Error	CI_Lower_95	CI_Upper_95
0.749	0.703	0.003	0.461	0.81

Source: Own Calculation based on VNL V2.2 Annual composite 2023, EOG

The Gini coefficient point estimate of 0.749, with a 95% confidence interval of (0.461, 0.81), indicates substantial inequality in the distribution of Night Time Light radiance per unit area in India. The result shows that there are significant disparities in infrastructure and economic activity across Indian states and Union Territories.

Among the plain regions of India, with areas above 50,000 km², Uttar Pradesh (9.08 nW/cm²/sr/km²), and Tamil Nadu (8.98), recorded the highest radiance per Area km², indicating robust electrification and economic activity. In contrast, Chhattisgarh (4.13), Odisha (4.40), and Andhra Pradesh (4.57) had the lowest radiance per unit area. Among plain regions with areas below 50,000 km², Chandigarh (150.33), Delhi (146.44), and Puducherry (34.41) exhibited the highest Radiance per Area km². Conversely, Kerala (6.94), and Goa (11.69) recorded the lowest values, owing to their sparser population densities.

In states with difficult terrain and remote locations, mostly in the Northeast and Himalayan regions, radiance patterns varied. Tripura (4.59 nW/cm²/sr/km²), Uttarakhand (4.07), and Assam (4.07) exhibited relatively high total radiance per area km² despite geographic constraints. Conversely, Arunachal Pradesh (0.37) and Mizoram (0.38) recorded the lowest radiance per unit area, reflecting infrastructural challenges due to sparse population, low economic activity, and complex terrain. Mizoram's low ranking highlights the need for targeted development to enhance economic growth in the state. The radiance data is visualised in Map 5.7.

Map 5.7 Night Time Light Radiance India 2023

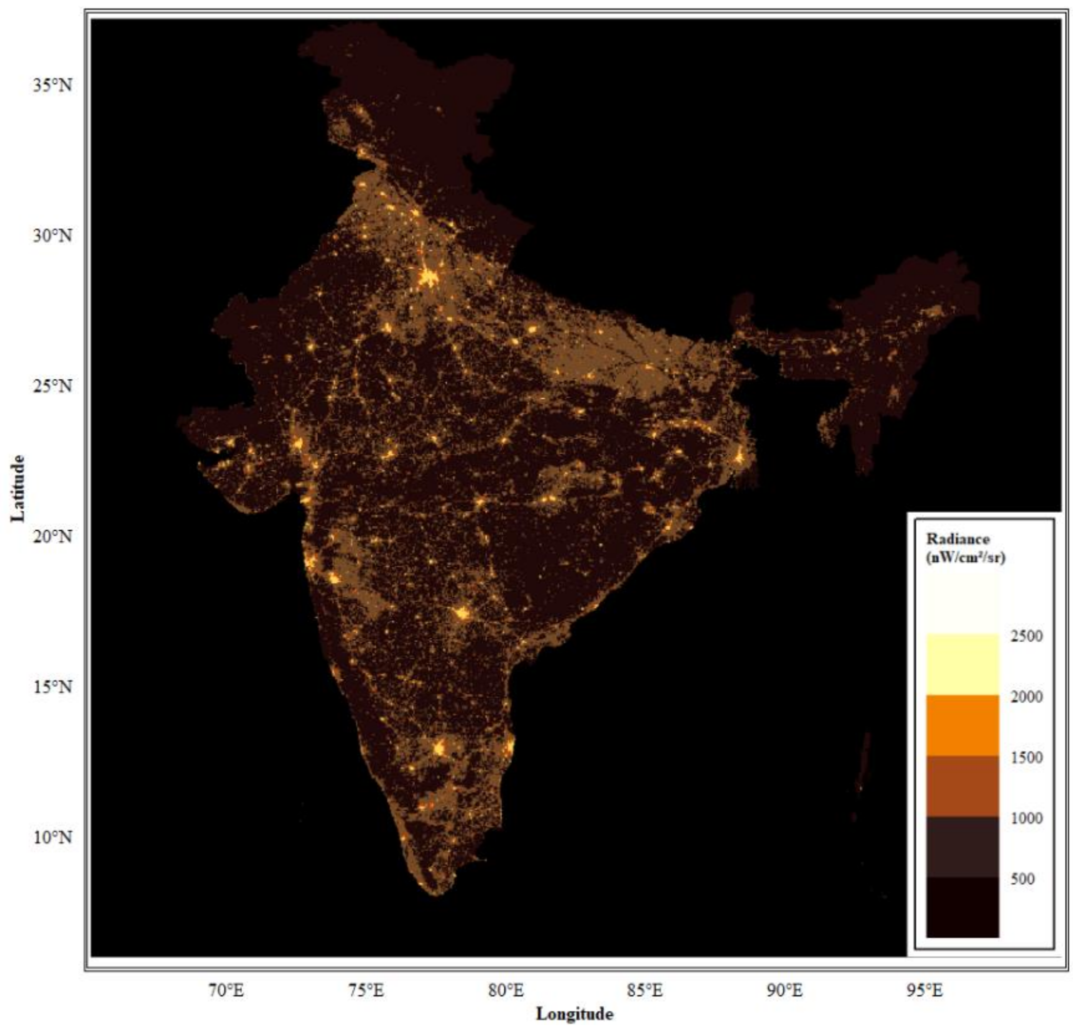

Source: Own visualisation based on GIS data from EOG V2.2 Annual Composite (2023) derived from NOAA VIIRS DNB & Survey of India map (2023)

5.6.2 Limitations of the Study

This analysis is subject to certain limitations. Four small disputed regions at the inter-state boundaries of Madhya Pradesh, Gujarat, Rajasthan, Bihar, Jharkhand, and West Bengal, with a combined area of 48.95 km² and total radiance of 103.86 nW/cm²/sr, are excluded from the Gini coefficient calculation due to their negligible contribution and unclear attribution to specific states. These regions are included in the national Total Radiance per Area km² to ensure completeness. The total analysed area of 3,270,051 km² using the Survey of India (2023) shapefile, is slightly less than India's official area of 3,287,263 km², plausible reasons being reprojections and cartographic generalisation in GIS mapping.

In mountainous and hilly regions, NTL values may underestimate electrification and economic activity due to terrain-induced occlusion and limited light dispersion. Thus, radiance values for such regions should be interpreted cautiously, particularly in inter-regional comparisons. The normalization of total radiance by area assumes uniform pixel quality after applying the Mizoram method threshold, which may not fully account for variations in data resolution across regions.

The study shows that Night Time Light data for India's 36 states and union territories exhibit large disparities in illumination. The national average Radiance per km² is 6.045 nW/cm²/sr/km², with a Gini coefficient of 0.749, indicates high inequality in artificial illumination in India. The analysis also shows that Mizoram records the lowest value at 0.382, far below states of similar size such as Tripura (4.585), Meghalaya (1.895) and Manipur (1.462). These figures point to Mizoram's distinct infrastructural and economic constraints even among its Northeastern counterparts. These results justify a closer examination of Mizoram to understand the spatial patterns and drivers of its low radiance.

5.6.3 Spatial Inequality in Night Time Light Radiance in Mizoram

To assess spatial patterns of Night Time Light distribution across districts in Mizoram, multiple inequality metrics derived from remote-sensed luminosity data is used. The analyses are based on Annual Composite Night Time Light (NTL) data from the VIIRS-DNB (Visible Infrared Imaging Radiometer Suite - Day/Night Band), VNL V2.2, provided by the Earth Observation Group (EOG) for the year 2023.

To balance the inclusion of meaningful low-level lighting with the exclusion of spatially dispersed or transient radiance, a 0.5 **(nW/cm^2/sr)** threshold was applied to the pixel-level NTL data. This thresholding accounts for the unique topography of Mizoram, where hilltop settlements often cast diffuse light onto adjacent downslopes, leading to spatial spillover. Additionally, low-radiance emissions from transient objects, such as jhum huts or temporary rural structures, do not reflect stable electrification but rather firelight or solar lanterns. By focusing on the radiance values above 0.5 nW/cm^2/sr, the method captures genuine settlement lighting, particularly from electrified areas, while reducing noise from slope diffusion and non-electrical light sources. This ensures that computed metrics reflect both rural and urban functional electrification zones. Two different measures are derived from this filtered high-radiance dataset, Intra-district inequality and Inter-district inequality.

For each district, mean radiance represents the average pixel value within its boundary, expressed in nanowatts per square centimetre per steradian (nW/cm^2/sr), while total radiance denotes the sum of all radiance values above the quality-control threshold of 0.5 nW/cm^2/sr. The lit pixels column indicates the number of pixels exceeding this threshold, each corresponding to an approximate ground area of 0.2147 km^2, given VIIRS's 30-arc-second spatial resolution. Radiance per km^2 normalises total radiance by the district's land area, providing a measure of light intensity relative to spatial extent. Table 5.14 summarises district-level Night Time Light metrics for Mizoram in 2023, derived from the VIIRS Nighttime Light (VNL) Version 2.2 annual composite provided by the Earth Observation Group (EOG).

Table 5.14 District-Level Night Time Light Metrics for Mizoram (2023)

SN	District	Mean Radiance ($nW/cm^2/sr$)	Total Radiance ($nW/cm^2/sr$)	Lit Pixels	Area in km2	Radiance per km^2 ($nW/cm^2/sr/km^2$)
1	Aizawl	1.2965	2656.49316	2049	2326.11	1.1420
2	Champhai	1.0055	663.658603	660	1532.73	0.4330
3	Hnahthial	0.6868	126.363782	184	1101.71	0.1147
4	Khawzawl	0.7582	255.52588	337	1134.47	0.2252
5	Kolasib	0.8024	772.674399	963	1347.11	0.5736
6	Lawngtlai	0.8678	1067.34447	1230	2485.98	0.4293
7	Lunglei	0.8854	904.903976	1022	3419.77	0.2646
8	Mamit	0.6824	691.989324	1014	3101.21	0.2231
9	Saiha	0.8072	448.817439	556	1498.94	0.2994
10	Saitual	0.8553	314.75154	368	1816.88	0.1732
11	Serchhip	0.8058	489.952636	608	1351.37	0.3626

Source: Own Calculation based on EOG V2.2 Annual Composite (2023) derived from NOAA VIIRS DNB

Aizawl has the highest total radiance, reflecting both a larger number of lit pixels and higher mean radiance values. Districts such as Kolasib and Champhai have smaller spatial extents of illumination but still register substantial total radiance. In contrast, Hnahthial records the lowest total radiance and the smallest lit pixel count, indicating minimal illuminated surface area. Radiance per km^2 provides a measure of illumination intensity relative to district size, allowing direct comparison between large and small districts. For example, Lawngtlai's total radiance exceeds that of Saitual, yet its much larger land area results in a lower radiance per km^2 value. The pixel size of 0.2147 km^2 means that even small differences in lit pixel counts represent sizeable differences in illuminated land area when aggregated at the district level.

Map 5.8 plots the pixel-level night time radiance across Mizoram for the year 2023, using the GIS data from the EOG VIIRS-DNB V 2.2 annual composite set. Mizoram being dimly lit compared to the rest of India, Radiance is displayed on a continuous gradient, with values clamped between 0.5 and 15 nW/cm²/sr to improve visualisation.

Map 5.8 Night Time Light Radiance Mizoram 2023

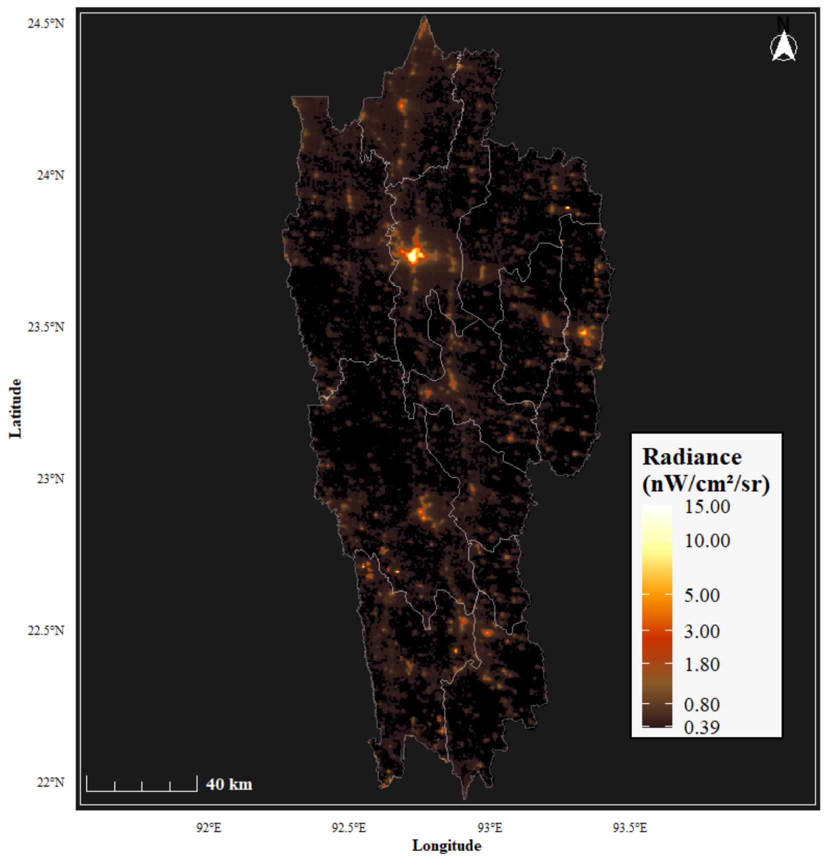

Source: EOG V2.2 Annual Composite (2023), NOAA VIIRS-DNB

The Night Time Light mapping highlights Aizawl as the state's most brightly lit region, its urban core radiating intense light due to dense infrastructure and economic activity. Lunglei town in the south and Champhai town in the east follow as secondary illuminated hubs, with moderate radiance reflecting their roles as district economic hubs, though significantly dimmer than Aizawl. Urban areas across the state consistently emit stronger light, forming distinct clusters on the map, while rural regions produce faint glows, often near the 0.5 nW/cm²/sr threshold, due to sparse electrification and low population density. Viewed from space, Lunglei District encompasses the largest dark expanse, its rural and forested areas minimally lit, followed closely by Mamit District, where light is confined to small market towns.

5.6.4 Intra-District Spatial Light Inequality

Intra-district spatial inequality is measured using the Gini coefficient, computed from the distribution of radiance values within each district after applying the filtering procedure described in Chapter 3. For each district, the NTL raster was cropped and masked to district boundaries, and all non-NA pixel values exceeding the 0.5 nW/cm²/sr threshold were extracted. The Gini coefficient was then calculated over this set of pixel values using R, with bootstrapping (1000 iterations) to estimate mean, standard error, and 95% confidence intervals. The Gini coefficient thus reflects the degree of spatial concentration of radiance within each district.

Table 5.15 Bootstrap Gini on Intra-District Nigh Time Light, Mizoram (2023)

SN	DISTRICT	Gini	Mean	Std Error	CI Lower (95%)	CI Upper (95%)
1	Aizawl	0.46	0.459	0.000	0.436	0.482
2	Champhai	0.348	0.347	0.001	0.311	0.382
3	Hnahthial	0.167	0.166	0.000	0.14	0.194
4	Khawzawl	0.215	0.214	0.000	0.19	0.238
5	Kolasib	0.25	0.249	0.000	0.227	0.27
6	Lawngtlai	0.286	0.286	0.000	0.261	0.31
7	Lunglei	0.300	0.300	0.001	0.259	0.347
8	Mamit	0.155	0.155	0.000	0.14	0.171
9	Saiha	0.26	0.259	0.001	0.229	0.292
10	Saitual	0.301	0.296	0.001	0.217	0.381
11	Serchhip	0.24	0.240	0.000	0.216	0.263

Source: Own Calculation based on EOG V2.2 Annual Composite (2023) derived from NOAA VIIRS DNB

The intra-district Gini coefficients range from 0.155 (Mamit) to 0.460 (Aizawl), reflecting variation in the spatial concentration of radiance across Mizoram. Aizawl (0.460) has the highest Gini coefficient, indicating a strong concentration of light in specific areas. As the administrative and economic centre of the state, the district contains dense urban cores with high radiance, contrasting with less illuminated peri-urban and rural areas. The distribution reflects a high degree of spatial disparity in lighting intensity in the district, consistent with its role as Mizoram's primary urban hub. Champhai (0.348) shows a relatively high Gini coefficient, indicating a moderate concentration of radiance in the district capital region, likely driven by localized commercial activity.

Hnahthial (0.167) and Mamit (0.155) record the lowest coefficients, indicating low spatial inequality in Night Time Light and an overall low level of Night Time Light radiance in the two districts. These low Gini values suggest limited infrastructure development, with sparse lighting distributed relatively evenly across rural landscapes. Khawzawl (0.215), Kolasib (0.250), Saiha (0.260), and Serchhip (0.240) fall in the low to moderate range. These districts exhibit balanced spatial distribution of radiance, with small clusters of concentrated light corresponding to administrative centres or road-based settlements. Lawngtlai (0.286), Lunglei (0.300), and Saitual (0.301) have moderate Gini coefficients, indicating the presence of sub-regional urban clusters of radiance within a wider rural setting.

The analysis shows that intra-district variation in NTL is moderate throughout the state in the year 2023. Most districts are clustered between a Gini Coefficient of 0.20 and 0.30. Champhai, with a moderately high inequality at 0.34 while Aizawl exhibits high intra-district inequality (0.46). Districts with relatively low intra-district inequality, such as Hnahthial and Mamit, suggests an overall low level of infrastructure development rather than equitable distribution of economic activity.

5.6.5 Inter-District Inequality in Total Night Time Light

This section evaluates the disparity in total radiance across administrative districts in Mizoram. For each district, total radiance is calculated based on the NTL data extracted for 2023. The total radiance of each district is further normalized by the area of each district. To assess the inequality in this distribution, a weighted Gini coefficient is estimated using a non-parametric bootstrap procedure with 1,000 replications. The result of the test is presented below.

Table 5.16 Bootstrap Gini Result on Inter District Total Radiance Mizoram (2023)

Gini	Mean	Std_Error	CI_Lower_95	CI_Upper_95
0.495	0.457	0.002	0.327	0.575

Source: Own Calculation based on VNL V2.2 Annual composite 2023, EOG

The Gini coefficient of 0.495 indicates moderate to high inequality in the distribution of total radiance across the 11 districts of Mizoram. A small number of districts, notably Aizawl with a total radiance of 1.1420 nW/cm²/sr/km², contributed disproportionately to the region's total radiance, while others, such as Hnahthial (0.1147 nW/cm²/sr/km²), contribute minimally. This disparity suggests there is moderate to high inequality in infrastructure and settlement density across districts. A

Table 5.17 below presents the top-ranking district within each quintile, based on radiance intensity normalised by land area (expressed in nW/cm²/sr/km²). This metric provides insight into the spatial density of artificial illumination, serving as a proxy for the concentration of infrastructure and economic activity. Districts in the first quintile, including Mamit (0.22), Hnahthial (0.11), and Saitual (0.17), exhibit the lowest radiance intensities per square kilometre. This indicates a relatively sparse spatial footprint of illuminated infrastructure. These areas are characterised by dispersed settlement patterns and limited infrastructure development. The second quintile features districts such as Lunglei (0.26) and Khawzawl (0.23), where moderate levels of lighting are observed, corresponding to few concentrated urban centres surrounded by underdeveloped rural settlements. In the third quintile, Serchhip (0.36) and Saiha (0.30) show relatively moderate levels of radiance values per km^2, reflecting their moderate concentration of light-emitting infrastructures and hitting at an evenly distributed economic activity.

Table 5.17 Quintile Analysis of Inter-District Total Radiance Mizoram

Quintile	District	Total Radiance ($nW/cm^2/sr/km^2$)
1st	Hnahthial	0.11
2nd	Khawzawl	0.22
3rd	Saiha	0.30
4th	Kolasib	0.40
5th	Aizawl	1.14

Source: Own calculations based on VNL V2.2 Annual Composite 2023, EOG

The fourth quintile comprises Champhai (0.43), Lawngtlai (0.43), and Kolasib (0.40), all of which demonstrate a substantial urban presence and increasing radiance concentration. Although these districts remain well below Aizawl in absolute terms, their relatively elevated radiance per km^2 suggests the emergence of secondary nodes of economic activity and infrastructure. Their presence contributes to a more balanced spatial distribution of development, thereby moderating overall spatial inequality within the state. In effect, these districts play a pivotal role in diffusing the concentration of infrastructure beyond the capital and supporting a more regionally distributed growth pattern.

Finally, Aizawl, the capital district, occupies the fifth quintile with a markedly higher radiance intensity of 1.14 $nW/cm^2/sr/km^2$, more than double that of the next highest district and exceeding the combined radiance of all districts in the first quintile.

Lorenz curve illustrating the cumulative distribution of total radiance is presented in Graph 5.1.

Graph 5.1 Lorenz Curve of Inter-District NTL Mizoram

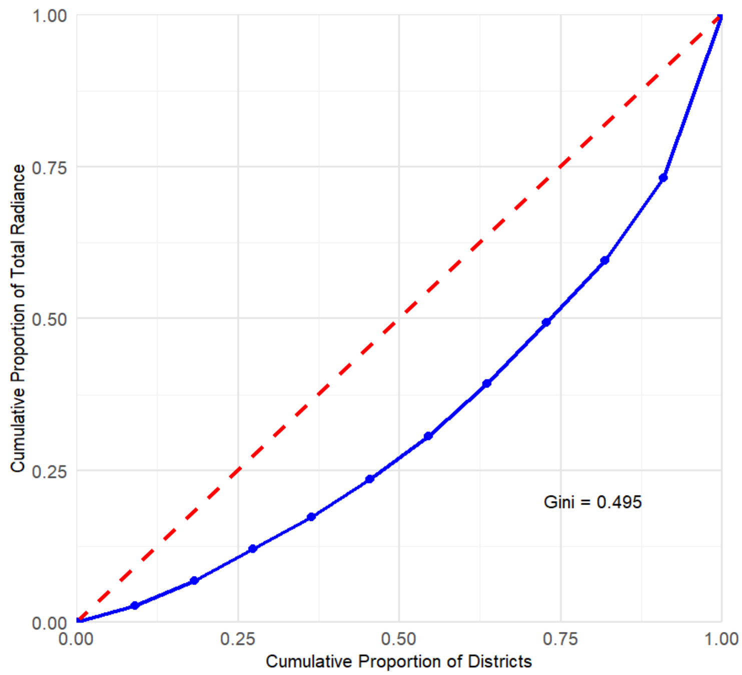

While the dominance of Aizawl district partly reflects its population share (over 30% as per the 2011 Census), its radiance intensity far surpasses what would be expected under proportional development. Unlike other capital districts that benefit from strategic locational advantages such as ports, mineral resources, or trade corridors, Aizawl's primacy is rooted in administrative centrality rather than intrinsic geographic endowments. This suggests a pattern of monocentric agglomeration, shaped by the centralisation of public institutions and services, rather than organic or market driven spatial development. In this context, Aizawl's disproportionate concentration of light, and by extension infrastructure and activity, reflects structural spatial inequality, whereby institutional factors reinforce uneven development patterns.

5.6.6 Limitations of the Study

While NTL data offers a powerful lens through which to observe patterns of spatial development, its application as a proxy for economic activity in Mizoram reveals several important limitations. Initial efforts to normalise radiance values by population, using per capita NTL, produced metrics that appeared counterintuitive. For instance, Hnahthial District consistently emerged with the highest per capita radiance, surpassing more urbanised and economically vibrant districts such as Aizawl, Champhai, and Lunglei. This unexpected outcome is likely a function of both the built environment in urban Mizoram and the way the VIIRS sensor detects radiance.

Urban centres such as Aizawl typically feature densely packed, multi-storey structures (ranging from four to seven storeys) in tightly constrained urban cores. The architectural form of these buildings often limits outward radiance emissions to the front and rear façades, significantly reducing the light detectable by the VIIRS instrument, which captures light reflected within a steradian field. As a result, the overall radiance emitted from high-density urban areas may be systematically underestimated. In contrast, rural or low-density areas with single-storey, widely spaced buildings tend to emit light more freely across surfaces and directions, potentially inflating the radiance signal relative to actual economic intensity.

Several studies have addressed these limitations by incorporating urban density correction factors or building morphology data (e.g., Elvidge et al., 2019; Li & Zhou, 2021). However, the absence of granular data on population distribution at the pixel level (500×500 m) renders such adjustments challenging to implement effectively in the context of Mizoram. Moreover, as urban areas agglomerate, their artificial light emissions tend to plateau, a phenomenon partly driven by the adoption of energy-efficient lighting and an economic shift toward non-illuminating assets (e.g., air conditioners). Consequently, low growth in NTL intensity within urban cores may reflect changes in consumption behaviour rather than stagnation in development.

An additional conceptual limitation arises from the non-rivalrous nature of artificial lighting. Unlike private goods, the benefit of public lighting is not diminished by the number of users, a single light source may simultaneously serve hundreds or thousands of individuals. As such, per capita NTL may misrepresent actual development: it risks overstating economic activity in sparsely populated areas with limited but intense lighting, while understating the infrastructure and functional density of well-lit urban centres.

Given these complexities, this study emphasises the use of spatially grounded indicators, such as the total radiance, extent of lit area, and mean intensity of illumination, to better approximate the functional scale of economic activity. These indicators are more robust to distortions introduced by urban morphology, population sparsity, or behavioural changes in lighting consumption, and therefore provide a more reliable basis for interpreting spatial development patterns in Mizoram.

To conclude, the Gini analysis shows that spatial inequality in radiance exists both within and between districts in Mizoram. Aizawl has the highest intra-district inequality and also contributes the largest share of total radiance across the state. Most other districts have moderate or low Gini values, which points to uneven development in infrastructure across regions. While NTL data has known limitations and should not be treated as a perfect measure of economic activity, it remains a useful proxy in contexts with limited ground-level data. The results align with observed patterns, such as Aizawl's dominant role as the administrative and economic centre, and reveal clear disparities in how development is distributed across the state.

5.7 TEMPORAL ANALYSIS OF NIGHT TIME LIGHT IN MIZORAM

This section evaluates the Spatio-temporal trends in Night Time Light (NTL) radiance across Mizoram over the period from 2014 to 2023, using the Mann-Kendall (MK) trend test on a 10x10 km grid comprising 237 with non-zero radiance values.

The analysis quantifies monotonic changes in NTL radiance, derived from VIIRS-DNB Annual Composites (VNL V2 for 2014–2021 and V2.2 for 2022–2023), with a threshold of 0.5 nW/cm²/sr applied to filter noise. A district level Mann-Kendall analysis is also conducted to complement the grid analysis. Mann-Kendal tau ranges from -1 to +1 with values closer to +1 indicates positive trend whereas values nearing -1 indicates negative trend. Results are summarized in statistical tables and visualized in map and figures, incorporating district boundaries to highlight spatial patterns.

5.7.1 Mann-Kendall Analysis Trend of NTL in Mizoram (2014-2023)

The Mann–Kendall (MK) test is applied to a 10×10 km grid covering 237 cells to assess monotonic temporal trends in Night Time Light (NTL) radiance over the 10-year period from 2014 to 2023. Of the total grid cells analysed, 135 (57.0%) shows statistically significant trends at the 5% significance level ($p < 0.05$). Among these, 133 cells (98.5% of significant cases) have positive tau values, indicating monotonic increases in radiance. Only 2 cells (1.5%) record negative tau values, reflecting decrease in NTL radiance.

Table 5.18 Summary of Mann-Kendall Trend Analysis (2014–2023)

Total Cells	Significant p < 0.05	Positive Trends	Negative Trends	Mean Tau	Median Tau	Min Tau	Max Tau
237	135	133	2	0.503	0.556	-0.867	1

Source: Own calculation from VNL V2 (2014–2021) and V2.2 (2022–2023), EOG

Across all cells, the Kendall's tau coefficient average 0.503, with a median of 0.556, indicating a central tendency towards positive monotonic change. The coefficients range from −0.867, representing a strong negative monotonic trend, to 1.000, representing a perfect positive monotonic trend. This range captures both the most pronounced declines and the maximum possible increases observed during the study period.

The highest positive tau was observed in cell 155 ($\tau = 1.000$, $p = 0.000083$), centred around Farkawn village in Champhai district, indicating a perfect positive monotonic trend in radiance. This is followed by cell 204, encompassing the corridor between Champhai town and the Zokhawthar border trading town, and cell 301, centred around Kanghmun town in the north-western tip of Mizoram, both with $\tau = 0.956$ ($p = 0.000172$). Other high-ranking cells include those in Champhai, Aizawl, Mamit, Saiha, and Lunglei districts, with τ values ranging from 0.911 to 0.8667. The top 10 cells are presented in Table 5.19.

Table 5.19 Top 10 Grid Cells of Significant MK trends (p < 0.05)

SN	Cell ID	Tau	P-Value	Trend Direction	District
1	155	1.0000	0.000083	Positive	Champhai
2	204	0.9560	0.000172	Positive	Champhai
3	301	0.9560	0.000172	Positive	Mamit
4	167	0.9110	0.000347	Positive	Champhai
5	234	0.9110	0.000347	Positive	Aizawl
6	235	0.9110	0.000347	Positive	Aizawl
7	208	0.8819	0.001088	Positive	Mamit
8	80	0.8667	0.000676	Positive	Saiha
9	123	0.8667	0.0006767	Positive	Lunglei
10	221	0.8667	0.000677	Positive	Aizawl

Source: Own calculation from VNL V2 (2014–2021) and V2.2 (2022–2023), EOG

Table 5.20 presents annual NTL statistics for the total radiance across the 237 grid cells. The mean total radiance per grid cell increased from 11.59 nW/cm²/sr in 2014 to 32.56 nW/cm²/sr in 2023. The maximum total radiance per grid cell rose from 682.33 nW/cm²/sr to 1031.86 nW/cm²/sr, with the standard deviation expanding from 50.49 to 83.78, reflecting growing variability across the grid.

Table 5.20 Annual Total Radiance Statistics (2014–2023)

Year	Mean Total Radiance	Min Total Radiance	Max Total Radiance	Std. Dev. Total Radiance
2014	11.59	0	682.33	50.49
2015	8.28	0	569.67	42.82
2016	8.5	0	610.56	45.26
2017	11.54	0	599.41	46.53
2018	11.47	0	636.45	49.71
2019	11.83	0	722.11	54.92
2020	18.69	0	758.45	60.78
2021	14.85	0	650.2	52.36
2022	21.41	0	891.74	71.2
2023	32.56	0	1031.86	83.78

Source: Own calculation from VNL V2 (2014–2021) and V2.2 (2022–2023), EOG

Graph 5.2 shows the Grid wise total radiance trend for the study period (2014-2023).

Graph 5.2 Grid-wise Total Radiance Trend, Mizoram (2014-2023)

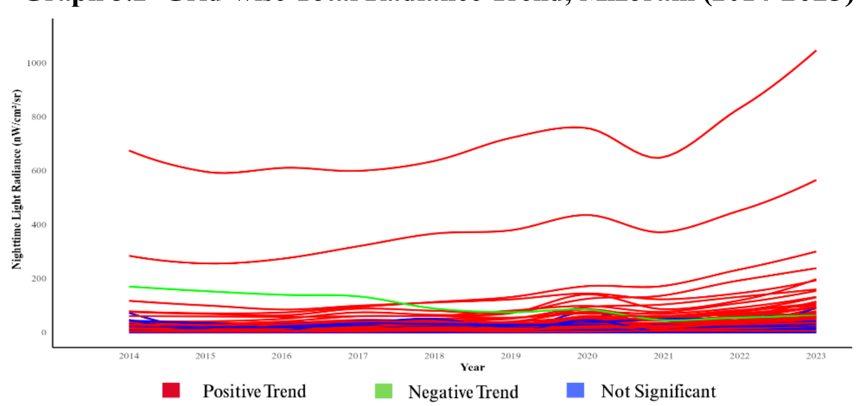

Source: Own visualisation based on VNL V2 (2014–2021) and V2.2 (2022–2023), EOG

Cell 233, 245 and 234, from Aizawl district, occupies the top positive radiance curves. The trend also shows a slight dip in radiance during the covid pandemic of 2021 and varying degrees of recovery among the regions.

The spatial distribution of Kendall's tau values is illustrated in Map 5.9, where Mizoram is divided into 258 grid cells. Significant positive trends with $\tau \geq 0.8$ are shown in yellow, while those with τ between 0.6 and 0.8 are shown in aquamarine, and those between 0.4 and 0.6 in cyan-blue. Cells with non-significant trends ($p > 0.05$) are depicted in deep blue. Negative monotonic trends are represented in red, and areas with no significant radiance above the 0.5 nW/cm²/sr threshold appear in grey.

Map 5.9 Mann-Kendall Tau Map of Mizoram (2014-2023)

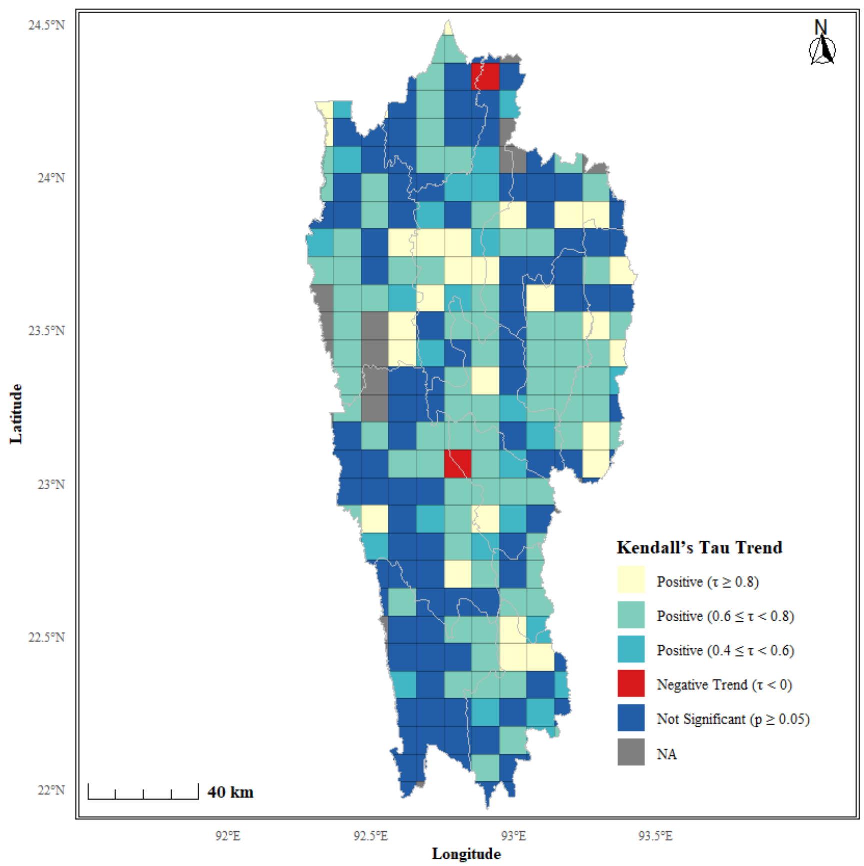

Source: Own visualisation based on VIIRS-DNB VNL V2 (2014–2021) and V2.2 (2022–2023), Earth Observation Group

Two cells display negative trends. Cell 319 (tau = -0.867, p = 6.77e-04), centred around Tuirial Dam, indicates a significant decline in total radiance. This is not surprising given the fact that the Tuirial Hydel Project was under construction during the study period, with significant declining trend of radiance since its opening in 2017. The next negative trending cell, Cell 150 (tau = -0.6000, p = 0.020044), contains Haulawng town and Hmuntlang village in Lunglei district, with a consistent decline in radiance, suggesting a lack of developmental infrastructure in this segment for the period between 2014 to 2023.

Overall, grid cells from districts such as, Lawngtlai, Lunglei, Mamit, Saiha, and Saitual account for the bottom not significant trends. The total radiance trajectories for 237 cells, confirms the prevalence of upward trends, with urban cells driving the steepest increases. The standard deviation of total radiance across grid cells, increasing from 50.49 in 2014 to 83.78 in 2023 suggests that there is a growing spatial disparity, with urban cells contributing disproportionately to peak radiance values. These results highlight that urban districts, particularly Aizawl, have experienced substantial gains in total radiance, while rural areas show limited increases or, in some cases, declining trends. The MK test results show that more than half of the grid cells experienced statistically significant monotonic change in NTL radiance between 2014 and 2023, with positive trends overwhelmingly more frequent than negative ones. Negative monotonic trends were rare and confined to a very small proportion of the study area.

5.7.2 Mann-Kendall District-Level Analysis of Mizoram

To assess the robustness of observed radiance trends, the Mann-Kendall test was applied to district-level aggregated radiance data. All 11 districts exhibited positive trends, with 10 showing statistically significant increases ($p < 0.05$). The mean tau was 0.677, and the median tau was 0.689, with values ranging from 0.467 to 0.822, confirming a strong tendency toward increasing radiance across Mizoram. Table 5.21 highlights the summary statistics

Table 5.21 Summary of District Mann-Kendall Trend Analysis (2014–2023)

Total Cells	Significant $p < 0.05$	Positive Trends	Negative Trends	Mean Tau	Median Tau	Min Tau	Max Tau
11	10	10	0	0.6768	0.6889	0.4667	0.8222

Source: Own calculation from VNL V2 (2014–2021) and V2.2 (2022–2023), EOG

At the district level, Kendall's tau values range from 0.5110 in Kolasib and Lawngtlai to 0.8220 in Aizawl, Champhai, and Mamit. Hnahthial, Khawzawl, Lunglei, Saiha, and Serchhip also record moderate to strong positive tau values (0.6000–0.7780). Ten districts display statistically significant positive trends ($p < 0.05$), while only Saitual district exhibits a non-significant trend ($p = 0.0736$, $\tau = 0.4667$)

Table 5.22 Mann-Kendall Trend Results by District

SN	District	Tau	P-Value	Trend Direction
1	Aizawl	0.8220	0.0013	Positive
2	Champhai	0.8220	0.0013	Positive
3	Hnahthial	0.6890	0.0073	Positive
4	Khawzawl	0.7780	0.0024	Positive
5	Kolasib	0.5110	0.0491	Positive
6	Lawngtlai	0.5110	0.0491	Positive
7	Lunglei	0.6000	0.0200	Positive
8	Mamit	0.8220	0.0013	Positive
9	Saiha	0.6440	0.0123	Positive
10	Serchhip	0.7780	0.0024	Positive
*	Saitual	0.4667	0.0736	Non-significant

Source: Own calculation based on VNL V2 (2014–2021) and V2.2 (2022–2023), Earth Observation Group

Annual Night Time Light (NTL) statistics for the study period show a sustained rise in total radiance across all districts of Mizoram. District mean total radiance increased from 279.72 nW/cm²/sr in 2014 to 740.28 nW/cm²/sr in 2023, while the maximum district radiance rose from 1316.64 nW/cm²/sr to 2615.53 nW/cm²/sr over the same period. Table 5.23 presents the total radiance in 2014 and 2023 for each district, along with their absolute and percentage gains over the 10-year period.

Across districts, the magnitude of change varies substantially. In absolute terms, Aizawl records the largest gain in total radiance (+1337.85 nW/cm²/sr), reflecting its already high baseline in 2014. In percentage terms, the largest relative increases occur in districts with comparatively low initial radiance values, most notably Khawzawl (+533.59%), Hnahthial (+443.73%), and Serchhip (+380.20%). Several mid-ranking districts, including Champhai (+318.82%), Mamit (+316.48%), and Saitual (+287.01%), also register substantial relative growth.

Table 5.23 Total Radiance and Gains by District (2014–2023)

SN	District	Total Radiance 2014	Total Radiance 2023	Radiance Gain	Percentage Radiance Gain
1	Aizawl	1318.64	2656.4932	1337.8532	101.46
2	Champhai	158.46	663.6586	505.1986	318.82
3	Hnahthial	23.24	126.3638	103.1238	443.73
4	Khawzawl	40.33	255.5259	215.1959	533.59
5	Kolasib	387.88	772.6744	384.7944	99.20
6	Lawngtlai	382.77	1067.3445	684.5745	178.85
7	Lunglei	286.36	904.9040	618.5440	216.00
8	Mamit	166.15	691.9893	525.8393	316.48
9	Saiha	129.74	448.8174	319.0774	245.94
10	Saitual	81.33	314.7515	233.4215	287.01
11	Serchhip	102.03	489.9526	387.9226	380.20

Source: Own Calculation base on VNL V2 (2014–2021) and V2.2 (2022–2023), Earth Observation Group

This pattern indicates that while radiance has increased across the entire state, the pace and scale of growth have not been uniform. Districts starting with higher initial radiance tend to see the largest absolute gains, whereas districts with lower initial levels experience higher percentage growth, narrowing the gap but not eliminating, differences in overall radiance levels by 2023.

5.7.3 Limitations

The Mann–Kendall analysis, applied at both the 10×10 km grid-cell and district levels, is not without limitations. The grid framework does not produce perfectly uniform cells, as those along the borders are smaller, which can affect aggregated totals; however, this is unavoidable given Mizoram's irregular boundaries, and still serves as an effective basis for trend detection. The COVID-19 lockdowns of 2021 introduced short-term disruptions, with urban radiance dropping while rural areas remained largely unaffected, reflecting their differing exposure to mobility restrictions.

The inclusion of VIIRS v2.2 data for 2022–2023, with enhanced filtering, may yield slightly higher radiance values than earlier v2 years (2014-2021), and the 0.5 $nW/cm^2/sr$ threshold, while necessary to exclude stray urban light, may also filter out genuine low-intensity rural lighting in the early years. Aggregation to the district level inevitably smooths local variations, and annual composites mask seasonal patterns, yet these approaches remain appropriate for detecting long-term monotonic change. Within these constraints, the Mann-Kendall test provides a statistically observable and consistent temporal picture of radiance change across Mizoram.

Overall, the Mann–Kendall trend analysis of night-time radiance in Mizoram highlights a steady and spatially widespread increase in artificial lighting across much of the state between 2014 and 2023. The consistency of trends across both 10×10 km grid cells and district-level units indicate that the observed patterns are not merely a result of spatial scaling, but are robust across different levels of aggregation. Strong positive trends were recorded in more than half of all grid cells, with only a small fraction showing significant declines, while district-level analysis confirms statistically significant increases in 10 out of 11 districts. Urban areas display more concentrated and sustained growth in radiance, whereas rural regions experience slower and more spatially dispersed change, with some recording high relative percentage gains from low initial baselines. Future research could build on this work by integrating higher-resolution Night Time Light data, preferably at 1 metre scale, to capture finer-scale patterns of change and further refine the understanding of lighting dynamics in both urban and rural contexts.

5.8 LINEAR TREND AND SPATIAL CLUSTERING OF NIGHT TIME LIGHT

To tests the hypothesis whether growth in economic activity across Mizoram is randomly distributed or show signs of uneven growth patterns, a temporal dynamic of Night Time Light (NTL) radiance across Mizoram from 2014 to 2023 is evaluated using a two-stage analytical framework that integrates temporal trend estimation with spatial clustering analysis.

In this study annual total radiance values are computed for 10 × 10 km grid cells covering the state, using the VIIRS-DNB composites from the Earth Observation Group (EOG). The analysis examines night time light radiance trends across a grid of cells in Mizoram from 2014 to 2023 to identify patterns of change in Radiance.

First, Ordinary Least Square (OLS) regression is applied to the annual total radiance for each cell, calculating the rate of change over time. These rates are then analysed to detect spatial clusters, where areas with significantly high growth in radiance are marked as hot spots, and those with minimal or negative change are identified as cold spots, revealing the spatial distribution of illumination trends over the decade.

5.8.1 Linear Trend Results

OLS regression is applied to the annual total radiance time series for each cell, yielding slope coefficients representing the average annual rate of radiance change. Table 5.24 summarizes the OLS results, showing that out of the 237 grid cells analysed, 128 (54.0%) displayed statistically significant trends ($p < 0.05$), with 126 showing positive slopes and only two exhibiting significant declines.

Table 5.24 Summary of OLS Regression Results for NTL Radiance Trends (2014–2023)

Metric	Value
Total Cells	237
Significant Trends ($p < 0.05$)	128
Positive Trends ($p < 0.05$)	126
Negative Trends ($p < 0.05$)	2
Mean Slope (nW/cm²/sr/year)	2.0255
Median Slope (nW/cm²/sr/year)	0.7489
Min Slope (nW/cm²/sr/year)	-13.4458
Max Slope (nW/cm²/sr/year)	37.3406
Mean R^2	0.43
NA Results	0

Source: Own calculations based on VIIRS-DNB VNL V2 & V2.2, EOG.

The mean slope across all cells is 2.03 nW/cm^2/sr/year and a median slope of 0.75 nW/cm^2/sr/year. While a small number of cells experience very large annual increases (up to 37.34), the majority show more moderate growth. The mean R^2 value is 0.43, which suggests that the linear model explained a moderate proportion of the temporal variation in NTL. Negative slopes are rare and spatially isolated, representing localised reductions in radiance rather than widespread declines. Only two cells with declining trends are observed during the study period. The top 10 significant cell are presented below in Table 5.25.

The top 10 significant cells ($p < 0.0001$), includes cell 155 (slope: 1.87, R^2: 0.97) and cell 301 (slope: 3.43, R^2: 0.95) with strong radiance growth, and cell 319 (slope: -13.45, R^2: 0.87) with a notable decline. These cells, derived from OLS regression on VIIRS-DNB VNL V2 (2014--2021) and V2.2 (2022--2023) data, highlight areas with the most significant changes in radiance, where slopes represent the average annual rate of change.

Table 5.25 Top 10 Significant OLS Regression Results for NTL Radiance Trends (2014–2023)

Cell_ID	Slope (nW/cm²/sr/year)	p-value	R^2
155	1.8668	0.0001	0.97
301	3.4335	0.0001	0.95
342	5.0089	0.0001	0.92
221	6.4584	0.0001	0.89
289	3.2039	0.0001	0.89
234	23.8582	0.0001	0.88
319	-13.4458	0.0001	0.87
80	11.7883	0.0001	0.87
244	10.5051	0.0001	0.87
208	0.4194	0.0001	0.86

Source: Own calculations based on VIIRS-DNB VNL V2 & V2.2, EOG.

5.8.2 Spatial Clustering of Changes in Night Time Ligh Radiance

The Getis-Ord-Gi* statistic is computed on the per-cell slope values to identify significant hot spots (clusters of high positive change) and cold spots (clusters of low or negative change). Getis-Ord Gi* statistics are computed on the OLS slopes for all 258 grid cells, including 21 cells with zero radiance assigned a slope of 0. Out of 258 cells, 20 are classified as significant hot spots and 4 as significant cold spots at the 5% significance level.

The top 10 significant Hotspots and Cold spots are presented in Table 5.26.

Table 5.26 Top Significant Gi* Clusters of NTL Trends (2014–2023)

Cell ID	Gi*	p-value	Neighbours	Cluster Type	District
246	7.671	0.0001	8	Hot Spot	Aizawl
234	7.323	0.0001	8	Hot Spot	Aizawl
233	7.175	0.0001	8	Hot Spot	Aizawl
245	7.031	0.0001	8	Hot Spot	Aizawl
232	6.172	0.0001	8	Hot Spot	Mamit
222	5.667	0.0001	8	Hot Spot	Aizawl
221	4.525	0.0001	8	Hot Spot	Aizawl
257	3.197	0.0014	8	Hot Spot	Aizawl
332	-2.507	0.0122	3	Cold Spot	Aizawl
308	-2.293	0.0219	5	Cold Spot	Aizawl
320	-2.281	0.0226	5	Cold Spot	Aizawl
307	-2.228	0.0259	8	Cold Spot	Aizawl

Source: Own Calculation base on VNL V2 (2014–2021) and V2.2 (2022–2023), Earth Observation Group

Hot spots are concentrated in Aizawl and its peri-urban fringes including parts of Mamit and Saitual districts, with clusters also found in Champhai, Lawngtlai and Saiha. These locations correspond to areas of sustained economic activity, urban expansion, and infrastructure investment. Cold spots were predominantly found in the far north of Aizawl district bordering Manipur State. These regions experienced low economic activity during the study period and are responsible for the high intra district inequality in the district. The complete table of the significant hotspots and cold spots is appended in appendix VII. Map 5.10 visualises the Getis-Ord-Gi* map, with red cells indicating Hot spots and blue cells indicating Cold spots.

Map 5.10 Getis-Ord Gi* Hot Spot Analysis of NTL Radiance Change Rates Mizoram (2014-2023)

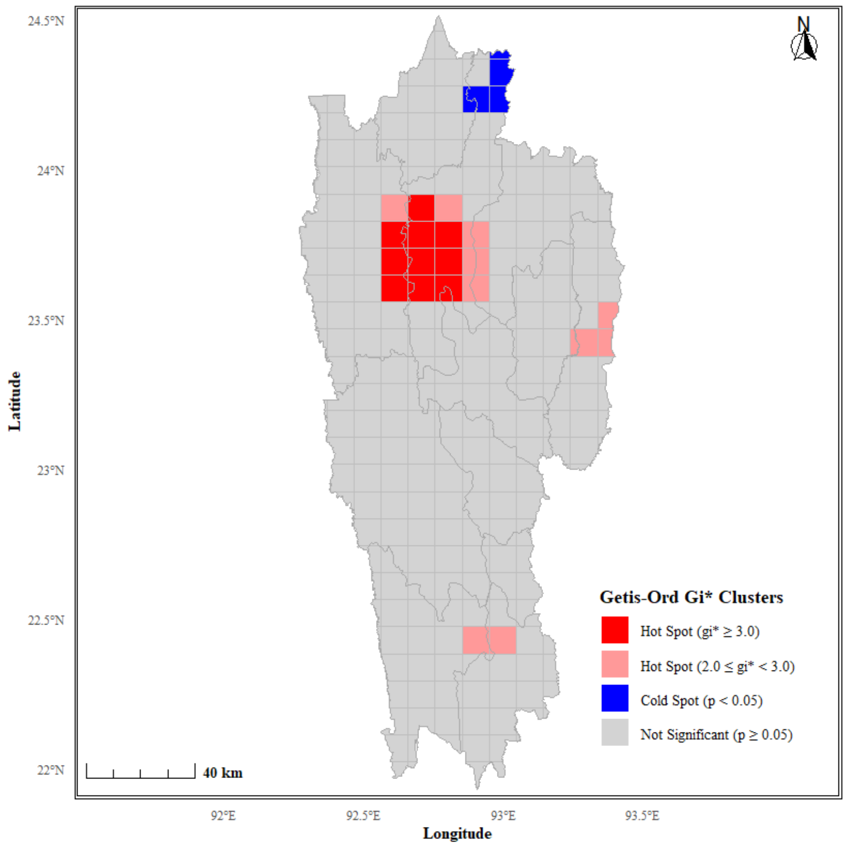

Source: Own visualisation based on VIIRS-DNB VNL V2 and V2.2, Earth Observation Group

5.8.3 Hypothesis Evaluation

Of the 237 valid grid cells analysed, 128 (54.0%) display statistically significant linear trends in total radiance ($p < 0.05$). Almost all of these (126) are positive, indicating widespread radiance growth across the state. The highest slopes are concentrated in and around Aizawl, Mamit, and parts of Champhai, reflecting sustained increases in artificial lighting over the decade.

When the slope values are subjected to the Gi* spatial clustering test, 20 significant hot spots and 4 significant cold spots ($p < 0.05$) are identified. Hot spots correspond closely with urban cores and their immediate peripheries, while cold spots occur in rural and remote area where radiance change is minimal or negative.

The co-occurrence of statistically significant positive slopes and spatially coherent hot spots demonstrates that the increase in night-time radiance is both temporally persistent and geographically concentrated. This pattern is inconsistent with the null hypothesis (H_0) of random spatial distribution and supports the alternative hypothesis (H_1) that radiance growth over the study period is not evenly spread across Mizoram but instead reflects spatial clustering, with hot spots concentrated in urban and peri-urban centres and cold spots in sparsely populated rural areas.

5.8.4 Robustness of the Model

The model employed in this study uses a two-stage approach comprising ordinary least squares (OLS) regression and Getis–Ord Gi* spatial clustering. A radiance threshold of 0.5 nW/cm²/sr is applied to filter noise and ephemeral light sources, such as urban light spillover or transient events like fires. This ensures reliable radiance measurements for 237 grid cells with non-zero radiance, consistent with established NTL methodologies. The OLS regression identifies significant trends in 128 cells ($p < .05$), with high coefficients of determination observed in the most significant cells (e.g., $R^2 = .97$ for cell 155; $R^2 = .95$ for cell 301), indicating strong linear fits for key areas of radiance change. The Getis–Ord Gi* analysis, applied to all 258 grid cells using a queen contiguity matrix, is well suited to Mizoram's irregular terrain as it captures spatial relationships without reliance on distance-based measures, which are less applicable in hilly regions. Sensitivity analysis conducted across 5 × 5 km (704 cells, 282 significant trends, 71 clusters) and 20 × 20 km (71 cells, 45 significant trends, 7 clusters) grids confirmed the robustness of the 10 × 10 km model, with consistent proportions of significant trends (40–63%) and stable cluster detection (24 clusters, compared to 71 and 7), balancing granularity with noise reduction. The use of annual composite data from VIIRS-DNB VNL V2 (2014–2021) and V2.2

(2022–2023) supports robust trend detection over a decade, with calibration differences exerting minimal influence on rate-of-change estimates.

5.8.5 Limitations of the Study

This study of NTL radiance trends and spatial clustering in Mizoram from 2014 to 2023 is not without several limitations, as such several data and terrain-related constraints should be noted. The application of a 0.5 nW/cm²/sr threshold, while effective for filtering noise and transient light sources such as urban light spillover, fires, and temporary structures (e.g., construction sites, jhum huts), may also exclude genuine low-intensity radiance from small rural settlements. This effect may be amplified in Mizoram's hilly terrain, where topographic shading can attenuate radiance signals.

The mean R^2 value of 0.43 across the 237 non-zero radiance cells are influenced by the inclusion of cells with weak or noisy signals, consistent with previous findings that non-urban NTL measurements can contain transient components. The absence of village or local council-level boundary data necessitates the adoption of a 10 × 10 km grid, which may not fully capture fine-scale spatial variability in radiance. Similarly, reliance on annual composite datasets limits temporal resolution such as detection of seasonal variations.

Despite these constraints, the study identifies statistically significant trends and spatial clusters, with the queen contiguity matrix proving well suited to Mizoram's irregular terrain. Future work could improve precision by incorporating higher-resolution datasets (e.g., ≤1 m imagery) and integrating village-level boundaries to better capture localised radiance changes.

The study provides robust evidence to reject the null hypothesis of random spatial distribution of Night Time Light (NTL) radiance trends in Mizoram (2014–2023), supporting the view that radiance growth is both temporally persistent and geographically clustered. Significant trends are concentrated in urban and peri-urban centres around Aizawl city, while several districts and rural hinterlands exhibit relative stagnation. Spatial clustering analyses and multi-resolution sensitivity checks confirm consistent patterns that supports the robustness of the model employed for the study. These results also support prior findings of this chapter that there exist pronounced spatial inequalities in economic activity in the state, reflecting its urban-centric development policies that risk marginalisation of peripheral rural regions and offers valuable insights for regional planning and policy.

5.9 SPATIAL INEQUALITY IN ECONOMIC ACTIVITY

This section examines spatial inequalities in economic activity across Mizoram, India, using Night Time Light (NTL) radiance density as a proxy, with a focus on disparities in road and health facility infrastructures. Night time light data are sourced from the Visible Infrared Imaging Radiometer Suite (VIIRS) Day/Night Band (DNB) Version 2.2 annual composite for 2023, provided by the Earth Observation Group. The analysis employs 10 km × 10 km grid shapefile with 258 cells and projected to UTM Zone 46N, EPSG 32646. Radiance density is calculated as total radiance count per cell divided by area (100 km^2), proxying the economic vitality of each grid cells in Mizoram.

Standardised predictors included 3 main types, hard infrastructure, soft infrastructure and socio-economic parameters. Hard infrastructure densities measures of roads in each grid cells such as National highways Density (NH_dnst), State highways Density (SH_dnst), Rural Roads Density (RR_dnst), Agricultural Link Roads Density (ALR_dns), Residential roads Density (RsR_dns) and Buildings Area Density (bldg_ar). Soft infrastructure facility count such as Hospital (cnt_Hsp), Sub-District Hospital (cnt_SDH), Community Health Centre (cnt_CHC) and Primary Health Center (cnt_PHC) are also added in count per grid cell. Socio-economic variables such as population estimates for 2023 (POP_2023), BPL percentage

(BPL_prc), Mean Elevation (elev_mn) and access to District headquarter (rd_HQ) in km are also included in the analysis. The grid shapefile is further masked with a district shapefile to support spatial clustering analysis.

To filter the initial variables, Outlier test, Zero-variance test and Variance Inflation Factor (VIF) test for non-zero variance was conducted. The Ordinary Least Squares (OLS) regression is then employed on selected variables, followed by robustness checks via heteroscedasticity tests and a Spatial Lag Model (SLM) to address spatial autocorrelation. Spatial Error Model (SEM) is also performed as a sensitivity check. This analysis offers a synthesis to the study of spatial inequality in hard and soft infrastructure in Mizoram explored in chapter 4 and chapter 5. It is as attempt to explore how spatial inequalities in road and health facilities are associated with uneven economic outcome, as proxied by NTL, in the state.

5.9.1 Results of Variable Filtering and Selection

The analysis follows a structured sequence to identify factors influencing NTL radiance density, progressing from diagnostics to regression models, ensuring findings reflect spatial dynamics. Initial diagnostics identifies cell_id 341 as an influential outlier, with a Cook's distance of 0.3243 exceeding the threshold of 0.0155 (4/n, where n = 258). Its exclusion results in 257 complete cases. No variable exhibits zero variance, preserving all for further evaluation.

Correlation analysis identifies high pairwise correlations ($r > 0.8$) among Residential Road density (correlated with Population density, $r = 0.8714$; Building Area density, $r = 0.9188$; and Hospital count, $r = 0.9670$). Building area density correlates with population density, $r = 0.9012$; and hospital count, $r = 0.9534$). Hospitals correlate with population density, $r = 0.8949$). These variables are excluded to prevent multicollinearity. Variance inflation factor analysis confirms that retained predictors had VIF values below 5.

Table 5.27 Summary of Variance Inflation Factors of Predictors

Predictors	VIF
POP_2023_std	2.433
BPL_prc_std	1.3539
NH_dnst_std	1.3996
SH_dnst_std	1.2628
RR_dnst_std	1.125
ALR_dns_std	1.29
elev_mn_std	1.4387
cnt_SDH_std	2.0159
cnt_CHC_std	1.0604
cnt_PHC_std	1.4961
rd_dst_std	1.6231

Source: Own calculation

5.9.2 Results of Ordinary Least Squares Regression on Night Time Light in Mizoram, 2023

The Ordinary Least Squares (OLS) regression is employed to explore the baseline associations between the explanatory variables and Night Time Light (NTL) radiance density. The model explains 72.76% of the variance in NTL density (R-squared = 0.7276, adjusted R-squared = 0.7153). The Akaike Information Criterion (AIC) is 396.55, and the Bayesian Information Criterion (BIC) is 442.69. The parameter estimates, standard errors, t-values, and p-values are presented in Table 5.28.

The results reveal several notable associations. Population density (POP_2023_std) exhibits the strongest positive effect (coefficient = 0.6468, $p < .001$). A one-standard-deviation increase in population density is associated with a 0.6468 standard deviation increase in NTL density.

Table 5.28 OLS Regression Results for Nighttime Light Radiance Density

Predictors	Estimate	Std. Error	t-value	p-value
(Intercept)	0.4409	0.0318	13.8671	0.0001 ***
POP_2023_std	0.6457	0.0496	13.0202	0.0001***
BPL_prc_std	-0.0569	0.0372	-1.5311	0.127
NH_dnst_std	0.3151	0.0376	8.3738	0.0001 ***
SH_dnst_std	0.0506	0.0358	1.4139	0.1587
RR_dnst_std	0.0656	0.0337	1.9458	0.0528 *
ALR_dns_std	0.0517	0.0362	1.4294	0.1542
Elev_mn_std	-0.0784	0.0383	-2.0501	0.0414 *
SDH_cnt_std	-0.0324	0.0451	-0.7173	0.4738
CHC_cnt_std	0.0393	0.0327	1.202	0.2305
PHC_cnt_std	0.0956	0.0389	2.4564	0.0147 *
Rd_dst_std	-0.0412	0.0405	-1.0168	0.3102
Model Fit Statistics				
Residual standard error: 0.5096 (245 degrees of freedom)				
Multiple R-squared: 0.7276				
Adjusted R-squared: 0.7153				
F-statistic: 59.4827 (df = 11 and 245, p < .001)				
AIC: 396.55				
BIC: 442.69				
*** p < .001, ** p < .01, * p < .05				

Source: Own Calculation

National highway density (NH_dnst_std) also shows a significant positive association (coefficient = 0.3155, $p < .001$) Primary health centre count (PHC_cnt_std) is also positively associated with NTL density (coefficient = 0.0957, $p = .015$), implying that regions with more primary health facilities tend to have elevated economic activity, particularly in rural areas where primary health centres are critical service hubs. Elevation (elev_mn_std) shows a significant negative association (coefficient = -0.0783, $p = .041$), suggesting that higher-altitude areas, due to the difficulty of the terrain in Mizoram are associated with lower NTL density.

Other explanatory variables show weaker or non-significant associations. Rural road density (RR_dnst_std) approaches significance (coefficient = 0.0657, p = .053), at a potential positive relationship with NTL density. State highway density (SH_dnst_std, coefficient = 0.0506, p = .159) and Agricultural Link Road density (ALR_dns_std, coefficient = 0.0517, p = .154) are not significant.

Community health centre count (CHC_cnt_std, coefficient = 0.0394, p = .231) and sub-district hospital count (SDH_cnt_std, coefficient = -0.0324, p = .474) also lack significance. Below-poverty-line percentage (BPL_prc_std, coefficient = -0.0567, p = .127) and road distance to district headquarters (rd_dst_std, coefficient = -0.0413, p = .310) are also not significant.

5.9.3 Model Diagnostics

Following the OLS regression, diagnostic tests are conducted to assess the model's assumptions and suitability for capturing spatial patterns in Night Time Light (NTL) radiance density across Mizoram. The Breusch-Pagan test yields a statistic of 54.02 (df = 11, p < 0.001), indicating significant heteroscedasticity in OLS residuals, reflecting regional variations in elevation and infrastructure not fully captured by OLS.

Table 5.29 Heteroscedasticity and Spatial Autocorrelation Test on OLS Residuals

Test	Estimate	df	p-value
Breusch-Pagan	54.02	11	0.001***
Moran's I	3.2644		0.0011**
LMerr	8.8212		0.003 **
LMlag	32.5897		0.001 ***
RLMerr	1.3036		0.253
RLMlag	25.072		0.001 ***

Source: Own Calculation

Note: *** p < .001, ** p < .01, * p < .05

The Moran's I test, with a statistic of 3.2644 ($p = 0.0011$), confirms significant spatial autocorrelation, suggesting NTL density in a grid cell is influenced by neighbouring cells, consistent with clustered economic activity in urban and peri-urban areas. Lagrange Multiplier tests clarify the spatial dependence: LMlag (32.5897, $p < 0.001$) and robust RLMlag (25.0720, $p < 0.001$) indicate strong spatial lag dependence, while LMerr (8.8212, $p = 0.003$) is significant but robust RLMerr (1.3036, $p = 0.254$) is not, supporting the Spatial Lag Model (SLM) over the Spatial Error Model (SEM) to address these spatial patterns effectively.

5.9.4 Spatial Lag Model (SLM) on NTL Radiance of Mizoram

The spatial lag model (SLM) is estimated to address the spatial autocorrelation identified in the OLS residuals. This model is central to the analysis, as it accounts for spatial dependencies that reflect the region's clustered infrastructure and the spatial extent of economic activity. Test statistics, including parameter estimates, standard errors, z-values, p-values, and model fit statistics, are presented below.

Significant explanatory variables include Population density (coefficient = 0.6251, SE = 0.0449, $p < .001$), National Highway density (coefficient = 0.2872, SE = 0.0347, $p < .001$), and Primary Health Centre (coefficient = 0.0886, SE = 0.0353, $p = .012$). Population density exhibited the strongest effect, with a one-standard-deviation increase associated with a 0.6251 standard deviation rise in NTL Radiance density.

The SLM substantially improved the model fit over the OLS, achieving a Nagelkerke pseudo-R-squared of 0.7601, indicating that 76.01% of the variance in NTL radiance density is explained by the model. The Akaike Information Criterion (AIC = 365.85) reflects a 30.7-point improvement over the OLS model (AIC = 396.55), and the Bayesian Information Criterion (BIC = 415.54) also supports the SLM's relevance over the OLS analysis. The log likelihood is -168.9262 which strengthens the model's ability to capture spatial dependencies.

Table 5.30 Spatial Lag Model Estimates for NTL Density

Predictors	Estimate	Std. Error	z-value	p-value
(Intercept)	0.2688	0.0392	6.8536	0.0001 ***
POP_2023_std	0.6239	0.0449	13.9112	0.0001 ***
BPL_prc_std	-0.0567	0.0336	-1.6883	0.0913
NH_dnst_std	0.2868	0.0346	8.2811	0.0001 ***
SH_dnst_std	0.0451	0.0323	1.3955	0.1629
RR_dnst_std	0.0515	0.0305	1.6887	0.0913
ALR_dns_std	0.0291	0.0329	0.8836	0.3769
Elev_mn_std	-0.0409	0.0351	-1.1673	0.2431
SDH_cnt_std	-0.0278	0.0408	-0.6807	0.4961
CHC_cnt_std	0.0405	0.0296	1.3697	0.1708
PHC_cnt_std	0.0884	0.0353	2.5072	0.0122*
Rd_dst_std	0.0189	0.0381	0.4963	0.6197

Model Fit Statistics

Nagelkerke pseudo-R-squared: 0.7601

Log likelihood: -168.9262

AIC: 365.85

BIC: 415.54

LR test for spatial lag: $\chi^2(1) = 32.6955$, $p < 0.001$

Source: Own calculation

Note: *** p < .001, ** p < .01, * p < .05

The findings substantiate the role of urban agglomeration in driving economic activity, as densely populated areas in Mizoram, often near administrative or commercial hubs, concentrate resources and infrastructure as witnessed in the Getis Ord Gi* results earlier. National highway density shows a robust positive association, with a one-standard-deviation increase linked to a 0.2872 standard deviation increase in NTL Radiance density. This cements the critical role of quality road infrastructure in facilitating economic connectivity in hilly or mountainous regions, particularly in Mizoram where the National Highways are considered the lifeline of the state.

Primary Health Centre (PHC) also shows significant positive association, with a one-standard-deviation increase corresponding to a 0.0884 standard deviation increase in NTL Radiance density. The significance of PHCs highlights the importance of a spatially distributed health facility network in reducing spatial inequality. PHCs, despite being smaller in size and operation compared to other health facilities, are better distributed throughout the state which supports their strong association with economic activity.

Map 5.11 Significant Predictors of NTL in Spatial Lag Model, Mizoram 2023

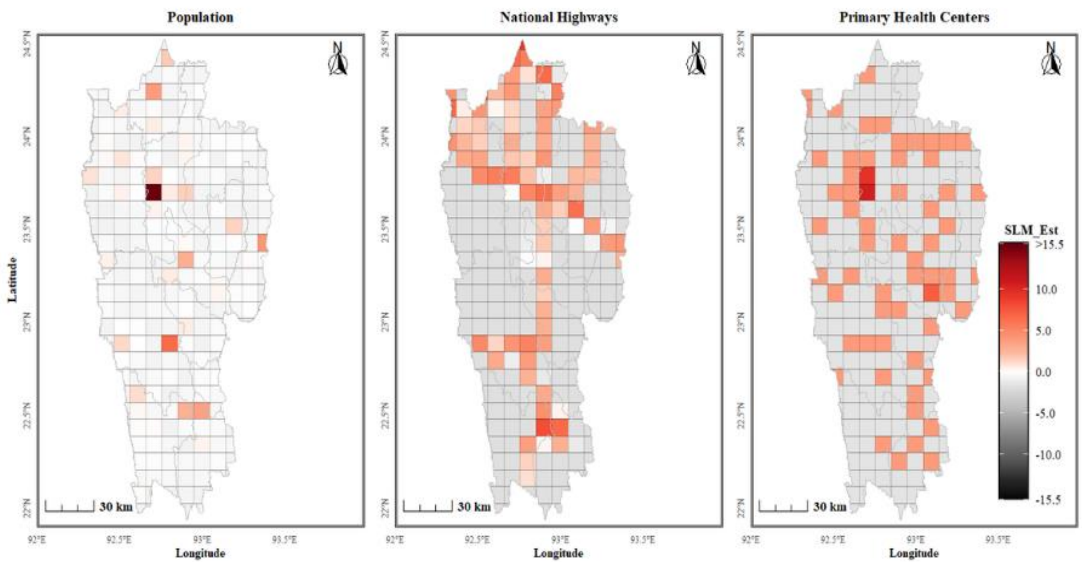

Source: Own visualisation based on GIS data from NTL data from V2.2 Annual Composite, EOG (2023), Population projected from Census 2011

Note- Map 5.11 presents the three significant predictors used in the Spatial linear model (SLM) for Mizoram, 2023. Population density (POP_2023_std), National Highway (NH_dnst_std), and Primary Health Centre density (PHC_cnt_std). The red-grey divergent colour scale indicates standardised values, with grey representing negative values, white representing zero, and red representing positive values (SLM_Est: -15.5 to >15.5).

Rural road density (coefficient = 0.0516, SE = 0.0305, p = .091) approaches significance with positive while Below Poverty Line (BPL) percentage (coefficient = -0.0566, SE = 0.0335, p = .091) hints at potential negative influence. The result shows that while Rural roads may contribute to connectivity, their effects are marginal unless connectivity is couple with other socio-economic investments. The near significance of BPL percentage is also remarkable, given that the standardization uses district level poverty rates for the grid cells, as village level data was unavailable at the time of this study. Although not significant at the 95% threshold, the negative trend in both the OLS and SLM show that poverty elevation is a critical component is spurring economic activity of a region.

Non-significant variables include State Highway density (coefficient = 0.0452, SE = 0.0324, p = .163), Agriculture Link Road density (coefficient = 0.0291, SE = 0.0329, p = .377), elevation (coefficient = -0.0409, SE = 0.0350, p = .243), Sub-District Hospital count (coefficient = -0.0278, SE = 0.0409, p = .496), Community Health Centre count (coefficient = 0.0406, SE = 0.0296, p = .171), and Road distance to district headquarters (coefficient = 0.0189, SE = 0.0381, p = .620).

The non-significance of State Highways reflects its dynamic role as linkage between urban hubs and peripheral regions, often linking far and remote regions where economic activity is low. The result does not negate its importance but rather highlights its unique dual role, connectivity between urban hubs as well as between rural areas.

In the same way the non-significance of Agriculture Link Road in an agrarian sate like Mizoram may seem counter intuitive at first. However, the location of agricultural fields in low artificially illuminated areas, inhibit its effects in a model measured by night time artificial illumination. The non-significant health facility variables, Sub-District Hospitals and Community Health Centres, also suggests that spatial coverage is most paramount when the effects of healthcare services is translated into its overall effect on economic well-being.

The non-significance of elevation, which was significant in OLS (p = .041), suggests that spatial dependencies captured by the SLM mitigated the direct effect of topography, as economic activity in neighbouring cells offset elevation-related constraints. This non-significance can also be understood better if the human settlement pattern of the state is taken into consideration. Contrary to many hill countries around the world, settlements in Mizoram are usually at higher elevations as people generally avoid settling in the low humid valleys. This unique feature of Mizoram is captured by the model, which may not hold true for other parts of the world.

Overall, the model's improved fit over OLS highlights its ability to address the spatial autocorrelation identified earlier, providing a more robust framework for understanding how infrastructure disparities shape economic activity in the state of Mizoram, India.

5.9.5 Hypothesis Evaluation

The study tests the hypothesis that spatial inequalities in road and health facility infrastructures are associated with disparities in economic activity, as measured by Night Time Light (NTL) radiance density in Mizoram. The null hypothesis H_0 posits no association, whereas the alternative hypothesis H_1 asserts a significant association.

Results from the spatial lag model (SLM) indicate strong support for rejecting H_0, in favour of H_1. National highway density, a key indicator of road infrastructure, exhibits a significant positive relationship with NTL density (coefficient = 0.2872, $p < .001$) which suggests that better-connected areas experience higher levels of economic activity. The number of Primary Health Centres also shows a positive and statistically significant effect (coefficient = 0.0886, $p = .012$), showing that greater health infrastructure is aligned with higher economic concentration. Population density, included as a control variable, displays a strong and significant effect (coefficient = 0.6251, $p < .001$) which is expected to have a strong association with economic outcomes. At the same time, Agriculture Link Roads and Community Health Centres are not significant predictors, which suggests that the magnitude of contribution of infrastructure types to economic activity in the state also rest on spatial spread. The model explains a substantial proportion of the variance in NTL density (Nagelkerke pseudo-R^2 = 0.7601), which supports the hypothesis that disparities in economic activity, as proxied by NTL radiance are strongly linked to unequal distributions of infrastructure across Mizoram.

5.9.6 Robustness and Sensitivity Tests

The analysis employs a set of methods to ensure reliable results. Outlier removal addresses influential observations, while correlation analysis eliminates variables with pairwise correlations above 0.8. The removal of VIF values below 5 confirms the absence of multicollinearity. The Breusch-Pagan test (BP = 54.02, $p < .001$) detects heteroscedasticity, and Moran's I test (I = 3.2644, p = .0011) confirms spatial autocorrelation. To account for the heteroscedasticity robustness is further tested using OLS with HC1 robust standard errors and clustered standard errors by district, detailed tables appended in Appendix VII & IX. These models produce consistent estimates for significant predictors.

Although the spatial lag model (SLM) served as the primary analytical framework, a spatial error model (SEM) was additionally estimated as a sensitivity test to verify the robustness of the findings, with detailed results presented in Table 5.31.

The SEM achieved a Nagelkerke pseudo-R-squared of 0.7387 and an Akaike information criterion (AIC) of 387.79, revealing significant positive associations for standardised Population in 2023 (estimate = 0.605, $p < 0.001$), National Highway density (estimate = 0.3058, $p < 0.001$), and Primary Health Centre count (estimate = 0.1048, $p < 0.01$), alongside similarities to the SLM in predictor significance and an enhanced level of statistical significance for the standardised primary health centre variable. This alignment in key predictors across models, including the absence of other significance for variables strengthens the reliability of the overall results in explaining the inequality observed in economic activity as proxied by night-time lights density radiance in Mizoram.

Table 5.31 Spatial Error Model Estimates for NTL Density

Predictors	Estimate	Std. Error	z-value	p-value
(Intercept)	0.4485	0.0483	9.2805	0.001 ***
POP_2023_std	0.605	0.0461	13.1324	0.001 ***
BPL_prc_std	-0.0615	0.0394	-1.5618	0.1183
NH_dnst_std	0.3058	0.0378	8.0918	0.001 ***
SH_dnst_std	0.0522	0.0346	1.5094	0.1312
RR_dnst_std	0.0392	0.0322	1.2159	0.224
ALR_dns_std	0.0453	0.0371	1.2235	0.2212
Elev_mn_std	-0.0568	0.0475	-1.1972	0.2312
SDH_cnt_std	-0.0367	0.042	-0.8732	0.3826
CHC_cnt_std	0.0405	0.0301	1.3445	0.1788
PHC_cnt_std	0.1048	0.0366	2.8674	0.0041**
Rd_dst_std	-0.0548	0.0486	-1.1278	0.2594
Model Fit Statistics				
Nagelkerke pseudo-R-squared: 0.7387				
AIC: 387.79				
BIC: 437.48				

Source: Own calculation

Note: *** p < .001, ** p < .01, * p < .05

A comprehensive model comparison is provided in Table 5.32. The SLM's better fit is evidenced by the lowest AIC and highest R-squared, validating its selection as the primary model for capturing spatial dependencies.

Table 5.32 Comparison of Models

Model		R-squared	AIC	BIC
OLS	Standard SE	0.7276	396.55	442.69
OLS	Robust SE	0.7276	396.55	442.69
OLS	Clustered SE	0.7276	396.55	442.69
SLM	Standard SE	0.7601	365.85	415.54
SEM	Standard SE	0.7387	387.79	437.48

Source: Own calculation

5.9.7 Limitations of the Study

This study presents several challenges and limitations, many of which arise from the nature of the spatial data and the technical constraints in the execution of the analysis. The use of the Night Time Light data as a proxy for economic activity is a methodological choice arising out of necessity rather than convenience, due to the absence of a reliable district level economic output parameter. It also poses several limitations such as the exclusion of non-illuminated economic activities, including agriculture and the plateauing of lighting intensity in urban core areas, and growing usage of energy efficient lighting systems.

The coarse resolution, 500-meter, of the data from VIIRS, while widely adopted, inevitably introduces challenges such as terrain masking and light dispersion from hilltop settlements which a finer resolution could have mitigated. Similarly, working with a grid framework involved a necessary trade-off: although it enables the detection of spatial patterns that would have been obscured by aggregation at the district level, the grid may have smooth over hyper-local variations and hot spots.

The standardisation of predictors also imposes an assumption of linear relationships, which can oversimplify complex spatial dynamics, including non-linear effects of infrastructure clustering. However, it is apparent that in large-scale spatial analyses, standardization is a necessity that ensures comparability and prevents scale-driven distortions. The allocation of district-level poverty percentages to grid cells presents another limitation, as it introduces uniformity that cannot fully capture intra-district heterogeneity between urban and rural areas. Evidence from the near-significance of poverty as a covariate suggests that finer-scale data, if available, would likely yield stronger associations. Additionally, the exclusion of highly correlated predictors such as building area density reduces the scope of analysing urbanization effects. While this decision prevents distortion from vertical variation in building sizes, the inclusion of population density presents itself as a more consistent control variable. Finally, the exclusion of testing with robust standard errors within the SLM and SEM frameworks are a technical constraint rather than a methodological choice. Nonetheless, sensitivity tests conducted using OLS robust and clustered standard errors provided reassurance regarding the stability of the results. Future studies can benefit from taking into account these limitations.

Despite these limitations, the spatial lag model shows that infrastructure inequalities are closely linked with differences in economic activity across Mizoram. The model explains a large share of the variation in night-time light density (Nagelkerke pseudo-R^2 = 0.7601), which indicates that areas with weaker access to roads and health facilities also tend to show lower economic output. Some predictors are not significant, but the general pattern is clear: unequal infrastructure provision contributes to spatial inequality in economic activity. In a state with difficult terrain and scattered settlements, these results point to the importance of reducing infrastructure gaps if balanced regional development is to be achieved.

5.10 SYNTHESIS AND DISCUSSION

The analysis across multiple datasets confirms that Mizoram's hard infrastructure is unevenly distributed, both between districts and within them. Building counts highlight clear disparities, with Aizawl far ahead of smaller districts. The Atkinson Index values indicate that inequality grows when more weight is placed on under-served areas, showing that the gap widens for districts at the lower end of infrastructure provision. Road infrastructure also reveals imbalances. Coefficients of variation point to high disparities, especially in residential and agricultural link roads. Spatial autocorrelation results confirm clustering patterns, with significant hot spots and cold spots that underline how some areas concentrate investment while others remain neglected.

Night Time Light radiance, used as a proxy for economic activity, shows Mizoram at the lowest end of India's per-area radiance. The inter- and intra-district

Gini values demonstrate that inequality is not only between districts but also within them, with Aizawl showing the highest intra-district concentration. Electricity transmission and distribution losses further highlight systemic inefficiencies that contribute to weaker radiance levels.

The temporal analysis of NTL from 2014 to 2023 shows that, while most districts and grid cells experience significant positive growth. Regions in the border experience the high growth trend owing to advantages in trade, both domestic and international. Higher radiance districts record the largest absolute increases, while lower radiance districts see relatively higher percentage growth, the scale of growth remains far behind. Spatial clustering of NTL growth, confirmed by Getis-Ord Gi* statistics, shows hot spots concentrated around Aizawl and peri-urban centres, while large parts of rural Mizoram remain stagnant.

The econometric models strengthen these observations. The SLM model explains a large share of the variance in radiance and confirms that spatial inequality in infrastructure is associated with inequality in economic output. While some predictors are not significant, the general finding is that lack of infrastructure provision, combined with difficult terrain and dispersed settlement, drives uneven economic patterns across the state. The non significance of nearness to the district capitals, proximity to administrative centres, suggests that some regions receive infrastructure investments despite being in the peripheral areas of their districts. This could be the result of political bias or a result of differences in natural endowments such as land and trade opportunities, which unfortunately is beyond the reasonable analytical scope of this study.

One important limitation of this study is the use of night time lights as a proxy for economic activity. As demonstrated in this chapter, artificial illumination does not scale neatly with population or output: a single concentrated light source may serve a large number of people, while vast unlit areas can still sustain significant agricultural or informal activity. Controlling ephemeral lighting and stray light is important, especially in regions like Mizoram where hill-top settlements project lights downhill. This means that NTL can overstate economic activity in sparsely populated areas and understate the density and functionality of urban economies where illumination is more diffused by terrain and urban structures. These biases, combined with the inability of radiance data to capture non-illuminated sectors such as agriculture, warrants caution in drawing blanket conclusions from NTL alone. The results need to be interpreted as an indicative measure of spatial disparities, complemented by socio-economic and sectoral data.

Taken together, these results point to systemic spatial inequality in Mizoram's infrastructure and its economic consequences. Aizawl and its surroundings emerge as dominant clusters of both infrastructure and economic activity, while rural and remote showed signs of growth, the scale may not be enough to reverse the trend of hyper agglomeration in Mizoram. The strong spatial clustering in roads, especially in Agriculture Link Roads, shows that inequality is not random but systematically reproduced, marginalising many in an economy where the major chunk of the population receives their livelihood through agriculture.

The results of this study show that economic infrastructure in Mizoram is unevenly distributed and that this contributes to spatial disparities in economic activity. Although these disparities are not extreme, their persistence has important implications. Unequal infrastructure access can reinforce existing disadvantages, especially for poorer populations who depend more heavily on public services and targeted investment. It also risks concentrating growth in a few urban centres, leading to problems such as congestion, higher living costs, land price inflation, and pressure on public health systems. At the same time, peripheral areas may continue to face low levels of development, deepening regional divides. These dynamics create costs for both core and peripheral regions and may, over time, translate into social or political tensions. To avoid such outcomes and to move toward more equitable growth, spatially targeted interventions are needed. Allocating resources purely on the basis of population is unlikely to address these imbalances; instead, investment strategies must account for geographic disparities to promote balanced and inclusive development across the state.

5.11 CONCLUSION

This chapter shows that spatial inequality in hard infrastructure is present in Mizoram, though the pattern is not as severe as at the national level. The Gini values for Night Time Light radiance indicate that, compared to India as a whole, inequality within Mizoram is more contained. At the same time, Mizoram records the lowest radiance per unit area in the country. Even accounting for terrain effects, this is consistently low level compared with other Himalayan and special category states points to limited infrastructure and economic activity across the state.

The picture that emerges is one of inequality in the context of generally low development. While some districts, especially Aizawl, have stronger infrastructure and economic concentration, the overall level of provision across the state remains weak. Good quality roads and rural health facilities stand out as areas where improvements could make the most difference. The uneven distribution of roads contributes to economic divides, while the spatial distribution of healthcare facilities mitigates the centripetal pull of agglomeration, associating with nodes of regional and peripheral hubs. The high transmission and distribution losses in the power sector reflects systemic inefficiencies that needs a good amount of investment. The evidence strongly suggests that policies should focus not only on reducing disparities between districts but also on raising the overall level of infrastructure in Mizoram. Targeted investment in road connectivity, integration with the national highway system, spatial intervention in healthcare and strengthening of the electricity grid would help address both inequality and over all low development in the state of Mizoram.

CHAPTER-VI

FINDINGS, RECOMMENDATIONS AND CONCLUSION

This chapter synthesises the key findings from the analyses conducted in Chapters 4 and 5, which investigated the soft infrastructure (healthcare) and hard infrastructure (buildings and roads) of Mizoram, respectively, with a focus on spatial inequality in infrastructure distribution across the region. It further examines the association between these infrastructure components and economic activity, using Night-Time Light radiance as a proxy. Drawing on a series of descriptive and inferential statistical tests performed in the preceding chapters, this section presents the outcomes, provides recommendations to address identified spatial disparities, and concludes with insights into the implications of these findings to mitigate spatial inequality and promote equitable economic development in Mizoram.

6.1. FINDINGS

Main Findings on Spatial Inequality in Health Infrastructure

- SaTScan analysis reveals a dominant healthcare facility cluster in Aizawl district with a radius of 4.72 km and a relative risk of 10.81 ($p < 0.001$), encompassing 18.5% of 119 facilities which indicates spatial clustering.

- The Gini coefficient (0.2407 for facilities, 0.302 for density) and Theil-T Index (0.2532 for beds, 47.7% between-district) reveal moderate inequality in facility and bed distribution, with southern districts (Lawngtlai: 1.34, Lunglei: 1.99 per 1,000) and western Mamit (1.31 per 1,000) significantly under-resourced. Within-district urban-rural disparities (52.3%) dominate in southern regions, indicating allocative inefficiencies.

- SaTScan analysis shows equipment usage cluster (relative risk = 5.10, $p < 0.001$) capturing 71.7% of 196,385 cases in Aizawl District. No other significant clusters were found in the state which suggests that medical equipment usage is highly concentrated in Mizoram.

- The Atkinson Index for medical equipment usage for different levels of inequality aversion were 0.597 ($\varepsilon = 0.5$), 0.714 ($\varepsilon = 0.1$), 0.812 ($\varepsilon = 1.5$) and 0.877 ($\varepsilon = 2$) respectively, this suggests high inequality at low aversion that progresses to severe inequality as more weight is given to the bottom of the distribution.

- Global Moran's I ($I = 0.071$, $Z = 0.9707$, $p = 0.1720$) suggests negligible spatial autocorrelation in health personnel density, while Local Moran's I identifies significant high-high clusters in eastern Serchhip and Khawzawl, low-low clusters in northern Saitual and Kolasib, and a high-low outlier in Saiha. This indicates imbalance in workforce distribution, contributing to regional inequality in personnel allocation.

- The Health Infrastructure Index, created through the Principal Component Analysis (PCA) indicates Aizawl's PC1 score (3.517) is driven by high bed density (4.62 per 1,000) and equipment density (0.206 per 1,000). Districts in southern (Lawngtlai, Lunglei) and western (Mamit) districts scored the lowest, highlighting pronounced disparities in resource availability in the most vulnerable lowlands districts.

- Spatial trap mapping, employing 7 km buffers around 118 facility centroids, identifies 248 settlements (33% of 752) requiring over 1 hour to access medical care, primarily in the southern districts (Lawngtlai: 89, Lunglei: 51) and western (Mamit: 31) districts. These access gaps are intensified in lowland districts with high tropical disease risk (mean Malaria API: 7.6).

Main Findings on Spatial Inequality in Hard Infrastructure in Mizoram

- The Atkinson index per capita at $\varepsilon = 1$ is 0.009, with bootstrap mean 0.008 (SE = 0.003) and 95% CI (0.003–0.014). The result indicates that districts moderate level of inequality with higher population density possess more building stock relative to demographic needs. The Atkinson Index for building density at $\varepsilon = 2.0$ yields 0.185 (bootstrap mean 0.160, 95% CI: 0.034–0.324), indicating high inequality.

- Road density exhibits strong spatial dependence. Global Moran's I across 258 grid cells (10x10km) are significant for all road types at $p \leq 0.001$: National Highways (0.274), State Highways (0.118), Rural Roads (0.101), Agricultural Link Roads (0.386), and Residential Roads (0.141). Agricultural link roads show the strongest clustering in central and eastern regions, while southern and western regions exhibit low-low clusters, indicating uneven connectivity critical for agrarian economies.

- The Mann-Kendall test across 237 grid cells (2014-2023) identifies significant positive NTL radiance trends in 135 cells (57%, $p < 0.05$, mean tau 0.503). The central and eastern regions exhibited the strongest monotonic increases, reflecting concentration of radiance growth in Aizawl and eastern districts, while southern and western districts lag.

- OLS regression identified significant radiance trends ($p < 0.05$), with a mean NTL slope of 2.0255 nW/cm²/sr/year and median of 0.7489 nW/cm²/sr/year, indicating that economic activity as proxied by NTL witnesses an increasing trend across Mizoram during 2014 to 2023.

- The spatial lag model (SLM) reveals significant associations between population density (coefficient 0.6251, $p < 0.001$), national highway density (coefficient 0.2872, $p < 0.001$), and primary health centre count (coefficient 0.0886, $p = 0.012$) with night-time light (NTL) radiance density, with a Nagelkerke pseudo-R^2 of 0.7601. The result indicates that disparities in road and health infrastructure is associated with economic inequalities, particularly in urban Aizawl and Champhai compared to southern and western regions.

- Getis-Ord analysis identifies 20 significant hot spots ($p < 0.05$) in Aizawl (e.g., cell 246, $Gi^* = 7.671$) and 4 cold spots in northern Aizawl (e.g., cell 332, $Gi^* = -2.507$) where the trend of NTL radiance slope (2014-2023) is clustered which suggests that although Mizoram experiences growth in economic activity, growth is significantly uneven.

Findings on Elevation based Tropical Disease Risk Zoning

- Mizoram's elevation spans 17 m to 2,149 m above sea level, with a mean of 610.2 m and a median of 565 m, which shows that there is considerable topographical diversity among the districts.

- Champhai District records the highest mean elevation (1,150.1 m) and median (1,139 m), while Kolasib has the lowest mean (263 m) and median (193 m). Lawngtlai contains the highest point (2,149 m), and Lunglei the lowest (17 m).

- Spearman correlation analysis reveals a strong negative relationship between settlement elevation and malaria Annual Parasite Incidence (API) across 2017–2021. The correlations are significant for 2017 ($r = -0.857$, $p = 0.011$), 2018 ($r = -0.857$, $p = 0.011$), 2019 ($r = -0.707$, $p = 0.050$), and 2020 ($r = -0.810$, $p = 0.022$), but weaker and non-significant for 2021 ($r = 0.286$, $p = 0.501$), likely reflecting reduced mobility during COVID-19 restrictions.

- Classification of districts based on elevation zones, Lowlands (17–432 m), Midlands (565–869.5 m) and Highlands (985.2–1,150.1 m) can help preparedness against vector-borne diseases with altitude-linked prevalence patterns, such as malaria.

Findings on Health Infrastructure Distribution in Mizoram 2021

- Mizoram has 119 health facilities in 2021, including 67 Primary Health Centres (PHCs), 9 Community Health Centres (CHCs), 2 Sub-District Hospitals (SDHs), and 41 hospitals (15 government, 26 private) in 2021. PHCs dominate as the most widespread facility type, distributed across both rural and urban areas.

- Aizawl District accounts for 29.4% of total health facilities, with a pronounced concentration in tertiary (48.8%) and secondary (30.0%) healthcare, establishing it as the primary hub for advanced medical services.

- CHCs are limited to 9 units across Mizoram, located in Aizawl (3), Khawzawl (1), Kolasib (1), Lawngtlai (1), Mamit (1), Saitual (1), and Serchhip (1). Southern districts, particularly Lunglei and Saiha, lack CHCs, compromising referral efficiency.

- Spatial analysis reveals health facilities align closely with the National Highway, forming a linear pattern from northern to southern Mizoram. Settlements distant from this axis face reduced access, exacerbating spatial disparities.

- A North–South spatial divide in PHC distribution was evident, with northern districts (e.g., Aizawl, Kolasib) showing denser, more uniform coverage compared to sparser southern districts (e.g., Lawngtlai, Saiha). An East–West gradient also exists, with eastern zones (e.g., Khawzawl, Champhai) exhibiting better spatial reach than western areas.

- Tertiary care is heavily concentrated in Aizawl's urban core (hospital density: 0.042 per 1,000), contrasting with low densities in southern districts like Lawngtlai (0.021) and Saiha (0.029), despite their higher disease burdens and ecological vulnerabilities.
- The population-based allocation of facilities overlooks regions with elevated malaria risk, as identified in prior analysis, leading to intra-district disparities, particularly in western and southern peripheral areas, where access remains limited.
- Facility density analysis yields a Gini coefficient of 0.302 (95% CI: 0.242–0.334, 1,000 bootstrap iterations), indicating a moderate level of inequality. Hnahthial (0.142 facilities per 1,000 population), Khawzawl (0.135), and Serchhip (0.112) rank highest due to low populations and numerous low-tier facilities, while urban Aizawl (0.078) appears under-resourced relative to its population and service breadth.

Findings on Distribution of Health Facility Beds in Mizoram

- Mizoram has 3,744 health facility beds across 11 districts in 2021, comprising 648 Primary Health Centre (PHC) beds, 270 Community Health Centre (CHC) beds, 80 Sub-District Hospital (SDH) beds, and 2,746 District Hospital beds, averaging 340 beds per district.
- Aizawl District dominates with 2,079 beds (55.5% of total), including 1,841 in District Hospitals (88.6% of its total), yielding a bed density of 4.62 per 1,000 population, exceeding the OECD average (4.4 per 1,000). Hnahthial has the fewest beds (70, 1.9%), primarily in PHCs (40 beds).

- The state average bed density of 2.76 per 1,000 population falls below the World Health Organization's recommended 3.5 per 1,000, with Aizawl (4.62) as the only district surpassing this threshold.
- GIS mapping highlights southern districts (Lawngtlai, Lunglei, Saiha) and eastern Champhai with low primary and secondary care bed availability (CHC and SDH beds total 350 state-wide). Aizawl leads in tertiary level bed density, followed by Saiha and Lunglei. Hnahthial, Khawzawl, Saitual, Kolasib, and Mamit have the lowest.
- Low bed density in high-risk tropical districts (Mamit: 1.31, Kolasib: 1.54, Lawngtlai: 1.34, Lunglei: 1.99 per 1,000) exacerbates risk for endemic diseases like malaria and limits epidemic preparedness.
- The Theil-T Index of 0.2532 indicates moderate inequality in bed allocation across Mizoram, reflecting disparities in healthcare access driven by both district-level and urban-rural variations.
- Within-group inequality (0.1324, 52.3% of total) is driven by pronounced urban-rural disparities in Lawngtlai (0.0358, urban: 4.08 vs. rural: 0.75 beds per 1,000) and Lunglei (0.0325, urban: 4.06 vs. rural: 0.88), highlighting severe rural bed shortages in southern districts.
- Between-group inequality (0.1209, 47.7% of total) is largely influenced by Aizawl's high bed density (4.62 per 1,000, contribution: 0.2848) compared to under-resourced districts like Mamit (1.31, -0.0278), Lawngtlai (1.34, -0.0377), and Saitual (1.20, -0.0179).
- These findings, aligned with GIS mapping, confirm that southern districts like Lawngtlai and Lunglei, with high within-group inequality and 18 spatial deserts within 7 km facility buffers, face acute access challenges, while low between-group contributions in Mamit and Kolasib reflect broader resource scarcity, exacerbating vulnerabilities in high-disease-burden zones.

Findings on Distribution of Medical Equipment in Mizoram in 2021

- Of the 10 diagnostic equipment analysed, X-ray machines (37 units), ECG (34 units), and Ultrasound (29 units) are the most abundant. Advanced equipment like Chemotherapy (6 units) and Radiotherapy (1 unit) is scarce, while Dialysis (12 units) and Endoscopy (21 units) are moderately available but concentrated.

- Aizawl District dominates with 93 units (58.1%), including 18 X-rays, 16 Ultrasounds, 17 ECGs, 9 CT-Scans, 7 ECHO machines, 4 Chemotherapy units, 1 Radiotherapy unit, 7 Dialysis units, 3 Bronchoscopy units, and 11 Endoscopy units. Hnahthial, Khawzawl, and Saitual each have only one X-ray unit, while Lunglei (16 units) and Lawngtlai (12 units) lack advanced diagnostics.

- Statewide, equipment density averages 0.118 units per 1,000 population, with X-ray (0.027) most prevalent and Radiotherapy (0.001) least. Aizawl has the highest per capita availability (0.206 units), followed by Champhai (0.114) and Serchhip (0.112). Saitual (0.015), Khawzawl (0.023), and Hnahthial (0.028) have the lowest density, relying almost exclusively on X-rays.

- Usage analysis shows Aizawl absorbs 140,888 diagnostic procedures against an expected 65,293 based on population share, with a usage-to-expected ratio of 2.158, indicating significant patient migration (75,595 users) from other districts. Lawngtlai (ratio: 0.350) and Mamit (ratio: 0.186) experience the highest outward migration, reflecting severe equipment shortages.

- The Atkinson Index, calculated with bootstrapping at inequality aversion levels ($\varepsilon = 0.5, 1, 1.5, 2$), confirms pronounced disparities in equipment usage. At $\varepsilon = 0.5$, the index is 0.597 (mean: 0.578, 95% CI: 0.251–0.789), indicating severe inequality even at low aversion thresholds. At $\varepsilon = 2$, the index rises to 0.877

(mean: 0.842, 95% CI: 0.581–0.937), highlighting acute disparities, particularly for underserved districts.

- The rising Atkinson Index with higher ε values suggests that inequality is most severe at the lower end of the distribution, with districts like Lawngtlai, Mamit, and Saitual facing critical shortages in essential diagnostic equipment, exacerbating access gaps for vulnerable populations.

- These disparities align with healthcare centralisation patterns observed in other developing regions, suggesting that redistributing equipment to align with population shares could improve equity without reducing total service provision, though Mizoram's overall lag in medical technology compared to broader India remains a concern.

- The Atkinson Index findings complement GIS mapping, reinforcing that the southern and peripheral districts, with limited access to advanced diagnostics, bear a disproportionate burden of inequality, driving patient migration to Aizawl and straining urban facilities.

Findings on Distribution of Health Personnel Density in Mizoram

- Mizoram's medical workforce in 2021 includes 685 doctors (0.506 per 1,000 population) and 1,902 nurses and health workers (1.671 per 1,000). Aizawl dominates with a doctor density of 0.877 and nurse/health worker density of 1.800 per 1,000, while Saitual (0.224 doctors) and Khawzawl (0.248 doctors) are significantly below the state average.

- Nurse and health worker distribution shows Hnahthial leading at 2.048 per 1,000, contrasted by critical shortages in Lawngtlai (0.728) and Saiha (1.016), indicating uneven workforce allocation across districts.

- Global Moran's I ($I = 0.071$, $Z = 0.9707$, $p = 0.1720$, 999 permutations) reveals weak, non-significant spatial autocorrelation, reflecting Aizawl's isolated concentration as the healthcare hub without comparable staffing in neighbouring districts.

- Local Moran's I analysis identifies significant spatial patterns: Serchhip ($Z = 1.6856$, $p = 0.0485$) and Khawzawl form high-high clusters, indicating localized staffing concentrations, while Saiha ($Z = 1.7289$, $p = 0.0411$) is a high-low outlier with higher personnel density than its neighbours. Saitual ($Z = -1.791$, $p = 0.0394$) and Kolasib ($Z = -1.8872$, $p = 0.0267$) form low-low clusters, marking areas of structural deprivation.

- Western lowland districts (Lawngtlai, Mamit), previously identified as high malaria risk zones, lack significant high-high or high-low clusters, exacerbating healthcare access inequities in regions with elevated disease burdens.

- The absence of significant clustering in high-risk western districts, highlights a critical mismatch between personnel distribution and health needs, particularly in infrastructure-poor western belts.

- Aizawl's low-high classification, despite its high workforce density, highlights its spatial isolation as a resource hub, with no spillover to adjacent districts, reinforcing systemic centralisation and regional disparities.

Findings on Healthcare Catchment Area and Deprivation Pockets

- The mapping of catchment areas, defined by a 7 km buffer around 118 reveal several healthcare access voids across Mizoram.

- 32.9% (totalling 248) of 752 settlements in Mizoram, requires more than one hour of travel to reach an institutional doctor. Another 33.24%, totalling 250 settlements are within a one-hour travel window, while 33.77% (totalling 254 settlements) are well within thirty minutes of care.

- Aizawl District, exhibits extensive catchment coverage, with both urban and rural areas well covered by extensive overlapping of buffers from PHCs, CHCs, and hospitals.

- Southern districts (Lawngtlai, Lunglei, Saiha) and western areas (Mamit) display significant underserviced pockets, with Lawngtlai hosting 89 of 248 settlements (33% of total) requiring over 1 hour to reach a health facility. Lunglei (51) and Mamit (31) follow, together accounting for over two-thirds of Mizoram's "far" settlements (>1 hour travel).

- Northern and eastern districts (Serchhip, Khawzawl, Kolasib) have fewer underserved settlements, with 254 settlements state-wide within 30 minutes of care and 250 within 1 hour, reflecting a pronounced North-South and East-West spatial divide in access.

- Clustering and overlapping of catchment areas are evident in central and eastern regions, particularly in Aizawl and Serchhip, indicating inefficient facility allocation driven by population of host village or town rather than spatial coverage considerations, leading to costly overlaps and underserved peripheral areas.

- Western and southern low-lying districts, identified as high-disease-burden zones due to tropical conditions, face compounded access challenges from terrain, seasonal flooding, and landslides, exacerbating spatial health traps where remoteness and limited First Referral Units (FRUs) force patient migration to urban centres like Aizawl, straining tertiary facilities.

Findings on Health Insurance in Mizoram

- Mizoram's healthcare system exhibits moral hazard, driven by the concentration of private hospitals in Aizawl (83% of state total), which absorb 57.51% of inpatient admissions (175,173 vs. expected 101,241.22) despite Aizawl hosting only 33.25% of the population, indicating significant inpatient migration from rural districts like Khawzawl (-87.88% IPD proxy) and Saitual (-80.10%).

- Analysis of Rashtriya Swasthya Bima Yojana (RSBY) and Mizoram State Health Care Scheme (MSHCS) shows claims outpacing enrolment, with RSBY claims growing at a 33.22% CAGR (2010–2021) against a 29.32% enrolment CAGR, and a 97.5% payout ratio in 2020–21, suggesting potential provider overbilling due to lax oversight in the 90:10 Central-state funded scheme.

- MSHCS claims rose at a 14.69% CAGR against a 12.30% enrolment CAGR, with a 0.671 claims-per-family ratio in 2019–20 but a low 29.7% payout ratio in 2020–21, reflecting stringent state scrutiny that rejected excessive claims, yet high utilisation (25% claims rate) indicates demand-side moral hazard driven by low enrolment fees (₹100 BPL, ₹1,000 APL) and transport allowances (₹1,000 in-state, ₹10,000 out-of-state).

- Aizawl's private hospitals registered a high OPD-to-IPD conversion rate ranging from 7.37% to 48.02% compared to government hospitals 4.08% (Aizawl Civil Hospital) and 4.66% Civil Hospital Lunglei, suggesting supply-side moral hazard

- The proportion of non-surgical and non-delivery IPD cases is notably higher in private hospitals, ranging from 21.88% (Ebenezer Medical Centre) to 100% (Redeem Hospital, College Veng), with most exceeding 60% of IPD. This suggests that private hospital may have admitted low acuity condition whereas government hospitals (-34% for Aizawl DH, 0.61% for Lunglei DH) barely admit non critical patients.

- The IPD migration proxy suggests that Aizawl (73.02%), Lunglei (23.06) and Siaha (40.92%) receive more IPD than their population warrants. This significant migration from other districts.

Findings on Health Infrastructure Index

- Bartlett's Test of Sphericity ($\chi^2 = 15.03$, $p = 0.0018$) and a strong beds-equipment correlation ($r = 0.905$) validate PCA for the Mizoram Composite Health Infrastructure Index (HII), though the small sample (11 districts) limits KMO (0.50)

- Principal component one (PC1) with a standard deviation of 1.421 explains 67.3% of the variance whereas as PC2 explains 29.8% of the variance, in total PC1 and PC2 explain 97.1% of the variance. Whereas PC3 explains 2.9% of the variance only, suggesting that all meaningful variability in the dataset is concentrated within the first two dimensions.

- The loading of PC1 emphasized bed (-0.680) and equipment (-0.662) capacity over heath buildings (-0.316).

- Aizawl's high Z-scores (beds: 1.52, equipment: 0.024 per 1,000) drive its top PC1 ranking (3.517), while low Z-scores in Mamit (beds: 0.23) and Saitual (beds: 0.32) result in bottom ranks (-1.556, -1.391).

- Eastern and southern districts such as Saiha (PC1: 0.761, PC2: -0.740), Serchhip (PC1: 0.665, PC2: 1.113), and Champhai (PC1: 0.599, PC2: 0.204) form a mid-tier, showing resilience in clinical capacity, with Serchhip also having high facility density while Saiha and Champhai shows signs of low facility density.

- Eastern districts Khawzawl (PC1: -0.583, PC2: 1.477) and Hnahthial (-0.435, 1.396) lead PC2 due to high building Z-scores (0.021), but low PC1 scores. indicating limited bed and equipment capacity. This mismatch reveals structural misalignment between facility spread and functional capacity.

- Northern/western districts Mamit (PC1: -1.556, PC2: -0.654), Saitual (-PC1: 1.391, PC2: -0.017), and Kolasib (PC1: -0.871, PC2: -0.927) show dual deficits in clinical capacity and facility density

- Southern districts such as Lawngtlai and Lunglei consistently underperform across both PC1 and PC2, facing low facility density and weak clinical capacity. These areas align with high tropical disease-burden zones, exacerbating spatial treatment bottlenecks.

Findings on SaTScan Statistics on Healthcare Facilities

- SaTScan analysis identifies a primary cluster in Aizawl district, centred at Redeem Hospital (23.724261 N, 92.726685 E, radius 4.72 km), containing 22 facilities (18 hospitals, 4 PHCs), representing 18.5% of Mizoram's 119 facilities in 0.33% of its 21,087 km² area.

- The Aizawl cluster's relative risk (RR = 10.81, 95% CI: 8.12–14.39) and p-value ($< 10^{-15}$, LLR = 47.24) confirm significant facility concentration, far exceeding the expected 2.45 facilities.

- A Gini coefficient of 0.2407 (optimal at 3%) highlights Aizawl's disproportionate facility share, with 22 facilities in a 70 km² area, indicating centralized resource allocation.

- A secondary cluster in southern Lunglei (22.879495 N, 92.761851 E, radius 4.37 km) includes seven facilities (5 hospitals, 2 PHCs), with RR = 7.71 and p = 0.013 (LLR = 11.32), suggesting a smaller hub.

- Non-significant clusters in Lengpui/Sairang (RR = 9.62, p = 0.701), Champhai (RR = 9.62, p = 0.701), Lawngtlai (RR = 9.62, p = 0.701), and Serchhip (RR = 7.21, p = 0.987) indicate limited facility concentration in northern, eastern, and southern districts.

- The Aizawl cluster's dominance reflects its role as Mizoram's administrative hub, with 18 of 20 hospitals concentrated within a 4.72 km radius, limiting access in peripheral districts.

- Southern and western districts (e.g., Lawngtlai, Mamit) show sparse facility distribution, with non-significant clusters highlighting infrastructure deficits in remote areas.

Findings on SaTScan Analysis on Medical Equipment Access

- SaTScan analysis of 196,385 medical equipment usage cases (2021) identifies a significant cluster in Aizawl district, centred at 23.724350 N, 92.719174 E, covering 450,444 people (33.3% of Mizoram's 1,354,830 population).

- The Aizawl cluster captures 140,888 cases (71.7% of total), far exceeding the expected 65,292.65, with a relative risk (RR) of 5.10 indicating usage 5.10 times higher than other districts.

- The cluster's log likelihood ratio (LLR = 60,651.23) and p-value (< 0.001, Monte Carlo rank 1/1000) confirm high statistical significance of concentrated diagnostic usage.

- No secondary clusters were detected, even with a 20% population-at-risk limit (270,966) indicating Aizawl's overwhelming dominance in equipment usage in the state.

- Eastern districts like Khawzawl (146 cases) and Hnahthial (488 cases) show minimal usage, limited to basic diagnostics (e.g., X-rays), indicating technological deficits.

- Southern and western districts such as Lawngtlai and Mamit, exhibit low case counts, reinforcing sparse access to advanced diagnostics.

- The absence of secondary clusters suggests a lack of uniform technological standards, with Aizawl monopolizing advanced diagnostic services across Mizoram.

Findings on Distribution of Building Infrastructure in Mizoram

- The Atkinson Index on building density, at $\varepsilon = 0.5$, yields 0.066 (bootstrap mean: 0.055, 95% CI: 0.010–0.108), indicating low inequality in building density at low aversion to disparities. This indicates that some level of inequality exists in the distributed across Mizoram, with Aizawl's dense concentration (43.13 buildings/km^2) dwarfs the rest of the districts.

- At higher inequality aversion ($\varepsilon = 2.0$), the Atkinson Index in buildings per km^2 density rises to 0.185 (bootstrap mean: 0.160, 95% CI: 0.034–0.324), signalling moderate inequality in building density across the state.

- Aizawl dominates with 90,101 buildings and a density of 43.13 buildings per km^2, far exceeding the state average of 15.84 buildings per km^2, highlighting a concentrated buildup area in the central district compared to peripheral regions.

- Southern districts Hnahthial (9,287 buildings, 8.44 buildings/km^2) and Lunglei (33,528 buildings, 9.82 buildings/km^2), and western Mamit (27,284 buildings, 8.81 buildings/km^2) show low building density, reflecting dispersed settlements and limited infrastructure access.

- Eastern Champhai (27,350 buildings, 17.87 buildings/km^2) and northern Kolasib (27,326 buildings, 17.27 buildings/km^2) exhibit higher building density, indicating more compact settlement patterns than southern and western districts.

- District areas vary widely, from Hnahthial's 1,100.89 km² to Lunglei's 3,415.74 km², driving low density in larger southern districts like Lunglei and Lawngtlai (34,240 buildings, 13.84 buildings/km²) despite moderate building counts, reflecting dispersed under developed settlement patterns

- The Atkinson index for buildings per capita at ε = 1 is 0.009, with a bootstrap mean of 0.008 and a standard error of 0.003. The 95% confidence interval ranges from 0.003 to 0.014, cementing the existence of spatial inequality in building infrastructure in Mizoram.

- Sensitivity tests across all epsilon values, at the 95% confidence intervals, exclude zero, consistently supporting the existence of spatial inequality. The Atkinson index increases with higher epsilon values, from 0.004 at epsilon = 0.5 to 0.018 at epsilon = 2.0, reflecting greater sensitivity to districts with lower buildings per capita. Although the result of Atkinson index on buildings per capita can be interpreted as low inequality, the data uses buildings footprints which doesn't not consider vertical floor spaces in highly urbanised settlements, in effect they result may understate true extend of inequality.

Findings on Distribution of Roads Infrastructure in Mizoram

- The GIS mapping of Roads is segregated into National Highways (1450.02 km), State Highway (1741.39), Rural Roads (3734.18 km), Agricultural Link Roads (5188.64 km) and Residential roads (2263.15 km), with a total road network of 14377.37 km.

- The Coefficient of Variation (CV) for road density reveals severe inequality, with Residential Roads (80%) and Agricultural Link Roads (57%) showing the highest disparities across Mizoram's 11 districts.

- National Highways (CV: 48%) and Rural Roads (CV: 37%) exhibit substantial variation in density, with a total road density CV of 32% masking significant allocative disparities.

- Central and eastern regions display strengths in total road density, often exceeding 80 km/100 km², driven by dense Agricultural Link Roads (e.g., up to 58.66 km/100 km² in eastern areas) and Rural Roads (e.g., 24–25 km/100 km² in central and eastern zones), supporting robust rural connectivity.

- Southern and western regions show weaknesses in total road density (40–60 km/100 km²), with sparse Residential Roads (4–7 km/100 km²) and Agricultural Link Roads (6–20 km/100 km²), restricting access to infrastructure critical for urban and rural development in these peripheral areas.

- Northern regions exhibit mixed patterns, with strong National Highway density (e.g., 12.21 km/100 km² in some areas) but weaker Residential and Agricultural Link Road density (7–12 km/100 km²), indicating partial connectivity that supports major routes but limits local access.

- Total road length across Mizoram (14,377.37 km) is dominated by Agricultural Link Roads (5,188.64 km) and Rural Roads (3,734.18 km), large southern areas (e.g., over 3,000 km²) dilute over all road density in the state, reflecting dispersed infrastructure patterns that may exacerbate spatial imbalances in peripheral zones.

Finding on Spatial Inequality of Road Infrastructure in Mizoram

- Global Moran's I analysis of road density on 258 grid cells finds significant clustering of all road types at $p \leq 0.001$: National Highways (0.274), State

Highways (0.118), Rural Roads (0.101), Agricultural Link Roads (0.386), Residential Roads (0.141). Agricultural Link Road shows the strongest clustering, concentrated in central, northern, and eastern regions compared to western and southern areas.

- LISA analysis for ALR reveals 28 High-High clusters in central and eastern zones and 21 Low-Low clusters in southern and western regions ($p \leq 0.05$), highlighting uneven connectivity for agricultural areas, which may impede aggregate agriculture output critical for an agrarian economy.
- National Highways show 19 High-High clusters in central-eastern and northern corridors and Low-High cells in southern and western zones ($p \leq 0.05$), indicating sparse major road access in peripheral areas.

- State Highways and Rural Roads have weaker clustering, with 11 and 7 High-High clusters, respectively, in northern and central areas, and 2 Low-Low (SH) and 11 Low-High (RR) cells in southern borders ($p \leq 0.05$), showing limited rural access.

- Residential Roads exhibit 8 High-High clusters in central urban zones and 4 Low-High cells in peripheral northern, southern, and western areas ($p \leq 0.05$), reflecting urban-biased connectivity.

- Central and eastern regions have high total road density (80–108 km/100 km^2), driven by National Highways, Agricultural Link and Rural Roads, while southern and western regions (40–60 km/100 km^2) face sparse infrastructure.

- Total road length (14,377.37 km) is led by Agricultural Link Roads (5,188.64 km) and Rural Roads (3,734.18 km).

Findings on Mizoram Electricity Infrastructure

- Near-complete electrification is achieved, with 98.9% of settlements electrified, suggesting that Mizoram has a spatially equal electrification infrastructure.

- Installed power capacity doubled from 29.35 MW (2016–17) to 62.70 MW (2022–23), driven by hydroelectric (38.35 MW) and solar (23.85 MW) expansion, boosting access across all regions.

- Per capita electricity consumption rose from 322 kWh (2016–17) to 439 kWh (2022–23), with urban central areas leading, though rural northern, southern, and western regions show improved usage.

- Transmission and distribution losses remain high at 24% (2022–23), down from 29% (2020–21), indicating persistent inefficiencies that burden state finances and limit reliable supply.

- Power line infrastructure is dominated by low-capacity 11 kV and LT lines (8,900+ km) over high/medium-voltage lines (2,200 km), indicates high losses and outages.

- Limited substation infrastructure (11 high-voltage, 62 medium-voltage) forces reliance on long, weak lines that potentially exacerbate costs and service disruptions.

Findings on Night Time Light (NTL) Radiance Inequality in India 2023

- The Gini coefficient for NTL Radiance per Area km² in India in 2023 is 0.749 with a bootstrap mean of 0.703, and standard deviation of 0.003, indicating substantial inequality in artificial illumination across India's 36 states and union territories.

- Northern and southern plain regions with large areas (>50,000 km²) show high radiance (8–9 nW/cm²/sr/km²), while central plains (e.g., 4–5 nW/cm²/sr/km²) have lower radiance, highlighting disparities in electrification.

- Smaller union territories (<50,000 km²) in northern and eastern regions exhibit intense radiance (34–150 nW/cm²/sr/km²), driven by urban density, whereas southern smaller states (6–12 nW/cm²/sr/km²) show moderate illumination.

- Northeastern and Himalayan states have varied radiance, with some areas (4–5 nW/cm²/sr/km²) exhibiting moderate illumination despite terrain challenges, while others (0.37–0.38 nW/cm²/sr/km²) such as Mizoram rank the lowest in India, indicating an overall lack of infrastructure and economic activity compared to the rest of India.

- India's total Radiance per Area km² is 6.045 nW/cm²/sr/km², derived from 19,762,916.841 nW/cm²/sr across 3,270,051 km², indicating moderate national illumination, indicative of a developing economy.

Findings on Night Time Light Radiance in Mizoram

- Inter-district Gini coefficient for total radiance is 0.495 (bootstrap mean: 0.457, 95% CI: 0.327–0.575), indicating moderate to high inequality in economic activity as proxied by NTL across Mizoram's 11 districts.

- Intra-district Gini coefficients range from 0.155 (western region) to 0.460 (central region), showing varied spatial concentration of radiance, with the state capital district region having the highest disparity.

- Aizawl leads in radiance per km^2 (1.1420 $nW/cm^2/sr/km^2$) and total radiance (2656.49316 $nW/cm^2/sr$), driven by dense urban illumination.

- Northern and eastern regions show moderate radiance per km^2 (0.43–0.57 $nW/cm^2/sr/km^2$), with substantial total radiance in northern district such as Kolasib (772.674399 $nW/cm^2/sr$).

- Southern and western regions have low radiance per km^2 (0.11–0.26 $nW/cm^2/sr/km^2$), with southern areas showing moderate total radiance (e.g., 1067.34447 $nW/cm^2/sr$) suggesting low economic activity in these regions.

- Mean radiance varies from 0.6824 $nW/cm^2/sr$ (western region) to 1.2965 $nW/cm^2/sr$ (central region), reflecting uneven lighting intensity across districts.

- Quintile analysis ranks Aizawl district the highest (1.14 $nW/cm^2/sr/km^2$), followed by eastern (0.43), central (0.36), southern (0.26), and western (0.22) regions, showing graded illumination disparities.

Findings on Temporal Analysis of Night-time Light in Mizoram (2014–2023)

- The Mann-Kendall test across 237 grid cells reveals significant positive trends in 135 cells (57%, $p < 0.05$), with a mean tau of 0.503. Grid cells in the central and eastern regions of Mizoram exhibit the strongest monotonic increases in radiance.

- District-level Mann-Kendall analysis indicates significant positive trends for 10 of 11 districts ($p < 0.05$, tau: 0.511–0.822). Central, eastern, and western regions show the most pronounced increases. Only Saitual district ($p = 0.0736$, Tau: 0.4667) registered non significance at 95% confidence level.

- Total radiance per grid cell rises from 11.59 nW/cm²/sr in 2014 to 32.56 nW/cm²/sr in 2023. Maximum radiance increases from 682.33 to 1031.86 nW/cm²/sr, indicating a moderate and positive increase in economic activity in Mizoram.

- The mean total radiance grows from 279.72 nW/cm²/sr in 2014 to 740.28 nW/cm²/sr in 2023, implying that most district see a positive increase in economic activity.

- The absolute radiance gained by each district indicates that growth is uneven as the largest absolute gain is found in Aizawl district (1337.85 nW/cm²/sr), followed by Lawngtlai district (684.5745 nW/cm²/sr). On the other hand, Hnahthial district (103.1238 nW/cm²/sr) registered the lowest absolute radiance gained, followed by Khawzawl district (215.1959 nW/cm²/sr).

- In terms of radiance growth percentage, Khawzawl district sees the highest gain (+533.59%) in radiance, followed by Hnahthial district (+443.73 %). These districts had a relatively low radiance (40.33 and 23.24 nW/cm²/sr) level in 2014, indicating accelerated illumination during the study period.

- In contrast Kolasib district (+99 %) sees the lowest radiance gain, followed by Aizawl (+101.46%), indicating that radiance growth has plateaued in these districts. The data also suggests, particularly in the case of Aizawl, that vertical expansion rather than horizontal expansion took place in the urban core.

- Increase in Spatial heterogeneity in radiance is observed, with grid-level standard deviation rising from 50.49 in 2014 to 83.78 in 2023, divergent growth trends across regions.

Findings on Linear Trend and Spatial Clustering Analysis of NTL Radiance in Mizoram (2014-2023)

- For 128 of 237 grid cells or 54.0% of the total, OLS regression shows significant radiance trends ($p < 0.05$), with a mean NTL slope of 2.0255 nW/cm²/sr/year and median of 0.7489 nW/cm²/sr/year, indicating considerable growth in economic activity across Mizoram.

- 20 significant hot spots ($p < 0.05$) cluster in Aizawl, with high Gi* value (7.671 for cell 246), reflects concentrated economic growth driven by urbanisation and investment.

- 4 significant cold spots ($p < 0.05$) in northern Aizawl (cell 332, Gi*: -2.507) highlight minimal or negative radiance change, suggesting that economic activity as proxied by NTL is not evenly distributed.

- Top cells show extreme radiance changes, with cell 234 (slope: 23.8582, R^2: 0.88) and cell 80 (slope: 11.7883, R^2: 0.87) indicating these areas experienced rapid development, while cell 319 (slope -13.4458, R^2 0.87) reflects rare economic decline.

- Mean R^2 of 0.43, with high values in key cells (0.97 for cell 155), confirms reliable linear trend detection, validated by sensitivity analysis across 5×5 km and 20×20 km grids, ensuring robustness of the 10×10 km grid spatial model.

- 20 hot spots and 4 cold spots confirm the alternative hypothesis (H1) of spatially clustered radiance growth, rejecting the null hypothesis (H0) of random spatial distribution.

Findings on Spatial Modelling of NTL with Infrastructure in Mizoram

- Population density (coefficient 0.6239, $p < 0.001$ in SLM) is strongly associated with NTL radiance density (0.6239 SD increase per SD), reflecting higher economic activity in densely populated districts.

- National highway density (coefficient 0.2868, $p < 0.001$ in SLM) is positively associated with NTL density (0.2868 SD per SD), which suggest that regions well connected with good quality roads see higher economic activity.
- Primary health centre count (coefficient 0.0884, $p = 0.012$ in SLM) is positively associated with NTL density (0.0884 SD per SD), indicating that spatial spread of health infrastructure plays a vital role in economic vitality, particularly for peripheral regions.

- Rural road density (coefficient 0.0515, $p = 0.091$ in SLM) shows a marginal positive association with NTL density, suggesting connectivity benefits rural area in economic activity via access to markets.

- BPL percentage (coefficient -0.0567, $p = 0.091$ in SLM) is marginally negatively associated with NTL density, pointing to poverty's role in constraining economic activity across districts. The absence of grid level poverty may have reduced the significance level at 95% CI, nonetheless, the result suggests poverty is associated with lack of infrastructure.

- State highways ($p = 0.163$), agricultural link roads ($p = 0.377$), sub-district hospitals ($p = 0.496$) and Community Health Centres ($p = 0.171$) show no significant association with NTL density, indicating limited direct links to economic disparities.

- Distance to district headquarters ($p = 0.620$ in SLM) lacks significance, indicating intra-district disparities where proximity to capitals does not ensure increase in economic activity.

- Elevation's negative association in OLS (coefficient -0.0784, $p = 0.041$) suggests lower economic activity in high-altitude areas, but its non-significance in SLM ($p = 0.243$) reflects spatial dependencies.

- The Breusch-Pagan test (statistic = 54.02, df = 11, $p < 0.001$) indicates significant heteroscedasticity in OLS residuals, while Moran's I (statistic = 3.2644, $p = 0.0011$) confirms significant spatial autocorrelation.

- Lagrange Multiplier tests show strong spatial lag dependence (LMlag = 32.5897, $p < 0.001$; robust RLMlag = 25.0720, $p < 0.001$) compared to weaker spatial error dependence (LMerr = 8.8212, $p = 0.003$; robust RLMerr = 1.3036, $p = 0.254$), supporting the use of SLM over SEM to address spatial patterns.

- SLM (Nagelkerke pseudo-$R^2 = 0.7601$, AIC = 365.85) outperforms OLS ($R^2 = 0.7276$, AIC = 396.55), capturing spatial dependencies in infrastructure-driven economic disparities.

- SLM and SEM ($R^2 = 0.7387$, AIC = 387.79) confirm consistent predictors (population, National Highways, Primary Health Centres), with SEM strengthening PHC's association ($p = 0.004$).

- The consistent significance of certain infrastructure such as National Highway and Primary Heath Care, and the near significance of other infrastructure such as State Highway, Rural Roads and CHCs, in the model supports rejection of the null hypothesis (H_0) of random spatial distribution and favours the alternative hypothesis (H_1) that disparity in infrastructure is associated with inequality in economic activity.

6.2 EMPERICAL BASED RECOMMENDATIONS

Recommendation to reduce Health Infrastructure inequality in Mizoram

- To improve overall health outcome of the state in the short run, public investment much first prioritise investment towards districts with low health infrastructure presence, such as Mamit, Saitual, Lawngtlai, Kolasib, Khawzawl, Hnahthial and Lunglei. In the long run the state must consider de-centralising tertiary care from Aizawl, establishing regional centres in the east, west and southern part of the state emphasizing spatial coverage so that everyone can benefit equitably.

- Reduce health care deprivation pockets by allocating spatially optimal rural PHCs. Facility allocation should be based on geographic coverage, not just host village population, to reflect Mizoram's heterogeneous terrain. Policy must ensure that every legally recognised, permanently inhabited settlement has access to a qualified medical officer within one hour's motorable distance, except in cases of extreme remoteness. This can be achieved through public–private and community partnerships.

- Increase bed capacity in regions where high patient migration takes place such as Khawzawl, Mamit, Lawngtlai, Saitual, and Hnahthial districts. It must be noted though that increasing bed capacity alone is not enough, as investment in bed should also be accompanied by investment to improve the overall quality of care.

- Close the technological gap between rural and urban health facilities by ensuring not just equipment supply but functional capacity, trained technicians, maintenance, and integration into service delivery. Public investment should prioritise this sector, in line with IPHC 2020 recommendations, to guarantee broad coverage of endemic and common conditions.

- Address manpower shortages in PHCs by enforcing minimum staffing standards. Health personnel must be made available to ensure uniform service availability across all facilities, fulfilling the last-mile delivery goal of the National Rural Health Mission.

- Mizoram lacks a functional hierarchical healthcare network due to the poor spatial distribution of Community Health Centres (CHCs). Policy must ensure that CHCs complement existing PHCs by serving as effective referral hubs and bridges to tertiary care. Their allocation should follow road networks and traffic flow to district capitals, recognising that CHCs are not just supervisorial units but a vital link in the health system network of the state.

- The service capacity of CHCs requires urgent policy review. Many function no differently from PHCs in terms of technology and specialist manpower. Existing CHCs should be evaluated against IPHC (2020) benchmarks for clinical relevance, technological adequacy, and spatial appropriateness. Administrative convenience must not override the need to strengthen the state's referral network.

- To reduce rural healthcare avoidance and unnecessary patient migration to urban centres, public trust in primary and secondary care must be restored. This requires both awareness campaigns clarifying the service deliverables of each tier and a publicly accessible real-time health portal displaying facility capacity, staff availability, wait times, and specialist schedules. Together, these measures will give citizens certainty in care and help rationalise patient flows across the health system.

- Strengthening rural healthcare is not only about serving rural populations; it has a multiplier effect. A revitalised rural system reduces patient migration, thereby easing pressure on overburdened urban facilities. This indirectly benefits urban dwellers, many of whom are poor and reliant on public services. Aligning rural investments with IPHS (2020) guidelines offers a policy pathway that maximises welfare and minimises economic externalities across both rural and urban populations.

- The two existing Sub-District Hospitals at Kulikawn and Tlabung serve important functions, but their current designation risks being perceived as inequity and may encourage unsustainable demands for upgradation of CHCs to SDH in notified towns. A more viable policy is to reclassify them as Urban Community Hospitals (UCHs), functionally equivalent to CHCs, while retaining their existing clinical and technological capacity. This redefinition positions them clearly as primary and secondary-level urban facilities rather than as intermediate "sub-district" institutions.

- Urban Primary Health Centres (U-PHCs) are underutilised, as they do not address a distinct service gap between Health Sub-Centres and District Hospitals. Their proliferation has been shaped more by funding streams under the National Urban Health Mission (NUHM) than by functional suitability. At the same time, they divert manpower and resources into facilities that remain technologically limited and clinically underused. A practical solution is to integrate U-PHCs into the proposed UCH system, preserving funding flows while aligning service delivery with actual urban health needs. This integration would eliminate duplication among U-PHCs, SDHs, and District Hospitals, producing a more coherent and efficient urban health structure.

- In Aizawl, with over 400,000 (2025 estimates) urban residence, the District Hospital currently provides primary, secondary, and tertiary care, an unsustainable arrangement that leaves many surgical patients unadmitted. To relieve this burden, the state should establish a network of Urban Community Hospitals (UCHs) at strategic locations across the city. UCHs would consolidate services now scattered across underutilised Urban Primary Health Centres, offering comprehensive outpatient care, 24/7 emergency and trauma stabilisation, essential surgeries, maternal and child health, diagnostics, and short-stay inpatient care. This two-tier urban system would decongest the District Hospital, enable it to focus on advanced tertiary care, and ensure equitable, clinically appropriate access to urban dwellers. The model can later be adapted to other districts as their populations grow.

- Referral Hospitals and specialised institutes must be reserved exclusively for advanced and super-specialist care. A stricter referral protocol is needed to prevent overload from cases manageable at the lower tier of the state’s health system. This would preserve specialist capacity, improve system efficiency, and build public confidence in lower tiers.

- To address regional disparities, a dedicated Regional Institute for Southern Mizoram should be established. This centre would serve southern Mizoram with a strong focus on non-communicable diseases such as cancer, diabetes, hypertension, and liver disease, which are highly prevalent in Mizoram. By situating advanced diagnostic and treatment facilities closer to these populations, the burden of long-distance travel to Aizawl from southern Mizoram would be reduced, while simultaneously strengthening public trust in regional institutions.

- Upgrading Khawzawl District Hospital into a Regional Referral Centre should be a medium-term priority. Equipped for non-communicable diseases, obstetric emergencies, and specialised surgeries, it would further reduce dependence on Aizawl.

- With Mizoram's extensive mobile coverage, telemedicine can strengthen early screening, triaging, and follow-up care, while directing patients to an appropriate health facility to reduce overcrowding. Graduates from nursing and paramedical institutions under medical supervision, can provide counselling, medication advice, and referral guidance. This would extend continuity of care to remote and peri-urban areas within an efficient referral chain.

- Policy should address the dual challenge of uneven distribution and overall technological backwardness in Mizoram's health system. Basic diagnostics and treatment equipment should be available at all district facilities, while advanced technologies must be developed in regional hubs with proper infrastructure. This targeted investment strategy will reduce intra-state disparities and bring Mizoram closer to national standards.

Recommendation to reduce overall Infrastructure inequality in the state

- Road connectivity should not be pursued for its own sake but should be linked with economic activity. New road project should be accompanied by supporting infrastructure such as agricultural storage facilities, wholesale markets, and small-scale enterprises, so that connectivity directly translates into jobs and income.

- Current roads in Mizoram mostly follow mountain ridges (north–south direction) due to lower construction costs. While cost-effective, this limits economic activity, since farmland and river valleys where most productive economic potential lies remain disconnected. In the long term, Mizoram should adopt a valley road corridor policy, under which key roads will be developed along low-lying riverine valleys. Although more expensive (due to bridges and tunnels), this approach will unlock large-scale agricultural and trade opportunities. Successive governments can progressively implement sections of these corridors so that the system is built over time without overburdening budgets.

- National Highways form the backbone of Mizoram's transport system, and their routine maintenance must be treated as a top policy priority. Poorly maintained stretches directly undermine economic activity, increase transport costs, and weaken the state's trade competitiveness. A dedicated, ring-fenced budget for highway upkeep, with strict monitoring mechanisms, is essential.

- The current National Highway alignment bypasses large parts of western and southern Mizoram, leaving them reliant on weaker state and rural roads. Expansion of the network into these underserved regions is necessary, with new alignments designed to maximise trade flows. Strategic priority should be given to routes that connect eastern and western Mizoram to the Kaladan Multi-Modal Transit Transport Project (KMMTTP), thereby strengthening domestic integration and international market access.

- State Highways require a comprehensive policy review to ensure uniform service quality across their entire length. Currently, officially designated continuous roads, such as the World Bank Road, show stark variation in width from satellite imagery. This inconsistency undermines reliability and increases costs. A unified management and quality-control framework is needed so that all segments of a roads meet the same service standards.

- Rural road construction in Mizoram leads to unnecessarily winding alignments where bridges and culverts are avoided. This increases travel time, maintenance costs, and road safety risks, creating an inefficient and unsustainable rural network. Policy must prioritise engineering designs that minimise distance and enhance safety through adequate investment in bridges, culverts, and slope protection. In the long run, such investments reduce costs while delivering a more reliable and efficient rural transport system.

- Residential roads are among the most unevenly distributed in the state, creating the potential to restrict housing supply and inflate land and rental costs. In several towns, the absence of adequate residential roads has already slowed horizontal growth, as evidenced by stagnation in night-time light radiance over the past decade. Policy must therefore prioritise the systematic expansion of residential (town) roads in urban centres across the state to enable balanced regional growth. New residential roads should be planned with future upgrades in mind, including provisions for drainage, underground utilities, and long-term expansion.

- Agricultural link roads are highly uneven in their distribution, concentrated in the northern and eastern highlands while the more arable southern and western lowlands remain under developed. This imbalance undermines productivity in an agrarian economy and skews regional growth. Policy must prioritise equitable agricultural connectivity, with a particular focus on unlocking the potential of the south and western lowlands, ensuring that infrastructure development aligns with arable land distribution and supports balanced state-wide growth.

- Lunglei, Hnahthial, and Mamit exhibit substantially lower total road densities (42.42 – 54.5 km/100 km^2) than the state average (68.14 km/100 km^2). Infrastructure investment on roads should prioritise these districts for a balanced regional growth.

- Analysis shows clustering and duplication of roads, with parallel alignments often serving the same destinations. A comprehensive review is needed to rationalise which roads qualify for state maintenance. All road construction, whether surfaced, unsurfaced, gravel, or dirt, should fall under the purview of the Public Works Department (PWD). This would ensure that engineering standards are followed for safety, future upgrades, and ecological sustainability. To achieve uniform standards and prevent duplication across schemes, every state or central programme involving road creation or maintenance should be implemented through the PWD, supported by a stronger horizontal reach of the department.

- The electricity grid in Mizoram needs a considerable amount of investment. The state needs to expand its 132 kV, 66 kV, and 33 kV lines and adding more medium-sized substations, while simultaneously upgrading older 11 kV and low-tension lines in rural areas and reconfiguring feeder networks to shorten transmission distances and reduce technical losses.

- Mizoram's extremely low night-time light radiance (0.38 $nW/cm^2/sr/km^2$), the lowest in India, reflects the state's infrastructural and economic underdevelopment. By strategically strengthening core networks improving connectivity between settlements, upgrading transport and electricity infrastructure, and enhancing the efficiency and resilience of these systems, the state can create the conditions necessary to stimulate economic activity, reduce spatial disparities, and gradually close the infrastructural gap with the rest of India.

- The analysis of intra-district Night Time Light indicates that districts such as Hnahthial and Mamit, suffer from a uniformly low infrastructural development. At the same time Aizawl district's rural area, especially it's far northern regions, witnessed with low economic activity. A targeted multi-prong economic intervention is needed in these regions.

- Mizoram's infrastructure and economic activity remain heavily concentrated in urban Aizawl, reflecting a structural monocentric pattern rather than balanced development. Strengthening other regions in the South, Western, and Northern region through targeted investments in transport, industry, health and human resource development can help redistribute activity and reduce spatial inequality.

- The 10 year Night Time Light radiance analyses reveal that while urban centres such as Aizawl and its peri-urban fringes exhibit robust recovery growth after the Covid pandemic, many rural and remote districts experience slow recovery, with some areas even showing declines. These patterns reflect how spatial disparities can exacerbate inequality if left unaddressed. Policy should therefore prioritise ensuring that all districts, receive comparable investments in core infrastructure, enabling equitable growth, reducing regional imbalances, and most importantly enhance resilience against economic shocks.

6.3 OTHER RECOMMENDATIONS

- Private hospitals must be regulated to prevent exploitative pricing practices, particularly when clinical outcomes remain below public sector standards. Pricing should be linked to transparent clinical quality indicators, aligning private incentives with patient welfare.

- Redistribute health personnel to correct the clustering pattern in the state and ensure vacancies are systematically filled through internship incentives eventually leading to permanent employment status. Increase domicile availability of doctors by upgrading one of the existing nursing institutes or District Hospital into a full fledge medical college, reducing capital costs. Link postgraduate opportunities to prior government services, at least to a minimum of 5 years' service, to strengthen retention and continuity of care.

- International best practices can be adapted to Mizoram's context. While IPHS (2020) offers a baseline, models such as Sweden's integrated system, where specialists rotate between secondary and tertiary facilities, could be incorporated into a two-tier UCH–District Hospital framework. This would optimise scarce human resources and ensure continuity of care.

- The state should discontinue its health insurance scheme, as they appear to be a liability than a public good in Mizoram. With the most advanced care infrastructures already under public control, subsidising private and out-of-state care through insurance is fiscally regressive and administratively redundant. In other words, the state government is currently creating incentives to avoid its own public health provisions and acts as a healthcare provider and insurer at the same time, which is unsustainable and risk intergenerational burden. Instead, redirecting funds into government facilities will expand capacity, reduce inequity, and ensure that resources strengthen Mizoram's own health system. This will also check demand side and supply side moral hazard in healthcare ecosystem.

- A "Mizoram Health Standard" should be codified to guarantee minimum levels of service delivery that are fiscally feasible and insulated from political cycles. This would provide citizens certainty in healthcare access regardless of politics or electoral cycles.

- Health planning must account for Mizoram's unique geography and demography. National programmes often reflect majority contexts that do not always align with the state's interest, as in the case of U-PHCs and surveillance systems such as Ayushman Bharat Digital Mission (ABDM). The state should retain the flexibility to adapt or even reject central schemes where they contradict local context and cultural values.

- Mizoram should establish a permanent Health Systems Research and Policy Unit within the Health Department, tasked with continuous monitoring, evaluation, and generation of state-specific evidence. Beyond health service delivery, the unit must actively support epidemic and pandemic preparedness by integrating expertise in epidemiology, virology, and disease surveillance. Such a unit would not only strengthen locally grounded policymaking but also ensure that recurring challenges such as scrub typhus, dengue, and other emerging infections are systematically addressed rather than reactively managed.

- Community participation mechanisms, including Village Health Committees and urban health boards, must be strengthened to improve accountability and ensure service delivery reflect local needs.

- Develop a public digital platform that displays real-time staff strength, facility capacity, waiting times, and specialist availability. Such transparency will reduce patient migration and bypassing of local facilities, strengthen referral discipline, and improve patient confidence in the local facilities.

- Building density analysis shows that urban Aizawl has expanded beyond sustainable limits. Government needs a long-term goal to de-congest and improve liveability. In this regard, government establishments can be moved out of the city in a phase manner, while digital communication and e-governance systems can ensure their functions continue effectively without being concentrated in the city centre, while also stimulating development in other regions.

- Introduce a building distance policy that clearly specifies how far new buildings must be constructed from the edge of public roads. This will ensure that space is available for future road expansion, pedestrian movement, and safe traffic flow. The rule should be applied uniformly across all new constructions.

- For existing buildings in congested urban centres, introduce zoning restrictions that clearly define what types of activities (commercial, residential, religious, institutional) can operate in them. This will prevent high-traffic activities (such as schools, shops, or religious gatherings) from being concentrated in buildings that directly obstruct traffic flow or road safety.

- Enforce strict protection of public roads from encroachment by private property, community groups, or religious institutions. Any encroachment should be removed through law, with relevant authorities given both the mandate and accountability to prevent re-encroachment.

- Existing ridge-based roads should be linked at regular intervals with valleys, so that agricultural products can reach markets faster and cheaper. This will also support river-basin economies such as fisheries, irrigation farming, and horticulture.

- The current health data capturing mechanism of the state needs a small, but important, refinement. A "city/town/village/locality of origin" field in the patient admission registers at all health facilities is needed and included in data reporting. Complementary to this, the Economics and Statistics Department should include a "district of origin" in the Death Certificate data. This inclusion will enable accurate disease mapping, reveal true intra and inter district mortality rates, and guide targeted interventions where they are most needed.

- During the GIS mapping, several misallocations of infrastructure was witnessed, particularly common was installation of sports infrastructure such as artificial turfs which doesn't seem to align with the settlement's sizes. The golf course in Thenzawl stands out as an unjustifiable allocation, lacking economic foresight in demand nor revenue. Given Mizoram's deficiency in basic infrastructure and high disease burden, such missteps in priority and allocation is costly and consequential. Future governments must prioritise essential infrastructure, transport, power, industry, and health. These are non-negotiables to drive economic growth and align Mizoram with India's development trajectory.

- Geographic Information Systems (GIS) is increasingly relevant in modern governance and policy planning. While geographers incorporate GIS technology to map economic phenomena, they often lack the theoretical grounding in market dynamics, incentives, public finance required for robust policy formulation. Integrating GIS into undergraduate and post-graduate economic programmes will equip economists to address modern economics challenges with analytical rigour, ensuring evidence-based policies that effectively tackle issues like regional inequality and resource allocation. This reform is essential to enhance the discipline's relevance and impact on policy-making in India.

6.4 CONCLUSION

This study shows that spatial inequality in infrastructure is a concerning dimension of economic development faced by hilly regions like Mizoram, where geography presents an extra barrier to economic progress. The evidence suggests that imbalances in infrastructure allocation, such as roads, buildings and health care systems, carry divergent economic outcomes among the central and peripheral regions, which may further reinforce regional disparities and perpetuate systemic marginalisation. The evidence also suggests that infrastructure allocation in the state rarely follow a systematic framework with no clear economic goals, resulting in the misallocation of scare resources. Addressing these spatial realities requires more than acknowledgement, it demands a policy review and an open dialogue among scholars, policymakers, community leaders, and the public. Correcting spatial inequality is not just a matter of balancing regional economic outcome but a vital public policy choice that can unleash the true economic potential of the state. By ensuring a more balanced distribution of infrastructure, Mizoram can lay the foundation for fast paced economic growth that converges with the wider economic progress of the nation.

APPENDICES

Appendix I

Distribution of Rural and Urban Beds in Mizoram 2021

	Districts	Population	Rural	Urban	Rural beds	Urban beds
1	Aizawl	450444	83889	347963	188	1891
2	Champhai	87929	87174	23728	80	142
3	Hnahthial	35152	26278	8874	40	30
4	Khawzawl	44368	27675	16692	70	21
5	Kolasib	103668	45783	57885	80	80
6	Lawngtlai	145575	119855	25721	90	105
7	Lunglei	164179	102656	61523	90	250
8	Mamit	106642	88245	18397	110	30
9	Saiha	69858	38852	31006	40	160
10	Saitual	66831	48103	14347	50	30
11	Serchhip	80184	40647	39537	80	87
*	Mizoram	1354830	709157	645673	918	2826

Note: Own calculation based on Population Projection (2021) & Mizoram Statistical Abstract (2021)

Appendix II

Thiel-T Subgroup Metric

Subgroup	Pop_Share	Beds per Capita	X/μ	$\ln(X/\mu)$	Theil Contribution
Aizawl_Rural	0.0619	0.002241	0.811	-0.209	-0.0105
Aizawl_Urban	0.2568	0.005434	1.9665	0.6761	0.3414
Champhai_Rural	0.0643	0.000918	0.3322	-1.1023	-0.0236
Champhai_Urban	0.0175	0.005985	2.1659	0.7726	0.0293
Hnahthial_Rural	0.0194	0.001522	0.5509	-0.5965	-0.0064
Hnahthial_Urban	0.0065	0.003379	1.1228	0.2013	0.0016
Khawzawl_Rural	0.0204	0.002529	0.9152	-0.0886	-0.0017
Khawzawl_Urban	0.0123	0.001258	0.4554	-0.7868	-0.0044
Kolasib_Rural	0.0338	0.001747	0.6323	-0.4584	-0.0098
Kolasib_Urban	0.0427	0.001382	0.5001	-0.693	-0.0148
Lawngtlai_Rural	0.0885	0.000751	0.2718	-1.303	-0.0313
Lawngtlai_Urban	0.019	0.004082	1.4773	0.3899	0.0109
Lunglei_Rural	0.0758	0.000877	0.3174	-1.148	-0.0276
Lunglei_Urban	0.0454	0.004064	1.4706	0.3854	0.0257
Mamit_Rural	0.0651	0.001247	0.4511	-0.7962	-0.0234
Mamit_Urban	0.0136	0.00163	0.59	-0.5276	-0.0042
Saiha_Rural	0.0287	0.001029	0.3725	-0.9878	-0.0106
Saiha_Urban	0.0229	0.005161	1.8678	0.6246	0.0267
Saitual_Rural	0.0355	0.001039	0.3761	-0.9779	-0.0131
Saitual_Urban	0.0106	0.002091	0.7567	-0.2787	-0.0022
Serchhip_Rural	0.03	0.001968	0.7122	-0.3394	-0.0073
Serchhip_Urban	0.0292	0.002201	0.7965	-0.2276	-0.0053

Note: Own calculation

Appendix III

RSBY and MSHSC Data

Year	Scheme	Enrolled	Claims	Paid
2011-12	RSBY	11951	1253	784
2012-13	RSBY	46789	9477	7444
2013-14	RSBY	103545	24012	21503
2014-15	RSBY	152983	29039	22016
2015-16	RSBY	152903	22624	17462
2016-17	RSBY	194886	21235	20251
2017-18	RSBY	194886	19013	18282
2018-19	RSBY	157414	14707	12759
2019-20	RSBY	267607	22229	22229
2020-21	RSBY	119872	16919	16504
2011-12	MSHCS	40185	8125	6276
2012-13	MSHCS	51344	4219	3853
2013-14	MSHCS	109100	5811	5596
2014-15	MSHCS	122913	8209	7843
2015-16	MSHCS	116322	5784	5258
2016-17	MSHCS	115221	7029	6603
2017-18	MSHCS	125459	5915	5685
2018-19	MSHCS	112732	4612	4257
2019-20	MSHCS	22229	14912	14713
2020-21	MSHCS	113720	28405	8398

Source: mizoramdata.mizoram.gov.in

Appendix IV

Capacity of Power Installed (MW)					
Year	**Diesel**	**Hydro**	**Thermal**	**Solar**	**Total**
2016 - 17	0	29.35	0	0	29.35
2017 - 18	0	29.35	0	0	29.35
2018 - 19	0	29.35	0	0.3	29.7
2019 - 20	0	29.35	0	0.35	29.7
2020 - 21	0.5	29.35	0	1.04	53.81
2021 - 22	0.5	29.35	0	2.35	32.2
2022 - 23	0.5	38.35	0	23.85	62.7

Source: Statistical Handbook of Mizoram 2023

Appendix V

Net Generation of Electricity with Imports (MU)						
Year	**Diesel**	**Hydro**	**Thermal**	**Solar**	**Import**	**Total**
2017 - 18	0	57.11	0	0	611.29	668.4
2018 - 19	0	40.09	0	0.17	623.24	663.6
2019 - 20	0	50.68	0	0.35	430.76	481.44
2020 - 21	0.01	29.57	0	1.77	413.57	444.92
2021 - 22	0	25.89	0	2.32	647.61	675.82
2022 - 23	0.01	29.38	0	0.03	29.833	59.253

Source: Statistical Handbook of Mizoram 2023

Appendix VI

Consumption of Electricity by Users (MU)

Year	KJP	Domestic	Commercial	Public Lighting	Public Water Works	Agri
2016 - 17	4.41	233.9	33.87	4.89	49.95	0.27
2017 - 18	3.56	235.14	47.34	2.24	41.59	0.14
2018 - 19	3.41	225.7	59.22	13.32	57.85	0.27
2019 - 20	5.6	208.96	36.4	0.43	50.6	0.11
2020 - 21	7.19	276.24	44.26	2.11	82.45	0.16
2021 - 22	5.63	280.24	47.89	2.35	80.55	0.14
2022 - 23	4.2	284.69	50.25	2.43	94.62	1.06

Year	Industrial	Bulk Supply	Others (Misc)	Total	Per Capita (kWh)
2016 - 17	10.47	15.28	0.5	353.54	322.22
2017 - 18	13.37	49.82	0.31	395.78	360.72
2018 - 19	14.38	13.37	0.24	387.76	353.41
2019 - 20	10.21	51.69	0.1	371.62	354.26
2020 - 21	9.6	13.92	8.99	444.92	407
2021 - 22	9.58	15.97	0.4	464.27	342.68
2022 - 23	13.18	12.98	16	479.42	439.42

Source: Statistical Handbook of Mizoram 2023

Appendix VII

Significant Gi* Clusters of NTL Trends (2014–2023)

Cell_id	gi*	gi_pvalue	Neighbors	Cluster type	District
246	7.671287	1.703E-14	8	Hot Spot	Aizawl
234	7.3234199	2.417E-13	8	Hot Spot	Aizawl
233	7.1747792	7.242E-13	8	Hot Spot	Aizawl
245	7.0312384	2.047E-12	8	Hot Spot	Aizawl
232	6.1723872	6.727E-10	8	Hot Spot	Mamit
222	5.6671389	1.452E-08	8	Hot Spot	Aizawl
244	5.643127	1.67E-08	8	Hot Spot	Mamit
221	4.5252533	6.032E-06	8	Hot Spot	Aizawl
257	3.1971864	0.0013878	8	Hot Spot	Aizawl
220	3.0419565	0.0023505	8	Hot Spot	Mamit
256	2.938726	0.0032956	8	Hot Spot	Mamit
247	2.712273	0.0066824	8	Hot Spot	Saitual
216	2.6787848	0.007389	5	Hot Spot	Champhai
258	2.6324598	0.0084769	8	Hot Spot	Aizawl
332	-2.5074123	0.0121619	3	Cold Spot	Aizawl
204	2.4801627	0.0131322	5	Hot Spot	Champhai
67	2.4513069	0.0142339	8	Hot Spot	Lawngtlai
308	-2.2926479	0.0218683	5	Cold Spot	Aizawl
320	-2.2809088	0.0225538	5	Cold Spot	Aizawl
203	2.2689933	0.0232687	8	Hot Spot	Champhai
68	2.243964	0.0248347	8	Hot Spot	Saiha
235	2.232197	0.0256019	8	Hot Spot	Saitual
307	-2.2275333	0.0259117	8	Cold Spot	Aizawl
223	2.0459075	0.0407655	8	Hot Spot	Saitual

Source: Own Calculation

Appendix VIII

OLS with HC1 ROBUST Standard Errors

Predictors	Estimate	Std. Error	t value	Pr(>|t|)
(Intercept)	0.4419	0.0318	13.9025	0
POP_2023_std	0.6468	0.0488	13.2645	0
BPL_prc_std	-0.0567	0.0365	-1.5549	0.1213
NH_dnst_std	0.3155	0.0727	4.3425	0
SH_dnst_std	0.0506	0.0296	1.7115	0.0883
RR_dnst_std	0.0657	0.0364	1.807	0.072
ALR_dns_std	0.0517	0.0275	1.8772	0.0617
elev_mn_std	-0.0783	0.0378	-2.0695	0.0395
cnt_SDH_std	-0.0324	0.0127	-2.5574	0.0111
cnt_CHC_std	0.0394	0.0687	0.574	0.5665
cnt_PHC_std	0.0957	0.1058	0.9042	0.3668
rd_dst_std	-0.0413	0.0431	-0.9575	0.3393

Source: Own Calculation

Appendix IX

OLS with Clustered Standard Errors by District

Predictors	**Estimate**	**Std. Error**	**t value**	**Pr(>|t|)**
(Intercept)	0.4419	0.0442	10.008	0
POP_2023_std	0.6468	0.0467	13.8439	0
BPL_prc_std	-0.0567	0.0351	-1.6174	0.1071
NH_dnst_std	0.3155	0.0864	3.6527	0.0003
SH_dnst_std	0.0506	0.0253	1.9987	0.0467
RR_dnst_std	0.0657	0.0579	1.1358	0.2572
ALR_dns_std	0.0517	0.0303	1.7083	0.0889
elev_mn_std	-0.0783	0.0459	-1.7064	0.0892
cnt_SDH_std	-0.0324	0.0164	-1.9783	0.049
cnt_CHC_std	0.0394	0.0765	0.5156	0.6066
cnt_PHC_std	0.0957	0.099	0.9667	0.3347
rd_dst_std	-0.0413	0.0675	-0.611	0.5418

Source: Own Calculation

BIBLIOGRAPHY

Abdi, H., & Williams, L. J. (2010). Principal component analysis. *Wiley Interdisciplinary Reviews: Computational Statistics, 2*(4), 433–459.

Abul Naga, R. H., & Yalcin, T. (2008). Inequality measurement for ordered response health data. *Journal of Health Economics, 27*(6), 1614–1625.

Ahluwalia, M. S. (2011). *Prospects and policy challenges in the Twelfth Plan. Economic and Political Weekly, 46*(21), 88–105.

Alonso, W. (1964). *Location and land use: Toward a general theory of land rent*. Harvard University Press.

Alqutaibi, A. Y., Borham, M., Alwadei, S., Alfotawi, R., Alshawkani, H. A., & Al-Jamaei, A. A. (2020). Socioeconomic status influences on awareness of oral cancer: WHO Eastern Mediterranean Region. *Asian Pacific Journal of Cancer Prevention, 21*(5), 1457–1462.

Amin, R., Khashan, A. S., & Rahman, M. (2020). Spatial clustering of childhood underweight in India: Evidence from the National Family Health Survey (NFHS-4). Spatial and Spatio-temporal Epidemiology, 35, Article 100374

Anand, S., & Bärnighausen, T. (2004). Human resources and health outcomes: Cross-country econometric study. *The Lancet, 364*(9445), 1603–1609.

Anh, T. T., & Sakai, H. (2022). Infrastructure, spatial inequality, and rural transformation: Evidence from Vietnam. *Asian Development Review, 39*(2), 85–113.

Anselin, L. (1988). *Spatial econometrics: Methods and models*. Kluwer Academic Publishers.

Anselin, L. (1995). Local indicators of spatial association—LISA. *Geographical Analysis, 27*(2), 93–115.

Anselin, L. (2003). Spatial externalities, spatial multipliers, and spatial econometrics. *International Regional Science Review, 26*(2), 153–166.

Anselin, L., & Le Gallo, J. (2006). Interpolation of air quality measures in hedonic house price models: Spatial aspects. In *Spatial Economic Analysis* (Vol. 1, pp. 31–52). Routledge.

Apparicio, P., Abdelmajid, M., Riva, M., & Shearmur, R. (2008). Comparing alternative approaches to measuring the geographical accessibility of urban health services: Distance types and aggregation-error issues. *International Journal of Health Geographics, 7*(1), Article 7.

Arbia, G. (2014). *A primer for spatial econometrics: With applications in R*. Palgrave Macmillan.

Arbués, P., Baños, J. F., & Mayor, M. (2015). *The spatial productivity of transportation infrastructure. Transportation Research Part A: Policy and Practice, 75*, 166–177.

Arrow, K. J. (1963). Uncertainty and the welfare economics of medical care. American Economic Review, 53(5), 941–973.

Aschauer, D. A. (1989). Is public expenditure productive? Journal of Monetary Economics, 23(2), 177–200.

Atkinson, A. B. (1970). On the measurement of inequality. *Journal of Economic Theory, 2*(3), 244–263.

Auchincloss, A. H., Gebreab, S. Y., Mair, C., & Diez Roux, A. V. (2012). A review of spatial methods in epidemiology, 2000–2010. *Annual Review of Public Health, 33*, 107–122.

Ayele, D. G., Zewotir, T., & Mwambi, H. (2021). Residential inequality and spatial patterns of infant mortality in Ethiopia: Evidence from Ethiopian Demographic and Health Surveys. *Tropical Medicine and Health, 49*(1), Article 15.

Bajar, S., & Rajeev, M. (2015). *The impact of infrastructure provisioning on inequality: Evidence from India* (Working Paper No. 349). Institute for Social and Economic Change.

Balarajan, Y., Selvaraj, S., & Subramanian, S. V. (2011). Health care and equity in India. *The Lancet, 377*(9764), 505–515.

Banerjee, A., & Iyer, L. (2005). History, institutions, and economic performance: The legacy of colonial land tenure systems in India. *American Economic Review, 95*(4), 1190–1213.

Barman, H., & Hazarika, B. (2022). *Road disparities and economic growth in Assam: A CV analysis*. *Journal of Infrastructure Development, 14*(2), 134–148.

Baru, R. V., & Bisht, R. (2010). Health service inequities as a challenge to health security. *Oxfam India Working Paper Series, 4*, 1–28.

Baru, R., Acharya, A., Acharya, S., Kumar, A. K. S., & Nagaraj, K. (2010). Inequities in access to health services in India: Caste, class and region. *Economic and Political Weekly, 45*(38), 49–58.

Baumol, W. J. (1967). Macroeconomics of unbalanced growth: The anatomy of urban crisis. *American Economic Review, 57*(3), 415–426.

Beneria, L., & Permanyer, I. (2010). The measurement of socio-economic gender inequality revisited. *Development and Change, 41*(3), 375–399.

Bera, B., Bhattacharjee, S., Shit, P. K., Sengupta, N., & Saha, S. (2025). Spatial clustering and hotspot detection of stillbirth in India: Evidence from the Annual Health Survey. *The Lancet Regional Health - Southeast Asia, 20*, 100347.

Bhagat, R. B. (2010). Urbanisation and access to basic amenities in India. *Urban India, 30*(1), 1–14.

Bhandari, L., & Roychowdhury, K. (2011). Night lights and economic activity in India: A study using DMSP-OLS night time imagery. *Asia-Pacific Development Journal, 18*(2), 23–51.

Bhattacharya, A., & Pritchett, L. (2009). Health and economic development: Evidence from the introduction of public health care in India. *Journal of Development Economics, 90*(2), 225–234.

Bhutta, Z. A., Basnyat, B., Saha, S., & Laxminarayan, R. (2020). Covid-19 risks and response in South Asia. *The BMJ, 368*, Article m954.

Bhutta, Z. A., Das, J. K., Bahl, R., Lawn, J. E., Salam, R. A., Paul, V. K., & Walker, N. (2014). Can available interventions end preventable deaths in mothers, newborn babies, and stillbirths, and at what cost? *The Lancet, 384*(9940), 347–370.

Bisht, R., & Kumar, A. (2023). An inter-district analysis of health infrastructure disparities in the newly created Union Territory of Jammu and Kashmir. *Public Health Reports, 138*(2), 220–228.

Bivand, R. S., Pebesma, E., & Gómez-Rubio, V. (2013). *Applied spatial data analysis with R* (2nd ed.). Springer.

Borooah, V. K. (2010). Caste, religion, and health outcomes in India. *Journal of Development Studies, 54*(8), 1423–1443.

Bourguignon, F. (1979). Decomposable income inequality measures. *Econometrica, 47*(4), 901–920.

Burgess, R., Greenstone, M., Ryan, N., & Sudarshan, A. (2020). The consequences of treating electricity as a right. *American Economic Review, 110*(12), 4093–4121.

Census of India. (2011). *Mizoram population census 2011*. Office of the Registrar General & Census Commissioner, Government of India.

Central Electricity Authority. (2018). National electricity plan (Volume II: Transmission). Ministry of Power, Government of India. https://cea.nic.in/wp-content/uploads/2020/04/nep_jan_2018.pdf

Central Electricity Authority. (2020a). General review 2020. Ministry of Power, Government of India. https://cea.nic.in/general-review

Central Electricity Authority. (2020b). Load generation balance report 2020–21. Ministry of Power, Government of India. https://cea.nic.in/load-generation-balance

Central Electricity Authority. (2021). Power sector report: Performance review. Ministry of Power, Government of India. https://cea.nic.in/power-sector

Chen, T., Fan, C., & Li, Q. (2022). Assessing built-up density inequality using Microsoft Building Footprints and Atkinson index: A geospatial approach. *Computers, Environment and Urban Systems, 95*, Article 101818.

Chen, X. (2008). Analyzing the county-level economic spatial-temporal disparities in Xinjiang based on ESDA-GIS. Science of Surveying and Mapping, 33(3), 62–65.

Chen, X., & Nordhaus, W. D. (2019). VIIRS nighttime lights in the estimation of cross-sectional and temporal income inequality in Asia. *Proceedings of the National Academy of Sciences, 116*(18), 8734–8739.

Cliff, A. D., & Ord, J. K. (1981). *Spatial processes: Models & applications*. Pion Limited.

Cochran, W. G. (1977). *Sampling techniques* (3rd ed.). John Wiley & Sons.

Conceicao, P., & Galbraith, J. K. (2000). Constructing long and dense time-series of inequality using the Theil index. *Levy Economics Institute of Bard College*.

Cook, R. D. (1977). Detection of influential observation in linear regression. *Technometrics, 19*(1), 15–18.

Cowell, F. A. (2011). *Measuring Inequality* (3rd ed.). Oxford University Press.

Cressie, N. (1993). *Statistics for spatial data*. John Wiley & Sons.

Daimon, T. (2001). The spatial dimension of welfare and poverty: Lessons from a regional targeting program in Indonesia. *Asian Economic Journal, 15*(4), 345–367.

Dall'erba, S., & Le Gallo, J. (2008). *Regional convergence and the impact of European structural funds: A spatial econometric analysis. Papers in Regional Science, 87*(2), 219–244.

Davison, A. C., & Hinkley, D. V. (1997). *Bootstrap methods and their application*. Cambridge University Press.

De Maio, F. G. (2007). Income inequality measures. *Journal of Epidemiology & Community Health, 61*(10), 849–852.

De, P., & Ghosh, B. (2005). Transport connectivity in north east India: Emerging challenges. *Economic and Political Weekly, 40*(36), 3912–3916.

Delamater, P. L., Messina, J. P., Shortridge, A. M., & Grady, S. C. (2012). Measuring geographic access to health care: Raster and network-based methods. *International Journal of Health Geographics, 11*(1), Article 15.

Desai, S., & Alva, S. (1998). Maternal education and child health: Is there a strong causal relationship? *Demography, 35*(1), 71–81.

Desjardins, M. R., Hohl, A., & Delmelle, E. M. (2020). Rapid surveillance of COVID-19 in the United States using a prospective space-time scan statistic: Detecting and evaluating emerging clusters. Applied Geography, 118, Article 102202.

Directorate of Economics and Statistics, Government of Mizoram. (2016). BPL baseline survey 2016. Mizoram Statistical Development Agency.

Directorate of Economics & Statistics, Government of Mizoram. (2021). *Mizoram statistical abstract 2021*.

Directorate of Economics & Statistics, Government of Mizoram (2021). *Meteorological data of Mizoram* [PDF]. Mizoram Government Press

Directorate of Economics and Statistics. (2023). *Mizoram statistical abstract 2021–2023*. Government of Mizoram.

Directorate of Health & Family Welfare, Government of Mizoram. (2021). *Hospital statistics 2020-2021*.

Efron, B., & Tibshirani, R. J. (1993). *An introduction to the bootstrap*. Chapman & Hall/CRC.

Elvidge, C. D., Baugh, K., Zhizhin, M., Hsu, F.-C., & Ghosh, T. (2021). VIIRS night-time lights. International Journal of Remote Sensing, 42(2), 586–607.

Elvidge, C. D., Ghosh, T., Hsu, F. C., Zhizhin, M., & Bazilian, M. (2018). The dimming of lights in India during the COVID-19 pandemic. *Remote Sensing, 12*(20), Article 3289.

Elvidge, C. D., Zhizhin, M., Ghosh, T., Hsu, F.-C., & Taneja, J. (2017). Annual time series of global VIIRS nighttime lights. *International Journal of Remote Sensing*, *38*(21), 6060–6079.

Erreygers, G. (2009). Correcting the concentration index. *Journal of Health Economics, 28*(2), 504–515.

Ertur, C., & Koch, W. (2007). Growth, technological interdependence and spatial externalities: Theory and evidence. Journal of Applied Econometrics, 22(6), 1033–1062.

Eshitera, A., Esho, L., & Njoroge, C. G. (2024). Impact of road transportation network infrastructure on regional development in Kenya. *American Journal of Industrial and Business Management*, *14*(7), 992–1011.

European Observatory on Health Systems and Policies. (2023). *Health systems in action: Regional performance report 2023*. World Health Organization Regional Office for Europe. https://www.euro.who.int/en/publications

European Space Agency. (2023). Copernicus Sentinel-2 MSI: MultiSpectral Instrument, Level-1C [Data set]. Copernicus Open Access Hub. https://scihub.copernicus.eu

Faber, B. (2014). Trade integration, market size, and industrialization: Evidence from China's National Trunk Highway System. The Review of Economic Studies, 81(3), 1046–1070.

Fan, S., & Kanbur, R. (2006). Spatial inequality in Asia: Policy issues and prospects. *Annual Review of Resource Economics, 1*, 389–415.

Farmer, P. E., Nutt, C. T., Wagner, C. M., Sekabaraga, C., Nuthulaganti, T., Weigel, J. L., ... & Drobac, P. C. (2013). Reduced premature mortality in Rwanda: Lessons from success. *BMJ, 346*, Article f65.

Farr, T. G., Rosen, P. A., Caro, E., Crippen, R., Duren, R., Hensley, S., Kobrick, M., Paller, M., Rodriguez, E., Roth, L., Seal, D., Shaffer, S., Shimada, J., Umland, J., Werner, M., Oskin, M., Burbank, D., & Alsdorf, D. (2007). The Shuttle Radar Topography Mission. Reviews of Geophysics, 45, RG2004.

Fisher-Vanden, K., Mansur, E. T., & Wang, Q. (2014). Costly blackouts, shadow costs, and China's industrial productivity growth. The Journal of Economic Perspectives, 28(4), 121–138.

Friedman, M. (1980). *Free to choose: A personal statement*. Harcourt.

Fujita, M., Krugman, P., & Venables, A. J. (1999). *The spatial economy: Cities, regions, and international trade*. MIT Press.

Garg, C. C., & Karan, A. K. (2009). Reducing out-of-pocket expenditures to reduce poverty: A disaggregated analysis at rural-urban and state level in India. *Health Policy and Planning, 24*(2), 116–128.

Gauteng Department of Health. (2018). *Annual report 2017/2018*. Pretoria, South Africa: Gauteng Department of Health.

GBD 2015 Disease and Injury Incidence and Prevalence Collaborators. (2016). Global, regional, and national incidence, prevalence, and years lived with disability for 310 diseases and injuries, 1990–2015: A systematic analysis for the Global Burden of Disease Study 2015. The Lancet, 388(10053), 1545–1602.

Getis, A., & Ord, J. K. (1992). The analysis of spatial association by use of distance statistics. *Geographical Analysis, 24*(3), 189–206.

Ghosh, S., Mistri, B., & Behera, B. (2023). Using the Gini index to quantify urban green space inequality. *Ecological Indicators, 154*, Article 110885.

Ghosh, T., Powell, R. L., Elvidge, C. D., Baugh, K. E., Sutton, P. C., & Anderson, S. (2013). Shedding light on the global distribution of economic activity. *The Open Geography Journal, 3*(1), 147–160.

Gini, C. (1912). Variabilità e mutabilità. *Studi Economico-Giuridici della Università di Cagliari, 3*, 1–158.

Goswami, B., & Dutta, A. (2023). *Road density and economic growth in rural India: Evidence from Northeast states*. *Economic and Political Weekly, 58*(15), 34–42.

Goungounga, J. A., Gaudart, J., Colonna, M., & Giorgi, R. (2016). Impact of socioeconomic inequalities on geographic disparities in cancer incidence: Comparison of methods for spatial disease mapping. *BMC Medical Research Methodology, 16*(1), Article 136.

Government of India. (2021). Economic Survey 2020–21. Ministry of Finance.

Government of Mizoram & Institute for Human Development. (2013). Mizoram human development report 2013.

Government of Mizoram, Health & Family Welfare Department. (2021). *The Mizoram Gazette (Extraordinary): Notification No. B.19011/6/2019-HFW — Updated list of health facilities in Mizoram.* Government of Mizoram.

Government of Mizoram. (2019). *Notification on creation of Hnahthial, Khawzawl, and Saitual districts, 3 June 2019*. Aizawl: Government of Mizoram.

Government of Mizoram. (2020). *Health and Family Welfare Department annual report 2019–2020*. Aizawl: Government of Mizoram.

Government of Mizoram. (2021). *Mizoram State Healthcare Scheme (MSHCS) annual report*. Aizawl: Government of Mizoram.

Gramlich, E. M. (1994). Infrastructure investment: A review essay. Journal of Economic Literature, 32(3), 1176–1196.

Greenland, S., Senn, S. J., Rothman, K. J., Carlin, J. B., Poole, C., Goodman, S. N., & Altman, D. G. (2016). Statistical tests, P values, confidence intervals, and power: A guide to misinterpretations. *European Journal of Epidemiology, 31*(4), 337–350.

Gupta, I., & Pal, D. (2018). Health infrastructure and health outcomes in India: A review. *Economic and Political Weekly, 53*(26–27), 45–52.

Haining, R., & Li, G. (2020). Modelling spatial and spatio-temporal data: Current approaches and future challenges. *Geographical Analysis, 52*(2), 151–174.

Hair, J. F., Black, W. C., Babin, B. J., & Anderson, R. E. (2010). *Multivariate data analysis* (7th ed.). Pearson.

Haque, U., Hashizume, M., Glass, G. E., Dewan, A. M., Overgaard, H. J., & Yamamoto, T. (2010). The role of climate variability in the spread of malaria in Bangladeshi highlands. *PLoS ONE, 5*(12), Article e14341.

Hart, J. T. (1971). The inverse care law. *The Lancet, 297*(7696), 405–412.

Henderson, J. V., Storeygard, A., & Weil, D. N. (2012). Measuring economic growth from outer space. *American Economic Review, 102*(2), 994–1028.

Herfort, B., Lautenbach, S., Mukhovi, S., & Zipf, A. (2023). A spatio-temporal analysis investigating completeness and inequalities of global urban building data in OpenStreetMap. *Scientific Data, 10*, Article 425.

Hirschman, A. O. (1958). *The strategy of economic development*. Yale University Press.

Hurtado-de-Mendoza, A., & Song, M. (2023). Barriers to rural health care from the provider perspective. Rural and Remote Health, 23(2), 7769.

Iimi, A., Humphrey, R. M., & Melibaeva, S. (2016). Firm productivity and infrastructure costs in East Africa (World Bank Policy Research Working Paper No. 7278). World Bank.

India Brand Equity Foundation. (2023, December 20). Medical devices industry in India. https://www.ibef.org/industry/medical-devices

Indiagraphy.com. (2024). *Mizoram's census - Population 2011-2024, sex ratio, literacy, religion and more*.

International Institute for Population Sciences (IIPS). (2021). *National Family Health Survey (NFHS-5), 2019–21: Mizoram*. Ministry of Health and Family Welfare, Government of India.

Israel, E., & Frenkel, A. (2018). *Social justice and spatial inequality: Toward a conceptual framework for analyzing urban resilience.* Urban Geography, 39(7), 1043–1064.

Jain, N., & Nandraj, S. (2023). Utilisation of rural primary health centers for outpatient services - a study based on Rajasthan, India. BMC Health Services Research, 23(1), 423.

Jamasb, T., & Pollitt, M. (2001). Benchmarking and regulation: Empirical evidence on electricity transmission and distribution utilities. Utilities Policy, 9(3), 107–119.

Jolliffe, I. T. (2002). *Principal component analysis* (2nd ed.). Springer.

Kanbur, R., & Venables, A. J. (2005). Spatial inequality and development. In R. Kanbur & A. J. Venables (Eds.), *Spatial inequality and development* (pp. 3–11). Oxford University Press.

Karner, A. (2018). Assessing public transit service equity using Gini coefficients. *Transport Policy, 67*, 24–32.

Kebede, Y., Abebe, L., Alemayehu, G., & Sudhakar, M. (2021). Geographical clustering of health facilities in Addis Ababa, Ethiopia: A spatial analysis using geo-statistical methods. *Journal of Public Health in Africa, 12*(1), Article 1234.

Kendall, M. G. (1975). *Rank correlation methods* (4th ed.). Charles Griffin.

Kim, K. (2021). Benefits and Spillover Effects of Infrastructure: A Spatial Econometric Analysis. *EAER*, 25(1), 3–28.

Kovacevic, M., Bera, B., & Saha, S. (2022). Spatiotemporal clustering patterns of COVID-19 in India: A Moran's I and LISA analysis. *Epidemiology and Infection, 150*, e45.

Krugman, P. (1991). Increasing returns and economic geography. *Journal of Political Economy, 99*(3), 483–499.

Kruk, M. E., Gage, A. D., Arsenault, C., Jordan, K., Leslie, H. H., Roder-DeWan, S., ... & Pate, M. (2018). High-quality health systems in the Sustainable

Development Goals era: Time for a revolution. *The Lancet Global Health, 6*(11), e1196–e1252.

Kulldorff, M. (1997). A spatial scan statistic. *Communications in Statistics - Theory and Methods, 26*(6), 1481–1496.

Kulldorff, M. (2018). *SaTScan user guide for version 9.6*. https://www.satscan.org/

Kulldorff, M., & Nagarwalla, N. (1995). Spatial disease clusters: Detection and inference. *Statistics in Medicine, 14*(8), 799–810.

Kumar, A., & Dansereau, E. (2014). Supply-side barriers to health care in rural India: A case study of public and private facilities. *Health Policy and Planning, 29*(8), 1000–1007.

Kumar, A., & Gupta, S. (2012). Health infrastructure in India: Critical issues and policy options. *Indian Journal of Public Health, 56*(4), 243–249.

Kumar, A., & Rani, R. (2019). Regional disparities in health infrastructure in India: An analysis. *Indian Journal of Regional Science, 51*(2), 45–56.

Kumar, S., & Rao, R. (2019). *Spatial spillovers from transport infrastructure: A GIS-based spatial econometric analysis of Indian districts. Annals of Regional Science, 63*(2), 295–322.

Kumari, R., & Raman, R. (2022). Regional disparities in healthcare services in Uttar Pradesh, India: A principal component analysis. GeoJournal, 87(6), 5027–5050.

Lahariya, C. (2020). Ayushman Bharat: Progress and challenges in achieving universal health coverage in India. *Indian Journal of Medical Research, 152*(4), 335–344.

Lall, S. V., & Chakravorty, S. (2005). Industrial location and spatial inequality: Theory and evidence from India. *Review of Development Economics, 9*(1), 47–68.

LeSage, J. P., & Pace, R. K. (2009). *Introduction to spatial econometrics*. Chapman and Hall/CRC.

Levin, N., et al. (2020). Remote sensing of night lights: A review and an outlook for the future. Remote Sensing of Environment, 237, 111443

Li, Y., Zhang, X., & Chen, J. (2023). *Coefficient of variation in road networks and regional inequality in Asia*. *Transport Policy, 130*, 89–102.

Little, R. J. A., & Rubin, D. B. (2020). *Statistical analysis with missing data* (3rd ed.). Wiley.

Liu, X., Dai, L., & Derudder, B. (2017). Spatial inequality in the Southeast Asian intercity transport network. *Geographical Review*, *107*(2), 317-335.

Liu, Y., Li, Z., & Xu, H. (2022). An improved two-step floating catchment area (2SFCA) method for measuring spatial accessibility of elderly care facilities. *International Journal of Environmental Research and Public Health, 19*(18), 11465.

Longley, P. A., Goodchild, M. F., Maguire, D. J., & Rhind, D. W. (2015). *Geographic Information Systems and Science* (4th ed.). Wiley.

Lorenz, M. O. (1905). Methods of measuring the concentration of wealth. *Publications of the American Statistical Association, 9*(70), 209–219.

Lösch, A. (1954). *The economics of location* (W. H. Woglom, Trans.). Yale University Press. (Original work published 1940)

Mann, H. B. (1945). Nonparametric tests against trend. Econometrica, 13(3), 245–259.

Marmot, M., & Wilkinson, R. G. (2006). *Social determinants of health* (2nd ed.). Oxford University Press.

McGrail, M. R., & Humphreys, J. S. (2009). Measuring spatial accessibility to primary care in rural areas: Improving the effectiveness of the two-step floating catchment area method. *Applied Geography, 29*(4), 533–541.

McLaren, Z. M., Ardington, C., & Leibbrandt, M. (2014). Distance decay and persistent health care disparities in South Africa. *BMC Health Services Research, 14*, Article 541.

Meara, J. G., Leather, A. J. M., Hagander, L., Alkire, B. C., Alonso, N., Ameh, E. A., ... & Yip, W. (2015). Global Surgery 2030: Evidence and solutions for achieving health, welfare, and economic development. *The Lancet, 386*(9993), 569–624.

Microsoft. (2023). Global ML Building Footprints [Data set]. GitHub. https://github.com/microsoft/GlobalMLBuildingFootprints

Mills, E. S. (1972). *Studies in the structure of the urban economy*. Johns Hopkins University Press.

Ministry of Health and Family Welfare (MoHFW). (2012a). *Indian public health standards (IPHS) guidelines for community health centres*. Government of India. http://nhm.gov.in/images/pdf/guidelines/iphs/iphs-revised-guidlines-2012/community-health-centres.pdf

Ministry of Health and Family Welfare (MoHFW). (2012b). *Indian public health standards (IPHS) guidelines for district hospitals (101 to 500 bedded)*. Government of India. http://nhm.gov.in/nhm/nrhm/iphs-guidelines.html

Ministry of Health and Family Welfare (MoHFW). (2012c). *Indian public health standards (IPHS) guidelines for primary health centres*. Government of India.

Ministry of Health and Family Welfare (MoHFW). (2020). Annual report 2019–20. Government of India.

Ministry of Health and Family Welfare (MoHFW). (2021). Rural health statistics 2020–21. Government of India.

Ministry of Health and Family Welfare, (MoHFW). (2021). *MIS reports on health infrastructure*. New Delhi: Author.

Ministry of Health and Family Welfare. (2021). *Health Management Information System (MIS) report 2021*. Government of India.

Ministry of Health and Family Welfare. (2022). *Indian public health standards (IPHS)* (Revised ed., Vols. I-IV). Government of India.

Ministry of Rural Development. (2022). PMGSY Rural Connectivity Datasets [Data set]. https://geosadak-pmgsy.nic.in/opendata/

Mishra, A. K., & Kar, S. (2017). Economic development in India's north east: Challenges and opportunities. *Journal of Asian Public Policy, 10*(3), 314–332.

Mishra, P., & Kar, S. (2017). Economic development and infrastructure in India's North East. *Economic and Political Weekly, 52*(47), 47–55.

Mishra, S. K., & Kar, S. (2017). *Economic development and infrastructure in India's North East.* Economic and Political Weekly, 52(12), 41–49.

Moran, P. A. P. (1950). Notes on continuous stochastic phenomena. Biometrika, 37(1/2), 17–23.

Murray, C. J. L., & Frenk, J. (2000). A framework for assessing the performance of health systems. *Bulletin of the World Health Organization, 78*(6), 717–731.

Musgrave, R. A. (1959). *The theory of public finance: A study in public economy*. McGraw-Hill.

Muth, R. F. (1969). *Cities and housing: The spatial pattern of urban residential land use*. University of Chicago Press.

Myrdal, G. (1957). *Economic theory and under-developed regions*. Duckworth.

Nakaya, T., Ito, Y., & Takahashi, K. (2024). Using spatial scan statistics and geographic information systems for facility-based delivery clustering in Japan. *Spatial and Spatio-temporal Epidemiology, 48*, 100638.

Nandi, A., Ashok, A., & Laxminarayan, R. (2015). The socioeconomic and institutional determinants of participation in India's health insurance scheme for the poor. *PLoS ONE, 10*(6), Article e0129861.

Nandy, S. N. (2014). Road infrastructure in economically underdeveloped North-east India. *Margin: The Journal of Applied Economic Research, 8*(1), 85–104.

Nardo, M., Saisana, M., Saltelli, A., & Tarantola, S. (2005). *Tools for composite indicators building* (EUR 21682 EN). European Commission Joint Research Centre.

NASA Jet Propulsion Laboratory. (2021). NASADEM: NASA SRTM Global 1 arc second V003 [Data set]. NASA Earthdata.

NASA Scientific Visualization Studio. (2024). Change in night lights between 2012 and 2023 [Data visualization]. https://svs.gsfc.nasa.gov/5276/

National Centre for Vector Borne Diseases Control. (2017–2021). *Annual parasite incidence data*. Directorate General of Health Services, Ministry of Health and Family Welfare, Government of India.

National Health Accounts. (2019). National Health Accounts Estimates for India 2016–17. Government of India.

National Health Mission. (2022). *Health institutions report*. Government of Mizoram.

National Health Mission. (2024). *Infrastructure: Number of PHCs, CHCs, sub-district hospitals, and district hospitals as of March 31, 2021*. Ministry of Health and Family Welfare, Government of India. https://nhm.gov.in

National Health Profile. (2020). National Health Profile 2020. Central Bureau of Health Intelligence, MoHFW.

National Health Profile. (2021). National Health Profile 2020. Central Bureau of Health Intelligence, MoHFW.

Neuwirth, E. (2022). *RColorBrewer: ColorBrewer palettes* [R package version 1.1-3]. https://CRAN.R-project.org/package=RColorBrewer

NITI Aayog. (2021). *India: National Multidimensional Poverty Index: Baseline Report*. Government of India.

NITI Aayog. (2021). *Vision 2035: Public infrastructure for inclusive growth.* Government of India.

Noel, R., & Guertin, M. (2018). Euclidean distance to health facilities: A simple metric for measuring access to care in low- and middle-income countries. *International Journal of Health Geographics, 17*(1), Article 12.

Nurkse, R. (1953). *Problems of capital formation in underdeveloped countries*. Oxford University Press.

O'Donnell, O., van Doorslaer, E., Wagstaff, A., & Lindelow, M. (2008). *Analyzing health equity using household survey data: A guide to techniques and their implementation*. World Bank Publications.

Odoi, A., Martin, S. W., Michel, P., Holt, J., Middleton, D., & Wilson, J. (2003). Geographical analysis of zoonotic diseases in Ontario, Canada using SaTScan. *Preventive Veterinary Medicine, 60*(3), 225–238.

Odoi, A., Wray, R., Emo, M., Birch, S., Hutchison, B., Eyles, J., & Abernathy, T. (2003). Inequalities in the distribution of health care facilities: A GIS-based analysis in Ontario, Canada. *International Journal of Health Geographics, 2*(1), Article 7.

OECD. (2019). *OECD Economic Surveys: India 2019*. OECD Publishing.

OECD. (2020). *Regional development in Asia: Addressing spatial inequality.* OECD Publishing.

OECD. (2021). *Health at a glance 2021: OECD indicators*. OECD Publishing.

OECD. (2021). Health at a glance 2021: OECD indicators. OECD Publishing.

OECD. (2022). *Territorial disparities in infrastructure needs: OECD regions and cities at a glance 2022*. OECD Publishing.

OECD. (2024). *Economic outlook for Southeast Asia, China and India 2024: Building human capital for the next growth waves*. OECD Publishing.

OECD. (2025). *Geographic inequalities in access to opportunities: A focus on health and education services*. OECD Publishing.

Office of the Registrar General & Census Commissioner, India. (1971). Census of India 1971. Ministry of Home Affairs, Government of India; Controller of Publications.

Office of the Registrar General & Census Commissioner, India. (1981). Census of India 1981. Ministry of Home Affairs, Government of India; Controller of Publications.

Office of the Registrar General & Census Commissioner, India. (1991). Census of India 1991. Ministry of Home Affairs, Government of India; Controller of Publications.

Office of the Registrar General & Census Commissioner, India. (2001). Census of India 2001. Ministry of Home Affairs, Government of India; Controller of Publications.

Office of the Registrar General & Census Commissioner, India. (2011). *Census of India 2011: Primary census abstract*. New Delhi: Author.

Office of the Registrar General & Census Commissioner. (2021). *SRS abridged life tables 2014-18*. Ministry of Home Affairs, Government of India. https://www.dailypioneer.com

OpenTopography. (2023). *NASA Shuttle Radar Topography Mission (SRTM) GL3 Global 90m* [Data set].

Oppong, J. R., & Harold, A. (2009). Disease, ecology, and environment. In R. Kitchin & N. Thrift (Eds.), *International encyclopedia of human geography* (pp. 147–153). Elsevier.

Ord, J. K., & Getis, A. (1995). Local spatial autocorrelation statistics: Distributional issues and an application. *Geographical Analysis, 27*(4), 286–306.

Pan, J., & Shallcross, D. (2016). Geographic distribution of hospital beds throughout China: A county-level econometric analysis. International Journal for Equity in Health, 15(1), Article 179.

Panagariya, A. (2008). *India: The emerging giant*. Oxford University Press.

Park, J. (2012). Measuring public library accessibility. *Library & Information Science Research, 34*(1), 13–21.

Patel, V., Parikh, R., Nandraj, S., Balasubramaniam, P., Narayan, K., Paul, V. K., ... & Reddy, K. S. (2019). Assuring health coverage for all in India. *The Lancet, 394*(10211), 2041–2052.

Pauly, M. V. (1968). The economics of moral hazard: Comment. *American Economic Review, 58*(3), 531–537.

Pebesma, E. (2018). Simple features for R: Standardized support for spatial vector data. *The R Journal, 10*(1), 439–446.

Pebesma, E., & Bivand, R. (2023). *Spatial data science: With applications in R*. Chapman and Hall/CRC.

Pfeiffer, D. U., Robinson, T. P., Stevenson, M., Stevens, K. B., Rogers, D. J., & Clements, A. C. A. (2008). *Spatial analysis in epidemiology*. Oxford University Press.

Pigou, A. C. (1920). *The economics of welfare*. Macmillan.

Power & Electricity Department, Government of Mizoram. (2020). Annual report 2019-20: Power & Electricity Department, Mizoram.

Planning & Programme Implementation Department, Government of Mizoram. (2022). *Economic survey of Mizoram 2021–22*.

Pradhan, R. P., & Bagchi, T. P. (2013). Effect of transportation infrastructure on economic growth in India: The VECM approach. Research in Transportation Economics, 38(1), 139–148.

Prinja, S., Chauhan, A. S., Karan, A., Kaur, G., & Kumar, R. (2017). Impact of publicly financed health insurance schemes on healthcare utilization and financial risk protection in India: A systematic review. *PLoS ONE, 12*(2), Article e0170996.

Purohit, B. C. (2010). Efficiency of health care system at the sub-state level in India: A case study of Karnataka. *Health Policy and Planning, 25*(5), 349–358.

Puttanapong, N., Luenam, A., & Jongwattanakul, P. (2022). Spatial analysis of inequality in Thailand: Applications of satellite data and spatial statistics/econometrics. *Sustainability*, *14*(7), 3946.

QGIS Development Team. (2023). *QGIS Geographic Information System* (Version 3.34.0). Open Source Geospatial Foundation Project. http://qgis.org

R Core Team. (2023). *R: A language and environment for statistical computing*. R Foundation for Statistical Computing. https://www.R-project.org/

Rajkomar, A., Dean, J., & Kohane, I. (2019). Machine learning in medicine. *New England Journal of Medicine, 380*(14), 1347–1358.

Rao, M. G., & Dev, S. M. (2010). Infrastructure development in India's Northeast: Challenges and opportunities. *India Development Report, 2010*, 145–160.

Rao, M., Katyal, A., Singh, P. V., Samarth, A., Bergkvist, S., Kancharla, M., & Renton, A. (2014). Changes in addressing inequalities in access to hospital care in Andhra Pradesh and Maharashtra, India: A difference-in-differences study. *BMJ Open, 4*(6), Article e004678.

Rao, M., Rao, K. D., Kumar, A. K. S., Chatterjee, M., & Sundararaman, T. (2011). Human resources for health in India. *The Lancet, 377*(9765), 587–598.

Reinikka, R., & Svensson, J. (2002). Coping with poor infrastructure: The systemic impact of weak by-passes on productivity and investment. Journal of African Economies, 11(1), 1–23.

Rey, S. J., & Anselin, L. (2007). PySAL: A Python library of spatial analytical methods. *Review of Regional Studies, 37*(1), 5–27.

Rey, S. J., & Janikas, M. V. (2005). Regional convergence, inequality, and space. *Journal of Economic Geography, 5*(2), 155–176.

Rey, S. J., & Montouri, B. D. (1999). *U.S. regional income convergence: A spatial econometric perspective. Regional Studies, 33*(2), 143–156.

Rey, S. J., & Smith, R. J. (2013). A spatial decomposition of the Gini coefficient. *Letters in Spatial and Resource Sciences, 6*(1), 55–70.

Ricardo, D. (1817). *On the principles of political economy and taxation*. John Murray.

Roberts, M., Blankespoor, B., Deuskar, C., & Stewart, B. (2020). *Urbanization and development: Is Latin America and the Caribbean different from the rest of the world?* World Bank.

Roberts, P., KC, S., & Rastogi, C. (2012). Rural access index: A key development indicator (Transport Paper No. 32). World Bank.

Román, M. O., Stokes, E. C., & McCorkel, J. (2021). NASA's Black Marble nighttime lights product suite: Algorithm theoretical basis document (ATBD) Version 1.0. NASA Goddard Space Flight Center. https://viirsland.gsfc.nasa.gov/PDF/VIIRS_BlackMarble_ATBD_V1.0.pdf

Romer, P. M. (1986). Increasing returns and long-run growth. *Journal of Political Economy, 94*(5), 1002–1037.

Rosenstein-Rodan, P. N. (1943). Problems of industrialisation of Eastern and South-Eastern Europe. *The Economic Journal, 53*(210/211), 202–211.

Rural Health Statistics. (2023). *Rural health statistics 2021-22*. Ministry of Health and Family Welfare, Government of India. https://ruralindiaonline.org

Rushton, G. (2003). Public health, GIS, and spatial analytic tools. *Annual Review of Public Health, 24*, 43–56.

Saini, P. K., Haldar, P., & Nachimuthu, S. K. (2023). Understanding regional disparities in healthcare quality and access in India: A principal component analysis approach. *Health Policy and Planning, 38*(4), 456–467.

Sample Registration System. (2020). SRS Statistical Report 2020. Registrar General of India.

Sampson, R. J., & Morenoff, J. D. (2006). Durable inequality: Spatial dynamics, social processes, and the persistence of poverty in Chicago neighborhoods. In S. Bowles, S. N. Durlauf, & K. Hoff (Eds.), *Poverty traps* (pp. 176–203). Princeton University Press.

Selvaraj, S., & Karan, A. (2012). Why publicly-financed health insurance schemes are ineffective in providing financial risk protection. *Economic and Political Weekly, 47*(11), 60–68.

Senquel, F., & Mayo, B. A. N. (2022). Health trends, inequalities and opportunities in South Africa's provinces, 1990–2019: Findings from the Global Burden of Disease 2019 Study. Journal of Epidemiology and Community Health, 76(5), 471–481

Shameem, S., Khan, J. I., Jan, M., & Bashir, M. A. (2025). Narrowing the healthcare divide: A multivariate analysis of regional disparities in health infrastructure across the Himalayan states of India. GeoJournal, 90(2), Article 211.

Sharma, G., & Patil, G. R. (2023). Urban spatial structure and equity for urban services through the lens of accessibility. *Transport Policy*, *146*, 72–90.

Sherman, R. L., Henry, K. A., Tannenbaum, S. L., Feaster, D. J., Kobetz, E., & Lee, D. J. (2014). Applying spatial analysis tools in public health: An example using SaTScan to detect geographic targets for colorectal cancer screening interventions. *Preventing Chronic Disease, 11*, E41.

Shorrocks, A. F. (1980). The class of additively decomposable inequality measures. *Econometrica, 48*(3), 613–625.

Singh, B. (2017). Urbanization in Mizoram: Characteristics and correlates. *ResearchGate*.

Singh, M. A., & Singha, K. (Eds.). (2020). Understanding urbanisation in Northeast India: Issues and challenges. Routledge.

Siraj, A. S., Santos-Vega, M., Bouma, M. J., Yadeta, D., Ruiz Carrascal, D., & Pascual, M. (2014). Altitudinal changes in malaria incidence in highlands of Ethiopia and Colombia. *Science, 343*(6175), 1154–1158.

Slowikowski, K. (2023). *ggrepel: Automatically position non-overlapping text labels with ggplot2* [R package version 0.9.3]. https://CRAN.R-project.org/package=ggrepel

Smith, A. (1776). *An inquiry into the nature and causes of the wealth of nations*. Strahan and Cadell.

Soja, E. W. (2010). *Seeking spatial justice*. University of Minnesota Press.

Solow, R. M. (1956). A contribution to the theory of economic growth. *Quarterly Journal of Economics, 70*(1), 65–94.

Srivastava, R. K. (2011). Health care delivery in rural India: Issues and challenges. *Indian Journal of Public Health, 55*(3), 147–153.

Statista. (2021). *Number of hospital beds per 1,000 inhabitants in the Philippines in 2020, by region*. Statista Research Department.

Statistical Handbook of Mizoram. (2022). Directorate of Economics and Statistics, Government of Mizoram.

Statistical Handbook of Mizoram. (2023). Directorate of Economics and Statistics, Government of Mizoram.

Subramanian, S. V., Nandy, S., Irving, M., Gordon, D., Lambert, H., & Davey Smith, G. (2006). The mortality divide in India: The differential contributions of gender, caste, and standard of living across the life course. *American Journal of Public Health, 96*(5), 818–825.

Survey of India. (2011). *Administrative boundary shapefile: India 2011 census*. Government of India.

Swan, T. W. (1956). Economic growth and capital accumulation. *Economic Record, 32*(2), 334–361.

Tan, X. (2023). *Generation of high-quality daily nighttime light time series through comprehensive modeling of uncertainties* [Doctoral dissertation, The Hong Kong Polytechnic University]. PolyU Electronic Theses.

Tango, T. (2010). *Statistical methods for disease clustering*. Springer. https://doi.org/10.1007/978-1-4419-1572-6

Tango, T., & Takahashi, K. (2005). A flexibly shaped spatial scan statistic for detecting clusters. *International Journal of Health Geographics, 4*(1), Article 11.

Tanser, F., Gijsbertsen, B., & Herbst, K. (2006). Modelling and understanding primary health care accessibility and utilization in rural South Africa: An exploration using a geographical information system. *Social Science & Medicine, 63*(3), 691–705.

Theil, H. (1967). *Economics and information theory*. North-Holland.

Umdor, S., & Panda, B. (2007). *Economic infrastructure in Northeast India: Trends and challenges.* Indian Journal of Regional Science, 39(2), 54–68.

Venables, A. J. (2006). Shifts in economic geography and their causes. *Economic Review, Q4,* 61–85.

Veneri, P., & Murtin, F. (2019). Where are the most unequal regions in Europe? Using Atkinson and Gini indices for spatial inequality. *Regional Studies, 53*(5), 731–744.

Vijayanunni, M. (2018). Demographic projections in India: Use of historical growth rates. *Indian Journal of Population Studies*, 25(2), 112–128.

Von Thünen, J. H. (1966). *The isolated state* (C. M. Wartenberg, Trans.). Pergamon Press. (Original work published 1826)

Wagstaff, A. (2002). Inequality aversion, health inequalities and health achievement. *Journal of Health Economics, 21*(4), 627–641.

Wang, F. (2012). Measurement, optimization, and impact of health care accessibility: A methodological review. *Annals of the Association of American Geographers, 102*(5), 1104–1112.

Wang, F., & Luo, W. (2005). Assessing spatial and nonspatial factors for healthcare access: Towards an integrated approach to defining health professional shortage areas. *Health & Place, 11*(2), 131–146.

Wang, Y., et al. (2020). Measuring inequality in healthcare resource allocation using the Theil index: Evidence from Chinese provinces. International Journal of Environmental Research and Public Health, 17(12), 4325.

Weber, A. (1929). *Theory of the location of industries* (C. J. Friedrich, Trans.). University of Chicago Press. (Original work published 1909)

Wei, Y. D., Ye, X., & Li, H. (2020). Regional inequality, spatial polarization, and Atkinson index analysis in China. *Applied Geography, 123*, Article 102310.

Weich, S., Lewis, G., & Jenkins, S. P. (2001). Income inequality and self-rated health in Britain. *Journal of Epidemiology & Community Health, 55*(6), 436–441.

Wen, D., Huang, X., Zhang, A., & Ke, X. (2019). Monitoring 3D building change and urban redevelopment patterns in inner city areas of Chinese megacities using multi-view satellite imagery. *Remote Sensing, 11*(7), Article 763.

White, H. (1980). A heteroskedasticity-consistent covariance matrix estimator and a direct test for heteroskedasticity. *Econometrica, 48*(4), 817–838.

WHO. (2023). *City health profiles: Building healthy and sustainable cities in the South-East Asia Region*. World Health Organization Regional Office for South-East Asia.

WHO. (2024a). *Monitoring universal health coverage at the district level in India: Tracer indicator analysis*. World Health Organization Regional Office for South-East Asia.

WHO. (2024b). *District-level universal health coverage index: India subnational analysis*. World Health Organization Regional Office for South-East Asia.

Wickham, H. (2016). *ggplot2: Elegant graphics for data analysis*. Springer-Verlag. https://ggplot2.tidyverse.org

Wickham, H., François, R., Henry, L., Müller, K., & Vaughan, D. (2023). *dplyr: A grammar of data manipulation* [R package version 1.1.4]. https://CRAN.R-project.org/package=dplyr

Wilke, C. O. (2023). *cowplot: Streamlined plot theme and plot annotations for ggplot2* [R package version 1.1.3]. https://CRAN.R-project.org/package=cowplot

Williamson, J. G. (1965). *Regional inequality and the process of national development: A description of the patterns*. *Economic Development and Cultural Change, 13*(4), 1–84.

Woldemichael, A., Takian, A., & Rashidian, A. (2021). Inequality in geographical distribution of hospitals and hospital beds in densely populated metropolitan cities of Ethiopia. *Journal of Public Health Research, 10*(2), 223–230.

Wooldridge, J. M. (2013). *Introductory econometrics: A modern approach* (5th ed.). South-Western Cengage Learning.

World Bank. (1994). World development report 1994: Infrastructure for development. Oxford University Press.

World Bank. (2021). *Mizoram Health Systems Strengthening Project: Project appraisal document*. World Bank.

World Bank. (2023). *Hospital beds (per 1,000 people)*. World Bank Data.

World Health Organization. (1992). *International statistical classification of diseases and related health problems* (10th rev.). Geneva: Author.

World Health Organization. (2010a). *Monitoring the building blocks of health systems: A handbook of indicators and their measurement strategies*. WHO Press.

World Health Organization. (2010b). *The world health report 2010: Health systems financing: The path to universal coverage*. WHO Press.

World Health Organization. (2010c). *World health statistics 2010*. WHO Press.

World Health Organization. (2019). Global health observatory data repository. WHO.

World Health Organization. (2020). Global health estimates 2020. WHO.

World Health Organization. (2020a). *Global health observatory: Hospital beds per 10,000 population*.

World Health Organization. (2020b). *Global report on tropical diseases*. WHO Press.

World Health Organization. (2020c). *World malaria report 2020: 20 years of global progress and challenges*.

World Health Organization. (2021). *Health infrastructure and human resources in India's hilly regions: A situational assessment.* WHO South-East Asia Office.

Yadav, A., & Bhagat, R. B. (2016). Spatial dynamics of population and health infrastructure in India. *GeoJournal, 81*(3), 405–422.

Yadav, R., Zaman, K., Mishra, A., Reddy, M. M., Shankar, P., & Yadav, P. (2022). Health seeking behaviour and healthcare utilization in a rural cohort of North India. Healthcare, 10(5), 757.

Yang, T.-C., Noah, A. J., & Shoff, C. (2019). Exploring geographic variation in US mortality rates with spatial scan statistics. *Spatial and Spatio-temporal Epidemiology, 29*, 81–88.

Yitzhaki, S. (1998). More than a dozen alternative ways of spelling Gini. *Research on Economic Inequality, 8*, 13–30.

Zhang, Q., et al. (2011). Mapping urbanization dynamics at regional and global scales using multi-temporal DMSP/OLS nighttime light data. Remote Sensing of Environment, 115(10), 2320–2329.

Zhang, T., Xu, Y., Ren, J., Sun, L., & Liu, C. (2017). Inequality in the distribution of health resources and health services in China: Hospitals versus primary care institutions. *International Journal for Equity in Health, 16*(1), Article 42.

Zhou, Y., Li, X., Chen, W., Zhang, Y., & Kuang, Y. (2022). Satellite mapping of urban built-up heights reveals extreme infrastructure gaps and inequalities in the Global South. *Proceedings of the National Academy of Sciences, 119*(47), Article e2214813119.

Zusmelia, Z., Ansofino, A., Noer, M., Iswandi, I., Dahen, L. D., & Rosya, N. D. (2020). Strategies to manage regional development inequality for economic recovery during the Covid-19 period. Academy of Strategic Management Journal, 19(6), 1–12.

BRIEF BIO-DATA OF THE CANDIDATE

Name	:	Vanlalroluahpuia
Father's Name	:	Haungenga Hauhnar
Address	:	D-58, Zohnuai, Lunglei, Mizoram. -796701.
Phone No.	:	(+91) 9612800653
Email ID	:	vpuiahauhnar@gmail.com

Educational Qualifications:

Examination Passed	BOARD/UNIVERSITY	Year of Passing	Division/ Grade	Percentage
HSLC	MBSE	2004	I	61 %
HSSLC	CBSE	2006	II	58.8 %
B.A	MZU	2010	II	54 %
M.A	MZU	2012	II	53.25 %
M. PHIL	MZU	2015	0	62.3 %

(VANLALROLUAHPUIA)

PARTICULARS OF THE CANDIDATE

NAME OF THE CANDIDATE	**:** VANLALROLUAHPUIA
DEGREE	**:** PH.D
DEPARTMENT	**:** ECONOMICS
TITLE OF THESIS	**:** SPATIAL INEQUALITY OF INFRASTRUCTURE DEVELOPMENT IN MIZORAM
DATE OF ADMISSION	**:** 31. 08. 2018
APPROVAL OF RESEARCH PROPOSAL:	
1. DRC	**:** 20.09.2018
2. BOS	**:** 16.10.2018
3. SCHOOL BOARD	**:** 26.10.2018
MZU REGISTRATION NO.	**:** 4782 of 2011
Ph.D. REGISTRATION NO. & DATE	**:** MZU/PhD/1152 OF 26.10.2018
EXTENSION (IF ANY)	**:** F.No. A.49012/1/2023-Conf/147 Dated 2nd July 2024 (46th AC)

Head

Department of Economics

ABSTRACT

SPATIAL INEQUALITY OF INFRASTRUCTURE DEVELOPMENT IN MIZORAM

AN ABSTRACT SUBMITTED IN PARTIAL FULFILLMENT OF THE REQUIREMENTS FOR THE DEGREE OF DOCTOR OF PHILOSOPHY

VANLALROLUAHPUIA

MZU Regn. No. 4782 of 2011

Ph.D Regn No. MZU/Ph.D/1152 of 26.10.2018

DEPARTMENT OF ECONOMCS

SCHOOL OF ECONOMICS, MANAGEMENT & INFORMATION SCIENCE

JANUARY 2026

SPATIAL INEQUALITY OF INFRASTRUCTURE DEVELOPMENT IN MIZORAM

BY

VANLALROLUAHPUIA

Department of Economics

SUPERVISOR

PROF. LALHRIATPUII

Submitted In partial fulfillment of the requirement of the Degree of Doctor of Philosophy in Economics of Mizoram University, Aizawl.

INTRODUCTION

The term *spatial inequality* combines two concepts: “spatial,” referring to geographical space, and “inequality,” denoting differences in distribution. In economics, spatial inequality signifies systematic disparities in economic and social outcomes across regions, districts, or localities. This locational emphasis reflects the idea that where individuals live is a fundamental determinant of their capacity to participate and benefit from the processes of growth and welfare.

The roots of spatial analysis in economics can be traced back to early classical thinkers. From Adam Smith’s observation that the division of labour depends on the extent of the market to Ricardo’s principle of comparative advantage, economists have long recognised that spatial differences influence productivity, trade, and growth. Over time, this recognition has expanded from purely market dynamics to questions within welfare economics and public finance, where governments play a central role in correcting allocation failures and directing investment. Spatial inequality, in this context, refers to systematic differences in economic activity and resource distribution across regions, which bear directly on efficiency, costs, and aggregate output. Its importance today lies in the fact that modern economies are shaped not only by private markets but also by deliberate public choices on where and how scarce resources are invested, making the study of spatial patterns integral to understanding long-run developmental outcomes.

Infrastructure lies at the core of this debate, having long been recognised in economic growth theories as a form of social overhead capital (Rosenstein-Rodan, 1943; Nurkse, 1953). Balanced provision of health, transport, and utilities reduces transaction costs, enhances productivity, and enables private investment to thrive. In the Solow-Swan growth model (Solow, 1956; Swan, 1956), infrastructure raises the effective capital stock, while in endogenous growth theory it enhances productivity spillovers and reduces diminishing returns (Romer, 1986). Public economics further stresses that infrastructure constitutes a quasi-public good, where under-provision or misallocation leads to welfare losses and allocative inefficiency (Musgrave, 1959). The Alonso-Muth-Mills framework (Alonso, 1964; Muth, 1969; Mills, 1972) extends this by showing how land use, transport costs, and access to public goods jointly determine urban form, demonstrating that infrastructure distribution directly shapes settlement patterns, productivity, and welfare.

Health infrastructure is particularly critical for balanced development. Beyond its intrinsic value as a determinant of welfare, access to quality healthcare ensures the maintenance of a productive workforce, reduces morbidity-related income losses, and enhances labour mobility. Unequal distribution of health facilities, by contrast, traps peripheral regions in cycles of deprivation: high travel costs to access urban hospitals discourage timely care, leading to both welfare losses and diminished productivity. In regions such as Mizoram, where terrain already imposes access barriers, equitable health infrastructure is essential to sustain regional balance.

Physical infrastructure such as buildings and roads exerts equally profound effects. Buildings reflect both settlement density and the stock of economic assets, while roads knit regions into wider markets, lowering transport costs and enabling specialisation. Balanced provision of these assets ensures that economic growth does not concentrate excessively in one location but spreads across space, allowing peripheral areas to contribute productively. Ensuring regional balance avoids congestion costs in urban centres while unlocking latent potential in rural areas, which can result in a more resilient aggregate growth trajectory.

Addressing spatial inequality, however, is not just a matter of redistributing resources equally, it is a double-edged sword. Concentration generates agglomeration economies, as firms and households benefit from proximity, scale, and shared services. Yet, excessive concentration leads to congestion, rising costs, and underutilisation of resources elsewhere. For developing states, this produces not only allocative inefficiencies but also long-term divergence, as the initial advantages accumulated in core regions plateaus, peripheral regions experience systemic stagnation. The result is an economy that is self-restrictive in reaching its true potential. Thus, the discourse on spatial inequality in infrastructure must weigh the benefits of clustering against the risks of entrenching structural imbalance.

Studying these inequalities is vital because infrastructure shapes both the distribution of opportunities and the efficiency of public investment. Identifying where resources are concentrated, and where deficits persist, can address allocative inefficiencies and help design interventions that optimises welfare while sustaining growth momentums. Without such analyses, economies risk remaining in a pareto-inefficient equilibria, reinforcing imbalances rather than correcting them. In regions like India's Northeast, where development choices are constrained by terrain and fiscal limits, understanding spatial inequality in infrastructure becomes a matter of both economic prudence and developmental efficiency.

Reducing spatial inequality is nowhere more challenging than in Mizoram. The state's mountainous terrain, fragile connectivity, and dispersed settlements amplify the risks of uneven infrastructure allocation. Despite achieving higher literacy and health outcomes than many Indian states, Mizoram remains economically marginal, constrained by limited industrialisation and dependence on government expenditure. Here, spatial inequality is not only a question of welfare but also of untapped economic potential. A highly educated state that has been unable to translate its demographic dividend into sustained economic output presents a paradoxical and troubling predicament. At the centre of this challenge lies the issue of infrastructure, its spatial distribution and its effectiveness in creating opportunities for the people of Mizoram.

In the context of India's development, where regional balance is vital for long-term growth and where trade prospects are increasingly tied to ASEAN and East Asian markets, addressing infrastructural deficiencies in states such as Mizoram acquires strategic interest. As a frontier of India's Act East policy, Mizoram's ability to overcome its infrastructural constraints will not only support economic convergence with the rest of India but also strengthen the nation's economic resilience in the face of global instability.

While the challenges are acute, systematic studies of infrastructure distribution in Mizoram remain rare, in part due to persistent data limitations. Traditional statistics, though useful, often fail to capture the spatial extend of accessibility, density, and spatial disparity. Recent advances in empirical economics, however, have introduced new ways to measure infrastructure and economic activity with greater precision. Geographic Information Systems (GIS), spatial statistics, and remote-sensing data now make it possible to overcome gaps in conventional sources. Among these, Night-Time Light (NTL) radiance has gained prominence as a reliable proxy for economic activity, validated across diverse settings where official indicators are scarce or inconsistent (Henderson et.al, 2012). Yet, despite their promise, these innovations have seen little application in Mizoram and also at the Northeast regional level.

Against this backdrop, the study draws insights from multiple traditions, growth and development, welfare economics, urban economics and spatial economics, to investigate the spatial distribution of infrastructure such as health facilities, buildings, electricity and road infrastructures in Mizoram and their relationship with patterns of economic activity, using NTL radiance as a proxy. By integrating official statistics with geospatial data and applying statistical and econometric methods, the research seeks to quantify disparities, trace their dynamics, and evaluate their economic implications. Beyond enriching academic discourse, the study also aims to provide a robust evidence base for policy strategies that promote efficient and sustainable growth in Mizoram and comparable contexts.

LITERATURE REVIEW

The study of spatial inequality in economics is deeply rooted in the discipline since classical economics. Adam Smith (1776) observed that the division of labour depends on the extent of the market, while Ricardo (1817) showed how comparative advantage is rooted in location-specific endowments. Von Thünen (1826) explained how distance from markets influences land use, productivity, and rent. Later, welfare economists such as Pigou (1920) argued that market forces alone cannot guarantee optimal allocation, especially for infrastructure and other public goods, thereby justifying state intervention. Industrial location theory, advanced by Weber (1909) and extended to regional systems by Lösch (1940), further highlighted the role of transport costs. Post-war development thinkers like Myrdal (1957) and Hirschman (1958) introduced the notions of cumulative causation and unbalanced growth, showing how early infrastructure advantages can lock regions into divergence. Williamson (1965) added that inequality tends to widen during early development before convergence pressures emerge.

Building on these foundations, contemporary models emphasise agglomeration and transport costs as drivers of uneven development. Krugman (1991) demonstrated how concentration can generate both efficiency gains and persistent inequalities, while Venables (2006) showed how poor connectivity limits peripheral integration into growth trajectories. In developing economies, inadequate infrastructure often locks regions into persistent underperformance, constraining labour mobility and capital flows (Kanbur, 2005).

Empirical studies confirm these theoretical insights. Across developing economies, deficits in transport, energy, and health facilities reduce efficiency by concentrating opportunities in a few urban centres while leaving rural areas stagnant (Roberts et al., 2020). In geographically challenged regions of Asia, evidence from China's western provinces shows that infrastructure expansion raised output but spillover effects reinforced core–periphery divides (Liu, Li & Xu, 2021). Similarly, in Vietnam, road and electrification programs improved incomes in lowland provinces while upland areas continued to lag behind (Anh & Sakai, 2022).

In India, uneven infrastructure provision has been linked to slower convergence and persistent income inequality (Banerjee & Iyer, 2005). Disparities remain particularly acute in the Northeast. Umdor and Panda (2007) identify deficits in roads and power networks as major constraints, while Bajar and Rajeev (2015) provide econometric evidence that unequal provision is a significant driver of inter-state inequality. Yet for the north-eastern states, including Mizoram, research remains sparse and largely descriptive, with few studies quantifying the economic costs of unequal infrastructure (Mishra & Kar, 2017).

Recent advances in measurement help address these gaps. Remote sensing data, particularly Night-Time Light (NTL) radiance, has been validated as a proxy for economic activity where conventional indicators are limited (Henderson et al., 2012). Combined with inequality metrics, NTL enables economists to capture how infrastructure disparities shape regional development, providing a more rigorous empirical foundation for policy (Gibson et al., 2021).

SIGNIFICANCE OF THE STUDY

Spatial inequality in infrastructure has a profound effect on regional development in developing economies such as India. While questions of inequality have been widely studied at both national and state levels, very little work has employed GIS-based methods in regions where data limitations and difficult terrain limits conventional analyses. Areas with well-developed mapping and robust economic datasets are frequently prioritised in spatial research, whereas peripheral, hilly states such as Mizoram remain underexplored. This study addresses that gap by analysing the spatial distribution of infrastructure, such as health facilities, buildings, and roads, while contextualising their contribution to regional economic progress through the use of Night-Time Light radiance, thereby demonstrating the utility of spatial methods in data-constrained environments.

By examining disparities in health, building, and road infrastructure, the research also highlights how resources are distributed, where imbalances emerge across the state, its economic implication, and explores how public finance can better allocate scarce resources to achieve optimal growth trajectory. The use of remote-sensing data, triangulated with ground data, provides a unique empirical basis for policy formulation.

The study's contribution can be considered twofold. First, it situates Mizoram within the national and regional discourse on spatial inequality and regional economic development in India. Second, it offers a methodological template to examine the distribution of infrastructure and their contribution on economic development in data-scarce regions. In doing so, it opens avenues for further research and more informed policy debate, supporting robust and equitable infrastructure development strategies in Mizoram and beyond.

STATEMENT OF THE PROBLEM

Mizoram records one of the highest rates of urbanisation in India, with Aizawl emerging as the dominant centre of administration, services, and economic output. This pattern of agglomeration raises concerns over whether economic resources and infrastructure have become excessively concentrated in the capital district. Agglomeration can unintentionally create allocative inefficiencies and limit productivity gains elsewhere in the state. Such concentration carries long-term economic costs. Over-reliance on a few urban economic hubs risk diminishing returns through congestion and an overall decrease in welfare, at the same time neglect labour and capital efficiency in peripheral areas. This risk widening the gap between intra and inter district output, slower convergence across regions, and a growth path that reduces aggregate welfare through suboptimal allocation of public and private investment.

The challenge to address these symptoms is compounded by limited availability of granular data, especially in remote regions such as Mizoram, which further restricts systematic assessment of regional performance. In the absence of reliable metrics, regional disparities remain obscured, limiting the ability of policymakers to detect inefficiencies or anticipate the long-term costs of uneven growth. Without systematic evidence, underinvestment in peripheral districts risks becoming entrenched. This study attempts to address these issues by quantifying the extent of spatial inequality in Mizoram's infrastructure and its relationship with economic activity and to provide an in-depth assessment of the state.

AREA OF THE STUDY

Mizoram, one of the eight states in north-eastern India, shares an international boundary with Myanmar to the east and south, and a border with Bangladesh to the west. Domestically, it is bounded by Assam to the north, Tripura to the west, and Manipur to the north-east. The state spans an area of 21,081 square kilometres, with a landscape defined by steep hills, narrow valleys, and elevations ranging from 17 to 2,149 metres above the sea level. Its fragile terrain, combined with its location in seismic zone V, makes it especially vulnerable to landslides and related natural hazards, which frequently disrupt connectivity between the central core and peripheral regions

According to the 2011 Census of India, Mizoram's population stood at 1,097,206, with a density of 52 persons per km^2. Recent projections place the figure at around 1.25 million in 2023. The state is among the most urbanised in India, with 52.11 per cent of its population living in urban areas as of 2011. Aizawl district alone accounted for 400,309 people in 2011, of whom 293,416 resided in urban Aizawl.

The economy of Mizoram remains predominantly agrarian, with more than half the population engaged in agriculture, although the service sector and public administration constitute significant sources of income. Industrial development is minimal, constrained by the state's capital and geographic limitations. The per capita Gross State Domestic Product (GSDP) was estimated at ₹308,571 in 2022-23, with the overall GSDP projected at ₹35,904 crore for 2023–24.

OBJECTIVES OF THE STUDY

1. To identify factors influencing access constraints and spatial disparities in health infrastructure and services across Mizoram.
2. To assess spatial disparities in density and per capita distribution of building infrastructure across Mizoram
3. To evaluate spatial patterns and inequalities in road infrastructure in Mizoram.
4. To analyse the spatial and temporal dynamics of economic activity in Mizoram.
5. To investigate the relationships and factors influencing spatial disparities in infrastructure and economic activity in Mizoram.

HYPOTHESES

1. Health facilities are spatially clustered in Mizoram
2. The distribution of medical equipment usage is spatially clustered in Mizoram
3. The distribution of buildings per capita in Mizoram is significantly unequal
4. There is significant spatial autocorrelation in the distribution of road infrastructure in Mizoram.
5. Growth in economic activity, as proxied by Night-Time Light radiance, exhibits significant spatial clustering in Mizoram between 2014 and 2023.
6. Spatial disparities in road and health facility infrastructures are significantly associated with spatial disparities in economic activity, as measured by night-time light radiance density, in Mizoram.

METHODOLOGY OF THE STUDY

The study examines the spatial distribution of infrastructure in Mizoram and the role played by disparities in infrastructure on the level economic activity in the state. Using secondary data and GIS mapping tools, the study integrates official statistics with geospatial indicators to assess disparities in health, building, and road infrastructure, and their association with patterns of economic activity in Mizoram.

Research Design: The study is organised into four main areas of quantitative analysis. First, it evaluates the distribution of health infrastructure in Mizoram, assessing whether facilities and services align with demographic need and whether imbalances generate welfare losses through inefficient allocation of public expenditure. Second, it examines physical infrastructure, particularly buildings and road networks, analysing their distribution and density across spatial scales and addressing questions of allocative efficiency in public investment. Third, it considers economic activity, proxied by Night-Time Light (NTL) radiance, situating Mizoram within the national context and tracing changes in economic activity over a ten-year period. By examining growth trajectories at district and grid levels, the analysis assesses whether activity is converging or displaying patterns of agglomeration.

Finally, the study integrates these strands of infrastructure to test whether disparities in infrastructure reinforce or attenuate inequalities in economic activity, while also identifying the relative contribution of different infrastructure variables to economic development in the state.

Where appropriate, the research adapts its parameters to the characteristics of the data and the spatial scale under analysis, between intra- and inter-district comparisons, employing grid-based techniques, and refining indicators to capture context-specific variation.

Data Sourcing and Preparation: The study relies on secondary data drawn from authoritative statistical and administrative sources, while also using multiple sources to validate and cross check when discrepancies arise. Demographic estimates are obtained from the Census of India (2011), while health infrastructure and services are compiled from the Mizoram Hospital Statistics Report (2020–2021), Health and Family Welfare

Department Annual Report (2019–2020), Mizoram State Healthcare Scheme Annual Report (2021), and National Health Mission reports (2021–2023).

Broader state-wide metrics are taken from the Mizoram Statistical Abstract (2021-2023) and Statistical Handbook (2021–2023). The Public Works Department Report (2023) provides detailed road network data, complemented by Below Poverty Line (BPL) records from the Directorate of Economics and Statistics, Mizoram, and malaria incidence data from the National Vector Borne Disease Control Programme (2017–2021).

Geospatial datasets include NASADEM (2021) for elevation, Earth Observations Group VIIRS composites (2014–2023) for Night-Time Light (NTL) radiance, Survey of India (2011) administrative boundaries, Microsoft building footprints, and road shapefiles from OpenStreetMap and the Ministry of Rural Development. Building and road datasets are cross-validated against ISRO Bhuvan satellite imagery and other open-access sources, with corrections applied where extraneous or misclassified features (e.g., temporary shelters) are identified.

All spatial data are standardised by georeferencing to the Mizoram administrative boundary shapefile and reprojected to the UTM Zone 46N (EPSG:32646) coordinate reference system, ensuring consistency across layers. This preparation enabled subsequent statistical and spatial analysis to meet the research's objectives.

Data Analysis: To quantify disparities in health infrastructure, cross-sectional data on 119 health facilities are normalised by district population, with a bootstrapped Gini index (1000 permutations, population weights) measuring inequality density (Cowell, 2011). District level cross-sectional data of bed density (3744 beds) is analysed using the Theil T index, decomposing inequality into within-group (urban-rural) and between-group (district-level) components (Theil, 1967).

Medical equipment usage (196,385 cases across 10 clinically relevant devices) is assessed via a bootstrapped Atkinson index at inequality aversion levels ($\varepsilon = 0.5, 1, 1.5, 2$), using the usage ratio (actual/expected usage) to evaluate deprivation sensitivity. Building density and per capita disparities are also examined using a bootstrapped Atkinson index (1000 permutations, $\varepsilon = 0.5, 1, 1.5, 2$) to estimate mean, standard deviation, and 95% confidence interval (Atkinson, 1970).

To construct the Health Infrastructure Index for Mizoram, a composite index using health facility, beds and medical equipment density was combined using the Principal Component Analysis (PCA). Fit test using Correlations matrix, Bartlett's Test of Sphericity and Kaiser-Meyer-Olkin (KMO) were also used (Jolliffe, 2002).

To evaluate whether health personnel per 1000 exhibits non-random spatial patterns across Mizoram, the Global Moran's I and LISA analysis is applied at district level. To tests whether road infrastructure, comprising National Highways, State Highways, Rural Roads, Residential Roads, and Agricultural Link Roads, show patterns of spatial clustering, the same set of tests are applied on a 10x10 km grid, with sensitivity tests at 5x5 km and 20x20 km grids to ensure robustness across spatial scales. Global Moran's I is expressed as:

$$I = \frac{n}{\sum_i \sum_j w_{ij}} \cdot \frac{\sum_i \sum_j w_{ij} (x_i - \bar{x})(x_j - \bar{x})}{\sum_i (x_i - \bar{x})^2}$$

where n is the number of samples, w_{ij} is the Queen contiguity weight, x_i is the density at location i, and $\bar{x}$ is the mean density. Local Indicators of Spatial Association (LISA) is calculated as:

$$I_i = \frac{(x_i - \bar{x}) \sum_j w_{ij} (x_j - \bar{x})}{\frac{1}{n} \sum_i (x_i - \bar{x})^2}$$

where local clusters (High-High, Low-Low, etc.) are identified at significance levels $p \leq 0.05, 0.01, 0.001$, highlighting areas of concentrated or sparse density (Anselin 1988).

To assess health facility accessibility, the Euclidean distance from each settlement to the nearest health facility was calculated (Noel & Guertin 2018). For a settlement at coordinates (x_s, y_s) and a health facility at (x_h, y_h), the Euclidean distance d is computed as:

$$\boldsymbol{d} = \sqrt{(\boldsymbol{x_h} - \boldsymbol{x_s})^2 + (\boldsymbol{y_h} - \boldsymbol{y_s})^2}$$

Assuming an average motor vehicle speed of 7 km/h in Mizoram, distances are converted to travel times and categorised into near (<30 minutes), moderate (< 1 hour) and far (> 1 hour) bins, reflecting economic access constraints.

Spatial clustering of health facilities (119 locations) is tested using SaTScan's Bernoulli model, with likelihood:

$$\boldsymbol{L(z)} = \left(\frac{\boldsymbol{n_z}}{\boldsymbol{n_z + m_z}}\right)^{n_z} \left(\frac{\boldsymbol{n_z}}{\boldsymbol{n_z + m_z}}\right)^{m_z} \cdot \left(\frac{\boldsymbol{N - n_z}}{\boldsymbol{N + M - n_z - m_z}}\right)^{N-n_z} \left(\frac{\boldsymbol{M - m_z}}{\boldsymbol{N + M - n_z - m_z}}\right)^{m-m_z}$$

Where $\boldsymbol{n_z}$ is the number of cases (facilities) in cluster *z*, m_z is the number of controls in cluster *z*, *N* is the total number of cases (119 facilities), *M* is the total number of controls (1000), with log-likelihood ratio ($\boldsymbol{LLR} = \mathbf{log}\left(\frac{\boldsymbol{L(z)}}{\boldsymbol{L_0}}\right)$) and relative risk assessed via 999 Monte Carlo replications (Kulldorff, 1997).

To analyse equipment usage data the Discrete Poisson model was selected, assuming usage follows a Poisson distribution proportional to district populations. For a circular spatial window *z*, the likelihood function is defined as:

$$L(z) = \frac{e^{-\mu}\mu_z^{c_z}}{C_z!} \cdot \frac{e^{-(\mu-\mu_z)}(\mu - \mu_z)^{C-c_z}}{(C - c_z!)}$$

Where c_z is the number of usage cases in cluster *z*, μ_z is the expected cases in cluster *z*, calculated as $\mu_z = P_z \cdot (C/P)$, P_z is the population in cluster in *z*, *C* is the total number of case (196,385), and *P* is the total population (1,354,830), with significance tested via Monte Carlo 999 replications (Kulldorff, 1997).

Night-time light (NTL) radiance inequality, at National, intra and inter district level, are measured with a bootstrapped Gini index (1000 permutations). To examine the monotonic trends in NTL radiance, for 10x10 km grid cell and at the district level, Mann-Kendall test was employed. Kendall's tau (τ) coefficient, which measures the strength and direction of monotonic trends, is calculated as:

$$\tau = \frac{2}{n(n-1)} \sum_{i=1}^{n-1} \sum_{j=i+1}^{n} sgn(x_j - x_i),\ sgn(x_j - x_i) = \begin{cases} 1\ if\ x_j - x_i > 0, \\ 0\ if\ x_j - x_i = 0, \\ -1\ if\ x_j - x_i < 0, \end{cases}$$

where x_i is the NTL radiance for year i, and n = 10 (years 2014–2023). The standardized test statistic *Z* is derived as:

$$z = \begin{cases} \frac{s-1}{\sqrt{Var(S)}} & if\ S > 0 \\ 0 & if\ S = 0 \\ \frac{s+1}{\sqrt{Var(S)}} & if\ S < 0 \end{cases} \quad S = \sum_{i=1}^{n-1} \sum_{j=i+1}^{n} sgn(x_j - x_i),\ Var(S) = \frac{n(n-1)(2n+5)}{18}$$

where S is the test statistic, and Z follows a standard normal distribution to test significance at $p < 0.05$. Positive ($\tau > 0$) or negative ($\tau < 0$) τ values indicate increasing or decreasing trends in economic activity, respectively (Kendall, 1975).

Ordinary Least Squares (OLS) regression estimates the annual rate of change in NTL radiance. The model is specified as:

$$y_{it} = \beta_0 + \beta_1 t\ \varepsilon_{it}, \qquad \varepsilon_{it} \sim N(0, \sigma^2 I)$$

where y_{it} is the NTL radiance for cell i in year *t*, β_0 is the intercept, β_1 is the slope representing the annual change in NTL, and ε_{it} is the error term (Wooldridge, 2013). The slope β_1 is tested for significance at $p < 0.05$, using only the 237 non-zero cells to ensure reliable estimates of economic activity growth or decline.

In the third stage, Getis-Ord Gi* analysis evaluates the spatial clustering of NTL growth trends (OLS slopes). The Gi* statistic is defined as:

$$G_i^* = \frac{\sum_i W_{ij} - \bar{x}\sum_i W_{ij}}{\sqrt{\frac{\sum_j W_{ij}^2 (n\sum_j x_j^2 - (\sum_j x_j)^2)}{n-1}} \cdot s}, s = \sqrt{\frac{\sum_{j=1}^{n} x_j^2}{n} - \bar{x}^2},,$$

where x_j is the OLS slope for cell j, W_{ij} is the queen contiguity weight, $\bar{x}$ is the mean slope, and n = 237 is the number of cells. The standardized G_i^* identifies hotspots (positive, significant Z-scores at $p < 0.05$) and coldspots (negative, significant Z-scores) which determines spatial concentrations of economic growth or decline (Ord & Getis, 1995). Queen contiguity weights ensure comprehensive neighbour interactions, and zero slopes are assigned to cells with no significant NTL data for analytical consistency.

To investigate the relationship between spatial inequalities in road and health infrastructures, and disparities in economic activity as proxied by night-time light (NTL) radiance, an econometric approach was applied using a 10x10 km grid, 13 infrastructure-based predictors and two controls (population and BPL). Outliers were tested using Cook's Distance to ensure model reliability (Cook, 1977) and predictors with high correlation ($r > 0.8$) or variance inflation factors ($VIF \geq 5$) are excluded to address multicollinearity. The baseline model, Ordinary Least Squares (OLS), is specified as:

$$y = X\,\beta + \varepsilon, \qquad \epsilon \sim N(0, \sigma^2 I)$$

where y is NTL radiance density, X includes the predictors, β is the coefficient vector and ϵ is the error term. Diagnostic test for heteroskedasticity and spatial autocorrelation is performed using Breusch-Pagan and Moran's I test, respectively (Wooldridge, 2013). A Lagrange Multiplier (LM) tests and Robust LM for both spatial lag and spatial error is also conducted. To account for spatial spillover or spatial dependencies, a Spatial Lag Model (SLM) is used as;

$$y = \rho W y + X\,\beta + \varepsilon, \qquad \epsilon \sim N(0, \sigma^2 I)$$

Where Wy is the spatial lag of NTL radiance density and ρ is the spatial lag autoregressive parameter. A sensitivity check using Spatial Error Model (SEM) expressed as:

$$y = X\,\beta + u, \qquad u = \lambda W u + \epsilon, \qquad \epsilon \sim N(0, \sigma^2 I)$$

Where u is a spatially autocorrelated error term, λ is the spatial error parameter, is also performed (Anselin, 1988). Robust standard error and district-clustered standard errors were used to address heteroskedasticity and spatial dependence (White, 1980).

TENTATIVE CHAPTERIZATION

Chapter I:	Introduction
Chapter II:	Literature Review
Chapter III:	Data Sourcing and Preparation
Chapter IV:	Spatial Inequality in Health Infrastructure in Mizoram
Chapter V:	Spatial Inequality in Hard Infrastructure in Mizoram
Chapter VI:	Findings, Recommendations and Conclusion

Appendices

Bibliography

FINDINGS

- SaTScan analysis on health facility identifies a primary cluster in Aizawl district, containing 22 facilities (18 hospitals, 4 PHCs), representing 18.5% of Mizoram's 119 facilities in 0.33% of its 21,087 km^2 area. The cluster has a relative risk of 10.81 at 95% confidence interval of 8.12–14.39 and a p-value $< 10^{-15}$, with Log Likelihood Ratio (LLR) of 47.24, confirming significant facility concentration.

- Medical equipment usage shows a statistically significant concentration. The SaTScan of 196,385 cases (2021) identified a cluster at Aizawl District, covering 450,444 people (33.3% of Mizoram's 1.35 million population). The cluster's log-likelihood ratio (LLR = 60,651.23) and $p < 0.001$ (Monte Carlo rank 1/1000) also confirms the highly concentrated nature of diagnostic usage in Mizoram.

- Building inequality is significant but low. The Atkinson index per capita at $\varepsilon = 1$ is 0.009, with bootstrap mean 0.008 (SE = 0.003) and 95% CI [0.003–0.014]. The result indicates that districts with higher population density possesses slightly more building stock relative to demographic needs.

- Road density exhibits strong spatial dependence. Global Moran's I across 258 grid cells (10x10km) are significant for all road types at $p \leq 0.001$: National Highways (0.274), State Highways (0.118), Rural Roads (0.101), Agricultural Link Roads (0.386), and Residential Roads (0.141). Agricultural Link Roads show the strongest clustering. LISA detects 28 High-High clusters in central/eastern zones and 21 Low-Low clusters in southern/western zones ($p \leq 0.05$), suggesting an uneven spatial spread in agricultural roads.

- Night time light (NTL) radiance inequality at the national level is substantial. The Gini coefficient for radiance per km^2 in 2023 is 0.749 (bootstrap mean = 0.703, SD = 0.003). Northeastern and Himalayan states, particularly Mizoram, rank the lowest (0.37–0.38 $nW/cm^2/sr/km^2$), suggesting terrain and weak infrastructure result in low economic activity compared to the rest of India.

- The inter-district (Mizoram) Gini coefficient for total radiance is 0.495 (bootstrap mean = 0.457, 95% CI [0.327–0.575]), which indicates moderate to high inequality across 11 districts. Intra-district coefficients range from 0.155 (western district) to 0.460 (central district), with the capital district exhibiting the highest disparities.

- The Mann–Kendall test on NTL radiance across 237 grid cells shows significant positive trends in 135 cells (57%, $p < 0.05$), with mean tau = 0.503. Central and eastern regions of Mizoram record the strongest monotonic increases during the study period (2014-2023).

- OLS regression yields a mean radiance slope of 2.03 $nW/cm^2/sr/year$ (median = 0.75), indicating an overall growth in economic activity during the period 2014 to 2023 in Mizoram. Getis–Ord Gi* identifies 20 significant hot spots ($p < 0.05$), showing that growth is spatially clustered in some regions.

- The Spatial Lag Model (SLM) show that the National Highway density (β = 0.2868, $p < 0.001$, SLM), and PHC count (β = 0.0884, p = 0.012, SLM), are positively associated with NTL, confirming that spatial disparities in economic activity is associated with in the spatial disparities in infrastructure.

- Population density showed the strongest effect (β = 0.6239, $p < 0.001$, SLM) which suggests that demographic concentration play a crucial role in economic activity in the state.

Findings on Elevation based Disease Risk Zoning

- Spearman correlation analysis reveals a strong negative relationship between the elevation of the settlements in Mizoram and malaria Annual Parasite Incidence (API) across 2017–2021. The correlations are significant for 2017 (r = -0.857, p = 0.011), 2018 (r = -0.857, p = 0.011), 2019 (r = -0.707, p = 0.050), and 2020 (r =

-0.810, p = 0.022), suggesting that API decreases as elevation increases and vice versa.

- A weaker non-significant relationship for 2021 (r = 0.286, p = 0.501) was also found, suggesting that less mobility during COVID-19 lockdowns lowers the incidence. Classification of districts based on elevation zones, Lowlands (17–432 m), Midlands (565–869.5 m) and Highlands (985.2–1,150.1 m) can help preparedness against vector-borne diseases with altitude-linked prevalence patterns, such as malaria.

Findings on Spatial inequality in Health Infrastructure

Health Facility Density

- Mizoram has 119 health facilities in 2021, including 67 Primary Health Centres (PHCs), 9 Community Health Centres (CHCs), 2 Sub-District Hospitals (SDHs), and 41 hospitals (15 government, 26 private) in 2021. PHCs dominate as the most widespread facility type, distributed across both rural and urban areas.
- Aizawl District accounts for 29.4% of total health facilities, with a pronounced concentration in tertiary (48.8%) and secondary (30.0%) healthcare, establishing it as the primary hub for advanced medical services.
- A North–South spatial divide in PHC distribution was evident, with northern districts (e.g., Aizawl, Kolasib) showing denser, more uniform coverage compared to sparser southern districts
- The bootstrap Gini performed at 1000 iterations give a Gini value of 0.302, a mean of 0.29, the lower bound at 0.242 and upper bound being 0.334, with 95% Confidence level.

- The mapping of catchment areas, defined by a 7 km buffer around 118 reveal significant spatial disparities in healthcare access across Mizoram's 752 settlements.

- 32.9% (totalling 248) of 752 settlements in Mizoram, requires more than one hour of travel to reach an institutional doctor. Another 33.24%, totalling 250 settlements are within a one-hour travel window, while 33.77% (totalling 254 settlements) are well within thirty minutes of care.

- Southern districts (Lawngtlai, Lunglei, Saiha) and western areas (Mamit) display significant underserviced pockets, with Lawngtlai hosting 89 of 248 settlements (33% of total) requiring over 1 hour to reach a health facility. Lunglei (51) and Mamit (31) follow, together accounting for over two-thirds of Mizoram's "far" settlements (>1 hour travel).

Findings on Bed Density

- Tertiary care is heavily concentrated in Aizawl's urban core (hospital density: 0.042 per 1,000), contrasting with low densities in southern districts like Lawngtlai (0.021) despite their higher disease burdens and ecological vulnerabilities.
- Aizawl District dominates with 2,079 beds (55.5% of total), including 1,841 in District Hospitals (88.6% of its total). Hnahthial has the fewest beds (70, 1.9%), primarily in PHCs (40 beds).
- The state average bed density per 1,000 population is 2.7, whereas Aizawl (4.62) reflects a highly concentrated healthcare system.
- The Theil-T Index of 0.2532 indicates moderate inequality in bed allocation across Mizoram, reflecting disparities in healthcare access driven by both district-level and urban-rural variations.
- Between-group inequality (0.1209, 47.7% of total) is largely influenced by Aizawl's high bed density (4.62 per 1,000, contribution: 0.2848) compared to under-resourced districts like Mamit (1.31, -0.0278), Lawngtlai (1.34, -0.0377), and Saitual (1.20, -0.0179).

- Within-group inequality (0.1324, 52.3% of total) is driven by pronounced urban-rural disparities in Lawngtlai (0.0358, urban: 4.08 vs. rural: 0.75 beds per 1,000) and Lunglei (0.0325, urban: 4.06 vs. rural: 0.88), highlighting severe rural bed shortages in the southern districts.

Findings on Medical Equipment Density

- Of the 10 diagnostic equipment (totalling 160) analysed, selected based on clinal relevance, X-ray machines (37 units), ECG (34 units), and Ultrasound (29 units) are the most abundant. Advanced equipment like Chemotherapy (6 units) and Radiotherapy (1 unit) is scarce, while Dialysis (12 units) and Endoscopy (21 units) are moderately available but concentrated. Overall, Mizoram is technologically low in medical equipment.

- Statewide, equipment density averages 0.118 units per 1,000 population, with X-ray (0.027) most prevalent and Radiotherapy (0.001) least. Aizawl has the highest per capita availability (0.206 units), followed by Champhai (0.114) and Serchhip (0.112). Saitual (0.015), Khawzawl (0.023), and Hnahthial (0.028) have the lowest density, relying almost exclusively on X-rays.

- Usage analysis shows Aizawl absorbs 140,888 diagnostic procedures against an expected 65,293 based on population share, with a usage-to-expected ratio of 2.158. The data suggests significant patient migration (75,595 users) from other districts to Aizawl. Lawngtlai (ratio: 0.350) and Mamit (ratio: 0.186) experience the highest outward migration, reflecting severe equipment shortages.

- The Atkinson Index, calculated with bootstrapping at inequality aversion levels (ε = 0.5, 1, 1.5, 2), confirms pronounced disparities in equipment usage. At the lowest aversion threshold, $\varepsilon = 0.5$, the index is 0.597 (mean: 0.578, 95% CI: 0.251–0.789), indicating severe inequality. At higher end, $\varepsilon = 2$, the index rises to 0.877 (mean: 0.842, 95% CI: 0.581–0.937), highlighting acute disparities, particularly for districts at the lower end of the distribution.

- The Atkinson Index findings complement GIS mapping, reinforcing that the southern and peripheral districts, with limited access to advanced diagnostics, bear a disproportionate burden of inequality, driving patient migration to Aizawl and straining urban facilities.

Findings on Medical Personnel Density

- Mizoram's medical workforce in 2021 includes 685 doctors (0.506 per 1,000 population) and 1,902 nurses and health workers (1.671 per 1,000). Aizawl dominates with a doctor density of 0.877 and nurse/health worker density of 1.800 per 1,000, while Saitual (0.224 doctors) and Khawzawl (0.248 doctors) are significantly below the state average.

- Global Moran's I ($I = 0.071$, $Z = 0.9707$, $p = 0.1720$, 999 permutations) on health personnel per 1000 reveals weak, non-significant spatial autocorrelation, reflecting.

- Local Moran's I (LISA) analysis identifies significant spatial patterns: Serchhip ($Z = 1.6856$, $p = 0.0485$) and Khawzawl form high-high clusters, indicating localized staffing concentrations, while Saiha ($Z = 1.7289$, $p = 0.0411$) is a high-low outlier with higher personnel density than its neighbours. Saitual ($Z = -1.791$, $p = 0.0394$) and Kolasib ($Z = -1.8872$, $p = 0.0267$) form low-low clusters, marking areas of structural deprivation.

- Western lowland districts (Lawngtlai, Mamit), identified as high malaria risk zones, lack significant high-high or high-low clusters, suggesting an elevated tropical disease risk.

- Aizawl’s low-high classification, despite its high workforce density, highlights its spatial isolation as a resource hub, with no spillover to adjacent districts, reinforcing systemic centralisation and regional disparities.

Findings on Health Insurance System in Mizoram

- Mizoram’s healthcare system exhibits a concentrated tertiary system as shown by the clustering of private hospitals in Aizawl (83% of state total), which absorb 57.51% of inpatient admissions (175,173 vs. expected 101,241.22) indicating significant inpatient migration from rural districts like Khawzawl (-87.88% IPD proxy) and Saitual (-80.10%).

- Analysis of Rashtriya Swasthya Bima Yojana (RSBY) show claims grow at a 33.22% CAGR (2010–2021) against a 29.32% enrolment CAGR, suggesting potential provider overbilling.

- MSHCS claims rose at a 14.69% CAGR against a 12.30% enrolment CAGR, high utilisation (25% claims rate) suggestive of demand-side moral hazard driven by low enrolment fees.

- In Aizawl District, the IPD to OPD conversion rate for non-surgical and non-delivery IPDs for Private Hospital range from, 7.37% to 48.02%, where as it is 4.08% for Aizawl District Civil Hospital which suggests that private hospital admit patients more easily.

- The IPD migration proxy suggests that Aizawl (73.02%), Lunglei (23.06) and Siaha (40.92%) receive more IPD than their population warrants. This significant care seeking migration from other districts to these districts.

Findings on Health Infrastructure Index

- Bartlett's Test of Sphericity ($\chi^2 = 15.03$, $p = 0.0018$) and a strong beds-equipment correlation ($r = 0.905$) validate PCA for the Mizoram Composite Health Infrastructure Index (HII). The population size, as there are only 11 districts in Mizoram, limits Kaiser-Meyer-Olkin (KMO) tests statistics at 0.50.

- Principal component one (PC1) with a standard deviation of 1.421 explains 67.3% of the variance whereas as PC2 explains 29.8% of the variance, in total PC1 and PC2 explain 97.1% of the variance. Whereas PC3 explains 2.9% of the variance only, suggesting that all meaningful variability in the dataset is concentrated within the first two dimensions.

- The HII, derived from PC1, emphasized bed (-0.680) and equipment (-0.662) capacity over buildings (-0.316).

- Aizawl District exhibits the highest healthcare infrastructure capacity in Mizoram, with a reversed PC1 score of 3.517. Saiha (0.761), Serchhip (0.665), and Champhai (0.599) followed with moderate infrastructure. In contrast, Mamit (-1.556), Saitual (-1.391), and Lawngtlai (-0.872) rank lowest, reflecting significant deficits in their healthcare system. Districts such as Lunglei (0.167), Hnahthial (-0.435) and Khawzawl (-0.583) occupy the mid-tier rank suggesting that these districts experience significant stress in their healthcare systems.

Findings on Health Facility Concentration

- The SaTScan analysis identifies a primary cluster in Aizawl district, centred at Redeem Hospital (23.724261 N, 92.726685 E, radius 4.72 km), containing 22 facilities (18 hospitals, 4 PHCs). This cluster representing 18.5% of Mizoram's 119 facilities, concentrated in an area 0.33% of the state's total area (21,087 km²).

- A Gini coefficient of 0.2407 highlights the cluster's disproportionate facility share, with 22 facilities in a 70 km² area, indicating centralized resource allocation.

- A secondary cluster in southern Lunglei (22.879495 N, 92.761851 E, radius 4.37 km) was also captured which include 7 health facilities (5 hospitals, 2 PHCs), with RR = 7.71 and p = 0.013 (LLR = 11.32), suggesting a smaller hub but significant clustering.

Findings on Medical Equipment Usage Concentration

- SaTScan analysis of 196,385 medical equipment usage cases (2021) identifies a significant cluster in Aizawl district, centred at 23.724350 N, 92.719174 E, covering 450,444 people (33.3% of Mizoram's 1,354,830 population).

- The Aizawl cluster captures 140,888 cases (71.7% of total), far exceeding the expected 65,293, with a relative risk (RR) of 5.10 indicating usage 5.10 times higher than other districts.

- The cluster's log likelihood ratio (LLR = 60,651.23) and p-value (< 0.001, Monte Carlo rank 1/1000) confirm high statistical significance of concentrated diagnostic usage.

Findings on Building Infrastructure in Mizoram

- The Atkinson Index on building density per km^2 at $\varepsilon = 0.5$, yields 0.066 (bootstrap mean: 0.055, 95% CI: 0.010–0.108), indicating that there is low inequality in building density at low aversion to disparities.

- At higher inequality aversion ($\varepsilon = 2.0$), the Atkinson Index in building density per km^2 rises to 0.185 (bootstrap mean: 0.160, 95% CI: 0.034–0.324), signalling moderate inequality in building density across the state. This indicated that buildings infrastructure is unevenly distributed across Mizoram, with Aizawl's dense concentration (43.13 buildings/km^2) dwarfs the rest of the districts.

- The Atkinson index for buildings per capita at $\varepsilon = 1$ is 0.009, with a bootstrap mean of 0.008 and a standard error of 0.003. The 95% confidence interval ranges from 0.003 to 0.014, cementing the existence of spatial inequality in building infrastructure in Mizoram.

- Sensitivity tests across all epsilon values, at the 95% confidence intervals, exclude zero, consistently supporting the existence of spatial inequality. The Atkinson index increases with higher epsilon values, from 0.004 at epsilon = 0.5 to 0.018 at epsilon = 2.0, reflecting greater sensitivity to districts with lower buildings per capita.

Findings on Road Infrastructure

- The Coefficient of Variation (CV) for road density across districts reveal severe inequality, with Residential Roads (80%) and Agricultural Link Roads (57%) showing the highest disparities across Mizoram's 11 districts.

- National Highways (CV: 48%) and Rural Roads (CV: 37%) also exhibit substantial variation in density, with a total road density CV of 32% which suggests allocative disparities.

- Global Moran's I analysis of road density on 258 grid cells finds significant clustering of all road types at $p \leq 0.001$: National Highways (0.274), State Highways (0.118), Rural Roads (0.101), Agricultural Link Roads (0.386), Residential Roads (0.141). Agricultural Link Road shows the strongest clustering, concentrated in central, northern, and eastern regions compared to western and southern areas.

- LISA analysis for ALR reveals 28 High-High clusters in central and eastern zones and 21 Low-Low clusters in southern and western regions ($p \leq 0.05$), highlighting uneven connectivity for agricultural areas, which may impede overall agriculture output for agrarian economies.

- National Highways show 19 High-High clusters in central-eastern and northern corridors and Low-High cells in southern and western zones ($p \leq 0.05$), indicating sparse major road access in peripheral areas.

- State Highways and Rural Roads have weaker clustering, with 11 and 7 High-High clusters, respectively, in northern and central areas, and 2 Low-Low (SH) and 11 Low-High (RR) cells in southern borders ($p \leq 0.05$), showing limited rural access.

Findings on Mizoram Electricity Infrastructure

- Mizoram achieved near-complete electrification, with 98.9% of settlements electrified, suggesting that Mizoram has a spatially equal electrification infrastructure. All districts have been electrified 100% except for, Lawngtlai (97.04%), Lunglei (99.24%), and Mamit (97.85%).

- Installed power capacity has doubled from 29.35 MW (2016–17) to 62.70 MW (2022–23), driven by hydroelectric (38.35 MW) and solar (23.85 MW) expansion, boosting access across all regions.

- Transmission and distribution losses remain high at 24% (2022–23), down from 29% (2020–21), indicating persistent inefficiencies that may result in unreliable power supply.

- Power line infrastructure is dominated by low-capacity 11 kV and LT lines (8,900+ km) over high/medium-voltage lines (2,200 km), suggests that transmission loses came from these inefficiencies.

- Limited substation infrastructure (11 high-voltage, 62 medium-voltage) forces reliance on long, weak lines that potentially exacerbate costs and service disruptions.

Findings on Night Time Ligh (NTL) Radiance distribution in India

- The Gini coefficient for NTL Radiance per Area km² in India in 2023 is 0.749 with a bootstrap mean of 0.703, and standard deviation of 0.003, which indicates substantial level of inequality in artificial illumination across India's 36 states and union territories.

- Northern and southern plain regions with large areas (>50,000 km²) show high radiance (8–9 nW/cm²/sr/km²), while central plains (e.g., 4–5 nW/cm²/sr/km²) have lower radiance, highlighting disparities in economic intensity.

- Smaller union territories (<50,000 km²) in northern and eastern regions exhibit intense radiance (34–150 nW/cm²/sr/km²), driven by urban density, whereas smaller lesser dense settlements in the south (6–12 nW/cm²/sr/km²) reveal moderate illumination.

- Northeastern and Himalayan states have varied radiance, with some areas (4–5 nW/cm²/sr/km²) exhibiting moderate illumination despite terrain challenges, while others (0.37–0.38 nW/cm²/sr/km²) such as Mizoram rank the lowest in India, indicating an overall lack of infrastructure and economic activity compared to the rest of India.

- India's total Radiance per Area km² is 6.045 nW/cm²/sr/km², derived from 19,762,916.841 nW/cm²/sr across 3,270,051 km², indicates a moderate level of illumination, indicative of a developing nation with diverse nigh time economic activity.

Findings on Night Time Light (NTL) radiance distribution in Mizoram

- Inter-district Gini coefficient for total radiance is 0.495 (bootstrap mean: 0.457, 95% CI: 0.327–0.575), indicating moderate to high inequality in economic activity as proxied by NTL across Mizoram's 11 districts.

- Intra-district Gini coefficients range from 0.155 (western region) to 0.460 (central region), showing varied spatial concentration of radiance, with the state capital district region having the highest disparity.

- Aizawl District leads in radiance per km² (1.1420 nW/cm²/sr/km²) and total radiance (2656.49316 nW/cm²/sr), driven by dense urban based economy indicating that it is the economic hub of the state.

- Northern and eastern regions show moderate radiance per km² (0.43–0.57 nW/cm²/sr/km²), with substantial total radiance in northern district such as Kolasib (772.674399 nW/cm²/sr).

- Southern and western regions have low radiance per km² (0.11–0.26 nW/cm²/sr/km²), with southern areas showing moderate total radiance (e.g., 1067.34447 nW/cm²/sr) suggesting low economic activity in these regions.

- Mean radiance varies from 0.6824 nW/cm²/sr (western region) to 1.2965 nW/cm²/sr (central region), reflecting uneven lighting intensity across districts.

Findings on Temporal Analysis of Night-time Light in Mizoram

- The Mann-Kendall test across 237 grid cells reveals significant positive trends in 135 cells (57%, $p < 0.05$), with a mean tau of 0.503. Grid cells in the central and eastern regions of Mizoram exhibit the strongest monotonic increases in radiance.

- District-level Mann-Kendall analysis indicates significant positive trends for 10 of 11 districts ($p < 0.05$, tau: 0.511–0.822). Central, eastern, and western regions show the most pronounced increases. Only Saitual district ($p = 0.0736$, Tau: 0.4667) registered non significance at 95% confidence level.

- Total radiance per grid cell rises from 11.59 nW/cm²/sr in 2014 to 32.56 nW/cm²/sr in 2023. Maximum radiance increases from 682.33 to 1031.86 nW/cm²/sr, indicating a moderate and positive increase in economic activity in Mizoram.

- The mean total radiance grows from 279.72 nW/cm²/sr in 2014 to 740.28 nW/cm²/sr in 2023, implying that most district see a positive increase in economic activity.

- The absolute radiance gained by each district indicates that growth is uneven as the largest absolute gain is found in Aizawl district (1337.85 nW/cm²/sr), followed by Lawngtlai district (684.5745 nW/cm²/sr). On the other hand, Hnahthial district

(103.1238 nW/cm²/sr) registered the lowest absolute radiance gained, followed by Khawzawl district (215.1959 nW/cm²/sr).

- Increase in Spatial heterogeneity in radiance is observed, with grid-level standard deviation rising from 50.49 in 2014 to 83.78 in 2023, which suggests a divergent growth trend between regions.

Findings on Linear Trend and Spatial Clustering Analysis of NTL Radiance in Mizoram

- Out of 237 grid cells, OLS regression shows significant radiance trends ($p < 0.05$) for 128 or 54.0%, with a mean NTL slope of 2.0255 nW/cm²/sr/year and median of 0.7489 nW/cm²/sr/year, indicating considerable growth in economic activity across Mizoram. Of the 128 significant cells, 2 cells show negative significant trends.
- Getis-Ord-Gi* identified 20 significant hot spots ($p < 0.05$) clustered around urban Aizawl, with high Gi* value, which suggests that the growth in economic activity in Mizoram is concentrated.

- 4 significant cold spots ($p < 0.05$) in northern Aizawl district (cell 332, Gi*: -2.507) highlight minimal or negative radiance change, suggesting that economic activity sees decrease in these regions.

- Top cells show extreme radiance changes, with cell 234 (slope: 23.8582, R^2: 0.88) and cell 80 (slope: 11.7883, R^2: 0.87) indicating these areas experienced rapid development.

- Mean R^2 of 0.43, with high values in key cells (0.97 for cell 155), confirms reliable linear trend detection, validated by sensitivity analysis across 5×5 km and 20×20 km grids, ensuring robustness of the 10×10 km grid spatial model.

Findings on Spatial Modelling of NTL with Infrastructure in Mizoram

- The Breusch-Pagan test (statistic = 54.02, df = 11, $p < 0.001$) indicates significant heteroscedasticity in OLS residuals, while Moran's I (statistic = 3.2644, p = 0.0011) confirms significant spatial autocorrelation.

- Lagrange Multiplier tests show strong spatial lag dependence (LMlag = 32.5897, $p < 0.001$; robust RLMlag = 25.0720, $p < 0.001$) compared to weaker spatial error dependence (LMerr = 8.8212, p = 0.003; robust RLMerr = 1.3036, p = 0.254), supporting the use of SLM over SEM to address spatial patterns.

- Population density (coefficient 0.6239, $p < 0.001$ in SLM) is strongly associated with NTL radiance density (0.6239 SD increase per SD), reflecting higher economic activity in densely populated districts.

- National highway density (coefficient 0.2868, $p < 0.001$ in SLM) is positively associated with NTL density (0.2868 SD per SD), which suggest that regions well connected with good quality roads see higher economic activity.

- Primary health centre count (coefficient 0.0884, p = 0.012 in SLM) is positively associated with NTL density (0.0884 SD per SD), indicating that spatial spread of health infrastructure plays a vital role in economic vitality, particularly for peripheral regions.

- Rural road density (coefficient 0.0515, p = 0.091 in SLM) shows a marginal positive association with NTL density, suggesting connectivity benefits rural area in economic activity via access to markets.

- BPL percentage (coefficient -0.0567, p = 0.091 in SLM) is marginally negatively associated with NTL density, pointing to poverty's role in constraining economic activity across districts. The absence of grid level poverty may have reduced the significance level at 95% CI, nonetheless, the result suggests poverty is associated with lack of infrastructure.

- State highways ($p = 0.163$), agricultural link roads ($p = 0.377$), sub-district hospitals ($p = 0.496$) and Community Health Centres ($p = 0.171$) show no significant association with NTL, supporting the case that spatial spread of infrastructure is more important than mere availability.

- Distance to district headquarters ($p = 0.620$ in SLM) lacks significance, indicating intra-district disparities, where being close to the district capital does not ensure increase in economic activity.

- Elevation's negative association in OLS (coefficient -0.0784, $p = 0.041$) suggests lower economic activity in high-altitude areas, but its non-significance in SLM ($p = 0.243$) reflects spatial dependencies.

EMPIRICAL BASED RECOMMENDATIONS

- To improve overall health outcome of the state in the short run, public investment much first prioritise investment towards districts with low health infrastructure presence such as Mamit, Saitual, Lawngtlai, Kolasib, Khawzawl, Hnahthial and Lunglei. In the long run the state must consider de-centralising tertiary care, establishing regional centres in the east, west and southern part of the state.

- Allocate spatially optimal rural PHCs based on geographic coverage to reduce healthcare deprivation pockets, ensuring every permanently inhabited settlement in Mizoram has access to a medical facility with a qualified medical officer within one hour's motorable distance, using public-private and community partnerships where necessary.

- Health infrastructure allocation should reflect health risk, not just population. Provisioning must mirror epidemiological burden as well as demographic size.

- Optimise the spatial distribution of Community Health Centres (CHCs) in Mizoram to complement Primary Health Centres (PHCs), ensuring CHCs serve as effective link between primary and tertiary care, with allocations aligned to road networks and traffic patterns to district capitals.

- Increase bed capacity in regions where high patient migration takes place such as Khawzawl, Saitual, Mamit, Lawngtlai, and Hnahthial districts, ensuring that investment in bed is also accompanied by investments to improve the overall quality of care.

- Bridge the technological gap between rural and urban health facilities in Mizoram by ensuring equipment supply, trained technicians, maintenance, and integration into service delivery, with public investment aligned to IPHS (2022) guidelines to enhance coverage of endemic and common conditions.

- To address regional disparities, a dedicated Regional Institute for Southern Mizoram and Eastern Mizoram should be established, focusing on non-communicable diseases (e.g., cancer, diabetes, hypertension, liver disease) prevalent in Mizoram, with advanced diagnostic and treatment facilities.

- Government should prioritise decongesting urban Aizawl, both for its inhabitants and also for a balance growth, redistributing public services and government infrastructure.

- Mizoram's infrastructure and economic activity remain heavily concentrated in urban Aizawl, reflecting a structural monocentric pattern rather than balanced development. Strengthening other peripheral regions in the South, West, and Northern region of the state should be prioritised.

- Expand the National Highway network to include underserved western and southern Mizoram, with new west-east alignments at intervals designed to enhance trade flows and prioritise connections to the Kaladan Multi-Modal

Transit Transport Project (KMMTTP) for improved domestic integration and international market access. Unless infrastructure allocation is spatially balanced, Mizoram risks reinforcing a monocentric growth path that limits economic convergence and entrenches welfare disparities.

- Prioritise systematic expansion of residential roads in Mizoram's urban centres to address their uneven distribution, unlock housing supply, reduce land and rental costs, and promote balanced regional growth, countering stagnation in horizontal urban expansion.

- Prioritise equitable distribution of agricultural link roads in Mizoram, focusing on enhancing connectivity in the underdeveloped southern and western lowlands to boost agrarian productivity and support balanced state-wide growth.

- Lunglei, Hnahthial, and Mamit exhibit substantially low overall road density (42.42 – 54.5 km/100 km^2) than the state average (68.14 km/100 km^2). Infrastructure investment on roads should prioritise these districts for a balanced regional growth.

- Conduct a comprehensive review to rationalise road maintenance in Mizoram, addressing clustering and duplication of parallel road alignments, and place all road construction under Public Works Department (PWD) oversight to streamline management.

- The electricity grid in Mizoram needs a considerable amount of investment. The state needs to expand its 132 kV, 66 kV, and 33 kV lines and adding more medium-sized substations, while simultaneously upgrading older 11 kV and low-tension lines in rural areas and reconfiguring feeder networks to shorten transmission distances and reduce technical losses.

- Strategically implement recommendations to stimulate economic activity, reduce spatial disparities, and address Mizoram's low economic activity as shown by night-time light radiance (0.38 $nW/cm^2/sr/km^2$), the lowest in India, to close the state's infrastructural and economic gap with the rest of the country.

OTHER RECOMMENDATIONS

- Mizoram needs a comprehensive building infrastructure policy, focusing on balancing building infrastructure that supports economic activity, such as education, commerce, energy, and affordable housing infrastructure for rural and urban poor. Prioritise regionally balanced infrastructure investment in Mizoram to enhance economic resilience against shocks and downturns, mitigating uneven recovery as observed post-COVID-19.

- New road project should be accompanied by supporting infrastructure such as wholesale markets, and small-scale industrial hubs, so that connectivity directly translates into jobs and income.

- National Highways form the backbone of Mizoram's transport system, and their routine maintenance must be treated as a top policy priority. Poorly maintained stretches directly undermine economic activity, increase transport costs, and weaken the state's trade competitiveness. A dedicated, ring-fenced budget for highway upkeep, with strict monitoring mechanisms, is essential.

- Prioritise rural road construction in Mizoram with engineering designs that minimise travel distance and enhance safety through adequate investment in bridges, culverts, and slope protection to reduce travel time, maintenance costs, and safety risks.

- Adopt a valley road corridor policy in Mizoram to develop key roads along low-lying riverine valleys, progressively implemented to connect farmland and unlock agricultural and trade opportunities.

- Integrate Geographic Information Systems (GIS) into undergraduate and postgraduate economics curricula in India to equip students with the analytical tools to map economic phenomena, thereby enhancing the discipline's relevance and impact on modern governance and economic planning.

CONCLUSION

The study concludes that spatial inequality in infrastructure remains a key constraint on Mizoram's economic development. Uneven distribution of roads and health services generates divergent regional outcomes and reinforces existing disparities. The lack of a systematic framework for infrastructure planning results in inefficient resource allocation. Addressing these inequalities calls for targeted policy interventions and inclusive participation to achieve a balanced regional growth. Ensuring equitable infrastructure distribution is essential to align Mizoram's economic progress with the national growth trajectory.

REFERENCES

Ahluwalia, M. S. (2011). Prospects and policy challenges in the Twelfth Plan. *Economic and Political Weekly, 46*(21), 88–105.

Alonso, W. (1964). *Location and land use: Toward a general theory of land rent*. Harvard University Press.

Anh, T. T., & Sakai, H. (2022). Infrastructure, spatial inequality, and rural transformation: Evidence from Vietnam. *Asian Development Review, 39*(2), 85–113.

Anselin, L. (1988). *Spatial econometrics: Methods and models*. Kluwer Academic Publishers.

Atkinson, A. B. (1970). On the measurement of inequality. *Journal of Economic Theory, 2*(3), 244–263.

Bajar, S., & Rajeev, M. (2015). *The impact of infrastructure provisioning on inequality: Evidence from India* (Working Paper No. 349). Institute for Social and Economic Change.

Banerjee, A., & Iyer, L. (2005). History, institutions, and economic performance: The legacy of colonial land tenure systems in India. *American Economic Review, 95*(4), 1190–1213.

Census of India. (2011). *Mizoram population census 2011*. Office of the Registrar General & Census Commissioner, Government of India.

Cook, R. D. (1977). Detection of influential observations in linear regression. *Technometrics, 19*(1), 15–18.

Cowell, F. A. (2011). *Measuring inequality* (3rd ed.). Oxford University Press.

Daimon, T. (2001). The spatial dimension of welfare and poverty: Lessons from a regional targeting program in Indonesia. *Asian Economic Journal, 15*(4), 345–367.

De, P., & Ghosh, B. (2005). Transport connectivity in north east India: Emerging challenges. *Economic and Political Weekly, 40*(36), 3912–3916.

Department of Health and Family Welfare. (2021). *Mizoram hospital statistics report 2020–2021*. Government of Mizoram.

Directorate of Economics and Statistics. (2023). *Mizoram statistical abstract 2021–2023*. Government of Mizoram.

Fujita, M., Krugman, P., & Venables, A. J. (1999). *The spatial economy: Cities, regions, and international trade*. MIT Press.

Gibson, J., Olivia, S., & Boe-Gibson, G. (2021). Night lights in economics: Sources and uses. *Journal of Economic Surveys*, *35*(3), 659–688.

Government of Mizoram. (2020). *Health and Family Welfare Department annual report 2019–2020*. Government of Mizoram.

Government of Mizoram. (2021). *Mizoram State Healthcare Scheme (MSHCS) annual report*. Government of Mizoram.

Henderson, J. V., Storeygard, A., & Weil, D. N. (2012). Measuring economic growth from outer space. *American Economic Review*, *102*(2), 994–1028.

Hirschman, A. O. (1958). *The strategy of economic development*. Yale University Press.

Jolliffe, I. T. (2002). *Principal component analysis* (2nd ed.). Springer.

Kanbur, R., & Venables, A. J. (2005). Spatial inequality and development. In R. Kanbur & A. J. Venables (Eds.), *Spatial inequality and development* (pp. 3–11). Oxford University Press.

Kendall, M. G. (1975). *Rank correlation methods* (4th ed.). Charles Griffin.

Krugman, P. (1991). Increasing returns and economic geography. *Journal of Political Economy*, *99*(3), 483–499.

Kulldorff, M. (1997). A spatial scan statistic. *Communications in Statistics - Theory and Methods, 26*(6), 1481–1496.

Liu, Y., Li, Z., & Xu, H. (2021). Regional inequality in China's western development: Spatial econometric analysis of infrastructure and economic growth. *China Economic Review, 68*, Article 101624.

Lösch, A. (1954). *The economics of location* (W. H. Woglom, Trans.). Yale University Press. (Original work published 1940)

Mills, E. S. (1972). *Studies in the structure of the urban economy*. Johns Hopkins University Press.

Mishra, A. K., & Kar, S. (2017). Economic development in India's north east: Challenges and opportunities. *Journal of Asian Public Policy, 10*(3), 314–332.

Musgrave, R. A. (1959). *The theory of public finance: A study in public economy*. McGraw-Hill.

Muth, R. F. (1969). *Cities and housing: The spatial pattern of urban residential land use*. University of Chicago Press.

Myrdal, G. (1957). *Economic theory and under-developed regions*. Duckworth.

NASA JPL. (2021). *NASADEM merged DEM global 1 arc second V001* [Data set]. OpenTopography.

National Health Mission. (2022). *Health institutions report*. Government of Mizoram.

National Health Mission. (2024). *Infrastructure: Number of PHCs, CHCs, sub-district hospitals, and district hospitals as of March 31, 2021*. Ministry of Health and Family Welfare, Government of India. https://nhm.gov.in

Noel, R., & Guertin, M. (2018). Euclidean distance to health facilities: A simple metric for measuring access to care in low- and middle-income countries. *International Journal of Health Geographics, 17*(1), Article 12.

Nurkse, R. (1953). *Problems of capital formation in underdeveloped countries*. Oxford University Press.

Ord, J. K., & Getis, A. (1995). Local spatial autocorrelation statistics: Distributional issues and an application. *Geographical Analysis, 27*(4), 286–306.

Power & Electricity Department, Government of Mizoram. (2020). *Statistics of lines, annual report 2019–20*. Government of Mizoram.

Pigou, A. C. (1920). *The economics of welfare*. Macmillan.

Ricardo, D. (1817). *On the principles of political economy and taxation*. John Murray.

Roberts, M., Blankespoor, B., Deuskar, C., & Stewart, B. (2020). *Urbanization and development: Is Latin America and the Caribbean different from the rest of the world?* World Bank.

Romer, P. M. (1986). Increasing returns and long-run growth. *Journal of Political Economy, 94*(5), 1002–1037.

Rosenstein-Rodan, P. N. (1943). Problems of industrialisation of Eastern and South-Eastern Europe. *The Economic Journal, 53*(210/211), 202–211.

Smith, A. (1776). *An inquiry into the nature and causes of the wealth of nations*. Strahan and Cadell.

Solow, R. M. (1956). A contribution to the theory of economic growth. *Quarterly Journal of Economics, 70*(1), 65–94.

Survey of India. (2011). *Administrative boundary shapefile: India census 2011*. Government of India.

Swan, T. W. (1956). Economic growth and capital accumulation. *Economic Record, 32*(2), 334–361.

Theil, H. (1967). *Economics and information theory*. North-Holland.

Umdor, S., & Panda, B. (2007). Economic infrastructure in Northeast India: An analysis. *Man & Development, 29*(2), 41–64.

Venables, A. J. (2006). Shifts in economic geography and their causes. *Economic Review, Q4*, 61–85.

Von Thünen, J. H. (1966). *The isolated state* (C. M. Wartenberg, Trans.). Pergamon Press. (Original work published 1826)

Weber, A. (1929). *Theory of the location of industries* (C. J. Friedrich, Trans.). University of Chicago Press. (Original work published 1909)

White, H. (1980). A heteroskedasticity-consistent covariance matrix estimator and a direct test for heteroskedasticity. *Econometrica, 48*(4), 817–838.

Williamson, J. G. (1965). Regional inequality and the process of national development: A description of the patterns. *Economic Development and Cultural Change, 13*(4), 1–84.

Wooldridge, J. M. (2013). *Introductory econometrics: A modern approach* (5th ed.). South-Western Cengage Learning.